DOCTOR OF PHILOSOPHY

The Chemistry and Ecology of British Bluebells (Hyacinthoides non-scripta)

Raheem, Dotsha

Award date:
2016

Awarding institution:
Bangor University

The Chemistry and Ecology of British Bluebells (*Hyacinthoides non-scripta*)

by

Dotsha Raheem

A Thesis Submitted in Partial Fulfilment of the

Requirements for the Degree of

Doctor of Philosophy

in the

School of Chemistry

College of Physical and Applied Sciences

Bangor University

Bangor University

2015

Declaration and Consent

Details of the Work

I hereby agree to deposit the following item in the digital repository maintained by Bangor University and/or in any other repository authorized for use by Bangor University.

Author Name:……..

Title: ……..…….

Supervisor/Department: .....

Funding body (if any): .....

Qualification/Degree obtained:…… …….

This item is a product of my own research endeavours and is covered by the agreement below in which the item is referred to as "the Work". It is identical in content to that deposited in the Library, subject to point 4 below.

Non-exclusive Rights

Rights granted to the digital repository through this agreement are entirely non-exclusive. I am free to publish the Work in its present version or future versions elsewhere.

I agree that Bangor University may electronically store, copy or translate the Work to any approved medium or format for the purpose of future preservation and accessibility. Bangor University is not under any obligation to reproduce or display the Work in the same formats or resolutions in which it was originally deposited.

Bangor University Digital Repository

I understand that work deposited in the digital repository will be accessible to a wide variety of people and institutions, including automated agents and search engines via the World Wide Web.

I understand that once the Work is deposited, the item and its metadata may be incorporated into public access catalogues or services, national databases of electronic theses and dissertations such as the British Library's EThOS or any service provided by the National Library of Wales.

I understand that the Work may be made available via the National Library of Wales Online Electronic Theses Service under the declared terms and conditions of use (http://www.llgc.org.uk/index.php?id=4676). I agree that as part of this service the National Library of Wales may electronically store, copy or convert the Work to any approved medium or format for the purpose of future preservation and accessibility. The National Library of Wales is not under any obligation to reproduce or display the Work in the same formats or resolutions in which it was originally deposited.

<u>Statement 1</u>:

This work has not previously been accepted in substance for any degree and is not being concurrently submitted in candidature for any degree unless as agreed by the University for approved dual awards.

Signed …….. (candidate)

Date ……..

Statement 2:

This thesis is the result of my own investigations, except where otherwise stated. Where correction services have been used, the extent and nature of the correction is clearly marked in a footnote(s).

Other sources are acknowledged by footnotes giving explicit references. A bibliography is appended.

Signed ……. (candidate)

Date …….

Statement 3:

I hereby give consent for my thesis, if accepted, to be available for photocopying, for inter-library loan and for electronic repositories, and for the title and summary to be made available to outside organisations.

Signed ……. (candidate)

Date …….

NB: Candidates on whose behalf a bar on access has been approved by the Academic Registry should use the following version of **Statement 3:**

Statement 3 (bar):

I hereby give consent for my thesis, if accepted, to be available for photocopying, for inter-library loans and for electronic repositories after expiry of a bar on access.

Signed …… (candidate)

Date ……

Statement 4:

Choose **one** of the following options

a) I agree to deposit an electronic copy of my thesis (the Work) in the Bangor University (BU) Institutional Digital Repository, the British Library ETHOS system, and/or in any other repository authorized for use by Bangor University and where necessary have gained the required permissions for the use of third party material.	X

b) I agree to deposit an electronic copy of my thesis (the Work) in the Bangor University (BU) Institutional Digital Repository, the British Library ETHOS system, and/or in any other repository authorized for use by Bangor University when the approved **bar on access** has been lifted.	
c) I agree to submit my thesis (the Work) electronically via Bangor University's e-submission system, however I **opt-out** of the electronic deposit to the Bangor University (BU) Institutional Digital Repository, the British Library ETHOS system, and/or in any other repository authorized for use by Bangor University, due to lack of permissions for use of third party material.	

Options B should only be used if a bar on access has been approved by the University.

In addition to the above I also agree to the following:

1. That I am the author or have the authority of the author(s) to make this agreement and do hereby give Bangor University the right to make available the Work in the way described above.

2. That the electronic copy of the Work deposited in the digital repository and covered by this agreement, is identical in content to the paper copy of the Work deposited in the Bangor University Library, subject to point 4 below.

3. That I have exercised reasonable care to ensure that the Work is original and, to the best of my knowledge, does not breach any laws – including those relating to defamation, libel and copyright.

4. That I have, in instances where the intellectual property of other authors or copyright holders is included in the Work, and where appropriate, gained explicit permission for the inclusion of that material in the Work, and in the electronic form of the Work as accessed through the open access digital repository, *or* that I have identified and removed that material for which adequate and appropriate permission has not been obtained and which will be inaccessible via the digital repository.

5. That Bangor University does not hold any obligation to take legal action on behalf of the Depositor, or other rights holders, in the event of a breach of intellectual property rights, or any other right, in the material deposited.

6. That I will indemnify and keep indemnified Bangor University and the National Library of Wales from and against any loss, liability, claim or damage, including without limitation any related legal fees and court costs (on a full indemnity bases), related to any breach by myself of any term of this agreement.

Signature: ……

Date : …….

Acknowledgments

I am sincerely thankful to my supervisors Dr Vera Thoss and Dr Martina Lahmann for their support, guidance and valuable advice throughout the study. Without whom this work could not have been realised. I would also like to acknowledge the role of the following people and groups who helped at various stages of the study

Dr Mohammed Nur-e-Alam for introducing me to the principles of natural product chemistry.

Dr Anna Santoro and members of the Plant Chemistry Group for the useful discussions, friendly support and suggestions that helped shaping early ideas into research outcomes.

My research committee, Prof. Bela Paizs and Dr Chris Gwenin for their support and useful suggestions throughout the study.

The clerical and technical staff at School of Chemistry, especially Dr David Hughes, Shon Glyn Jones and Toby Vye for their help with technical NMR and chromatography problems.

Prof. Deri Tomos, Mr Barry Grail from the School of Biological Sciences in Bangor University and Dr Mark Long for their help and advice regarding MALDI-ToF analysis of fructans.

Rizgar Hassan, Victor Ebuele and Jason Fitzsimmons for their help with the seasonal plant sampling.

Dr Ana Winters and Dr Barbara Hauck from the Institute of Biological, Environmental and Rural Sciences (IBERS) in Aberystwyth University for their help in the analysis of bluebell phenolics.

Dr Ahmed Tawfike and Dr RuAngelie Edrada-Ebel from Strathclyde Institute of Pharmacy and Biomedical Sciences (SIBPS), University of Strathclyde, Glasgow for enabling the metabolomics analysis of bluebell seasonal samples. BBSRC High Value Chemical from Plants Network for training grant to undertake metabolomics analysis.

Dr Marc Bouillon for helping out with derivatisation of sugars for NMR-based structural analysis.

Dr Carol Clements (SIBPS), University of Strathclyde for biological activity screening using MRSA, *Klebsiella pneumonia, Trypanosoma brucei,* and *Mycobacterium marinum*.

Prof. Steve Kelly's Group, University of Swansea for biological activity screening using *Candida albicans* mutans.

Dr Diane Irvin, Syngenta, UK for assessing pesticidal activity.

Prof Karl Hoffman and Dr Helen Whiteland, IBERS, Aberystwyth University for assessing the antihelmintic activity of bluebell saponins funded through the National Research Network.

The Kurdish Regional Government for the support and financial funding that made this study possible.

Last, but not least, my family for their endless love and support that gave me strength to make it through the tough times.

Contents

Abbreviations

1-BuOH	1-Butanol
AcOH	Acetic acid
ADP	Adenosine diphosphate
ATP	Adenosine triphosphate
COSY	Correlation Spectroscopy
DAD	Diode array detector
DEPTQ	Distortionless Enhancement by Polarisation Transfer
DHAP	Dihydroxyacetone phosphate
DP	Degree of polymerisation
DW	Dry weight
ELSD	Evaporative light scattering detection
F	Fructose
FA	Formic acid
FC	Flash chromatography
FEH	Fructan exohydrolase
FFT	Fructan-fructan fructosyltransferase
FW	Fresh weight
G	Glucose
GF	Sucrose
HCl	Hydrochloric acid
HMBC	Heteronuclear Multiple-Bond Correlation
HMF	Hydroxymethylfurfural
HSQC	Heteronuclear Single Quantum Correlation
HSQC-TOCSY	Heteronuclear Single Quantum Correlation with additional Total Correlation Spectroscopy transfer
MALDI-ToF-MS	Matrix-assisted laser desorption/ionisation – Time of flight – mass spectrometry
MeCN	Acetonitrile
MeOH	Methanol
MRSA	Methicillin-Resistant Staphylococcus aureus
MWt	Molecular weight
NOESY	Nuclear Overhauser Effect Spectroscopy

NP	Normal phase
R_f	Retention factor
RP	Reverse phase
SEM	Standard error of the mean
SST	Sucrose-sucrose fructosyltransferase
TFA	Triflouroacetic acid
TLC	Thin layer chromatography
TMS	Trimethysilyl
TNC	Total non-structural carbohydrates
t_R	Retention time
UV	Ultraviolet

Abstract

Bluebell chemistry was investigated in order to identify factors contributing to the success and survival of the plant in a bluebell-bracken dominated ecosystem. The plant was divided into roots, bulbs, leaves, scapes and flowers and three classes of compounds (carbohydrates, phenolics and saponins) were studied and their seasonal changes were followed.

Total non-structural carbohydrates (TNC) were quantified after acid hydrolysis of the dried plant material and analysis of the reaction product by high performance liquid chromatography with diode array detection (HPLC-DAD). The bulbs contained the highest carbohydrate content compared to the other parts with TNC levels ranging from 36 – 82% of dry weight. Highest values in bulbs were reached around anthesis and remained high until the end of above ground growth. The lowest values were recorded during the underground growth phase before shoot emergence in March. The above ground parts showed low TNC contents at the start of their growth and higher values were reached during the active above ground growth. Mono- and disaccharides were studied using gas chromatography-mass spectrometry (GC-MS) after conversion into volatile oxime-trimethyl silyl derivatives. Fructose, glucose and sucrose were detected in this pool with fructose being the major sugar in the underground organs versus glucose in the above-ground parts. The bulbs showed significant increase in monosaccharides, especially fructose, during the early growth. Fructans were also investigated and their amounts were determined in the above and below ground organs following an enzymatic assay. The results showed a trend similar to the TNC especially in the bulbs. The fructan pool was further studied with matrix-assisted laser desorption ionisation – time of flight (MALDI-ToF) spectroscopy to determine the chain length of the polymer. This revealed that short chains <10 units are more commonly found with DP3 and DP4 being the most abundant oligomers. Higher chain lengths (up to DP20) was also found, but in much lower quantities. The main trisaccharide was isolated using flash chromatography and preparative TLC in reverse phase mode. Structural elucidation was achieved using 1D and 2D NMR spectroscopy of the free and peracetylated forms and the trisaccharide was identified as 1-kestose.

The phenolic profile of bluebell flowers, scapes and leaves was thoroughly studied using HPLC-UV and ESI-MS/MS analysis. The results showed that apigenin was the main flavone aglycone in the plant in addition to minor quantities of luteolin, eriodycteol and other unidentified aglycones. Phenolic acids including *p*-coumaric and ferulic acids were also detected. Both *O*- and *C*-glycosides were detected. The glycosidic moieties identified as

hexoses, pentoses, rhamnose and glucuronic acid. The methanolic extract of bluebell flowers was investigated and four new metabolites were isolated including two phenylalkyl glycosides (benzyl-O-β-D-glucopyranosyluronic acid-(1→2)-glucopyranoside DR1 and 2-phenylethyl-O-β-D-glucopyranosyluronic acid-(1→2)-glucopyranoside DR2) and two apigenin glycosides (7-[*O*-*β*-D-glucopuranosyl-(1→3)-*O*-*β*-D-xylopyranosyl-(1→6)-*O*-*β*-D-glucopyranosyl-(1→2)-*O*-*β*-D-glucglucopyranoside uronic acid-(1→)] apigenin (DR3) and 7-[*O*-*β*-D-xylopyranosyl-(1→6)-*O*-*β*-D-glucopyranosyl-(1→2)-*O*-*β*-D-glucglucopyranoside uronic acid-(1→)] apigenin (DR4)). The structural elucidation of these compounds was based on NMR, accurate mass and MS/MS analysis. Apigenin and *p*-coumaric acid were the only aglycones quantified after acid hydrolysis of the hydrolysed dried plant. The results showed that the two aglycones accumulated to a higher extent in the above ground organs with anthesis being characterised with an increase in content of both compounds to up to 15 and 0.5 mg. g^{-1} DM, respectively.

A previously unreported saponin, (3*β*-[(*O*-*β*-D-glucopyranosyl-(1→3)-*O*- *β*-D-glucopyranosyl-(1→3)-[*α*-L-rhamnopyranosyl-(1→2)]-*O*-*β*-D-glucopyranosyl-(1→2)-*O*-*α*-L-arabinopyranosyl-(1→6)-*O*-*β*-D-glucopyranosyl)oxy]-17,23-epoxy-28,29-dihydroxy-27-norlanost-8-en-24-one (DR1), was isolated from bluebell flowers using RP flash chromatography. The structure was elucidated with extensive 1D and 2D NMR, acid hydrolysis and GC-MS analysis of the sugars, accurate mass and MS/MS analysis. The isolated saponin was investigated for potential anti-trypanosomal, antimicrobial, antifungal, pesticidal and schistosomicidal activities. DR1 showed high biological activities against *Trypanosoma brucei* and *Schistosoma mansoni*. Crude fractions (aqueous and 1-butanol fractions of the methanolic extracts) from bluebell seeds were also investigated for schistosomicidal activities and found to show comparable results to DR1. The metabolomics approach and multivariate analysis approach was used in order to investigate the saponins and follow their seasonal changes. The seasonal samples of different plant parts were analysed with LC-MS in positive and negative modes. The resulting spectra were processed and the data produced were compared to databases for possible identification of metabolites. Multivariate analysis highlighted the difference between bulb metabolites from the above ground organs. The LC-MS spectra obtained and peak data used to study the changes in saponin contents between the different organs throughout the study period. The bulbs were found to contain the lowest amounts of total saponins (only about 20% of the other organs) with the highest ratios being in March-April at the start of the growth then decrease afterwards. Amongst the above-ground organs,

the flowers showed relatively higher contents. The LC-MS spectra from the metabolomics study were utilised in tentatively identifying a number of saponins. Two other metabolites were identified as steroidal aglycones from their HR-ESI-MS spectra. These metabolites were of 470 and 456 mass units and were characteristic of the bulbs.

Chapter summaries

Chapter 1: Introduction

This chapter highlights the aims of the study followed by a brief description of British bluebells. Aspects related to the plant's ecology were addressed including its geographical distribution, habitats and phenological phases are also explained. In addition to a review of the current knowledge about the chemistry of the plant.

Chapter 2: Carbohydrates in Bluebell Ecology

An introduction is given to the fructans as the main storage carbohydrate in the plant, their biosynthesis, ecological significance and methods of analysis. Different carbohydrate pools are investigated including total non-structural carbohydrates (TNC), mono- and disaccharides and fructans. The seasonal changes in each of the pools was determined in relation to the different phenological phases of the plant's life. The main trisaccharides in the plant was isolated and its structure was elucidated.

Chapter 3: Bluebell phenolics

An introduction is given to the main aspects of plant phenolics including biosynthesis, localisation, ecological significance and methods of their analysis. A complete investigation of the phenolic profile of the above-ground parts and isolation of 4 new compounds and their structural elucidation from the flowers. Quantification of apigenin and *p*-coumaric acid in different parts, their seasonal changes and ecological significance is discussed.

Chapter 4: Bluebell Saponins

General introduction to biosynthesis, localisation, ecological significance and techniques in the analysis of saponins. The metabolomics approach and multivariate analysis was used in general metabolite investigation and quantifying of the saponins. The seasonal changes in saponins in different bluebell parts were discussed in relation to changes in the plants phenology. LC-MS data was used in tentatively identifying saponins and steroid aglycones. Isolation and identification of the main flower saponin in addition to biological activity tests.

Chapter 1: Introduction

1.1. Aims of the study

The survival, success and dominance of a plant in a specific ecological niche is determined by the adequate employment of its physiological treats and chemical resources in response to different environmental stimuli. Such strategies may include:

1. Effective biomass production, storage and allocation to different organs.
2. Defence mechanisms against potential biotic threats (herbivores and pathogens).
3. Resistance against abiotic factors such as UV radiation, cold and heat stress through the accumulation of specific metabolites that can help control the osmotic pressure or modify cellular components to counteract the stress factor.
4. Sharing resources and competition with neighbouring plants often through affecting the availability of light and water or through the allelopathic effect of their chemicals on the establishment and growth of seedlings and availability of nutrients in the soil biosphere.
5. Strategies that guarantee the reproduction and continuation of the species via attraction of pollinators, production and spread of seeds.

The ecological success of a plant is additionally determined by the nature of these factors and the characteristic of the plant at different stages of its life.

The effect of availability of sunlight, nutrient supply, habitat and competition on British bluebell was studied by Blackman and Rutter in their paper series (1946 – 1950) in an investigation of the physiological and ecological aspects related to the plant's environment. Sunlight was identified as the limiting factor that influences the growth, function and uptake of N, P and K nutrients. The effect of competition from other plants reflected the amount of sunlight available for bluebell in the different habitats. Their work covered the effects of important factors on bluebell ecology and involved a detailed study of these factors, effects of their variation on the plant and their seasonal changes. Merryweather and Fitter (1995) studied the extent to which bluebells utilise mycorrhizal fungi in P acquisition and the allocation and seasonal changes of P and biomass in the plant. However, factors related to the biochemistry of the plant have received little attention even though they may be involved in the control of other ecosystem processes or affecting organisms nearby.

This work aims to investigate the chemistry of British bluebells and its relation to the ecological success of the plant through the following main steps:

- Identify and quantify the main reserve carbohydrate in the plant and study the quantitative and qualitative changes occurring at different phenological stages.
- Identify the main secondary metabolites as possible chemicals providing protection to the plant from biotic and abiotic factors and follow their seasonal changes.
- Investigation of the role of the secondary metabolites in plant protection. This is achieved by testing the biological activities of isolated secondary metabolites for potential applications against pathogens and also as candidates for drug discovery.

1.2. British bluebells

1.2.1. Nomenclature

British bluebells are currently known as *Hyacinthoides non-scripta* (L.) Chouard ex Rothm. (Rix 2004), but are also found in the literature under other synonyms with *Endymion non-scriptus* (L.) Garcke or *Scilla non-scripta* (Blackman and Rutter 1949; Knight 1964; WILSON 1959) used most often.

1.2.2. Description

The main parts of the plant are described in (Figure 1). The underground parts comprise a bulb and roots. The bulb is made up of 2-4 concentric tubes fused together. The roots are unbranched and rather thick and can grow up to 5 - 10 cm. Younger plants grow strong contractile roots in addition to those mentioned earlier to help the bulb descend further in the soil as the plant grows. Each plant has 4 - 6 linear, shiny, smooth leaves with acute tips, 20 – 45 cm long, and 0.7 - 2.5 cm wide. The leaves are upright and shiny during early growth of the plant, but become flaccid later towards the end of the season. The scapes are solitary and solid about 15 – 50 cm high. Racemes are unilateral (one-sided) with 4 – 16 flowers. Usually upright while young in the bud, but nodding as they mature. Flowers are made up of six perianth segments (petals), usually violet – blue, but rarely white. The petals meet at the base to form linear, tubular shaped bells, 1.3 – 2.0 cm long and about 0.4 cm wide with petal tips recurved out. Each flower contains six creamy – white anthers of unequal length (Blackman and Rutter 1954; Rix 2004).

Figure 1 *Hyacinthoides non-scripta* (British bluebell).

1.2.3. Geographical distribution and habitat

H. *non-scripta* is native to areas in north-west Europe including the British Isles, West of France and Spain, Belgium, The Netherlands and rarely in north-west Germany (Figure 2) (Blackman and Rutter 1954, Martyn Rix 2004, Michael Grundmann 2010).

The preferable soil type for the plant is low acidic (pH 4.5 – 5.0) and the plant is usually absent from areas of clay and flint. The bulbs can descend up to depths of 20 – 25 cm in light soils, this reduces to about 10 cm in heavier soils (Blackman and Rutter 1954; Knight 1964). The plant is found to be limited to areas where the average highest temperature is between 15 – 25 ^{o}C and the minimum during winter months is above freezing point. This reflects the sensitivity of the species to high temperature and drought during summer months as in areas around the Mediterranean basin. It also reflects its intolerance to longer periods of frost encountered in much of the continental Europe (THOMPSON and COX 1978).

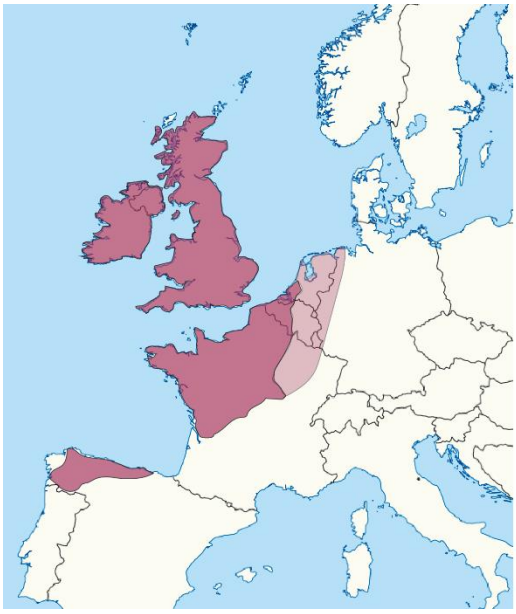

Figure 2 the geographical distribution of bluebells (*H. non-scripta*). The map is compiled based on maps and discerptions by (Blackman and Rutter 1954, Martin Rix 2004, Sebastian Van der Veken 2007, Michael Grundmann 2010). The lighter shade represent areas only described by (Blackman and Rutter 1954)

Bluebells are woodland species, but are also found on slopes, rock ledges and cliffs where they are protected from the effect of heavy grazing. In a deciduous woodland community (Figure 3 A), the plant exploits sunlight in early spring months, and most of the annual growth is achieved before the tree canopy is closed and light intensity decreases. This is reflected on the early flowering of bluebells in woodlands compared to open areas (Blackman and Rutter 1954). The open tree canopy can provide protection from heat loss during the cold nights in spring. Bluebells are sun plants, they are therefore either absent from coniferous woods or limited to the margins and edges (Knight 1964).

Bluebells are also found in south west of England and Wales accompanied by bracken (Figure 3 B). In fact, the rate of assimilation and hence the growth of bluebell in bracken communities is higher than it in woodlands. The co-existence of the two plants might be down to a number of factors including the fact that the active growth phase of bluebell is completed before the formation of bracken canopy which again means more availability and higher intensities of light during the growth time. Another factor is that their root systems are well adapted to the same type of soil. Additionally, the heavy shade cast by the bracken canopy will suppress the growth of other species and hence decrease competition on resources (Blackman and Rutter 1950).

A

B

Figure 3 A, British bluebells in a deciduous woodland and B, cohabiting a bracken community.

1.2.4. Phenology

The life cycle of the plant comprises a number of distinctive stages which have been described in detail by (Grabham and Packham 1983) and (Merryweather and Fitter 1995b) and summarised as follows:

Subterranean stage (September – late January):

Roots start to appear from the lower parts of the bulb in August and reach a considerable stage of development in winter. Around the same time, leaves also start their growth upwards in the soil. Leaf tips reach the surface soil in January where growth is held until February.

Active photosynthetic stage (February – May)

Leaves start a rapid growth and soon accumulate enough resources required for the growth of the new bulb (which is usually larger than the previous one) and flowering which starts in the following month. Previous year's leaf base in the bulb, which served as the main reserve over the winter, starts to become gelatinous in April and ready to be sloughed off.

Reproduction stage (April - June)

The rapid growth stage is followed a month later by flowering which extends to June. Fruit capsules are formed and seeds produced.

Senescence (June – July)

Leaves start to die in June and disappear completely towards the end of the month. Scapes and fruit capsules become desiccated, dried and ready to fall and disperse the seeds. Roots also disappear in preparation for dormancy. In June, and in addition to the aging process of the current year's tissues, flower initials start to form in the auxiliary buds inside the bulbs. These initials could be seen within the buds toward the end of the month, but the complete differentiation of the flower parts is not attained before September. For most of the time throughout the year, the bluebell bulb has two discs (stem bases). The base for the new bulb starts to form in August, the old bulb disk with the stem base from previous year will stay in the same bulb until they are shed in the next growth season in April. The bulbs therefore show one disc from only April to August- September.

Dormancy (July and August)

A period of no visible growth activity that extends until the emergence of new roots in August.

The start and duration of these stages might be slightly advanced or delayed between based on the habitat. Flowering may start in April in the south-west, but it could be delayed until June in areas like north-east Scotland.

1.2.5. Reproduction

Reproduction in bluebells could be either vegetative mostly through bulb division or sexual through seeds. (Knight 1964) placed the greatest responsibility in maintaining bluebell societies on the seeds. The same is concluded by (Grabham and packham 1983) whom upon comparison of bluebells in two sites, found that reproduction is mainly sexual, and vegetative reproduction is way less important. However, it was later found that vegetative reproduction can occur in bluebells at all ages, but this was observed when bulbs are planted individually rather than in crowded communities (Merryweather and Fitter 1995a).

1.3. Bluebell chemistry

Despite the wide spread of bluebell and its importance in the British natural heritage, their chemistry has not received much attention in comparison to other members of the same family. The current knowledge about the chemistry of the plant is limited to the three classes of compounds described below:

1.3.1. Sugars

The main polysaccharides present in the plant has been found to be fructan, a polymer of fructose. Bluebell bulbs were found to contain relatively high concentrations of 295.2 mg/g fresh weight as measured in July. Sucrose was also present as accompanying sugar of 13.8 mg/g fresh weight in the shoots (Brocklebank and Hendry 1989; Hendry 1987). A glucomannan was isolated from bluebell seeds consisting of glucose and mannose in 1:1.3 ratio. (Thompson and Jones 1964).

1.3.2. Bluebell oil

Bluebell seeds have been found containing oil at about 22-25% of dry weight. Detailed analysis of the oil revealed that it is made up of about 80% ω-9 monounsaturated (C18:1, C20:1 and C22:1), 10% ω-6,9 biunsaturated and 10% saturated fatty acids (Thoss et al. 2012). Minor oil ingredients have also been investigated. Steroids present were found to be primarily β-sitosterol followed by squalene, stigmasterol and camposterol in 132.6, 58.2, 34.3 and 12.5 mg/100g of oil. Tocopherols were also found in concentrations of 8.8, 44.5 and 38.2 mg/kg for α-, (β + γ)- and δ-tocopherols respectively (Mahmood 2013; Radine 2015).

1.3.3. Bluebell phenolics

The only reference to the phenolic compounds in the literature is related to delphinidine-based blue colour of the flowers. The pigment of bluebell flowers was identified as delphinidin-3-(6-*p*-coumarylglucoside)-5-(6-malonylglucoside) (Figure 4). The structural characterisation was based on using thin layer chromatography (TLC) and electrophoresis. Chemical treatments were also utilised including alkaline hydrolysis and H_2O_2 oxidation to help identify the acid and sugars moieties and their linkage positions. The identity of the isolated anthocyanin was confirmed by comparing its TLC behaviour in different solvents, NMR data and MS fragments with a previously identified compound from the flowers of *Commilina communis* with which the pigment was found to be identical (Goto et al. 1983; Takeda et al. 1986).

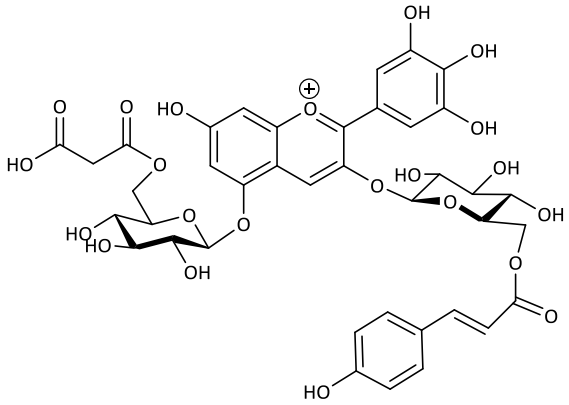

Delphinidin-3-(6-p-coumarylglucoside)-5-(6-malonylglucoside)

Figure 4 The anthocyanin identified as the blue-colour in bluebell flowers.

1.3.4. Iminosugars

Iminosugars are also known as polyhydroxy alkaloids and are sugar-resembling molecules that differ in that the endocyclic oxygen atom is replaced with nitrogen (Compain and Martin 2007). Early reports of iminosugars from bluebell were in 1997 when compounds 1 - 4 were isolated from bluebell leaves by (Watson et al. 1997). Further studies followed on the isolation of other iminosugars from bluebell (Kato et al. 1999) , on their therapeutic significance (Watson et al. 2001), and methods of their quantification (Egan et al. 1999). The major iminosugar found in bluebell is DMDP, followed by homoDMDP (Figure 5). The presence of iminosugars has been suggested as a possible reason behind cattle poisoning incidents when they graze on the plant (Watson et al. 1997). The fact that iminosugars are considered good candidates for future development of new therapies mainly due to their diverse structural parade and unique

biological and chemical characteristics (Horne et al. 2011; Nash et al. 2011) explains the interest in studying this class of compounds in bluebells.

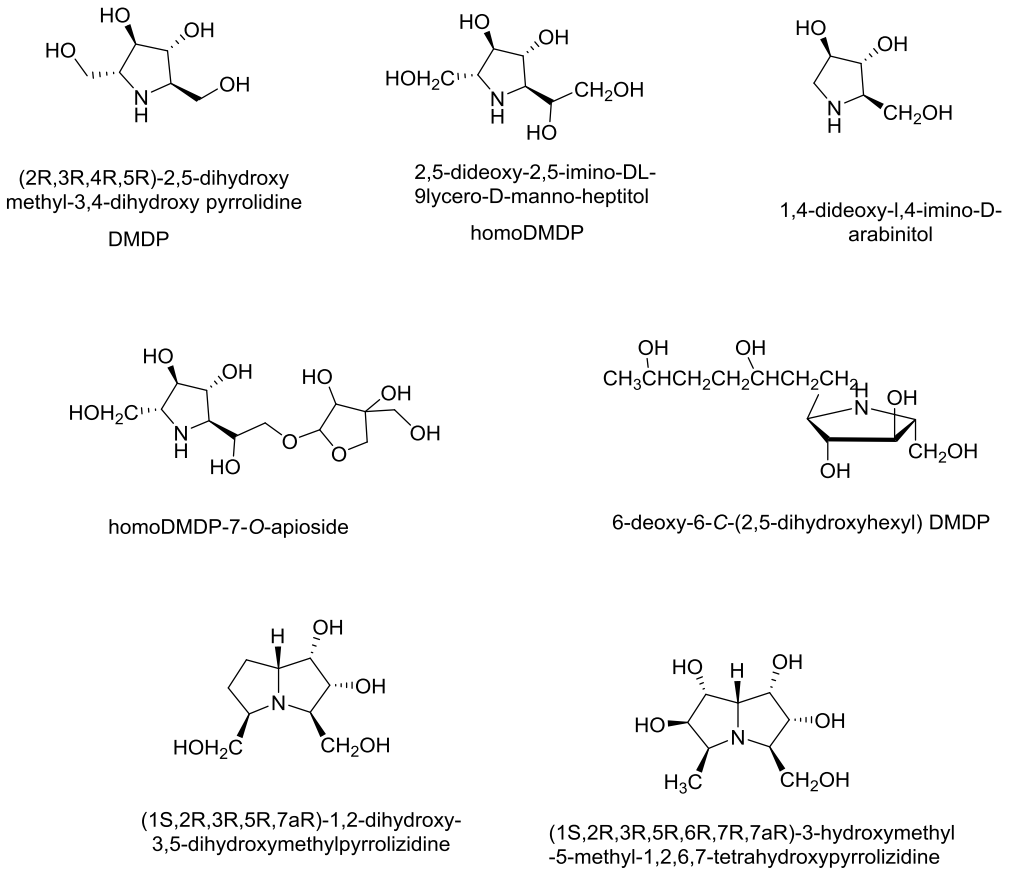

Figure 5 Iminosugars identified in bluebells (*H. non-scripta*)

Chapter 2: Carbohydrates in Bluebell Ecology

2.1. Introduction

2.1.1. Fructans in plants

Throughout their life-cycle, plants are challenged by various biotic and abiotic factors. Amongst these, competition from other plants, herbivory and environmental conditions such as temperature and availability of sunlight and water. The major factor limiting the start of different phenological phases of the plant's life is temperature (Halevy 1989; Kamenetsky et al. 2004). Changes in temperature at different times of the annual life cycle affect the onset and end of phenological stages such as dormancy or sprouting and re-growth. The response could be seen as direct simultaneous change and interconversion of carbohydrates (Risser and Cottam 1968). One successful survival strategy adapted by plants is the availability of secure reserves of carbohydrates represented by either starch or fructan in underground storage organs, such as rhizomes, tubers or bulbs. While starch or sucrose is most often stored, a smaller proportion of flowering plants (about 15%) are found to store fructans as their main reserve. These plants are distributed in different families many with economic significance including fodder crops and grasses, cereals (wheats and barley), food plants (onions, asparagus and lettuce) and ornamentals (tulips, hyacinths and narcissus) (Hendry and Wallace 1993b; Meier and Reid 1982). Bluebells belong to the smaller proportion of plants that store fructan as the main reserve carbohydrate. Bluebell bulbs have the capacity to accumulate large amounts of this polysaccharide reaching over 50% of dry weight. In fact, fructans were found to comprise 73% of the vacuolar carbohydrate concentration in the shoots with no significant presence of starch (Hendry 1987).

Besides being a source of carbon and energy during growth, fructans offer a number of other benefits. Vacuolar fructan synthesis lowers sucrose concentration in the cell and thus reduces osmotic pressure and prevents sugar-induced feedback inhibition of photosynthesis (Pollock 1986). Fructan accumulation has been linked to stress resistance. A geographical pattern could be drawn for the plants accumulating fructans including temperate zones with exposure to seasonal periods of drought or frost (Hendry and Wallace 1993a). When fructans and starch coexist in a plant it is found that starch is mainly consumed during growth while the fructan reserve undergoes much less change. This could be interpreted as that the plant mainly uses up the starch as a source for carbon and energy during re-sprouting and early growth, while

fructans can be involved in additional functions such as osmotic regulators and controlling water flux and in stress tolerance (Hendry and Wallace 1993a; Orthen 2001; Vijn and Smeekens 1999).

2.1.2. Fructan structure

Fructans are oligomers or polymers of fructose. They are synthesised from sucrose by the sequential addition of fructose units to give homologous series with wide structural diversity of linear and branched molecules (Edelman and Jefford 1968). Fructans are distinguished by their high water solubility, levo-rotation and non-reducing properties (Pollock 1986).

The basic structural unit of fructans commonly includes one glucosyl unit preserved from the starting sucrose molecule, but fructan molecules are also found where only fructosyl units are present (Ernst et al. 1996). Fructans are divided into five classes based on their structural variations (Livingston III et al. 2009; Meier and Reid 1982; Pollock and Chatterton 1988; Vijn and Smeekens 1999) which could be summarised below.

Inulin series

The simplest and best characterised plant fructans consisting of linear chains of (1→2) linked *β*-D-fructosyl units. The basic structure of this series could be represented as:

$$G\text{-}(1\rightarrow2)\text{-}[F\text{-}(1\rightarrow2)\text{-}F]_n\text{-}(1\rightarrow2)\text{-}F$$

Where G: glucose and F: fructose

The simplest fructan in this class is the trisaccharide 1-kestose (12Figure 6 A). It is found in sunflowers (*Helianthus tuberosus*) amongst other plants of the asterales order (Koops and Jonker 1996).

Levan series

In this series, adjacent fructosyl units are linked by *β*-(6→2) bonds as follows:

$$G\text{-}(1\rightarrow2)\text{-}[F\text{-}(6\rightarrow2)\text{-}F]_n\text{-}(6\rightarrow2)\text{-}F$$

Levan chains contain 6-kestose as their basic trisaccharide (Figure 6 B) and are mostly found in grasses within the poaceae family (Bonnett et al. 1997).

Mixed Levan

This type of fructan is found in wheat and is a variation of the levan series that contains both β-(1→2) and β-(6→2) linked fructosyl units (Bancal et al. 1992).

Inulin Neoseries

In the inulin neoseries, a glucose unit is linked to two fructosyl units at both C1 and C6 forming a neokestose molecule, the characteristic trisaccharide of this series. Fructosyl units are linked via β-(1→2) bonds to give inulin neoseries type fructans (Figure 6 C). A molecule in this series could be represented as follows:

$$F\text{-}(2\rightarrow1)\text{-}[F\text{-}(2\rightarrow1)\text{-}F]_m\text{-}(2\rightarrow 6)\text{- }G\text{-}(1\rightarrow2)\text{-}[F\text{-}(1\rightarrow2)\text{-}F]_n\text{-}(1\rightarrow2)\text{-}F$$

Fructooligosaccharides of this variety were found in *Asparagus officinalis* and onion (Shiomi 1981; Shiomi 1989)(Shiomi 1981)(Shiomi 1981).

Levan Neoseries

Similar to the inulin neoseries, the basic trisaccharide of this series is neokestose, but the linkages between fructosyl units are β-(6→2) instead of β-(1→2). This class of fructan is found in oats (Livingston et al. 1993).

Plants might contain more than one variety of fructans. For example, onions are found to contain both 1-kestose and neokestose trisaccharides (Darbyshire and Henry 1978; Fujishima et al. 2005).

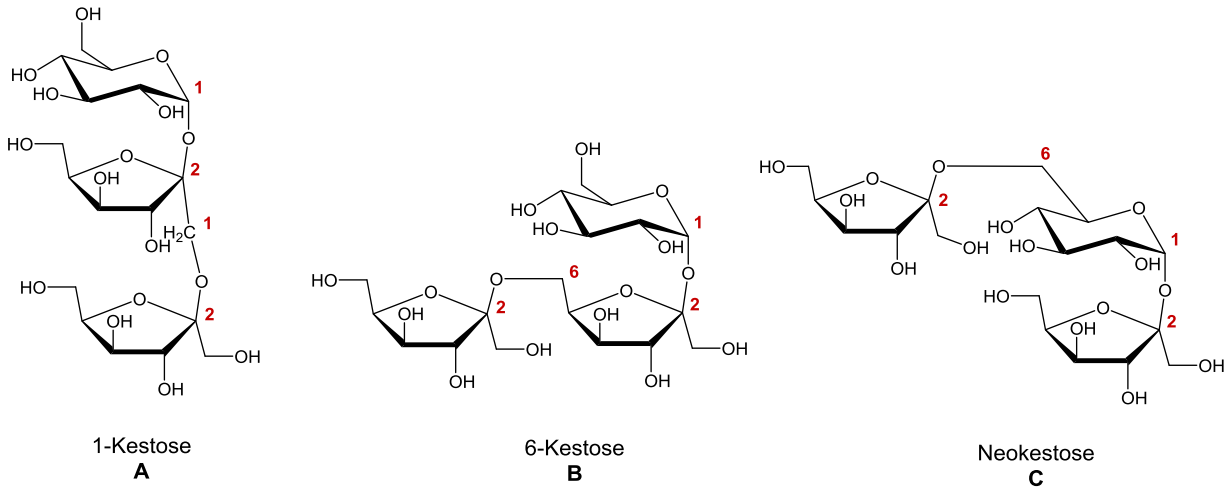

Figure 6 The three basic trisaccharides found in different fructan molecules. 1, Isokestose (or 1-kestose); 2, Kestose (or 6-kestose); 3, Neokestose.

2.1.3. Metabolism of fructans

2.1.3.1. Biosynthesis

Fructan biosynthesis takes place in the vacuole and two types of enzymes are involved in the process. The known model for the vacuolar biosynthesis and breakdown of fructans was first proposed by Edelman and Jefford (1968). It employs the involvement of two fructosyltransferases without the participation of sugar nucleotides or phosphorilation in the process. Although the model was originally proposed for the biosynthesis of fructans in tubers of *H. tuberosus* which consists principally of inulin type homologous series of fructooligosaccharides, it is widely applicable for other fructan types and in a wide range of plant systems. The first step in the biosynthesis of fructans is the reversible transfer of a fructosyl unit from a sucrose molecule to another by the action of the enzyme sucrose-sucrose fructosyltransferase (SST). The reaction leads to the formation of the trisaccharide 1-kestose and glucose (Figure 7). Sucrose is the primary substrate for fructan synthesis and the reaction is initiated only when a threshold concentration of the disaccharide is reached (Pollock 1984). The second stage of the reaction is chain elongation for which fructan-fructan fructosyltransferase (FFT) is the catalysing enzyme. This enzyme catalyses both chain elongation and shortening depending on the phenological stage of the plant's life (Figure 7 and Figure 8) (Pollock and Chatterton 1988). Enzymes catalysing biosynthesis of other fructan types have also been isolated. Asparagus and onion are found to contain an additional fructosyl transferase referred to as 6G-FFT. This enzyme catalyses the transformation of the fructose residue of 1-kestose to C6 of the glucose moiety producing neokestose. Continuous action of FFT on either ends of such trisaccharide produces fructans of the inulin neoseries (Shiomi 1989; Vijn et al. 1997).

2.1.3.2. Depolymerisation

The breakdown of fructan takes place either during translocation of temporary reserves in photosynthetic tissues or during re-sprouting in storage organs. The enzyme involved is known as fructan exohydrolase (FEH) and it catalyses the sequential removal of terminal fructosyl units (Figure 8). Free sucrose and fructose molecules thus produced are transferred to the cytoplasm where fructose is converted to sucrose and exported to growing vegetative organs (Edelman and Jefford 1968; Pollock 1986). Exohydrolases with specificity to different linkage types have also been isolated: a β-(1→2) - as well as a β-(2→6)-fructofuranosidase from

Jerusalem artichoke and *Lolium perenne* grasses respectively (Marx et al. 1997a; Marx et al. 1997b).

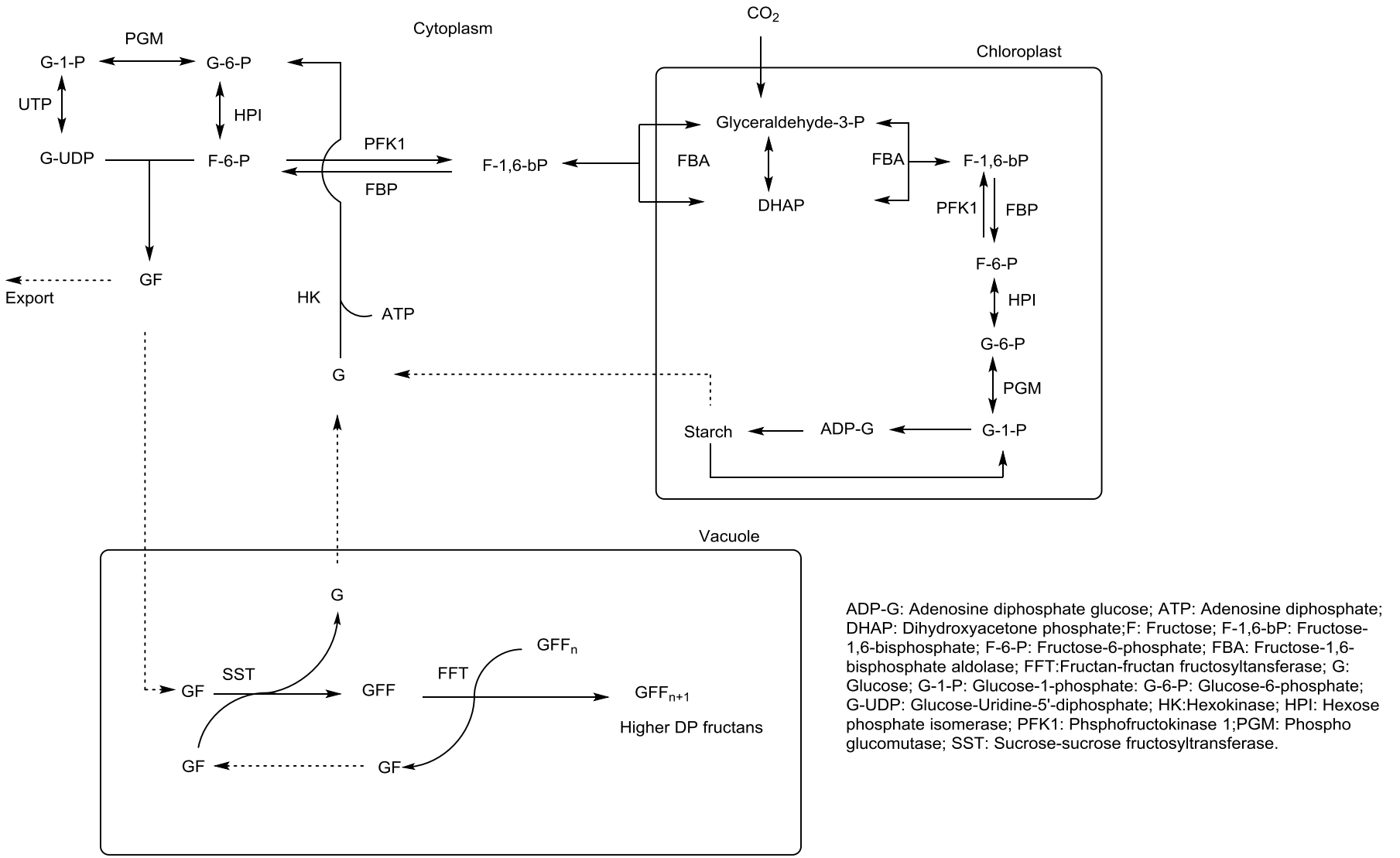

ADP-G: Adenosine diphosphate glucose; ATP: Adenosine diphosphate; DHAP: Dihydroxyacetone phosphate;F: Fructose; F-1,6-bP: Fructose-1,6-bisphosphate; F-6-P: Fructose-6-phosphate; FBA: Fructose-1,6-bisphosphate aldolase; FFT:Fructan-fructan fructosyltansferase; G: Glucose; G-1-P: Glucose-1-phosphate: G-6-P: Glucose-6-phosphate; G-UDP: Glucose-Uridine-5'-diphosphate; HK:Hexokinase; HPI: Hexose phosphate isomerase; PFK1: Phsphofructokinase 1;PGM: Phospho glucomutase; SST: Sucrose-sucrose fructosyltransferase.

Figure 7 The biosynthesis of fructans from sucrose. Adapted from (Edelman and Jefford 1968; Pollock and Chatterton 1988; Tarkowski and Van den Ende 2015).

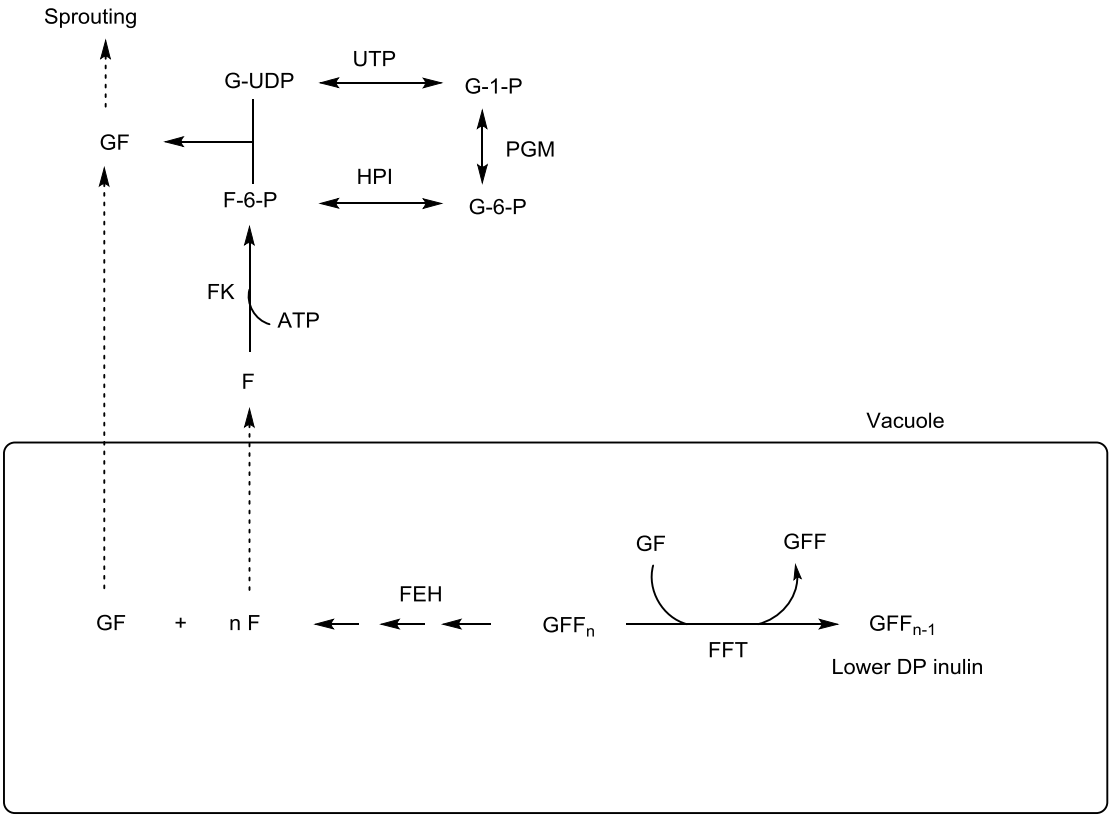

Figure 8 Fructans in storage organs. Chain shortening during cold winter months induced by the effect of FFT and depolymerisation by the action of fructan exohydrolase. Adapted from (Edelman and Jefford 1968; Pollock and Chatterton 1988; Tarkowski and Van den Ende 2015). Abbreviations are explained in Figure 7.

2.1.4. Ecological significance of fructans

2.1.4.1. Fructans in storage

Storage is defined broadly as resources that build up in the plant and can be mobilized in the future to support biosynthesis for growth and other plant functions (Chapin et al. 1990). Storage can be short-term (temporary) occurring usually in leaves due to high carbohydrate levels during photosynthesis. A triose phosphate molecule (glyceraldehyde-3-phosphate or dihydroxyacetone phosphate) produced during photosynthesis will either be converted into glucose or transferred to the cytoplasm in the form of fructose-1,6-bisphosphate (Figure 7). Glucose produced at this stage can be temporarily stored as starch in the chloroplast to be transferred later to the cytoplasm. Cytoplasmic hexoses can be utilised by the plant for building cellular components (fatty acids, proteins, phenolics, etc.) and to support growth and respiration or alternatively translocated to storage organs. In mature plants, a great proportion of the photosynthate is converted to sucrose and exported for storage. During active photosynthesis, the amount of sucrose produced can reach high levels. Fructan biosynthesis and the presence of a large storage compartment (the vacuole) in the photosynthetic tissue at

this stage provides a temporary sink that will prevent sugar induced feedback and ensures the continuation of photosynthesis. The accumulation of polysaccharides in the leaves is the result of supply from photosynthesis exceeding both cell's demand of sugars and export rate. The storage is temporary as the polysaccharides accumulated during the day are depolymerised and transported during the next dark period as indicated by the changes in enzyme activity of SST during day/night photoperiods (Wagner et al. 1986). However, fructans were found not to be subject to rapid daily turnover as in starch even when conditions inducing extensive mobilisation were applied. In an experiment on *Dactylis glomerata*, the plants were transferred to continuous darkness and extracts of leaf bases were harvested after different time intervals showing that fructan levels didn't decrease much for the first two days of darkness and 97% depletion was observed only after 4 days to be followed by 99.4% on the sixth day (Pollock 1982).

Long-term storage on the other hand, is usually associated with perennation (Edelman and Jefford 1968; Meier and Reid 1982). Perennials have the capacity to direct a large proportion of carbohydrates into their reserve organs (Rosnitschek-Schimmel 1983). Although this can diminish growth in the early stages of the plant's life, it can provide the plant with resources necessary for rapid early growth in the next season when the environmental conditions are still unfavourable for most annuals (Schulze 1982). Surveys of different plants have shown that despite that fructan accumulators are a minority compared to starch accumulators, they are the ones with the highest carbohydrate content in their reserve organs exceeding 50% and reaching over 70% of dry weight as in the case of bluebells. Most of these plants were also found to be active during cold seasons (late autumn, winter and early spring), better represented by the bulbous perennials (Brocklebank and Hendry 1989; Hendry and Wallace 1993b; Hendry 1987; Orthen 2001; Orthen and Wehrmeyer 2004). Brocklebank and Hendry (1989) investigated the storage carbohydrates in 20 species from the native and naturalised plants in Sheffield area. The plants were found to contain the main reserve carbohydrates: sucrose, starch and fructan most commonly present as combinations of two of the carbohydrates. Early growth was found to result in larger depletion of both fructose and starch reserves compared to fructan. In *Galanthus nivalis*, a bulbous perennial that stores both fructans and starch, Re-growth was accompanied by depletion of the starch content by more than 75%, whereas fructan consumption didn't exceed 40% during the same period (Orthen and Wehrmeyer 2004). These findings, in addition to the fact that fructan-accumulating plants share the characteristic of cold

season growth suggest that fructans contribute in other functions beyond being merely stored carbon reserves.

2.1.4.2. Fructans in cold hardiness and osmoregulation

The involvement of fructans in cold resistance or cryoprotection has been suggested repeatedly (Livingston III et al. 2009). They are found to be involved both directly and indirectly in the protection of plants during stress. Special characteristics of fructan molecules such as low crystallisation rate and relatively high water solubility enabled them to provide protection to the membrane from the damaging effects of freezing (Valluru and Van den Ende 2008). The first evidence for direct involvement was suggested by (Hincha et al. 2000) where they found that fructan but not starch stabilised liposomes during freeze –drying. This effect was further studied and the stabilisation was suggested to be due to the insertion of the fructan chains between the polar heads of phospholipid membranes (Vereyken et al. 2001). Despite their vacuolar location, fructans and FEH activity have been detected in the apoplast of plants under cold stress (Livingston and Henson 1998). A vesicle-mediated concept has been proposed by (Valluru et al. 2008) for the transport of fructans from the vacuoles to the apoplast for their subsequent participation in membrane stabilisation and cold stress protection.

Fructans also contribute indirectly to cold resistance via regulating the osmotic pressure of the cell. This is achieved via an increase in the concentration of soluble sugars and small molecular weight fructans that accompanies early growth. The high solute concentration at this stage facilitates uptake of water necessary for growth. The amount of water absorbed by the tissue is found to be directly proportional to the carbohydrate concentration as demonstrated in the inner scales of bulbous plants versus the low carbohydrate and water content in the outer ones (Darbyshire and Henry 1978; Orthen 2001). Water uptake is particularly important in plants undergoing growth via cell expansion rather than mitosis (Hendry 1987). The significance of osmotic potential in plants is not restricted to shoot growth. It is also the main contributor to flower petal expansion and opening (Le Roy et al. 2007) and to seed imbibition (Pollock and Lloyd 1994).

2.1.5. Carbohydrate analysis

2.1.5.1. Total non-structural carbohydrates (TNC) by acid hydrolysis

TNC is also known as total available carbohydrates and refers to all the carbohydrates available for use by the plant as energy sources or material for building other components. This includes mono- and disaccharides as well as polymeric starch and fructan. Structural components such

as cellulose and hemicellulose are not included in TNCs as they are not utilised by the plant in the same way. Evaluation of TNC levels of perennial (or biennial) plants is useful in determining periods of biosynthesis, storage and consumption of reserves. It also gives an insight into the plant's potential for regrowth in the new season.

TNC analysis commonly involves the hydrolysis of the carbohydrates into monosaccharides either enzymatically or by the effect of an acid. In most of the cases, the hydrolysed sugars are converted into furfurals which are then determined spectrophotometrically either with or without coupling to phenolic compounds used as colour-developing agents (Smith et al. 1964; Steele et al. 1984; Weinmann 1947; Zappala et al. 2005). HPLC has also been applied for the analysis of furfurals, and it was found to give high recoveries and better specificity compared to the colorimetric methods. Furthermore, it obviates the need of hazardous chemicals used in preparing the colour-developing reagents (Lee et al. 1986; Porretta and Sandei 1991).

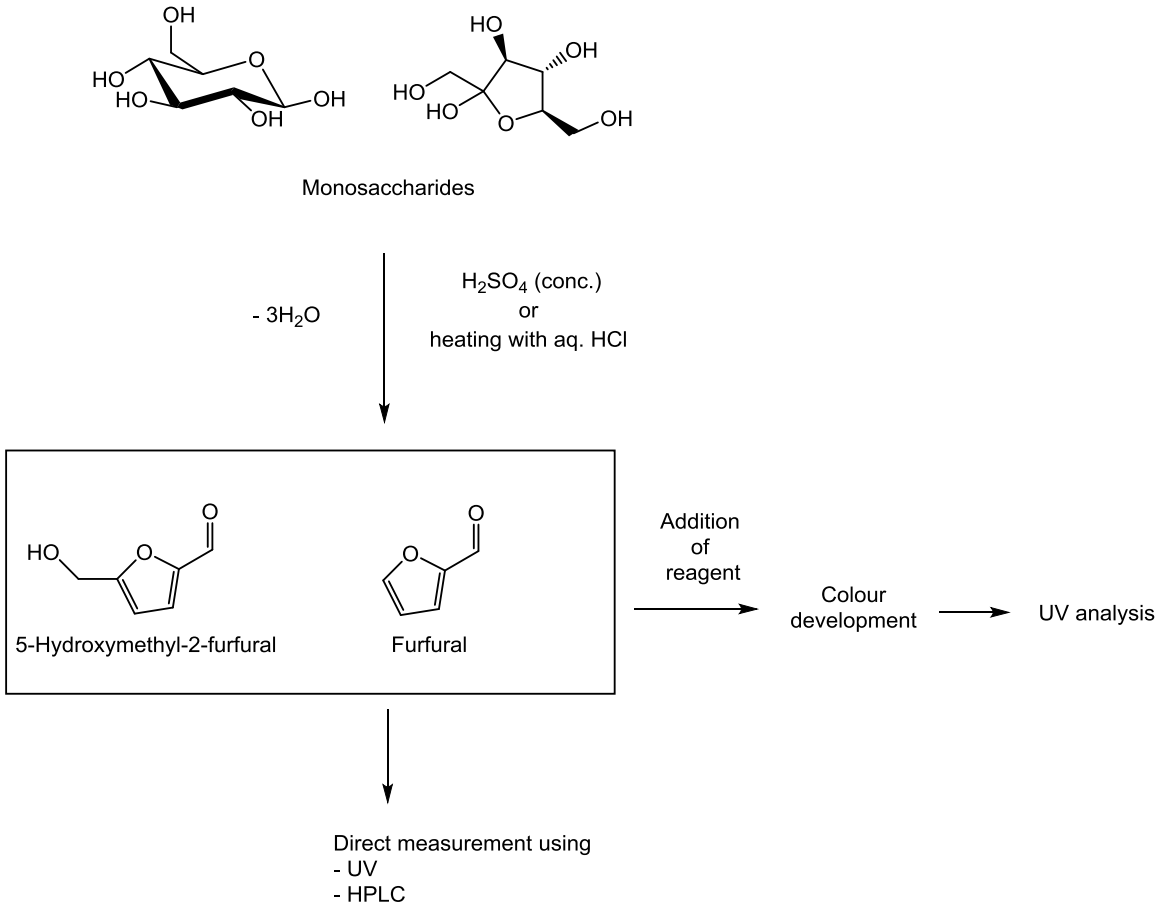

Figure 9 Outline of the principle of TNC analysis. The key step is the formation of furfurals which could then be quantified either colorimetrically or using HPLC.

2.1.5.2. Gas chromatography-mass spectrometry (GC-MS) analysis of mono- and disaccharides

Gas chromatography is a common and powerful tool in the analysis of mono and disaccharides. The analysis however, is not direct and derivatisation is required in order to convert the sugar molecule into a thermally stable and more volatile one. Derivatives include acetyl, silyl, oxime-trimethyl silyl, etc (Ruiz-Matute et al. 2011). Trimethylsilylation described by (Sweeley et al. 1963) is commonly used since the reaction is quick, sensitive and does not require high temperatures. The introduction of an oximation step prior to silylation is found to simplify the chromatogram by decreasing the number of peaks obtained for each sugar to 2 (syn and anti isomers) as opposed to several peaks (up to 6 for hexoses) when no oximation is used. Besides, the reaction products are comparably more stable and the method is applicable in general to both aldoses and ketoses (Molnár-Perl 2000; Ruiz-Matute et al. 2011). The routine approach for sugars analysis involves extracting the sample with either water, alcohol or aqueous alcoholic solutions. However, adding the reagents directly to the plant sample (Long and Chism, 1987 and Streeter and Strimbu 1998) has proven to be as efficient as the routine methods, yet quicker, less laborious and doesn't require lengthy solvent extractions.

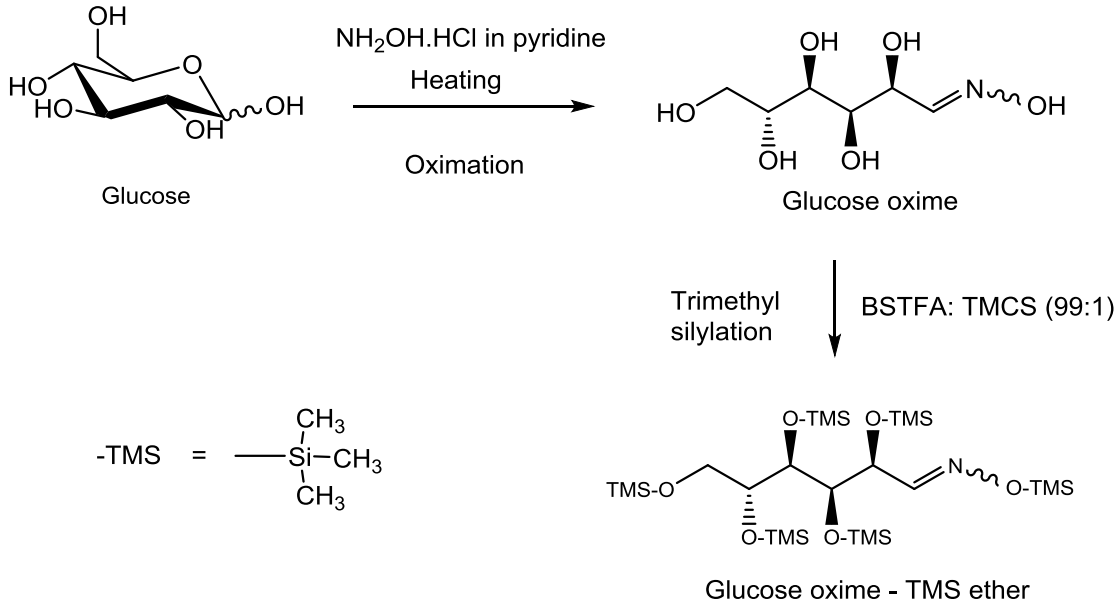

Figure 10 Oximation – silylation of mono- and disaccharides in preparation for analysis with GC-MS exemplified by a glucose molecule.

2.1.5.3. Matrix-assisted laser desorption/ionisation – Time of flight – mass spectrometry (MALDI-ToF-MS)

MALDI-ToF mass spectrometry is widely applicable for the analysis of biopolymers such as carohydrates and proteins with molecular mass lower than 50000 Da. The technique is based on desorption and ionisation induced by laser radiation energy of wavelength (260 - 350 nm or higher). Analytes are usually crystallised with excessive amounts of matrix. Since the process of ionisation is rather mild, intact molecules are usually detected by the ToF-MS detector rather than fragment ions (Hillenkamp et al. 1991; Pieles et al. 1993). MALDI-ToF is a sensitive, quick method and highly tolerant to impurities. The technique has been applied to crude extracts and plant tissues thus saving time and efforts often required for analyte purification. However, analytes of molecular weights higher than 10000 Da often give rise to poorly resolved mass peaks with low signal/ noise ratio compared to smaller molecules. This is mainly due to the difficulty in evaporating larger molecules. Additional limitations include the impossibility of distinguishing between isomeric saccharides having the same molecular mass. Furthermore the formation of adducts with potassium and sodium leading to multiple peaks per molecule and thus complicating the analysis (Harvey 2003; Harvey 1993; Stahl et al. 1997). The choice of the matrix is an important parameter in the analysis. Matrix compounds facilitate the ionisation process by absorbing the radiation energy and transferring it to the analyte molecule. The choice of a matrix for particular analysis is a process based on trial and error. Nonetheless, the choice lies among a list of compounds commonly used as matrices. Matrix compounds are often acidic and acting as proton donors in the ionisation process. The presence of conjugated double bonds in the compound help stabilising the ionised molecule. Acidic compounds as cinnamic, nicotinic and hydroxybenzoic acid derivatives, neutral molecules such as trihydroxyacetophenone and anthracene-based structures, and basic pyridine and pyrimidine related compounds are some of the most common matries (Fitzgerald et al. 1993; Harvey 2015; Harvey 1993; Hillenkamp et al. 1991; Zenobi and Knochenmuss 1998).

2.2. Methods

2.2.1. Materials and general methods

This section includes chemicals, some general techniques and instrumentation that apply to work common in this as well as the following chapters. Other experimental conditions that are more specific to a particular experiment are covered in their relevant sections.

2.2.1.1. Solvents and Chemical standards

Formic acid, HCl (both analytical reagent grade), and methanol, acetonitrile, hexane and water (HPLC grade) were purchased form Fisher Chemical, UK. 1-Kestose ≥99%, pyridine 99.8%, fucose ≥99%, glucose ≥99.5%, fructose ≥99%, sucrose ≥99.5% and hydroxylamine hydrochloride 99% (reagent plus grade) were from Sigma-Aldrich. The silylation reagent N,O-bis(trimethylsilyl) trifluoroacetamide: trimethylchlorosilane (BSTFA: TMCS (99:1)) from Supelco. Ethyl palmitate ≥95% from SAFC, USA. *p*-Coumaric acid was purchased from Lancaster Synthase. Apigenin, Methylapigenin-7-O-β-D-glucuronate and apigenin 7-O-β-D-glucuronic acid isolated from the flower extract were used as standards. Diaion HP20 gel was from Supelco. Silica gel 60 A for Normal phase (NP) chromatography was from Merck.

2.2.1.2. Mass spectrometry (MS)

High resolution mass for the isolated compounds was obtained using a Finnigan Surveyor PDA system coupled to Thermo-Finnigan LTQ Orbitrap (Thermo Scientific, Germany).

2.2.1.3. Nuclear magnetic spectroscopy (NMR)

NMR spectra were recorded on a Bruker Avance (400 or 500 MHz) spectrometer. For each compound a set of experiments were run including ^{1}H, ^{13}C, COSY, HSQC, HMBC, and HSQC-TOCSY NMR. Occasionally NOESY was also run. The obtained spectra were referenced using the internal signal from the solvent used. Deuterated solvents (D_2O, MeOD, pyridine-D_5) from Cambridge Isotope Laboratories, Inc. were used.

2.2.1.4. Automated flash chromatography

Automated flash chromatography was carried out using Reveleris automated flash system where the chromatographic run was monitored with both evaporative light scattering detector (ELSD) and UV. The columns used for automated chromatographic separation were 12 g Reveleris C18 columns. Flow rate of 18 mL. min^{-1} and the default fraction volume of 25 mL

was applied for all separations employing the Reveleris flash system. At the end of every chromatographic run (both FC and HPLC), the gradient was taken to 100% of the stronger solvent and held for 2-3 min to wash off the column, then again over 2-3 min to 100% of the weaker solvent with 2-3 min hold at the end of the run.

2.2.1.5. Thin layer chromatography (TLC)

NP TLC was carried out on precoated E. Merck TLC silica gel 60 F_{254} glass plates and reverse phase RP TLC on RP-18, F_{254}. The plates were visualised under UV lamp or using phosphomolybdic acid when the compounds were not UV-active.

2.2.1.6. Sample collection and pre-treatment

Bluebell plants were collected in an area located at 250 m above sea level in the Snowdonia National Park (Llanberis, United Kingdom). The site is classified as rough grazing for agricultural purposes, and falls under the upland vegetation type U20a (Pteridium aquilinum-Gallium saxatile community U20, Anthoxanthum odoratum sub-community U20a) and it is typical for an area where farmed lowlands adjoin the unenclosed uplands with well-drained and infertile soils (Figure 11). On the site a grid was applied measuring approximately 40 x 25 m and divided in 144 quadrants. Samples were collected from March 2014-July 2015. At each sampling occasion, alternate quadrants were sampled in duplicate by using a stainless steel (5 mm thick) square hollow section measuring 20 cm by 20 cm wide and 30 cm long. Sample collection followed the plant's growth pattern and thus weekly from leaf emergence to end of flowering (March- June), fortnightly after seed ripening until dormancy (June- October) and once every 6 weeks throughout the winter then once every three weeks until shoot emergence in March. From March to July plants were samples more or less fortnightly. Samples were collected always at the same time during the day, between 9:00 am and 11:00 am, in order to minimise the effect of diurnal variation.

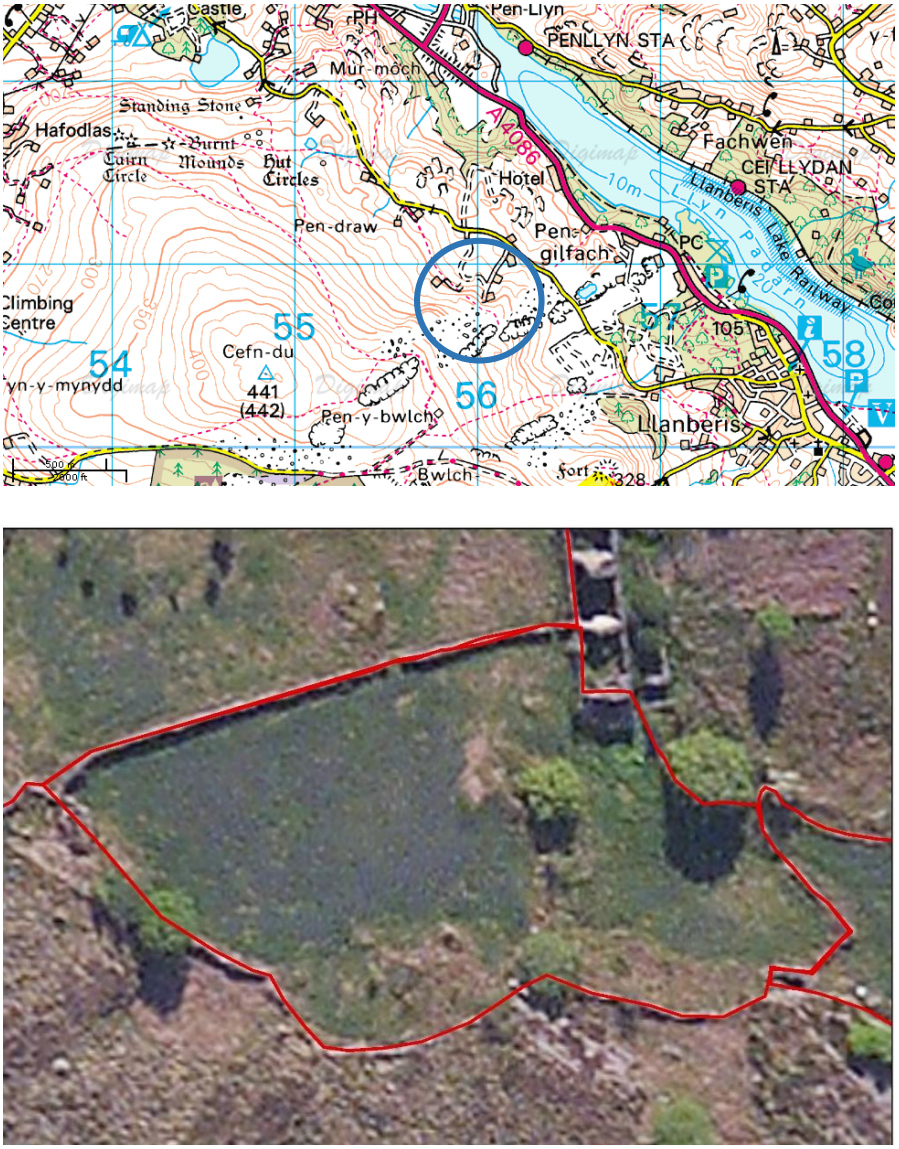

Figure 11 A, Sampling site location and B, aerial view of the sampling site with bluebell flowers visible as a purple hue.

In the laboratory, the bluebell plants were separated from the rest of the core, washed with deionised water to remove dirt and soil. The plants were then divided into roots, bulbs, leaves, scapes and flowers for total non-structural carbohydrate (TNC) analysis (Figure 12) or divided into shoots (leaves, scapes and flowers) and bulbs (bulbs and roots) for mono-, di-saccharides and fructan analysis. Samples were then freeze-dried using (CHRIST® Alpha 1-2 LD plus) freeze-dryer connected to (Vaccubrand, Germany) vacuum pump. The difference between fresh weight (FW) and dry weight (DW) was used to calculate the percentage of dry matter content (DW %) as in Equation 1. The freeze-dried samples were finally ground into a fine powder using a porcelain mortar and stored at -20 °C until further analysis. Samples collected from mid-May to the end of above-ground phase were ground using a (Retsch cyclone mill)

and passed through a 1 mm sieve since the lignification of the above ground parts and the formation of hard seed at the later stages made the use of a mortar and pestle impractical. The number of bulbs were counted for every sampling occasion by only taking bulbs with diameter above 8 mm and this number was considered as the number of plants per sample. The weights of different parts were divided by the number of bulbs in order to determine their weights per plant and the results were used in calculations on fresh plant basis. Leaf and scape heights were calculated (scapes heights including the flowers) by averaging 15 measurements in each core.

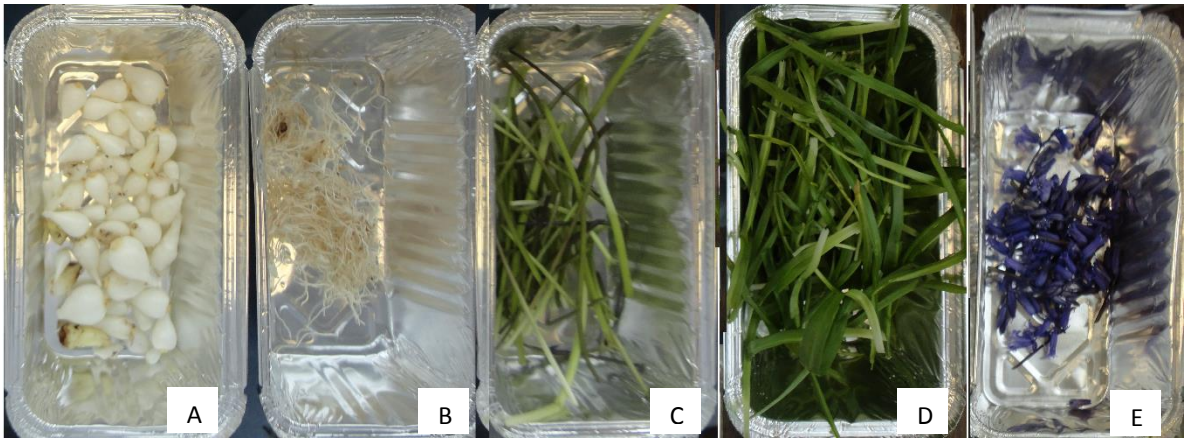

Figure 12 Separation of the plant into A, bulbs; B, roots; C, scapes; D, leaves and E, flowers.

Samples collected in 2015 comprised of one core per sampling occasion, and the plants were divided into two parts: shoots and bulbs with shoots collectively referring to leaves, scapes and flowers and bulbs composed of the underground parts (roots and bulbs).

$$DW\% = \left[1 - \left(\frac{FW - DW}{FW}\right)\right] \times 100 \qquad (1)$$

In addition to the seasonal sample collection, bluebell bulbs were harvested in August 2013 for isolation and NMR analysis of the main trisaccharide. Flowers were collected in May 2014 for the isolation of secondary metabolites.

2.2.2. Total non-structural carbohydrates (TNC)

All plant parts were analysed in duplicate for total hydrolysable carbohydrates (for 2014: 2 samples were taken one from each core and each analysed in triplicates; 2015: one sample per core analysed in duplicate). An amount of 20 mg of powdered freeze-dried sample was placed in a 25 mL glass vial and hydrolysed by adding 5 mL of 2 M HCl prepared in 50% MeOH. The

vials were screw-capped and heated on a block heater (Stuart, SBH130D/3) at 95 °C for 2 h. The reaction mixture was then filtered (Qualitative filter papers, Fisherbrand) and made up to 10 mL with 50% MeOH. Carbohydrate content was measured as hydroxymethylfurfurals (HMF) after injecting (20 µL) into a Dionex UltiMate 3000 High Performance Liquid Chromatography system equipped with a UV-VIS diode array variable wavelength detector utilising Chromeleon7 software for system operation and data analysis. The column used was Intersil ODS-3 column (5 µm, 4.6 mm x 150 mm). A gradient elution was applied using water and Acetonitrile (MeCN) both acidified with 0.1% formic acid (FA) from 0 to 100% MeCN in 35 min. Samples were analysed at 280 nm for this experiment. Additional higher wavelengths were used for phenolic acid and flavonoids in the same samples. The sum of areas of peaks 1 and 2 (Figure 13) were used in calculations. A series of 1-kestose solutions with concentrations ranging from 0.125 – 2.0 mg. mL^{-1} were hydrolysed under the same conditions and used to construct the calibration curve, y = 0.0023x, R^2 = 0.9833. The calculated amounts were converted from mg. mL^{-1} to mg. g^{-1} DW basis as follows:

$$C\ (mg.g^{-1}\ DW) = C\ (mg.mL^{-1}) \times 500 \qquad (2)$$

Where,

500 = the original 20 mg of dried and powdered sample was made up to 10 mL at the end which is equivalent to 2 mg of sample in every mL. By multiplying this by a factor of 500, the obtained quantity should represent the content per g DW.

Calculations to convert the calculated amounts from per g DW to per fresh plant part basis were done as follows:

$$C\ (mg.fresh\ plant\ part^{-1}) = C\ (mg.g^{-1}\ DW) \times DW\%\ (g\ DW.100\ g^{-1}\ FW) \times nFW(g\ FW.fresh\ plant\ part^{-1})\ /100 \qquad (3)$$

Where,

nFW = normalised fresh weight calculated by dividing the total fresh weight of a particular part of the plant by the number of bulbs in the sample core

100 = A factor to reduce the 100 in the DW%

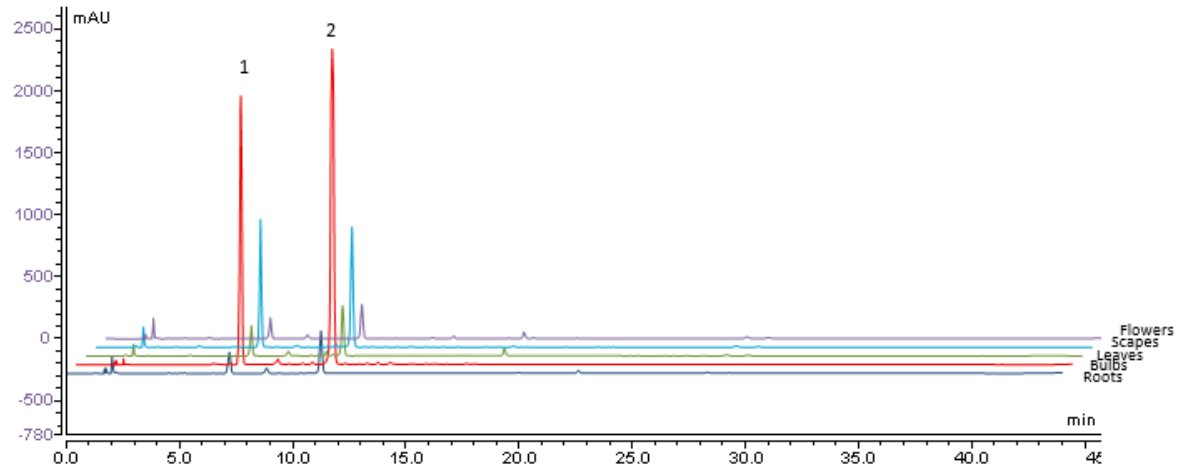

Figure 13 HPLC chromatogram of the acid hydrolysis products of the different parts of bluebell at 280 nm. The sum of areas of peaks 1 and 2 is equivalent to total hydroxymethyl furfulas produced during the reaction.

2.2.3. GC-MS analysis of mono- and disaccharides

Mono and disaccharides were analysed following the methods (Rojas-Escudero et al. 2004) and (Streeter and Strimbu 1998). The method was optimised for bluebell samples in terms of initial sample processing and preparation, reaction time and temperature and finally the extraction and clean-up of the product. Table 1 shows the optimised parameters and the conditions tested. In this analysis, mono- and disaccharides were converted into oxime-trimethyl silyl ethers and analysed by Gas Chromatography Mass Spectrometry (GC-MS).

Duplicate samples of 5 mg of freeze-dried powdered bulb were mixed in 2 mL glass vials with 100 µL of dry pyridine containing 0.5 mg. mL^{-1} of fucose as procedural standard, followed by 100 µL of a solution of 50 mg. mL^{-1} of $NH_2OH{\cdot}HCl$ in dry pyridine. The vials were heated on a block heater at 60 ºC for 3 h with occasional gentle mixing and then left to cool to room temperature (~ 20 ºC) before 100 µL of BSTFA: TMCS (99:1) was added. The resulting solution was left to react at room temperature for 30 min. Thereafter the reaction product was extracted by adding 1000 µL of hexane containing 0.1 mg mL^{-1} of ethyl palmitate as internal standard, vortex-mixed for 1 min then 300 µL de-ionised water was added to wash off inorganic salts and decompose any excess unreacted reagents. The solution was vortex-mixed for another minute and submitted for GC-MS analysis.

The GC-MS instrument used in this study was a Thermo Scientific 1300 Chromatograph equipped with a TRIPLUS RSH autosampler and an ITQ 900 MS detector. The sample was injected onto a TR-5 column (30 m x 0.25 mm ID x 0.25 µm). The following instrumental parameters were used: inlet temperature 250 °C, split flow 30 $mL.min^{-1}$, split ratio 20 and

helium was used as carrier gas with flow rate of 1.5 mL.min^{-1}. The temperature program started at 172 °C, with a 1 min hold, then increased at 10 °C.min^{-1} up to 210 °C, held for 1 min then increased at 20 °C.min^{-1} up to 220 °C, held for 1 min, then a final ramp of 10 °C. min^{-1} to 280 °C with 1.5 min hold at the end. As the sample vials contained both organic (hexane) and aqueous layers, the injector needle was set to draw 1.0 µL sample at a depth of 17 mm from the vial cap in order to avoid reaching the aqueous layer. Figure 14 shows chromatogram obtained using this method. Peaks were identified by comparison with reference compounds. The calibration standards used were glucose (0.005 – 0.1 mg.mL^{-1}), y = 0.0318x, R^2 = 0.9892; fructose (0.025 – 0.5 mg.mL^{-1}), y = 60.9348x, R^2 = 0.9915 and sucrose (0.0125 – 0.25 mg.mL^{-1}), y=0.0175x, R^2 = 0.9899. Relative response (area of peak/area of internal standard) was used in constructing the calibration curve and calculating analyte concentrations. The calculated amounts were converted from mg. mL^{-1} to mg. g^{-1} DW basis as follows:

$$C\ (mg.g^{-1}\ DW) = C\ \ (mg.mL^{-1}\ ) \times 200 \qquad (4)$$

Where,

200 = the original 5 mg of dried and powdered sample was made up to 1 mL at the end. By multiplying this by a factor of 200, the obtained quantity should represent the content per g DW.

The formula in Equation (3) was used in order to convert the calculated amounts from per g DW to per fresh plant part basis.

Table 1 Method optimisation for GC-MS analysis. The table shows different parameters and conditions tested with the optimum conditions in bold typeface.

Parameters	**Conditions tested**
Oximation reaction	Temp.: 20, 40, 50, **60**, 80, 100 (°C) time : 15, 30, 45, 60, 90, **120** (min)
Silylation reaction	Temp.: **20**, 40, 50, 60, 80 (°C) time : 15, **30**, 45, 60, 90, 120 (min) reagent volume: 25, 50, 75, **100**, 150 (µL)
Sample preparation and homogenisation	Oven drying, **freeze-drying**, grinding with liq N_2 , Ultra Turrax blending
Extraction method	Water, ethanol and **matrix (no solvent)**
Reaction solvent	**Pyridine**, aniline
Silylation reagent used	**BSTFA: TMCS (99:1)**, HMDS: TMCS (3:1), TMSI
GC column	**TR-5** , chiral column (DEX β120)

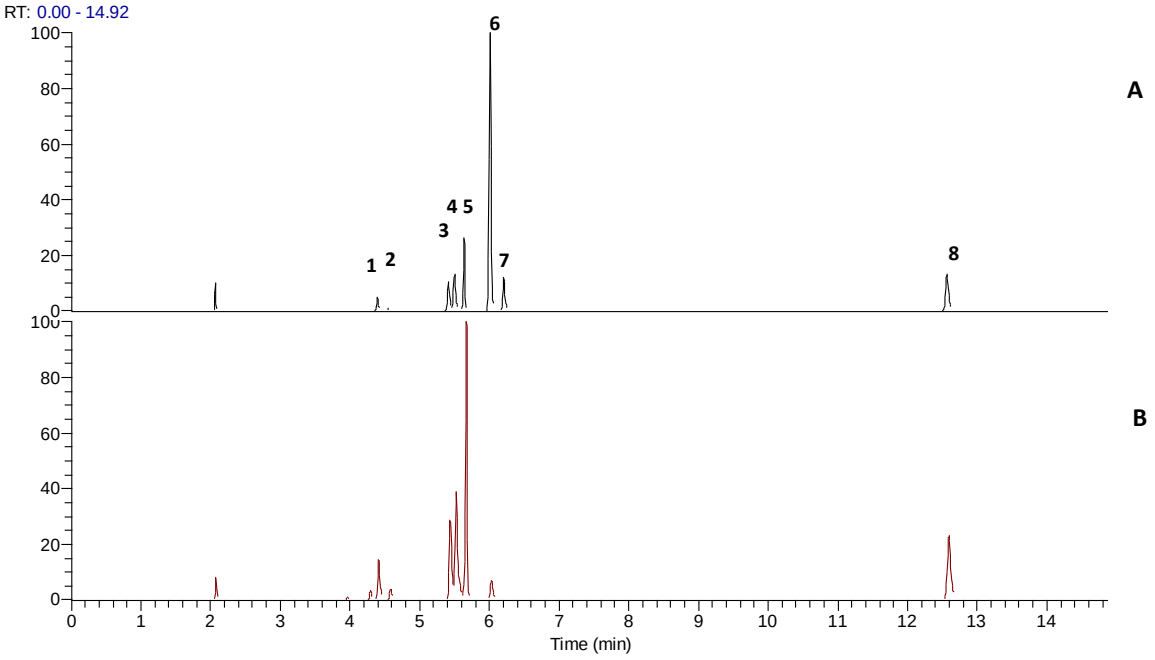

Figure 14 GC-MS chromatogram for A, bluebell leaf and B, bluebell bulb samples collected in 01/05/2014. Different compounds are detected as oxime-trimethylsilyl (TMS) ethers, TMS ethers or esters. 1,2: fucose oxime-TMS ether; 3,4: fructose oxime-TMS ether; 5: ethyl palmitate; 6,7: glucose oxime-TMS ether and 8: sucrose TMS ether.

2.2.4. Analysis of fructans

2.2.4.1. Quantification using enzymatic assay

In order to analyse fructans, Duplicate 20 mg aliquots of freeze-dried powdered bluebell bulbs and leaves were mixed with 8 mL of hot deionised water, stirred and heated at 80 ^{o}C for 15 min. The solution was allowed to cool to room temperature and made up to 10 mL with distilled water. Aliquots of 1 mL were centrifuged at 6000 rpm for 5 min and the clear supernatant was used in the analysis. The analysis of fructans was performed using a fructan HK enzyme kit (Megazyme International, Ireland). An aliquot of 20 µL of the sample was incubated with 20 µL of sucrase/maltase enzyme mixture in order to allow hydrolysis of sucrose and low DP maltosaccharides (if present) into glucose and fructose. After incubation, 50 µL of 100 mM sodium acetate buffer solution (pH 4.5) was added and vortex-mixed. The resulting mixture was denoted solution A. Two 20 µL aliquots were taken from this solution and transferred into two wells of a 96-well quartz microplate (Falcon, UK). Ten microliters of fructanase and indo-inulinase mixture was added to the first and 10 µL of buffer pH 4.5 solution to the second. The microplate was wrapped in cling film and incubated in an oven at 40 ^{o}C for 30 min so as to assist the hydrolysis of fructans into glucose and fructose. After the incubation period, 200 µL of de-ionised water, 20 µL of buffer pH 7.6 and 10 µL of $NADP^{+}$/ATP were added to both

aliquots. The absorbance of the plate was recorded after 3-5 min (A1), then the reaction was started by adding 10 µL of a mixture of hexokinase, phosphoglucose isomerase and glucose-6-phosphate dehydrogenase (HK/PGI/G-6-PDH) previously diluted 1:4 with a buffer solution (pH 7.6) on the day of analysis and kept in ice. The plate was left to stand at room temperature for 15 min and the absorbance was then recorded (A2). The sample absorbances (A1 and A2) at 340 nm wavelength was recorded using (BioTek PowerWaveTM XS) Microplate Spectrometer operated by Gen5 software. Pathlenghth correction was applied during the analysis to correct for the solution depth. The values for fructans were calculated as the differences between concentrations (C) of A1 and A2 calculated according to the formula:

$$\mathrm{C}\ (g.L^{-1}) = \frac{\mathrm{V} \times \mathrm{MWt}}{\varepsilon \times d \times v} \times \frac{0.09}{0.02} \times \Delta A \qquad (5)$$

Where,

V = final volume (mL)

MWt = molecular weight of glucose or fructose (180.16 g. mol^{-1})

ε = extinction coefficient of NADPH at 340 nm (6300 L. mol^{-1}. cm^{-1})

d = light path (cm)

v = sample volume (mL)

0.09/0.02 = volumes of solution A (0.09 mL) from which 0.02 mL aliquot was incubated with fructanse and indo-inulinase

The value of C in g. L^{-1} was changed to mg. g^{-1} DW using the following formula:

$$C_{fructans}\ (mg.g^{-1}DW) = \frac{C\ fructans\ (g.L^{-1})}{C\ sample\ (g.L^{-1})} \times\ 1000\ \times \frac{162}{180} \qquad (6)$$

Where,

162/180 = is a factor to convert from free glucose and fructose as calculated in the assay to their anhydrous forms as present originally in the fructan molecule

The formula in Equation (3) was used to calculate fructan contents per fresh plant part.

2.2.4.2. MALDI-TOF analysis

Bluebell bulbs were analysed using MALDI-TOF spectroscopy for two purposes: the first was to qualitatively investigate numbers and degrees of polymerisation (DP) of the fructans present in bluebell bulbs. The second was to compare the changes in chain lengths at different times during the season. Accordingly, two different approaches in matrix preparation and application to target were used that will be referred to as method 1 and 2 respectively.

Matrix preparation:

For method 1, using 2, 5-dihydroxybenzoic acid (DHB) 10 mg/mL in water. For method 2, the matrix was prepared by dissolving 18 mg/mL of DHB in a solution of water: MeCN (3:1). Another solution of 16 mg/mL of 2,4,6-trihydroxy acetophenone monohydrate (THAP) was prepared in a mixture of 0.1% TFA in water: MeCN (1:1) to be used as seeding layer. The combination of matrix and seeding solutions was found after testing solutions of DHB and THAP in different combinations of acetone, water and acetonitrile. DHB in water: MeCN 10 mg/mL was found to show higher mass fructans, but it doesn't crystallise very well and the spot could be seen as a circle with the analyte situated on the rim leaving the centre empty. Crystallinity and sample distribution could be improved to some extent by adding 10% of 2-hydroxy-5-methoxybenzoic acid to produce "super DHB", but even with that, shot to shot reproducibility was still very poor. Therefore, DHB was only used in method 1. THAP on the other hand, was producing a homogenous crystalline bed and the results were of reasonable reproducibility. The only drawback with using THAP was that it wasn't showing mass ranges higher than 1400. The optimised combination used in the quantitative analysis resulted in improved crystallinity and higher reproducibility, but still restricted to the relatively lower mass ranges. The DHB solution used in this test was of higher concentration in order to enhance crystallisation and water: MeCN used as a solvent rather than water to facilitate solvent evaporation.

Method 1: Qualitative analysis of bluebell bulbs' fructans:

Sample preparation: To 10 mg of freeze-dried and powdered bulb samples, 1000 µL of water was added, the mixture was vortex-mixed for 60 sec then centrifuged at 6000 rpm (technico Mini) for 10 min. the supernatant was analysed for fructooligosaccharides by mixing it with DHB solution (1:3). The seeding layer was prepared by applying 1 µL of the matrix solution onto the target and allowing it to dry. Then 0.5 µL of the sample: matrix mixture was added to it. A laser power of 40% was used and 100 shots were collected manually.

Method 2: Comparing fructan chain lengths at different times of the year:

Bluebell bulb samples were taken from 6 different time points in 2014 and aqueous extracts were prepared as above. The clear supernatants were analysed by mixing aliquots with equal volumes of DHB solution. Prior to applying the samples to the metal target, (1 µL) of THAP solution was applied as a seeding layer, allowed to dry at room temperature, then the sample: matrix mixture (0.5 µL) was dispensed onto it. A laser power of 43% was used, Samples were analysed using (Reflex IV MALDI-ToF Bruker Daltonics) mass spectrometer utilising the automatic collection (AutoX) feature to collect 240 laser shots per spot.

2.2.4.3. Analysis of the main trisaccharide of bluebell bulbs

2.2.4.3.1. Isolation

Bluebell bulbs collected in August 2013 (200 g) were used in this experiment. After washing with water, the bulbs were blended with 400 mL MeOH then another 400 mL was added and the mixture was left overnight. The extraction was repeated two more times applying mechanical stirring for 2 hr. The extracts were combined together and the solvent was removed on a rotary evaporator (Büchi Rotavapor R-210) at 40 ^{o}C leaving a residue of (4.5 g) with honey-like consistency. This was subjected to flash chromatography using Reveleris automated flash system. Approximately 500 mg of the extract was dissolved in 2 mL water and the resulting solution was injected onto a Reveleris C18 column. A solvent system of water acidified with 0.1% FA was used and peak elution was monitored with ELSD. A peak at t_R 1.0 min was collected and the solvent evaporated on a rotary evaporator at 40 ^{o}C. NMR analysis of this fraction showed that it mainly consisted of saccharides and TLC showed the presence of more than one compound. Accordingly, a solvent system was optimised for the best TLC separation and the compound was purified using preparative NP TLC. The plates were developed using a solvent system of n-BuOH: AcOH: water (5: 2.5: 1.5). 1-kestose Rf 0.13 was isolated as a white powder (9.7 mg) showing the following characteristics

Physical appearance: white powder

^{1}H NMR δ_H ppm (400 MHz, D_2O): 5.39 (1 H, d, *J* 3.8), 4.24 (1 H, d, *J* 8.7), 4.15 (1 H, d, *J* 8.5), 4.04 (1 H, t, *J* 7.3), 4.00 (1 H, t, *J* 7.7), 3.82 (1 H, m), 3.80 (1 H, dd, *J* 12.3, 4.5), 3.79 (1 H, d, *J* 12.4), 3.77 (2 H, m), 3.73 (2 H, m), 3.71 (1 H, t, *J* 9.6), 3.70 (1 H, d, *J* 12.3) 3.67 (1 H, d, *J* 12.0), 3.64 (1 H, d, *J* 12.3) 3.50 (1 H, dd, *J* 10.0, 3.9), 3.43 (1 H, t, *J* 9.4).

^{13}C NMR δ_C ppm (125 MHz, D_2O): 103.9, 103.4, 92.6, 81.3, 81.3, 76.7, 74.6, 74.0, 72.7, 72.5, 71.3, 69.3, 62.5, 62.3, 61.0, 60.5, 60.2, 49.0.

2.2.4.3.2. Peracetylation of the isolated trisaccharide

The isolated 1-kestose (9.7 mg) and standard 1-kestose (10 mg) were placed in glass vials and 500 µL of pyridine-D_5 was added to each followed by 100 µL of acetic anhydride. The vials' contents were sonicated for 1-2 min until clear solution was obtained. The solutions were then transferred to NMR tubes and sonicated for 5 min. The tubes were then submitted for NMR analysis giving the following chemical shift values:

^{1}H NMR δ_H ppm (400 MHz, Pyridine-D_5): 6.20 (1 H, d, *J* 3.7), 6.16 (1 H, d, *J* 7.7), 5.92 (1 H, d, *J* 6.7), 5.90 (2 H, t, *J* 10.0), 5.85 (1 H, d, *J* 8.0), 5.75 (1 H, t, *J* 6.5), 5.48 (1 H, t, *J* 9.9), 5.32 (1 H, dd, *J* 10.4, 3.8), 4.73 (1 H, ddd, *J* 10.2, 4.5, 2.3), 4.61 (7 H, ddd, *J* 17.1, 8.8, 4.5), 4.54 – 4.44 (2 H, m), 4.24 (1 H, d, *J* 9.7), 4.09 (1 H, d, *J* 9.7).

^{13}C NMR δ_C ppm (125 MHz, Pyridine-D_5): 173.5, 170.8, 170.7, 170.7, 170.6, 170.5, 170.4, 170.4, 170.3, 170.3, 170.2, 170.0, 167.2, 104.2, 103.8, 90.2, 79.1, 78.7, 77.5, 76.2, 75.9, 74.8, 70.9, 70.5, 69.2, 64.3, 64.0, 63.5, 63.2, 62.6.

2.3. Results and Discussion

2.3.1. Phenology

For 2014, the first sample was collected in March where the average shoot height was 10 cm above ground. Flower primers, enclosed by the leaves, were starting to become visible above ground during this week. Plant heights slowly increased in the following two weeks and reached up to 13.2 cm after which the plants exhibited a rapid growth and on April 16th the leaves grew to 21.6 cm and scapes became visible too at height of 9.7 cm. Over the next month the leaves and scapes grow up to an annual average height of 30 and 40 cm respectively and total weight averaging around 8 g per bulb. Anthesis started in May 1st and by the first week in June fruits had formed while seeds ripening completed in mid-July. Senescence started in the first week of June with the leaves starting to turn yellow and disappear completely by the end of the month followed by the scapes two weeks later thus ending the above-ground vegetative growth stage. Re-sprouting started in December of the following year and shoots with average height of 1.4 cm emerged from the bulbs. The subterranean growth continued at a slow rate and over the following two months shoots grew up to only 5 cm.

Bulbs, on the other hand, showed changes during different stages of the plant's annual life represented by variations in the percentage of dry weight (DW), shape and texture of the bulbs. DW was less than 10% in March 24th, increased slightly in the following week and remained around 12% for 3 weeks. In mid-April and with the start of rapid growth, the previous year's tissues in the bulbs started to become wrinkly and pale indicating that the previous year's reserve has been consumed and the tissues that contained them are now ready to be shed. Concurrent with shedding old bulb tissues, the current year's bulb started its growth and build-up of reserve. This was seen as an increase in DW from 12% in mid-April to a maximum of 29.6% over a period of 4 weeks. The DW remained more or less constant over the following month then it started to decrease gradually around the end of the vegetative growth. The bulbs entered a short period of dormancy for 2-3 weeks from the end of July until mid-August characterised by the disappearance of roots. Bulb elongation was observed in few sampling occasions after root growth in August, but the most remarkable was before shoot above-ground emergence in February, as bulbs grew to 4.0 – 6.5 cm length. Figure 15 shows the onset and duration of different phonological stages with the average vegetative growth represented by leaf and scapes height.

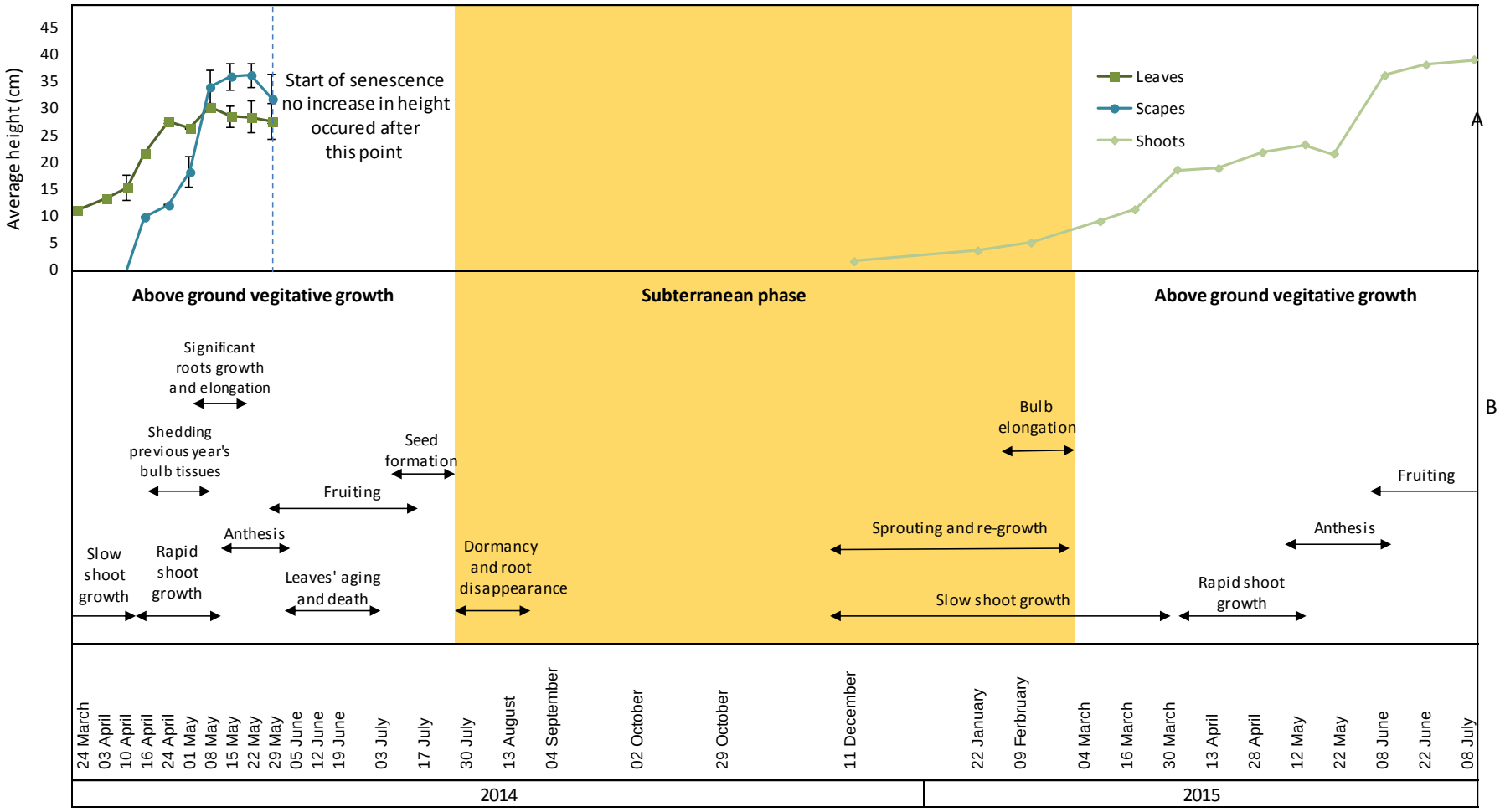

Figure 15 The phenology of bluebells observed during 2014-2015. A, Leaf and scape's heights for 2014, and shoots heights for 2015 samples. Error bars are SEM, n=2. B, The different phenological stages of the plant's life with the most significant characteristics of each stage.

2.3.2. Weather data

The exposure to periods of low temperature is usually linked to the depolymerisation of reserve polysaccharides into simple sugars which leads eventually to breaking dormancy and stating growth. In addition to the internal biochemical factors such as sugar and hormonal changes, environmental factors impose a great effect on the transition between different phenological stages (Horvath et al. 2003). A combination of long photoperiods and low temperature was found to promote scapes elongation in garlic (Kamenetsky et al. 2004). Both flowering and dormancy- two stages in the phenological cycle that ensures the continuity and the survival of the species- are highly affected by the changes in available light and temperature (Kamenetsky et al. 2012; Okubo 2012). Dormancy in spring ephemerals growing in woodlands coincides with the time when light intensity falls due to leaf growth and closing of the overhead tree canopy, concurrent with the decline in the available water which is being absorbed by roots of the accompanying growing trees (Lapointe 2001). Similarly and whether in a woodland community or accompanied by bracken, bluebells commonly exploit the light available in the early season prior to the growth of most of the other accompanying species. They are also sensitive to drought and require cool temperate climates for their growth (Blackman and Rutter 1950; Blackman and Rutter 1954; Knight 1964). Therefore, dormancy is a successful strategy to avoid the unfavourable environmental conditions by the plant at the start of summer to avoid the unfavourable conditions.

The active above-ground growth took place in the temperature range 4 – 14 ^{o}C in 2014 and 4 – 12 ^{o}C in 2015 which is in agreement with the growth temperature range stated for bluebell by (THOMPSON and COX 1978). The relatively lower temperatures in 2015 may have affected the duration of anthesis which extended for over a month compared to 3 weeks in 2014. It is also likely to have delayed fruiting and seed formation by about at least 1 week in 2015 (Figure 15).

Total daily rainfall data show the availability of water spread over the year. No periods of severe drought are seen. Rainfall profile during the above ground phase is rather spread compared to periods of continuous rain in winter. This probably makes the required balance ideal for the growth of bluebell represented by the availability of sufficient water for growth without water logging.

Light availability represented by total daily sunshine hours reveal that periods of maximum day length/light intensity don’t actually coincide with periods of maximum leaf growth as

might be expected. One reason might be the heavy growth of bracken preventing other plants from benefiting from radiation available at this period. However, in the case of bluebell, leaf senescence occurs long before the heavy growth of bracken canopy, which could suggest its relation to the limitation of sink capacity represented by the bulbs after reserve build-up as pointed out by (Lapointe 2001). Furthermore, temperatures are relatively higher at this time which also poses higher risk of drought.

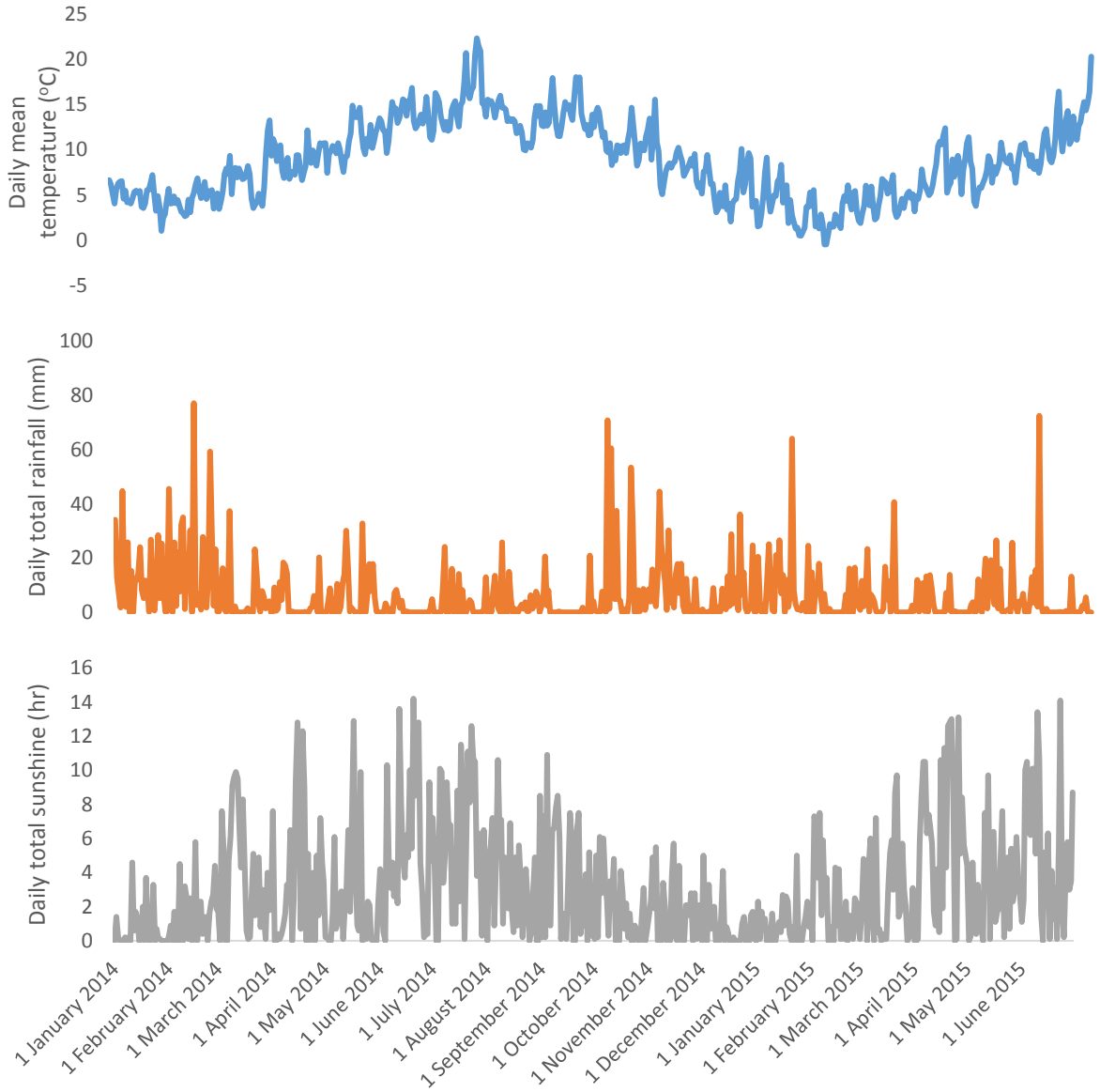

Figure 16 Weather data obtained from two stations close to the sampling location in north Wales.

2.3.3. Total non-structural carbohydrates (TNC)

Seasonal TNC and % DW measurements for samples collected in 2014 revealed that the bulbs are the major contributors to both parameters (Figure 17 - Figure 20). It also showed that these

two variables in the bulbs do not undergo severe depletion at any stage of the annual life cycle of the plant.

The minimum values measured were at the start of above-ground growth 653 mg. g^{-1} DW, while a maximum value of 823 mg. g^{-1} DW was reached on May 08th around the time when leaves are fully mature and photosynthesis is at its highest. The value remained relatively constant for the following week then started to decrease gradually towards the end of the growth season. A similar profile is seen for the bulbs when measurements are conducted on fresh plant weight's basis. The graph of dry matter content in bulbs (Figure 17 B) reflects the physiological changes occurring in this part of the plant. Bulbs' resource accumulation in May is a vital insurance for the plant's survival through the underground stage and also for its re-growth in the following season. The bulbs fresh weight (Figure 18 B) showed a decline during the same period due to shedding of old bulb tissues leaving behind the new bulb, which is physically smaller, but has higher dry mass content. The general trend for the bulbs is high TNC during peak above-ground growth followed by a decline through the subterranean phase to reach a minimum at late winter- early spring before plant shoot emergence. However, a number of fluctuations are seen along the line which could be either due to natural variations between different samples collected in the field or due to a number of events that happen through the plant's annual life cycle. Seed formation, for example, takes place around mid-July when the leaves are already dead and scapes are close to the end of their life. Carbon and energy required at this stage could be secured from the bulbs via the lignified scapes which may result in a decrease in bulbs TNC and/or mass. Another phenological milestone is bulbs entering dormancy towards the end of July, a stage that can also lead to an increase in TNC and/or mass by material recycling from the other parts. Another peak is seen at the start of October following root growth in the previous month. This increase is probably a result to the physiological changes in the plant after breaking dormancy and starting roots and shoot growth. In this case a similar and concurrent increase should occur in the levels of sucrose indicating fructan depolymerisation and resource mobilisation.

The decline in TNC levels during the subterranean phase is presented more clearly in the fresh plant based measurements as it takes into account the individualities and differences between different plant part's content of biomass (Figure 18 and Figure 22).

The roots showed a pattern similar to that of the bulbs featuring low TNC at the start of growth followed by an increase to reach a maximum of 189 mg. g^{-1} DW in mid-May then a gradual

decrease in the following month (Figure 17 A). The maximum TNC content in the roots 320 mg. g^{-1} DW was measured on July 17th (the last week before dormancy) which is probably an indication of mobilisation of carbohydrates from the roots in preparation for dormancy.

The roots exhibit a significant growth and elongation in mid-May and reached lengths of 13-15 cm. This results in higher root weight per plant and follows higher TNC in a similar profile (Figure 18 A). Plants sampled in September showed the presence of roots with relatively higher dry mass content than the previous season. Roots weight per plant were very low 0.01 g per plant and increased to 0.05 g by January. However, since both TNC levels and %DW decrease for the same period then most of the gained weight should come from water absorption by the root tissues.

The leaves showed relatively constant dry weight content ranging from 7-10 % throughout the growth period (Figure 19 A). Values of TNC were low at the beginning and measurements on fresh plant basis (Figure 20 A) emphasised the low amounts up to April 10th, then increased afterwards directly with leave's biomass. Highest concentrations reached during full expansion and growth of leaves then declined towards the end of their life.

The scapes comprised a much smaller weight proportion per plant compared to the leaves at the start of shoot growth in March. However, their TNC content per g DW was as 4 times higher (Figure 19 B). This shows the higher allocation of resources to the scapes. It additionally reflects the importance of this part in growth and development of flowers and eventually fruits and seeds. Fresh-weight based measurements showed a direct increase in TNC with increasing biomass (Figure 20 B). Dry-weight based measurements showed that the starting high concentrations of TNC were maintained until the start of anthesis in May then declined afterwards. Lignification of scapes tissues towards the end of June resulted in higher weights of scapes per plant even when the scapes were starting to die down.

The flowers which were already formed in the bulbs in the previous year, start their above ground growth with a DW content of about 15% and TNC of 70 mg. g^{-1} DW (Figure 19 C). The small proportion of flower (Le Roy et al. 2007)(Le Roy et al. 2007)(Le Roy et al. 2007)(Le Roy et al. 2007)(Le Roy et al. 2007)weights per plant made their sugar contents measured per plant basis appear very low at the early stages of above-ground growth. The flowers showed a pattern characterised by two distinctive maxima: one at the time of peak anthesis in mid-May and the second during seed ripening when it reached a maximum on June 12th (Figure 19 C). Anthesis is a distinctive stage in bluebell's phenology. Characterised by the formation of a

carpet of blue-purple flowers. An increase in simple sugars specifically fructose in the flowers is required to produce the osmotic driving force necessary for petal expansion during anthesis this agrees with the findings by (Le Roy et al. 2007; Vergauwen et al. 2000) in their detailed study of flowering in *Campanula rapunculoides*. Once the fruits are formed, the petals start to wither and dry down which explains the remarkable decrease in TNC and the increase in DW content at this time. Seed capsule expansion is accompanied by an increase in TNC which could also be considered a factor involved in tissue expansion and taking up water since the tissue dry weight decreases at this stage. The final stage is the ripening of seed which is accompanied by decrease in TNC and desiccation of the seed capsules as stated by (Housley and Daughtry 1987; Pollock and Lloyd 1994). The leaves start to show aging signs from the start of June to mark leaf death by the end of the month followed by the scapes two weeks later. Based on TNC values, carbohydrate levels in the scapes appear to be lower than that in the flowers in this period. This suggests the utilisation of carbohydrates from another source (in this case the bulbs).

For samples collected in 2015, the plants were divided into two parts: bulbs and shoots. Bulb DW agreed with results from 2014 where lowest values were observed in March-April. Fresh-weight based measurements shows better representation of the changes in TNC related to different phenological stages of the plant's life (Figure 21 and Figure 22). The results for shoots, representing a combination of the three above-ground parts, showed an increase in TNC and biomass steadily until full leaves and scapes growth (Figure 22 B). Another two peaks are seen in mid-May and early June for anthesis and seed formation respectively.

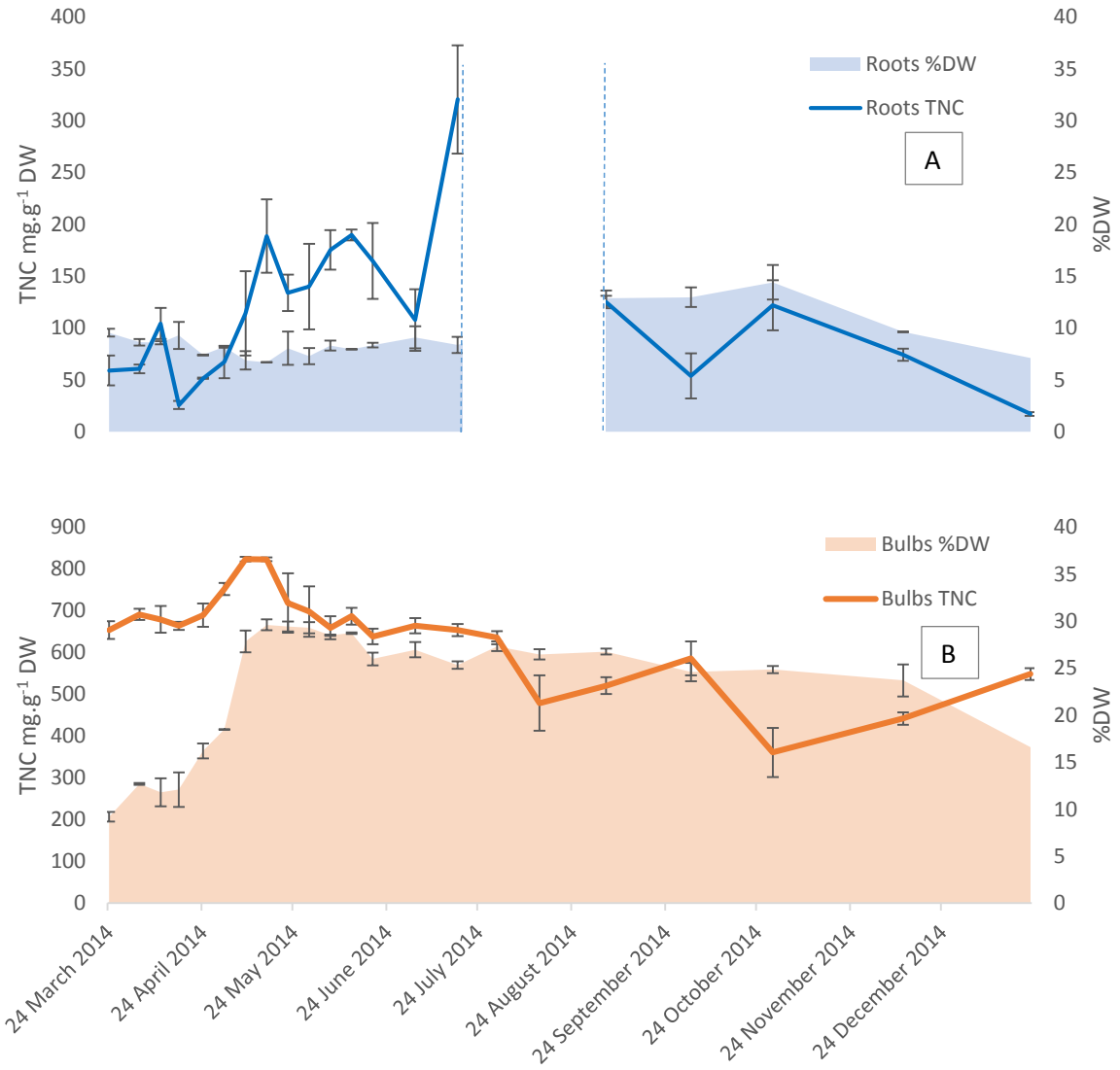

Figure 17 TNC in underground organs (A: roots and B: bulbs) calculated per dry weight basis for 2014 samples. The area between the dashed lines represents the time of root death during dormancy. The Error bars are SEM, n=2 each analysed in triplicates. The %DW of each part is plotted on the secondary axis. Error bars are SEM for n=2.

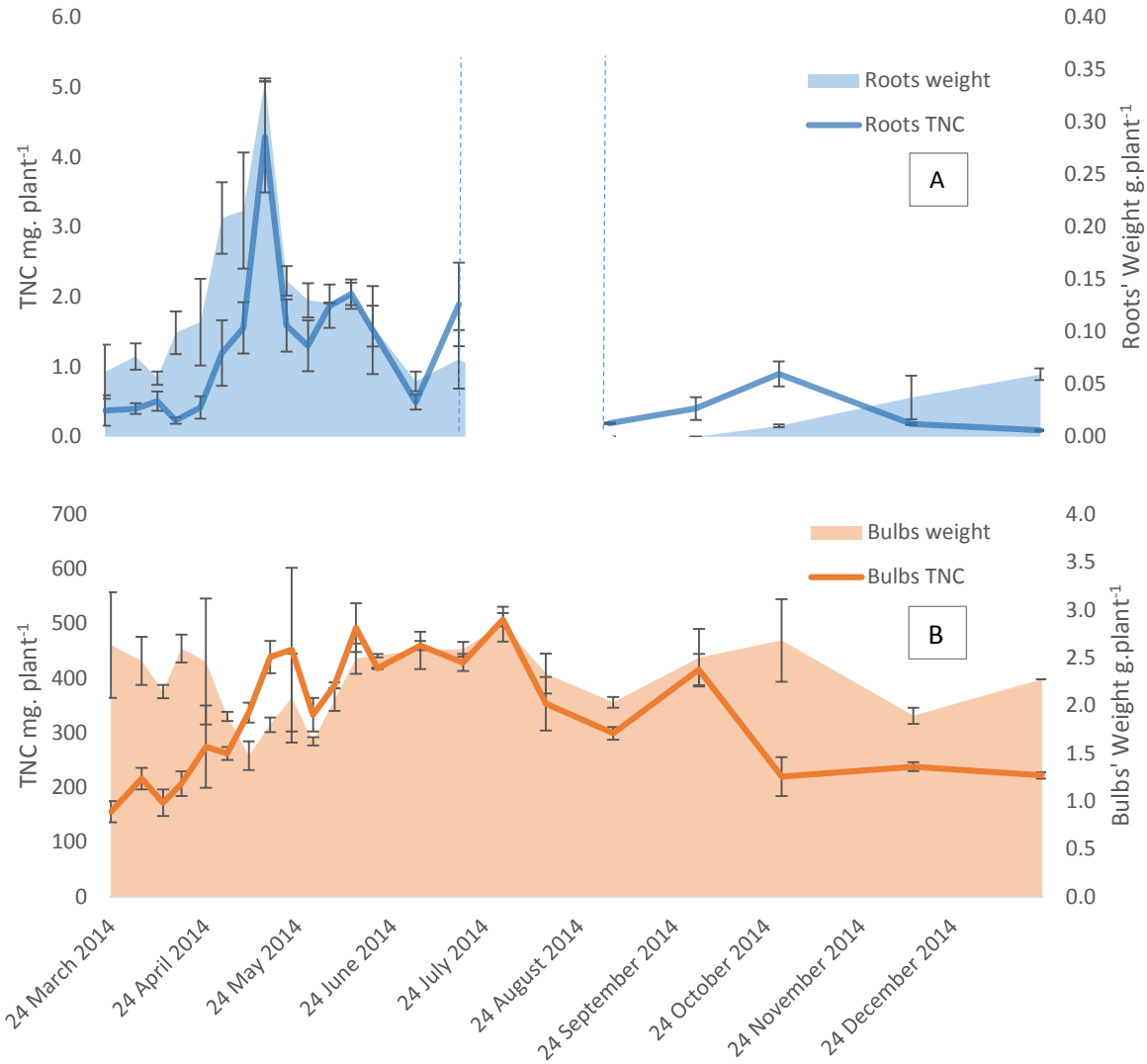

Figure 18 TNC in underground organs (A: roots and B: bulbs) calculated per fresh plant for 2014 samples. The area between the dashed lines represents the time of root disappearance during dormancy. Error bars are SEM, n=2 each analysed in triplicates. The fresh weight of each part plotted on the secondary axis. Error bars are SEM for n=2.

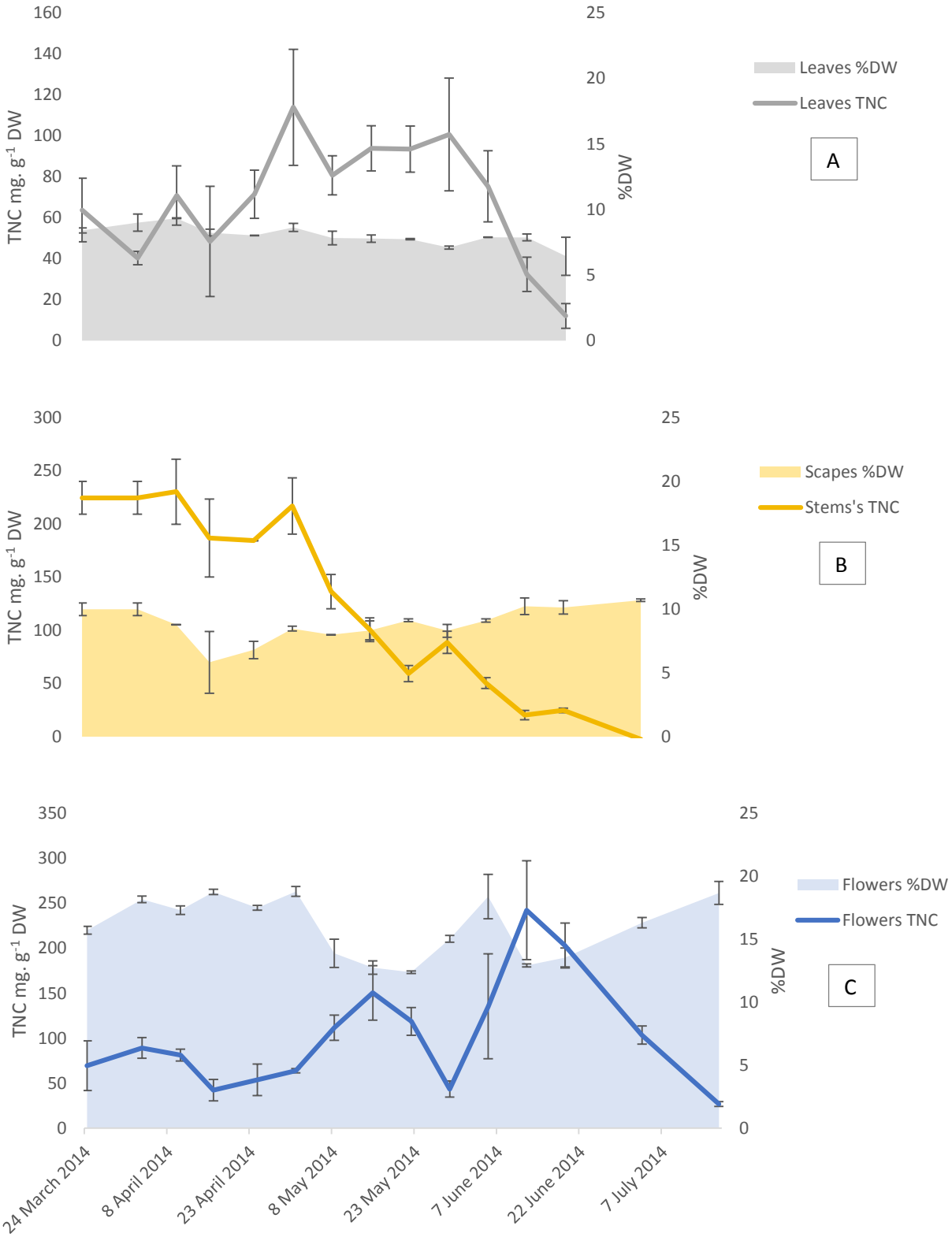

Figure 19 TNC in above ground organs (A: leaves, B: scapes and C: flowers) calculated per dry weight basis for 2014 samples. Error bars are SEM, n=2 each analysed in triplicates. The %DW of each part is plotted on the secondary axis with SEM bars of n=2.

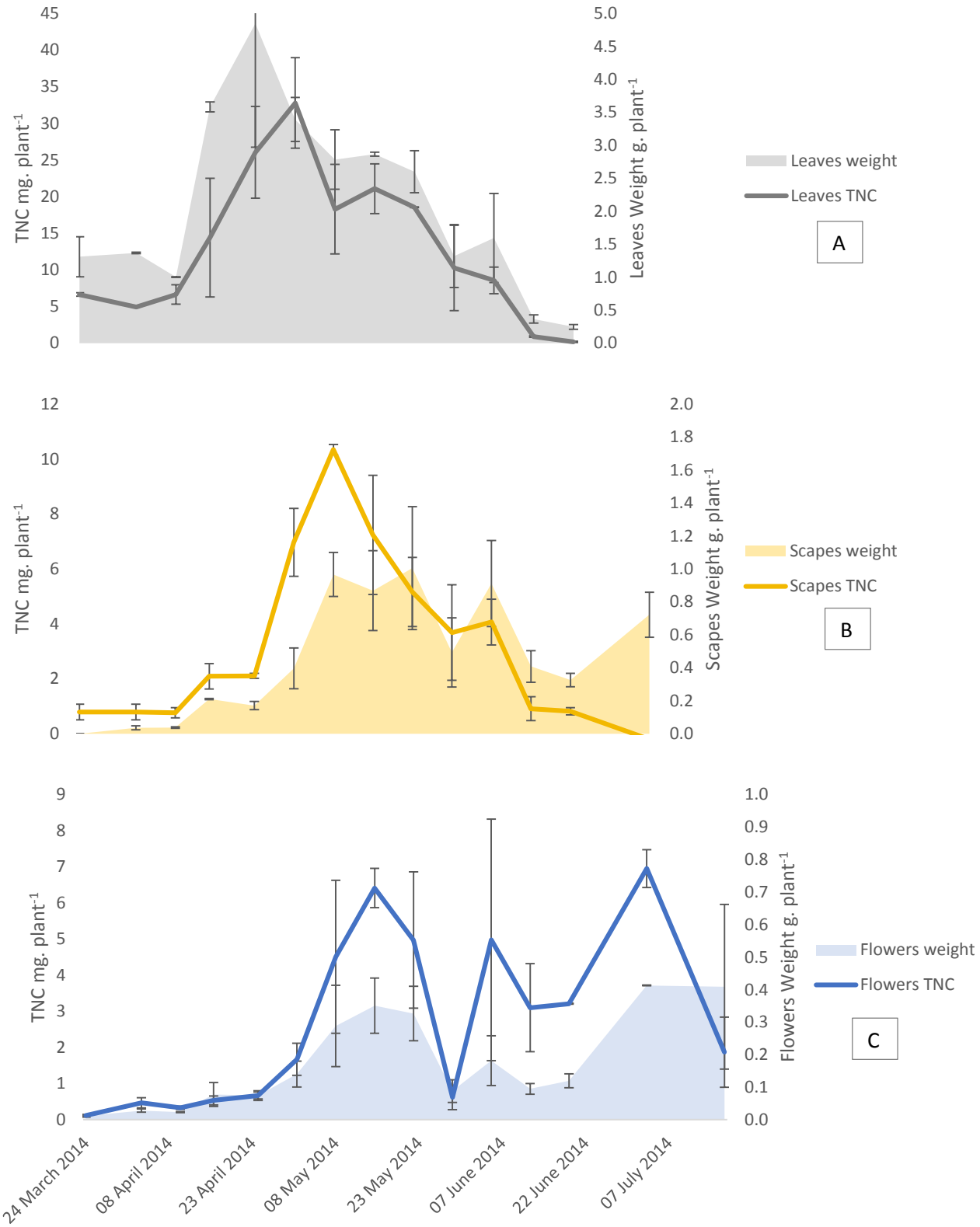

Figure 20 TNC in above ground organs (A: leaves, B: scapes and C: flowers) calculated per fresh plant for 2014 samples. Error bars are SEM, n=2 each analysed in triplicates. The fresh weight of each part plotted on the secondary axis. Error bars are SEM for n=2.

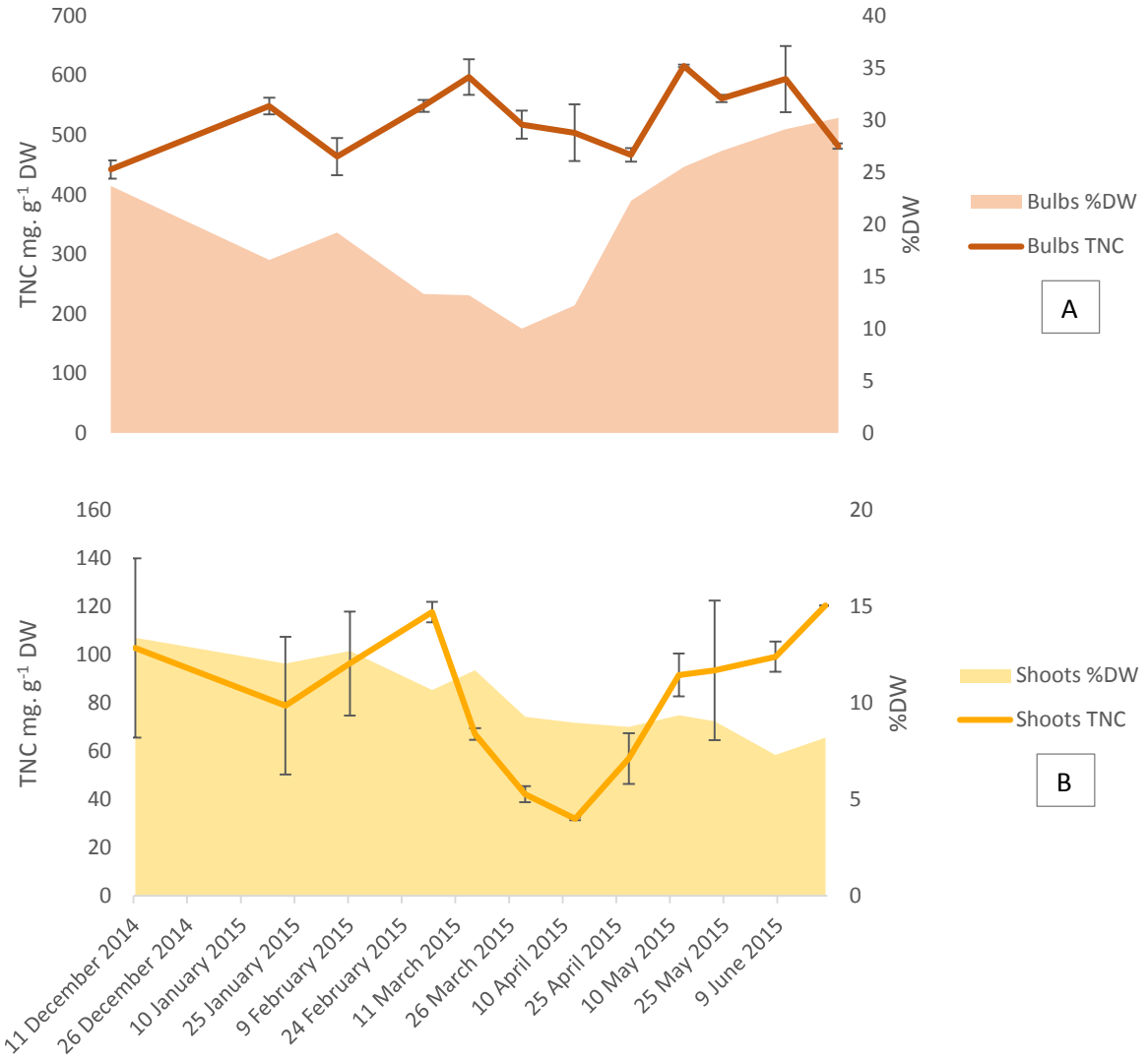

Figure 21 TNC in A: bulbs and B: shoots calculated per dry weight basis for 2015 samples. Error bars are SEM, n=2. The %DW of each part is plotted on the secondary axis. Only one measurement was taken.

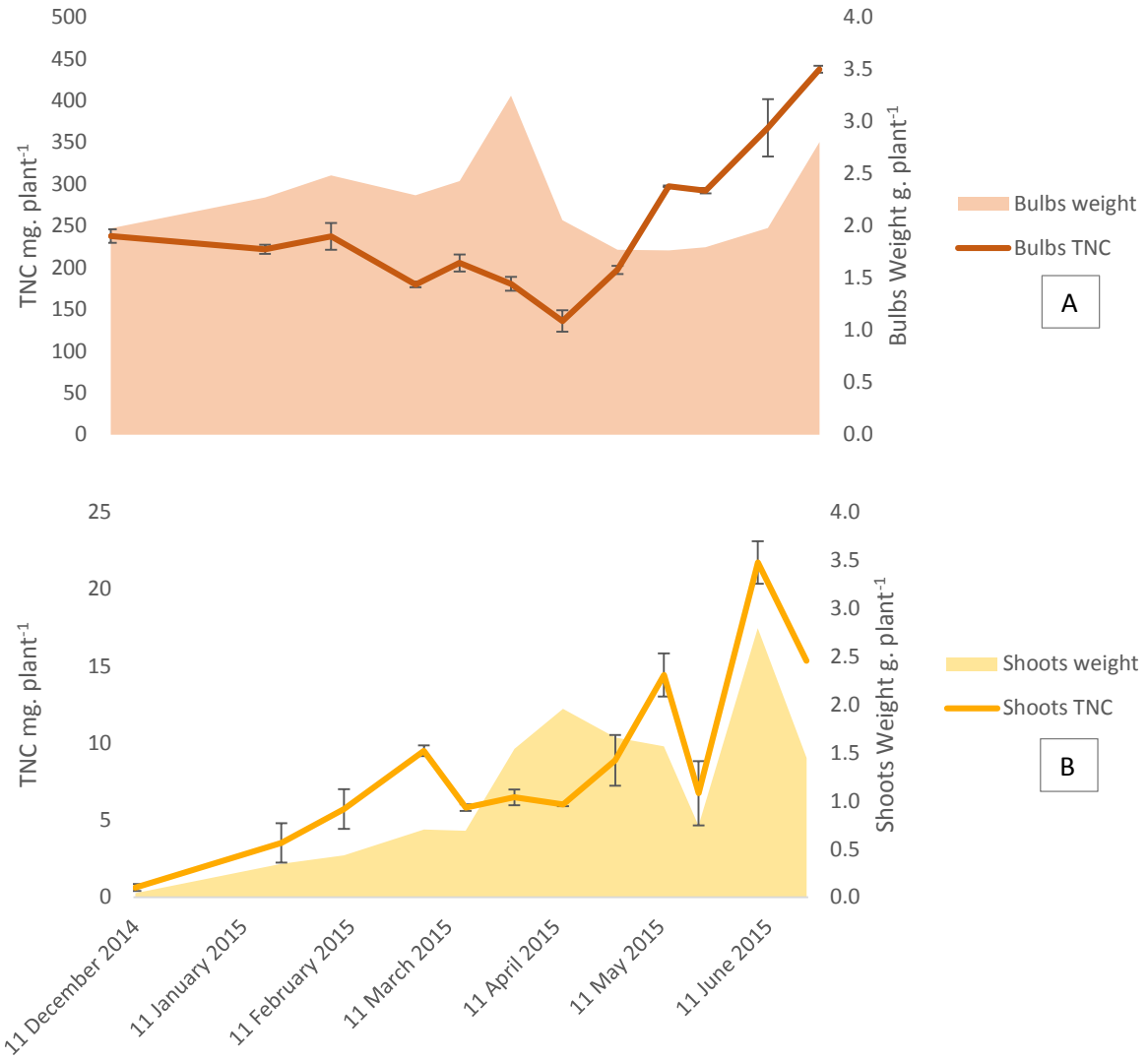

Figure 22 TNC in A: bulbs and B: shoots calculated per dry weight basis for 2015 samples. Error bars are SEM, n=2. The %DW of each part is plotted on the secondary axis. Only one measurement was taken.

2.3.4. Mono and disaccharides:

Analysis of the mono and disaccharides using GC MS showed the presence of three: fructose, glucose and sucrose. The most abundant sugar of this pool in the bulbs during the start of the season until mid-April was fructose followed by sucrose. The highest fructose concentration detected was 100.3 mg. g^{-1} DW in March 24th. Only small amounts (about 2.2 mg. g^{-1} DW) of glucose were detected in the same sample. The high amounts of fructose dropped quickly to 6.1 mg. g^{-1} DW by the start of May leaving sucrose as the main carbohydrate in the bulbs throughout the season (Figure 23). The increase in glucose levels was minor throughout the season. This is justifiable by the fact that the major polysaccharide present is fructan which contains usually only one glucose unit per molecule.

Sucrose is the cell's currency for transferring (both importing and exporting) material between different plant tissues. Therefore, changes in sucrose levels could be taken as indications of physiological activities at different stages. Sucrose accumulation can take place during the transfer of excess photosynthetic carbon from the leaves to storage organs. It can also indicate the depolymerisation of reserve polysaccharides in preparation for their translocation to growth sites.

Apart from the early-growth related increase in sugar levels that extended from January to April, other points along the timeline also showed some increase in sugar levels. The first increase was seen in May as a result of import from the leaves which were at their peak photosynthetic activity during this time. This level was maintained until the end of June when leaves start to die down. Transfer of sucrose to the bulbs results in their accumulation as fructans, in which case a similar increase in fructan levels should also take place. This was followed by a further increase at the end of July before dormancy and root death. A third increase is seen at the beginning of October coinciding with growth and establishment of roots.

In the shoots, Glucose was the major sugar present and both fructose and sucrose were of lower and relatively equal quantities (Figure 24). The only exception of this was during the first two weeks as sucrose was higher than both glucose and fructose when sucrose export from bulbs was the major source of carbon for the growing shoots. Glucose concentrations then started to show an increase proportional to the increase in the above-ground biomass. April 24th which was the point in time that characterised the beginning of fast growth in leaves was also the point where glucose amounts changed from 25.1 – 119.3 mg. g^{-1} DW in only two weeks. Furthermore it coincided with the transition of fructose from being the dominating sugar in the bulbs to its first low value at 15.8 mg. g^{-1} DW, and hence marking the end of export from this tissue.

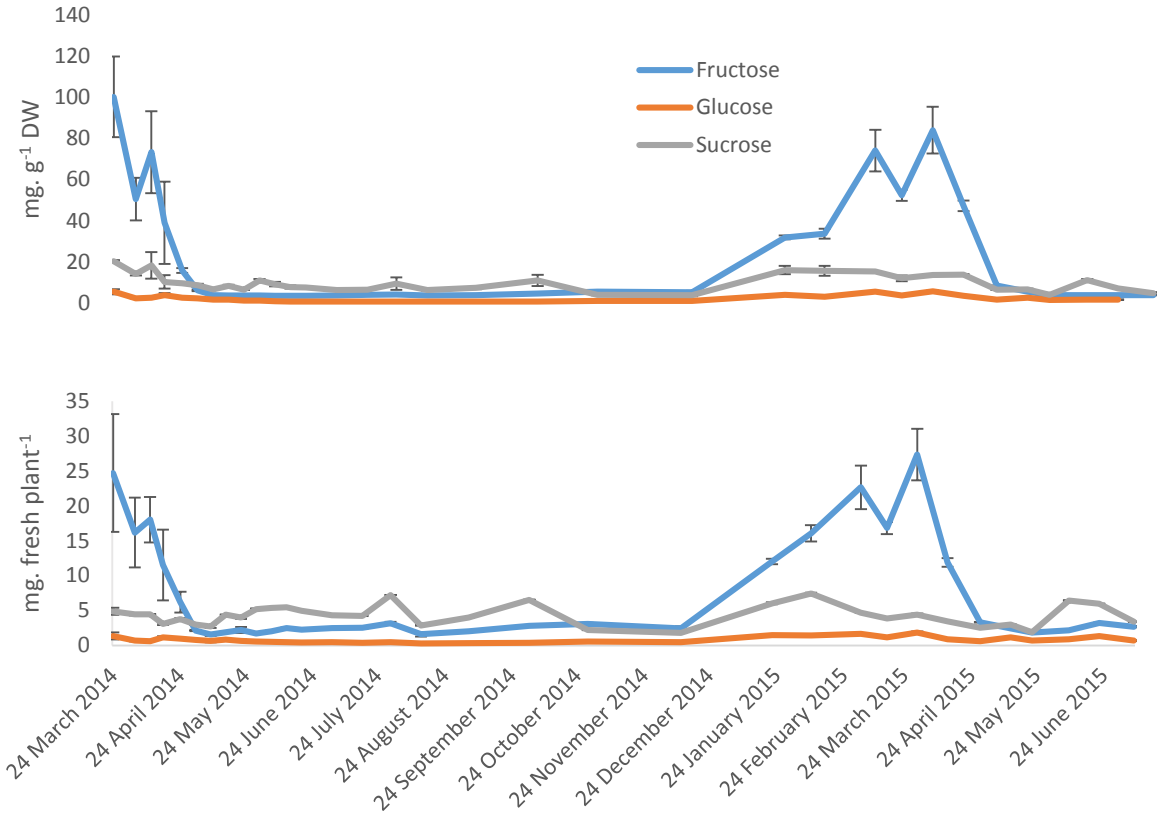

Figure 23 Seasonal variation of mono- and disaccharides in bluebell bulbs

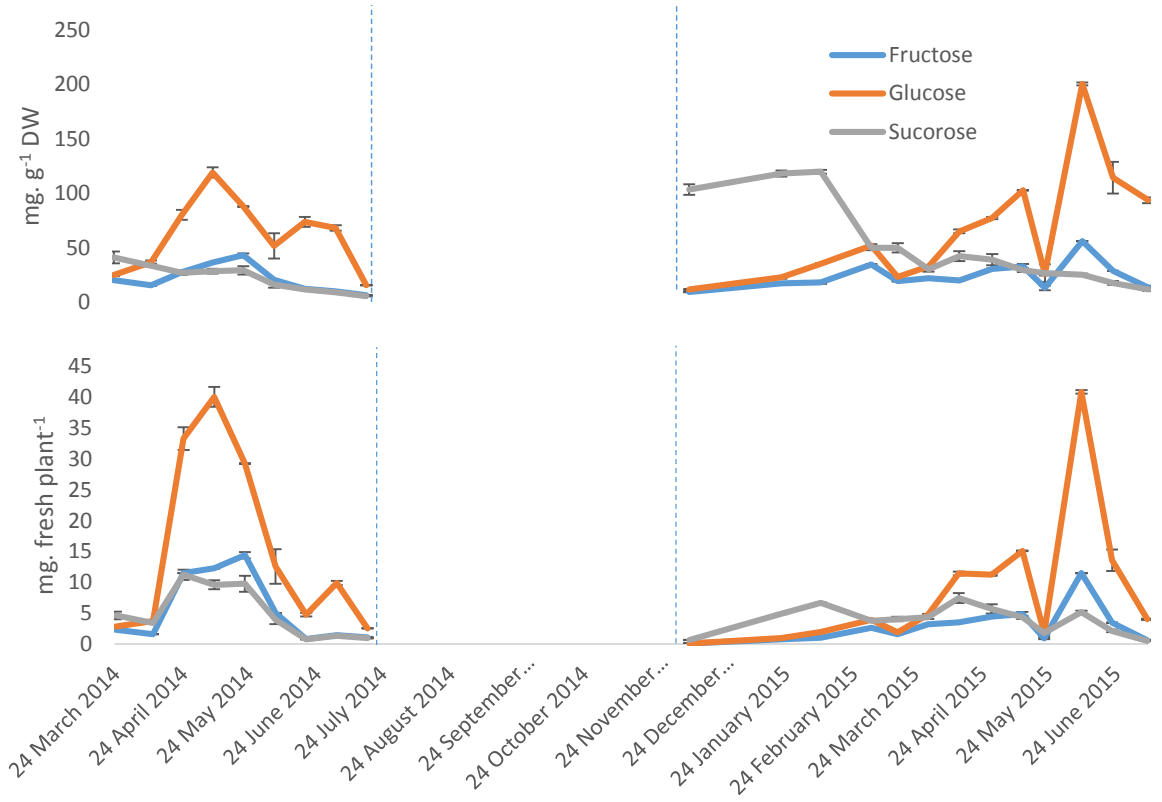

Figure 24 Seasonal variation of mono- and disaccharides in bluebell shoots. The area enclosed between the dashed lines represents the subterranean phase with no shoot growth. Error bars are SEM for at least n=2.

2.3.5. Bluebell fructans and their seasonal variation

Dry weight based calculations of the amount of fructans in the bulbs revealed changes in their profile in a manner similar to the changes in TNC throughout the year. Bulb fructans content was relatively low from end of March to end of April and started to increase concurrently with the growth of the above ground vegetation. Fructan concentrations reached over 740 mg. g^{-1} DW in May. Fructan values remained high in May and June then started to fluctuate in July with the general trend being downwards towards the end of the year (Figure 25). Export to bulbs (characterised by build-up of fructans and increase in % DW of bulbs) started once the leaves reached their highest content of dry matter on April 24th. At this point of time the scapes were at about half their annual heights and anthesis hadn't started yet. However, the amount of photosynthate seemed to be sufficient to meet the demands from both the growing above ground organs and refilling the underground reserves in bulbs.

The significance of bulbs appear obviously as the reserve organ responsible for the survival of the plant during the unfavourable cold months and re-growth in spring. Based on fructan analysis, bluebells consumed about 47% of the reserve during the subterranean stage. The highest decrease occurred at the start of the season prior to shoot emergence and concurrent with the increase in mono- and disaccharide levels. The amount of reserve consumption is relatively low in comparison with *Galanthus nivalis* L (snowdrops) that stores both fructan and starch. The amount of carbohydrates consumed in snowdrop bulbs was calculated as 40 and 30% of its fructan reserve in 1996-1997 and 1997-1998 growth periods respectively in addition to depletion of the starch reserve by 92 and 79% for the same period (Orthen and Wehrmeyer 2004). Bluebell bulbs accumulate fructans mainly and starch is only found in trace amounts (Hendry 1987), yet the utilisation of the fructan reserve was not much higher than in snowdrops. This could be justified by the differences in their re-growth and shoot emergence times. The earlier growth of snowdrops in winter months with flowering in January-February when both temperatures and photosynthesis rates are unfavourable has probably made the plant more dependent on the reserve during growth. While bluebell's shoot emergence is in mid – late March when temperature is relatively higher and longer sunshine hours enable the plant to photosynthesise in a more competent rate with early shoot emergence.

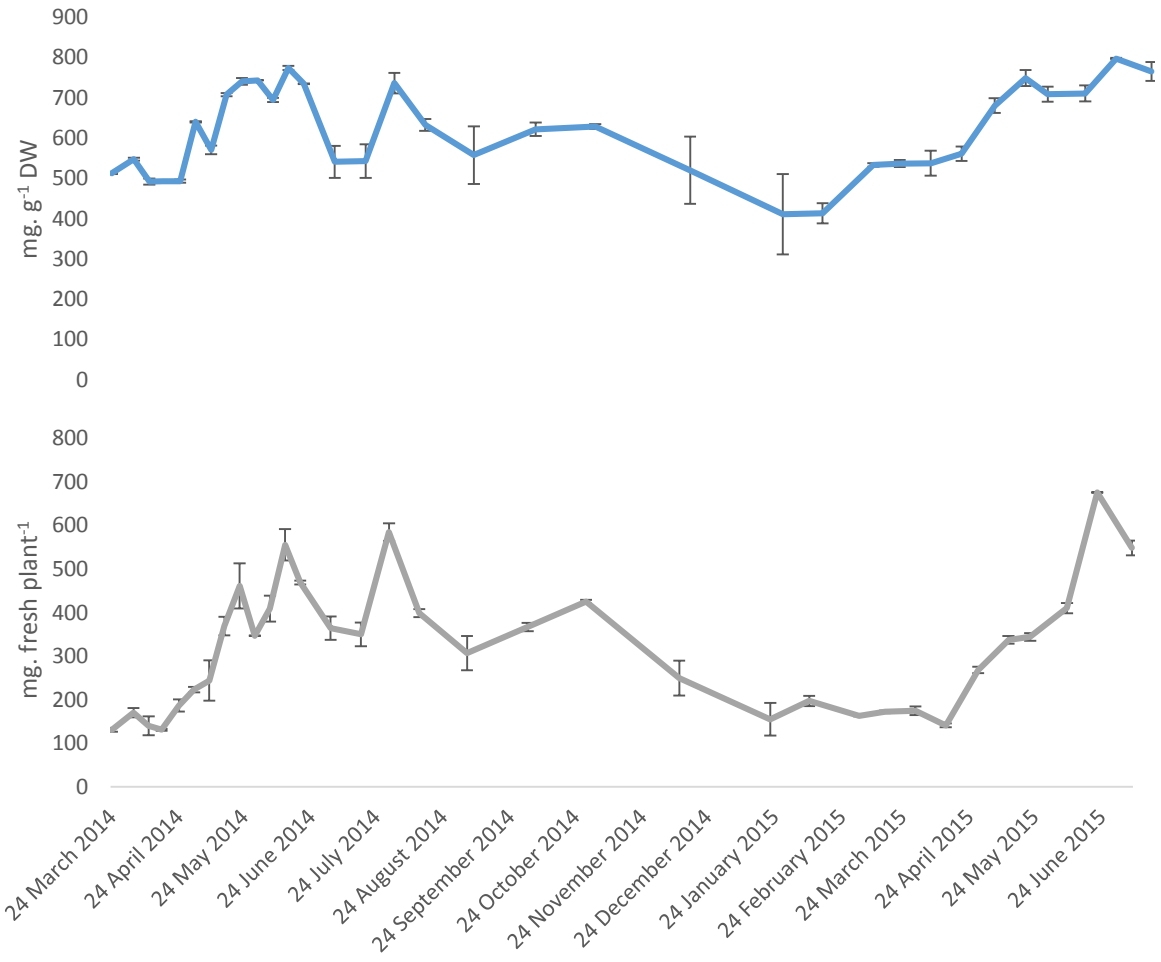

Figure 25 Seasonal variation of fructans in bluebell bulbs. Values are means with SEM for at least n=2.

The shoots on the other hand, showed a pattern similar to the mono- and disaccharides (Figure 26). Here again fluctuations are seen during the above-ground phase which could refer to periods of no or little photosynthesis allowing fructan depolymerisation and their translocation from the shoots to the bulbs. The presence of fructans and/or starch in photosynthetic tissues occurs when the rate of photosynthesis becomes higher than export rate. The excess amount of photosynthates is stored temporarily either in the form of starch in the cytoplasm or as fructans in the vacuole to be exported in the next dark period.

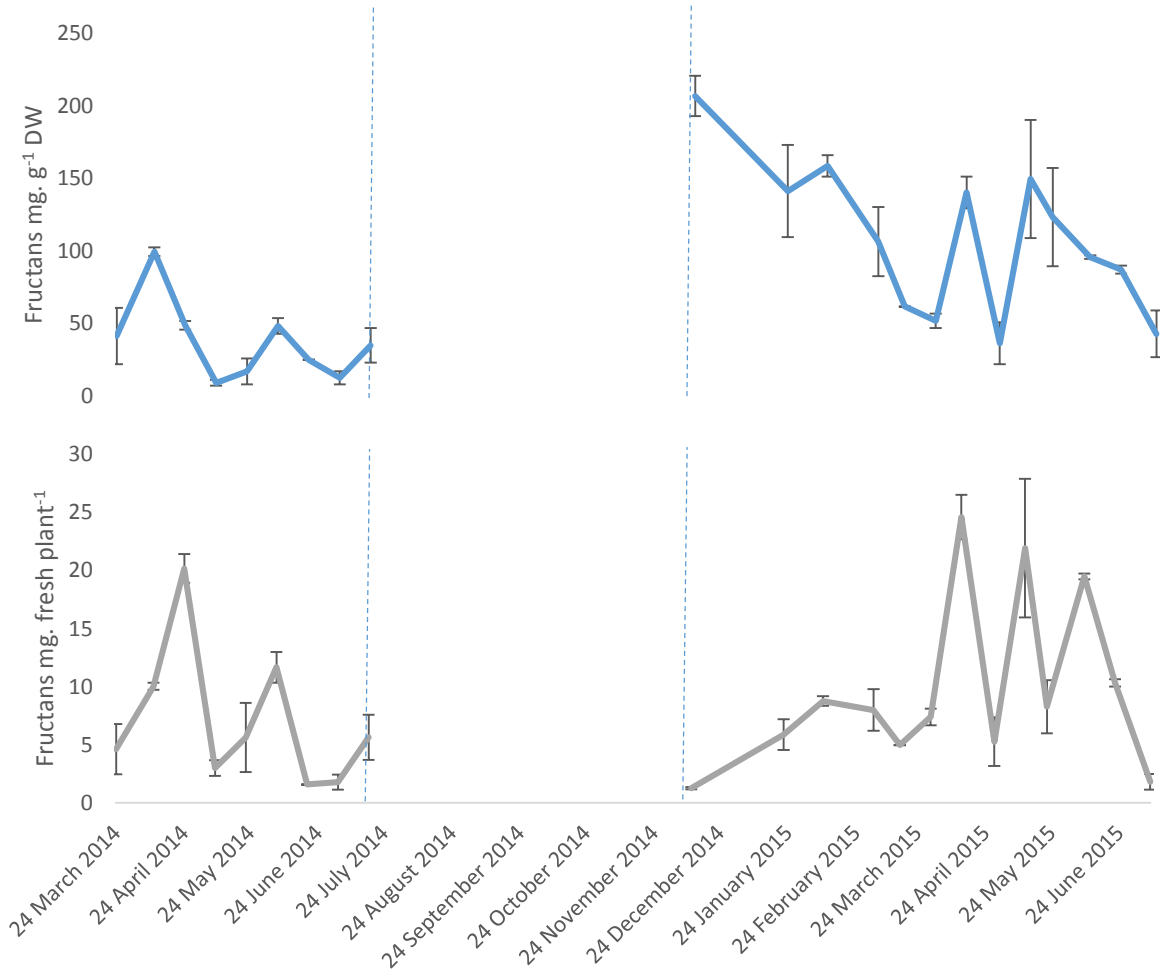

Figure 26 Seasonal variation of fructans in bluebell shoots. The area between the dashed lines represents the subterranean phase with no shoot growth. Error bars are SEM for at least n=2.

Fructan biosynthesis is beneficial to plants growing in environments with low temperature and short sunshine periods. Since fructan biosynthesis can continue in relatively low temperatures, diversion from accumulating starch to fructan is of a survival value for the plant. This, combined with the presence of large vacuoles enables the plant to photosynthesise efficiently under relatively stressful conditions. The fact that temporarily stored fructans in photosynthetic tissues is not prone to rapid turnover shows that fructan metabolism is tailored for plants subjected to cold temperatures and probably uncertainty of the availability of sunlight. As this will ensure the leaves access to carbon stores with short supply lines for the longest possible time if conditions didn't favour photosynthesis. Another factor in favour of fructan accumulation is that it doesn't undergo depletion during underground growth and early shoot emergence. This is most probably due to the fact that fructan degradation takes place by the action of one enzyme (FEH) that can target only terminal fructose moieties one at a time, a factor that adds to the longevity and prevents depletion of fructans as opposed to starch

polymers being hydrolysed by multiple enzymes targeting different locations (Beck and Ziegler 1989).

2.3.6. MALDI-ToF analysis of fructans in bluebell bulbs

Maldi-Tof analysis showed several peaks with separation of 162 mass units. Applying method 1 on the fructan fraction in bulbs revealed the dominance of short-chain fructooligosaccharides with DP3 and DP4 being the most common oligomers in all the samples tested and a decrease in the abundance of oligomers with increasing chain length. Figure 27 shows a bulb sample collected in March where the presence of chain lengths up to DP20 and even few other higher oligomers could be seen but with much lower signal/noise ratios.

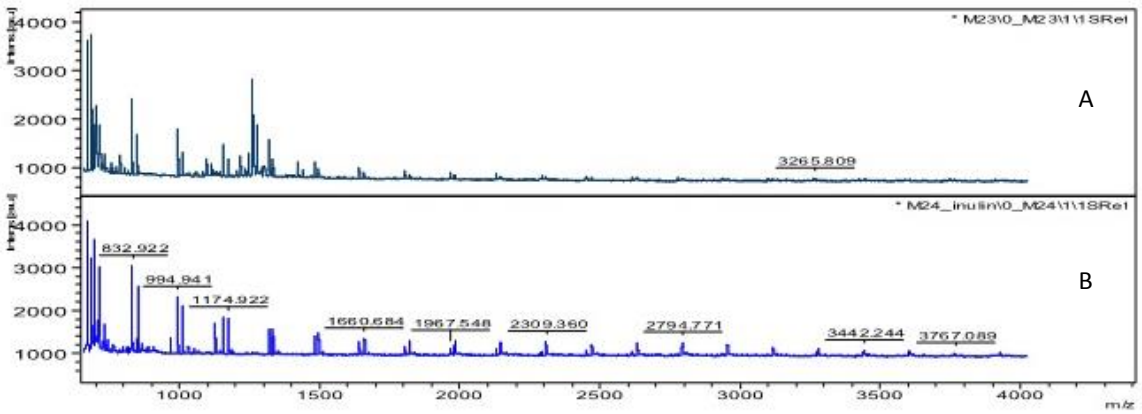

Figure 27 MALDI-ToF spectrum of bluebell bulb fructans (A) and inulin (B). Two peaks were detected for each oligomer representing $M+Na^{+}\cdot H_2O$ and $M+K^{+}\cdot H_2O$ respectively. Spectra obtained using method 1.

Method 2 was used for comparison of bulb samples collected at different times with regards to their contents of short chained fructans. The results (presented in Figure 28) showed that chains up to DP9 were found at the start of growth in March and disappeared in April-May, but were detected again in October. Figure 29 shows bulbs sampled in two different times of the year. April-May samples showed only the presence of DP3 and DP4 in addition to smaller quantities of DP5. It is likely that the longer chain fructans are also present at this stage, but their small quantities and higher difficulties in evaporating longer chains could resulted in them being undetected. Samples collected in October showed the typical case of different short-chain oligomers that occur in bulbs or tubers undergone cold treatment (Edelman and Jefford 1968). This stage is a result of depolymerisation of longer chain fructans in preparation for sprouting. Trace amounts of DP9-11 were also present, but they were below the detection limit of the method.

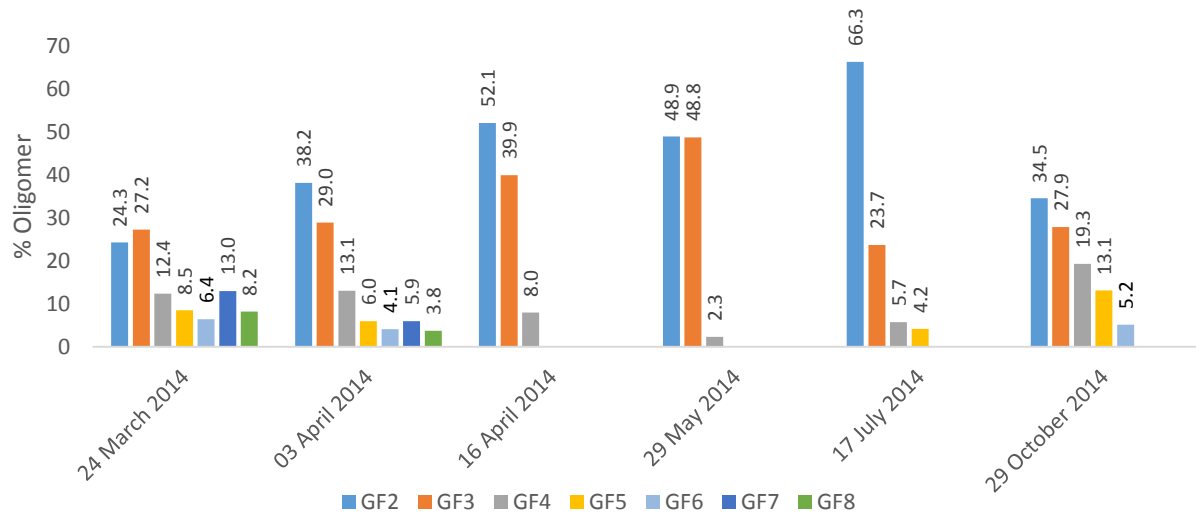

Figure 28 the percentage content of fructan oligomers in bluebell bulbs analysed by Maldi-ToF spectroscopy.

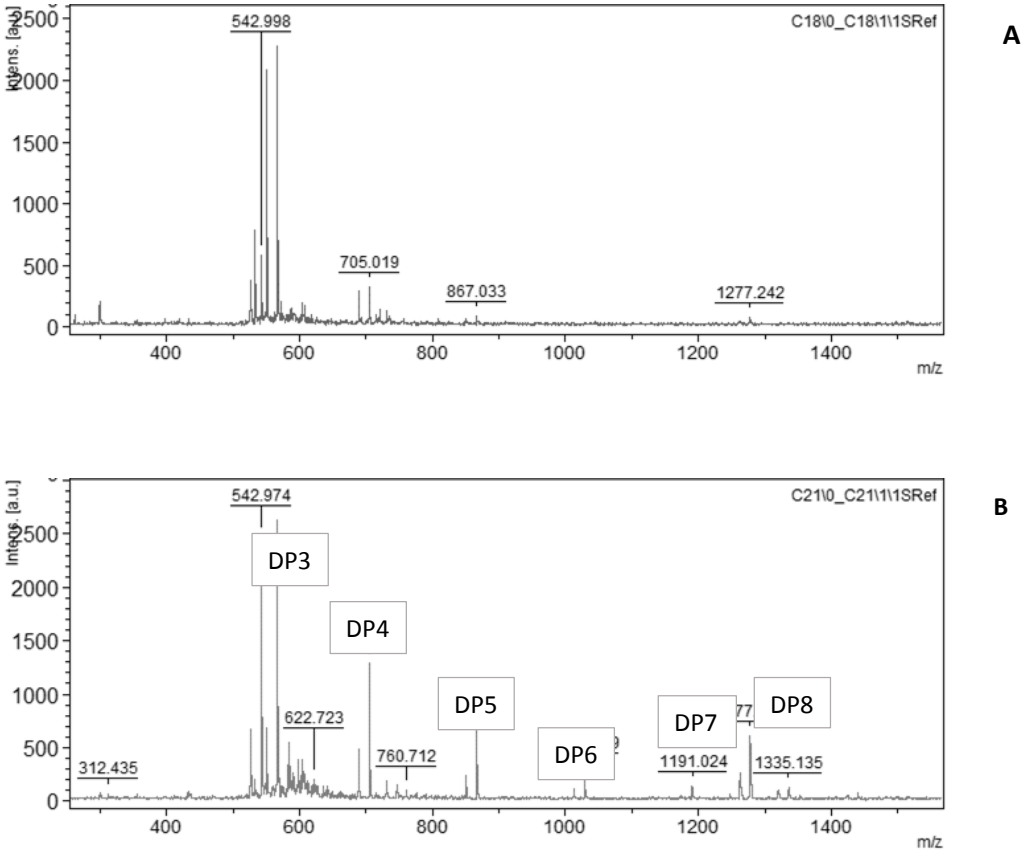

Figure 29 MALDI-ToF spectra of fructans in bluebell bulbs at two different times of the year: A, April during fructan build-up and B, October during depolymerisation in preparation for sprouting. Peaks represent $M+K^+$ ions of fructan homologs with DP 1-8. Spectra obtained using Method 2.

The changes in types and concentrations of carbohydrates over the annual life cycle is determined by the different phenological stages. The resources required for early growth in the shoots (leaves, scapes and flowers) are withdrawn from the bulbs reserve of stored carbohydrates. The mobilisation of carbohydrates from the bulbs takes place by the depolymerisation of the vacuolar storage of fructans through the action of the hydrolysing enzymes, fructan exo-hydrolases (FEH)s. As a result of the hydrolysis process, terminal fructose units are released leaving behind shorter chain lengths of the polymer. The monosaccharides hence formed are released to the cytoplasm where they are converted into sucrose by sucrose synthase to be exported to the growing organs where the supply of carbon and energy from photosynthesis is not yet sufficient to meet the demand (Edelman and Jefford 1968; Pollock 1986).

2.3.7. The main trisaccharide of bluebell bulbs

The structural elucidation of the isolated trisaccharide in its free and peracetylated form using 1D and 2D NMR spectroscopy was carried out providing the following observations:

The unknown molecule has 18 carbon atoms, as indicated by DEPTQ with a profile attributed to carbohydrates. The primary CH_2-OH carbons at 60-65 ppm, followed by the secondary CH-OH carbons at 70-80 ppm and finally the anomeric protons from 90-110 ppm. In this molecule, the anomeric region showed two peaks around 103 ppm indicating that they were quaternary carbon atoms. The third one showed a correlation to the doublet proton at 5.39 ppm in HSQC. This proton had a *J* value of 3.8 Hz indicating that it is an alpha anomer. Starting from this proton, COSY was used to assign most of the neighbouring protons, HMBC further confirmed the assignments and showed longer range ^{1}H-^{13}C correlations too. Neighbouring protons within the same spin system and their subsequent assignment to a particular sugar was confirmed with HSQC-TOCSY. This also included the protons that could not be identified using COSY due to signal-signal and signal-diagonal overlap of cross peaks. There is a clear and strong HMBC correlation between H1-G and C2-F1 which allowed the identification of the first fructose moiety attached to glucose. This was further supported by the presence of a weak HMBC correlation between C1-G and H1-F1. The obtained information indicated the presence of a trisaccharide from the kestose family (Figure 6).

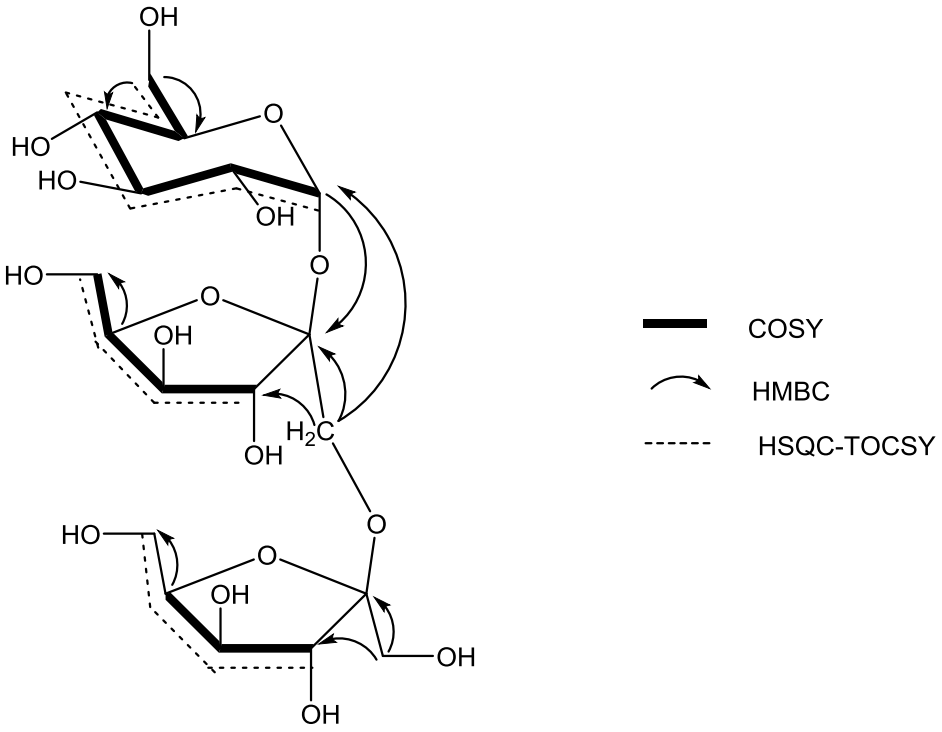

Figure 30 The structure of 1-kestose showing COSY, HSQC-TOCSY and some important HMBC correlation used in the structural assignment.

Previous assignments of the trisaccharides 1-kestose, 6-kestose and neokestose showed that the C and H chemical shift values vary only slightly and therefore comparison of NMR results with literature data can be ambiguous (Calub et al. 1990; De Bruyn and Van Loo 1991; Liu et al. 1991). Unfortunately, HMBC (for the free and peracetylated unknown trisaccharide) did not show any correlations between the second fructose moiety with neither glucose nor fructose 1 that would enable clear identification of the point of attachment and accordingly the type of isomer. It is, however, possible to distinguish the isomers when using reference spectra of the pure compounds. Since it was suspected from the available data that the unknown trisaccharide could have the structure of 1-kestose, an NMR dataset for both free and peracetylated 1-kestose was collected. The NMR spectra from the isolated trisaccharide were in good agreement with those of standard 1-kestose both in the free and peracetylated forms (Figure 118 and Figure 120). The acetylation reaction involves substitution of protons from 11 hydroxyl groups with acetyl groups. This appeared as correlations in HMBC between the sugar protons and their neighbouring acetyl groups (Figure 115 and Figure 123). From this, it was clear that the two protons at CH_2-F1 were not acetylated as no HMBC correlations were present. This indicated that the hydroxyl on CH_2-F1 is not free and must be involved in a glycosidic bond. From the three trisaccharide isomers, 1-kestose is the one with such characteristics and thus the isolated trisaccharide was identified as 1-kestose.

The isolation of 1-kestose from bluebell bulbs does not rule out the presence of the other trisaccharides (6-kestose and neokestose). It is not uncommon for fructan storing plants to contain combinations of more than one type of trisaccharide in varying rations examples include aspagarus (Forsythe and Feather 1989), tulip (Ohyama et al. 1985) and onion bulbs (Shiomi 1978).

Table 2 ^{1}H and ^{13}C chemical shift data of 1-kestose in D_2O and peracetylated 1-kestose in pyridine-D_5 isolated from bluebell bulbs.

Position	δ_H ppm (multiplicity, *J* Hz)		δ_C ppm	
	1-Kestose	**Peracetylated 1-kestose**	**1-Kestose**	**Peracetylated 1-kestose**
D-Glucose				
1	5.43 (d, 3.8)	6.20 (d, 3.7)	92.5	90.2
2	3.54 (dd, 3.9, 10.0)	5.31 (dd, 3.8, 10.4)	71.2	70.9
3	3.75 (t, 9.6)	5.90 (t, 10.0)	72.6	70.4
4	3.47 (t, 9.4)	5.48 (t, 9.9)	69.2	69.2
5	3.84 (m)	4.73 (ddd, 2.3, 4.5, 10.2)	72.4	69.2
6	3.81 (m)	4.49 (m), 4.59 (m)	60.1	62.7
D-Fructose 1				
1	3.71 (d, 12.0), 3.83 (d, 12.4)	4.09 (d, 9.7), 4.24 (d, 9.7)	60.9	63.3
2	-	-	103.2	104.4
3	4.28 (d, 8.7)	6.16 (d, 7.7)	76.6	75.9
4	4.04 (t, 7.7)	5.86 (d, 8.0)	73.8	74.8
5	3.86 (m)	4.57 (m)	81.2	78.8
6	3.77 (m)	4.60 (m), 4.66 (m)	62.2	64.0
D-Fructose 2				
1	3.67 (d, 12.3), 3.74 (d, 12.3)	4.60 (m), 4.67 (m)	60.4	63.6
2	-	-	103.7	103.80
3	4.27 (d, 8.5)	5.92 (d, 6.7)	76.6	77.5
4	4.08 (t, 7.3)	5.75 (t, 6.5)	74.4	76.2

Position	δ_H ppm (multiplicity, *J* Hz)		δ_C ppm	
	1-Kestose	**Peracetylated 1-kestose**	**1-Kestose**	**Peracetylated 1-kestose**
5	3.86 (m)	4.48 (m)	81.1	79.1
6	3.80 (m)	4.59 (m), 4.65 (m)	62.3	64.3

Chapter 3: Bluebell phenolics

3.1. Introduction

3.1.1. Phenolic compounds in plants

Plant phenolics comprise a diverse group of secondary metabolites. With varying chemical properties and physiological functions. They mostly exist as members of either the flavonoids or phenolic acids. Flavonoids, known for their contribution to flower and fruit colours (Brouillard 1988), are compounds with 15 C skeleton that share the basic structure C_6-C_3-C_6 (Figure 31). They are divided into sub-groups based on structural differences in the C_3 group of atoms. Flavonoids are commonly hydroxylated in 3, 5, 7, 3', 4'and/or 5' positions. Compounds within a particular sub-group can differ in the number and position of the hydroxyl groups as well as the presence of different substitution types including methylation, prenylation and acetylation or as sulphated derivatives. Although flavonoids are better known in their basic structural form, they are more commonly found as either *O*- or *C*-glycosides with the former being the more abundant form of glycosylation. *O*-glycosylation occurs through bond formation between a sugar molecule and either the 3- or 7- hydroxyl groups (Harborne and Williams 1988). The occurrence of 5-*O*-glycosides is rare for compounds with a carbonyl group at C4, since the hydroxyl group on C5 will be engaged in H-bonding with the neighbouring carbonyl group (Iwashina et al. 1995). *C*-glycosides on the other hand, are formed by direct bonding to either C_6 or C_8 of the aglycone (Harborne 1988; Vermerris and Nicholson 2007). Flavonoid glycosides can also occur in an acylated form through an ester linkage between the sugar hydroxyl groups and an organic acid which could be either aromatic as the hydroxycinnamic acids or aliphatic such as malonic acid (Heller and Forkmann 1988; Stafford 1990a).

The most common flavonoid glycosides are the mono glycosides. However, higher glycosylation with up to 4 sugar moieties are also frequent with glucose, galactose, rhamnose, arabinose, xylose, glucuronic and galacturonic acids being the most common glycosides (Markham 1989).

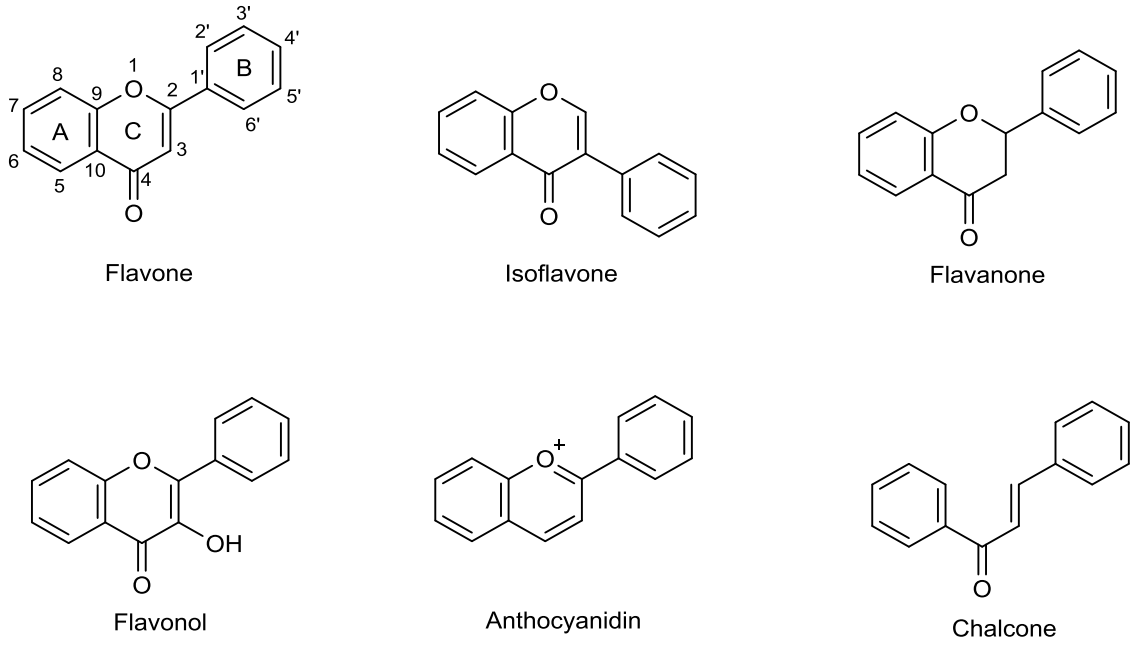

Figure 31 The basic structures of the main classes of flavonoids.

The second class of phenolic compounds are the phenolic acids. These compounds are most commonly found as members of the hydroxycinnamic acid group of compounds with a basic structure of C_6-C_3 (Figure 32). They usually occur as esters of sugars or organic acids such as quinic, shikimic and tartaric acids (Vermerris and Nicholson 2007). Another sub-class of the phenolic acids is the hydroxybenzoic acid group with the C_6-C_1 basic structure. Members of this family include compounds as protocatechuic, syringic and vanillic acid (Kuwatsuka and Shindo 1973; Raskin 1992). Variations in the basic structure of phenolic acids occur due to differences in the number and position of the hydroxyl and/or methoxy groups on 3 and 5 positions of the aromatic ring. In addition to the wide distribution of hydroxycinnamic acids in all plant families and their significant contribution to cell wall lignification (Harris and Hartley 1976), they are also known for their contribution to plant-plant communication and allelopathy (Inderjit 1996).

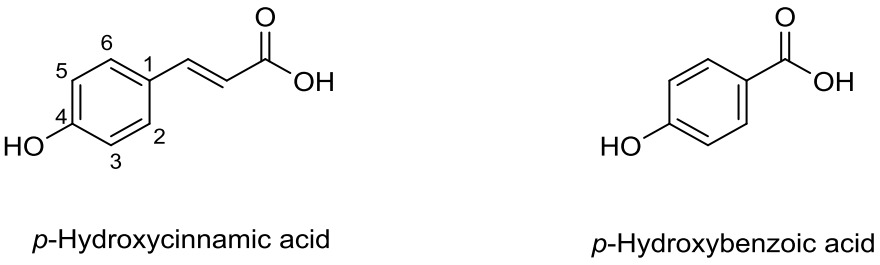

Figure 32 The basic structure of phenolic acids.

Another class of secondary metabolites is the phenylethanoid glycosides (Figure 33). This class includes polar compounds, biosynthetically related to the phenolics, and can also contain phenolic acids as part of the structure. These compounds are sometimes referred to as phenylpropanoids when cinnamic acid derivatives are linked to the sugar. The basic structure of these compounds comprises a glucose linked to a *β*-phenylethanol via a glycosidic linkage. High structural variations arise from the different structures and positions the R groups can take. These compounds commonly occur as either diglycosides or triglycosides in which case they mostly contain rhamnose linked to the central glucose moiety. R_1 and R_2 are the common points for the attachment of extra glycosidic units, whereas substitution on R_3 is rather restricted to hydroxycinnamic acids including caffeic and ferulic as the more common conjugates and to less extent coumaric acid. R_5 and R_6 are found to be either -H, -OH or -OCH_3. However, the substitution pattern is not restricted to the above order and different moieties can occur at various positions (Jiménez and Riguera 1994).

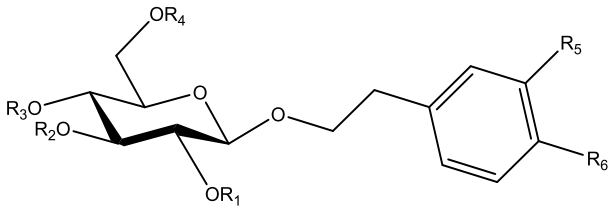

Figure 33 The basic structure of phenylethanoid glycosides.

3.1.2. Metabolism and localisation of plant phenolics

The biosynthesis of plant phenolics starts at the shikimate route which is also the synthetic pathway for aromatic amino acids. The resulting products encompass a large number of secondary metabolites containing a hydroxylated aromatic ring.

Hydroxycinnamic acid derivatives are synthesised from phenylalanine by the action of the enzyme phenylalanine ammonia-lyase (Figure 34) which produces cinnamic acid. This is then hydroxylated at the C4 position to give *p*-coumaric acid which could undergo futher hydroxylation and methylation resulting in different members of the hydroxyxinnamic acid family (Barz and Hoesel 1979). These compounds can be further polymerised into lignin and incorporated into cell walls. Additionally, the shikimate pathway also gives rise to the hydroxybenzoic acids either directly from shikimic acid or by the degradation of the C_3 side chain of hydroxycinnamic acids. Compounds produced in this route also include phenols and quinones (Harborne 1989; Raskin 1992).

The shikimate pathway can result in the production of phenylethanoid glycosides. The phenylpropanoid part of the molecule is found to arise from phenylalanine and cinnamic acid, while the hydroxyphenyl ethanol moiety is derived from either tyrosine or tyramine (Ellis 1983; Jia et al. 2015; Saimaru and Orihara 2010).

Flavonoids are biosynthesised by the condensation of hydroxycinnamic acids with 3 malonyl residues resulting in the formation of the C_6-C_3-C_6 basic structure. A step that is widely considered as a combination of the shikimate and the acetate pathways. The C_3 part of the molecule commonly undergoes cyclisation forming the middle ring (C) (Harborne 1989; Heller and Forkmann 1988).

Plants usually produce a range of phenolic compounds. HPLC analysis of leaves and flowers of Crataegus showed the presence of vitexin and quercetin (Rehwald et al. 1994) and a combination of different proportions of quercetin, kaempferol, myrecetin and luteolin was identified in a number of vegetables and fruits (Hertog et al. 1992).

Phenolic compounds are stored primarily in the vacuoles after their synthesis in the cytoplasm (Beckman 2000) predominantly as their glycosylated derivatives (Wollenweber et al. 1982). Glycosylation acts to detoxify and stabilise the aglycone and prevent their damaging effect on the cytoplasm. It also renders the compound (especially flavonoids) soluble in the vacuolar sap along with other polar constituents like fructans and inorganic ions (Miller et al. 2011). Polar phenolic compounds could also be transferred to the cell wall where they are incorporated in the polymeric structures leading to lignification. Non-polar phenolic compounds commonly present as either the aglycone structure or modified with less polar moieties such as methyl or prenyl groups are usually packaged into vesicles and transported to extracytoplasmic locations where they participate in defence against herbivores and pathogens and contribute to stress resistance (Beckman 2000; Hutzler et al. 1998; McClure 1979; Solovchenko 2010).

Methylation of the hydroxyl groups is found to occur at the levels of both hydroxycinnamic acid and the chalcone (Poulton 1981). Glycosylation occurs at different stages: *O*-linked glycosides are formed at the end of the metabolic pathway with the reaction taking place at the boundary of the tonoplast during the transfer of the phenolic compounds. However, incorporation of a *C*-glycoside is found to occur at an early stage of the biosynthetic pathway. This is supported by the fact that no *C*-glycosyltransferases have been found as opposed to the *O*-glycosyltransferases isolated from different sources. Another reason is that the *C*-glycosyl

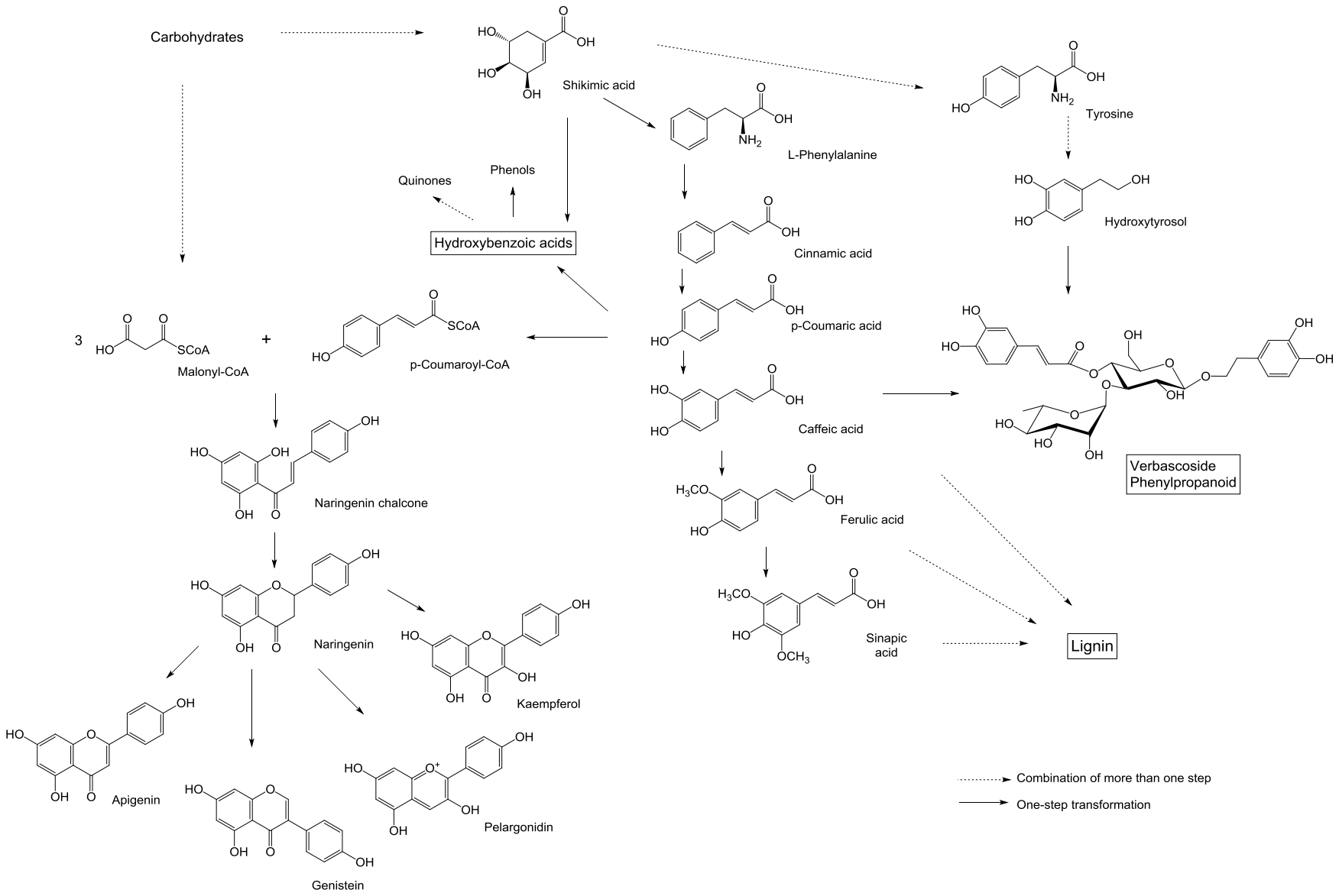

Figure 34 Biosynthsis of plant phenolics. {{366 Harborne, Jeffrey B. 1988; 369 Heller, Werner 1988; 450 Cheynier, Véronique 2013; 459 Alipieva, Kalina 2014; 514 Saimaru, Hiroshi 2010}}.

moieties are linked directly to the carbon backbone of ring (A) originally derived from 3 molecules of malonyl-CoA (Iwashina 2000; Stafford 1990a).Conjugation by the addition of acyl groups is also common and it involves the addition of both aromatic (mostly cinnamic acids) and aliphatic (e.g. malonic) acids to flavonoid glycosides. Acylation is reported to facilitate the uptake of the flavonoids into the vacuole (Matern et al. 1986; Stafford 1990a).

Metabolism of plant phenolics, as is the case with other secondary compounds, is an equilibrium between simultaneous synthesis and breakdown and this is linked to the larger system of complete metabolism in the plant (Barz and Köster 1981). Plant phenolics undergo turnover (also known as further metabolism) at different physiological stages. These changes can take the following forms:

1. Interconversion to other products in a particular sequence of the biosynthetic pathway as in the formation of coumarins from cinnamic acids.
2. Formation of new compounds by either addition or removal of chemical structures.
3. Conversion into higher molecular weight polymeric compounds by oxidative polymerisation such as tannins.
4. Catabolism resulting in the formation of simple products.

Degradation by peroxidising enzymes is the common catabolic reaction and it is found to yield C_6-C_1 and C_6-C_2 structures as a result for flavonoid breakdown in addition to CO_2 and other catabolites (Barz and Hoesel 1979; Stafford 1990b).

3.1.3. Ecological significance of plant phenolics

3.1.3.1. Allelopathy

Allelopathy is the ecological phenomenon involving chemical compounds produced and released to the environment by a plant (or organism in a wider context) that can affect the growth and survival of other plants and organisms within the ecosystem. This influence can be either adverse with negative influence on the surrounding species or beneficial (Li et al. 2010). Plant phenolics comprise a significant group of allelochemicals including the phenolic acids and flavonoids in addition to coumarins and tannins. Allelopathy is not restricted to phenolics as other classes of plant metabolites such as aliphatic aldehydes and ketones, straight chain fatty acids and alcohols, soluble organic acids, alkaloids can also show such effects (Narwal and Sampietro 2009).

Soil phenolics are commonly derived from plant root exudates or leaf litter leachates. Decomposition of flavonoids by microbial action can exert allelopathic effects that result in disruption of physiological processes in other plants. These can include negatively affecting the availability of phosphorous and potassium in soil, photosynthesis and respiration, protein synthesis and growth, membrane permeability, cell division and elongation in addition to other mechanisms including xylem element clogging and internal water transport relations (Cesco et al. 2012; Li et al. 2010; Narwal and Sampietro 2009). Phenolic allelochemicals can have beneficial effects for sustainable agricultural crop production by assisting root nodulation and their colonisation with beneficial bacteria such as arbuscular mycorrhizal fungi (AMF) and providing defence against plant parasites and insect pests. Plant seeds benefit from protection provided by phenolics through antimicrobial and antifungal flavonoids stored both inside and on the outer protective coatings (Mandal et al. 2010; Ndakidemi and Dakora 2003; Shirley 1998).

3.1.3.2. Plant defence

A general defence strategy against plant herbivores is through the lignified secondary cell wall since it can confer mechanical resistance due to its rigid and impermeable structures as well as chemical resistance offered by the monomeric precursors of lignin (e.g. *p*-coumaric and ferulic acids) (Bacic et al. 1988). In general, low plant phenolic concentration is linked to higher herbivory incidents (Zucker 1982). Leaf beetles were found to feed preferentially on willow plants with significantly low phenolic content compared to the control (Larsson et al. 1986). The concentration and distribution pattern of the compounds appear to confer different degrees of resistance (Tahvanainen et al. 1985). Other herbivores including mammals, birds and slugs also show preference for plants with low content of phenolics especially tannins (Bennett and Wallsgrove 1994; Hagerman and Robbins 1993). Phenolics deter herbivory through a range of mechanisms including: 1) the secretion of polymeric tannins that can bind with proteins or polymerise into glue-like substances and trap insects, 2) Hydrolysis of flavonoid glycosides and the release of toxic aglycones when the containing tissues are damaged or 3) by deposition on the outer surface of leaves as in the case of non-polar phenolics (Baldwin et al. 2001; Hagerman and Robbins 1993; Harborne 1979). It is worth mentioning however, that certain phenolic compounds can work as phagostimulants as in the case of quercetin-3-glucoside in the pollen of sunflower that attracts corn rootwarm that feeds on the pollen (Lin and Mullin 1999). There are also cases when a phenolic deterrent becomes attractant at lower

concentrations as with genistein from red clover when tested against red legged earth mites (Wang et al. 1998).

3.1.3.3. Pollinator attraction and seed dispersal

Flavonoids are responsible for the majority of flower colours. The anthocyanins give a wide range of colours such as blue, purple and red and the different shades in between. Other yellow and colourless flavonoids are responsible for white and cream flower petal colours (Harborne 1993; Miller et al. 2011). Flower colours work as general clues to attract pollinating insects and birds from a distance and lead them to the flower. In special cases, the distribution of the flavonoids is restricted to specific areas of the flower such as the flower base or on the petal tip. These patterns are known as pollen guides that absorb in the UV light and could be perceived by food seeking insects and orient them to where the pollen and nectar are located (Brouillard 1988; Harborne 1979). This is especially true when carotenoids are the main pigment as in yellow flower colours (Harborne and Nash 1984; Thompson et al. 1972). Flavonoids in fruits can also be a factor to attract fruit-eating animals that can assist in the dispersion of seeds (Gould and Lister 2006).

Flower colours are affected by a combination of chemical and physical factors such as pH, temperature, UV light, structural modifications including conjugation with sugars and acetylation, the presence of metal ions, and co-pigmentation with other flavonoids and their spatial orientation (Kondo et al. 1992; Miller et al. 2011; Yoshida et al. 2009). They are also affected by physiological changes of different stages in plant's life e.g., flowers pre- and post-pollination or fruits at different stages of maturation (Oren-Shamir et al. 1999).

3.1.3.4. Symbiosis and nutrient cycling

Flavonoid exuded from plant roots to the rhizosphere can act as signals to attract bacteria and fungi and also to induce gene transcription and protein synthesis in beneficial colonising bacteria (symbionts) which provide the plant with nutrients essential for growth and general fitness (Phillips and Tsai 1992; Treutter 2006). Colonisation by beneficial nitrogen-fixing bacteria in legume roots is an example on such a symbiotic relationship (Xie et al. 1995). This can occur in non-leguminous plants as well and a universal example is root colonisation by arbuscular mycorrhizal fungi which help provide mineral nutrients (in particular phosphorous) to plants growing in poor soils (Gianinazzi-Pearson 1996; Shirley 1996; Vierheilig et al. 1998).

Apart from nutrient uptake through symbiosis, phenolics can contribute to nutrient cycling and availability through either direct complex formation with metal ions or after humification

whereby phenolics in their oxidised quinone forms can form a metal holding matrix though covalent bonding to other chemical constituents such as sugars and amides (Appel 1993).

3.1.3.5. Stress resistance

Flavonoids are known to contribute to plant's resistance to different types of stress and their biosynthesis increases as a response mechanism to different unfavourable environmental factors (Bornman et al. 1997; Treutter 2006). The most remarkable is their antioxidant activity and contribution to plant protection from UV light. It has been argued that phenolic compounds require their antioxidant properties for most of their physiological activities and stress resistance (Appel 1993; Solovchenko 2010). In addition to the general increase in flavonoid synthesis under UV stress, it is found that some flavonoids show differential increase, especially those with additional hydroxyl groups on the B ring. Strong correlation was found between UV-B levels and the increase in luteolin: apigenin ratio in liverwort even when no change occurred in the total flavonoid content (Agati et al. 2012; Markham et al. 1998). One important feature of phenolic compounds in this aspect is their distribution in the tissues prone to oxidative damage. In rye leaves for example, esters of hydroxycinnamic acids were located in the epidermal part while anthocyanins and luteolin glucuronides were found in the mesophyll. Such a distribution of phenolic acids and flavonoids was found to contribute beneficially towards DNA repair after high level UV-B treatment in these tissues (Hutzler et al. 1998; Schmitz-Hoerner and Weissenböck 2003).

Phenolic compounds also contribute to cold hardening and cold stress resistance in plants. Extracellular ice formation in tissues under cold stress could be decreased through hardening of these tissues. One mechanism involved is deposition of lignin in their cell walls resulting in increased resistance to the damage from ice formation (Denness et al. 2011). Another mechanism is through super cooling of tissue water before freezing by intervening in the crystallisation (Chalker-Scott 1999; Sakai and Larcher 1987).

High temperature stress was also found to influence flavonoid synthesis (Gould and Lister 2006; Teklemariam and Blake 2003). Dehydration was found to increase anthocyanin synthesis up to 3-4 times compared to hydrated plants (Sherwin and Farrant 1998).

The effect from some of the stress factors can be synergetic (e.g., high temperature or draught and UV-B) (Sherwin and Farrant 1998; Teklemariam and Blake 2003). Cross resistance is also common as when increase in UV-B resistance can also cause increased tolerance to draught and cold stress (Chalker-Scott 1999).

3.1.4. Biological activity and health improving effects

Phenolic compounds have received significant attention for their health improving effects and biological activities. These compounds are broadly distributed in edible and medicinal plants (Hertog et al. 1992; Tawaha et al. 2007), have low dietary toxicity and high antioxidant activity (Li et al. 2008; Tawaha et al. 2007). Flavonoids possess cytotoxic activities and are found effective in diminishing tumour growth and propagation in different types of cancer including colon, lung, ovarian and prostate cancer amongst various others (Dai and Mumper 2010; Franzen et al. 2009; Hu et al. 2008; Shukla and Gupta 2010). Phenolic compounds also exhibit anti-inflammatory and antimicrobial effects (Oliveira et al. 2008; Pan et al. 2010; Pelzer et al. 1998), have the potential to prevent dementia (Commenges et al. 2000) and can contribute to protection against coronary heart diseases (Hertog et al. 1993; MOJŠIŁOVÊ and Kuchta 2001).

3.1.5. Sample preparation and techniques in plant phenolic analysis

3.1.5.1. Sample extraction, clean-up and fractionation

Extraction is the first stage in the isolation of phenolic compounds. Plant samples used could be either fresh, dried or frozen. Solvent extraction is the most common way of extraction due to its wide applicability, ease of use and efficiency. Extraction conditions can vary widely based on the plant matrix, the chemical nature of the target phenolic compounds, their concentration in the sample, their polarity and stability. Accordingly, a range of various solvents could be used such as water, methanol, ethanol, ethyl acetate and acetone. Factors like solvent: sample ratio, extraction time, temperature and pH can affect the recovery of the target compound from the sample.

Crude extracts usually contain large quantities of other compounds such as carbohydrates. One common strategy to remove these compounds is through the use of solid phase extraction (SPE) cartridges. Cartridges with various stationary phases are available that can provide separation based on polarity and acidity of the compounds, but the most common one being used is C_{18}. When an aqueous solution of the crude extract is passed through the cartridge, the phenolic compounds get adsorbed onto the cartridge while the more polar components could be washed off with water. The phenolics are then eluted with a less polar solvent such as methanol.

Column chromatography is used to provide further fractionation of the extract when isolation of pure compounds is required. Separation could be achieved either on silica or C_{18} stationary

phases with mobile phases ranging from non-polar mixtures such as MeOH: $CHCl_3$ to polar combinations of water: MeCN or MeOH (Dai and Mumper 2010; de Rijke et al. 2006; Khoddami et al. 2013; Stalikas 2007).

3.1.5.2. Acidic and alkaline hydrolysis

Hydrolysis of phenolic glycosides is commonly employed to assist characterisation and structural elucidation. Varying the concentration of the acid used in the hydrolysis and the reaction time can reveal different information about the number and nature of the sugars attached. Alkaline hydrolysis additionally releases the bound phenolic acids. Hydrolysis is also used to simplify chromatographic analyses, especially in situations where standards are not available (Markham 1989).

Acid hydrolysis is usually achieved using HCl with concentrations ranging from 1 – 2 M and heating at 100 ^{o}C for 1-2 hr. For alkaline hydrolysis, NaOH is used with concentrations ranging from 1 – 4 M at room temperature. Reaction time can vary from 15 min to overnight commonly in the dark and under inert condition of either N_2 or argon (Stalikas 2007).

Applying hydrolysis can have drawbacks on the analysis of phenolics as it results in the decrease of the amount of information obtained in a chromatographic run (Markham 1989). It can also result in underestimation due to decomposition of aglycones under reaction conditions. The time required for hydrolysis can vary based on the type of glycoside on the 7-hydroxyl group of the aglycone. For glucuronic acid, glucose and rhamnose moieties, the time required was 180, 25 and 5 min respectively (Harborne 1965). Similarly, the time required for the release of a particular aglycone can result in the decomposition of another. Therefore, the optimum hydrolysis condition for a particular analysis is a compromise between production of an aglycone and its decomposition (Nuutila et al. 2002). Another disadvantage is that under reaction conditions of acid hydrolysis, phenolic acids like *o*-coumaric and sinapic acids might undergo decomposition ranging from 15 – 95% (Krygier et al. 1982).

3.1.5.3. High-performance liquid chromatography with diode array detection (HPLC-DAD)

HPLC is the preferred and the most common technique for the separation and quantification of phenolic compounds in complex mixtures. Separation is achieved utilising the differences in affinities of the compounds to the packing material in the chromatographic column. Changing the ionic strength of the mobile phase or its pH, more commonly in a gradient elution, will allow the different compounds to elute separately (Khoddami et al. 2013; Vermerris and

Nicholson 2007). The elution of different compounds is monitored with a UV- visible DAD detector which is known to have high sensitivity, generally unaffected by fluctuations in temperature and well suited for use with gradient elutions. A significant advantage of these detectors is that they can provide useful information about peak purity (Meyer 2013).

Phenolic compounds absorb the electromagnetic radiation in the range 245 – 550 nm. Flavonoids are characterised by two absorption maxima. The first could be found in the range 245 - 285 nm (Band 1) due to ring B, and the second from 300 – 550 nm (Band 2) related to the pattern of substitution and conjugation on ring C (Giusti and Wrolstad 2001; Stalikas 2007).

In addition to its applicability in quantitative analysis, HPLC-DAD is also useful in general screening analysis to identify the sub-class of the flavonoids present. However, different phenolic glycosides belonging to the same sub-class cannot be distinguished (de Rijke et al. 2006).

3.1.5.4. Mass spectrometry (MS)

The identity of a compound could be confirmed from its MS data combined to LC-UV utilising reference database and standard compounds. However, for the identification and structural elucidation of an unknown compound, MS/MS or MS^n is required. LC-MS with atmospheric pressure chemical ionisation (APCI) and (electrospray ionisation) ESI are commonly used for this purpose with the latter being used more frequently. In the analysis of flavonoids, both negative (NI) and positive ionisation (PI) modes are used. Useful information about the structural identity of the compound is obtained in the PI mode, however, the NI mode is known to provide better sensitivity. MS/MS analysis of flavonoid glycosides is useful in identifying the type of the sugars present, although no information could be obtained about their stereochemistry. It also provides information about the type of glycosides (whether *O*- or *C*-linked). Furthermore, it can distinguish between the positions of glycosylation (3-*O*-, 7-*O*-, 6-*C*- or 8-*C*-) (de Rijke et al. 2006; Fossen and Andersen 2006; March et al. 2006).

For the structural analysis of flavonoid glycosides, a systematic nomenclature is used for the produced fragment ions which is based on combination of the models proposed by (Ma et al. 1997) and (Domon and Costello 1988) for the aglycone and glycan parts respectively (Figure 35) . In the case of free aglycones, fragments containing A- and B-rings are referred to as $^{ij}A_0$ and $^{ij}B_0$ respectively. Where the superscripts I and j represents the broken bonds in C-ring. For flavonoid glycosides, ions containing the aglycone are denoted X_j, Y_j and Z_j where the subscript *j* refers to the number of the glycosidic bonds broken counting from the aglycone. On

the other hand, fragments containing the glycan portions are labelled as A*i*, B*i* and C*i* where *i* represents the number of bonds broken counting from the terminal sugar. In the case of *C*-glycosides, the fragment Y_0 is produced when the *C*-glycosyl unit is lost.

Type of the sugar moieties can be identified from the mass of their different fragment ions A_i, B_i and C_i. The masses of these fragment ions can be calculated from the differences between the molecular ion mass and X_i, Y_i and Z_i fragments. This makes identifying these fragments possible even when they are not actually present in the spectrum. The loss of fragments of 162, 146 and 132 mass units indicates the presence of a hexose, a pentose and a deoxyhexose respectively (Vukics and Guttman 2010).

The type of glycosylation *O*- and *C*- glycosides could be distinguished from their fragment ions. For instance, at medium fragmentation energy, *C*-glycosides yield fragments resulting predominantly from intraglycosidic bond cleavage ^{ij}X and water molecule losses. *O*-glycosides on the other hand, give rise to distinctive Y*i* fragment ions (Vukics et al. 2008).

O-glycosides are found to occur more commonly at 3- and 7-positions. (Cuyckens and Claeys 2004). For a flavonoid-3,7- diglycoside molecule, the 3-glycan moiety can be identified by the notably higher intensity signal in the PI mode compared to that resulting from the 7-*O*-glycan of the same molecule (Sakushima et al. 1988). This also holds true when the two glycans are on different molecules as in flavonoid-3-glycosides in comparison to flavonoid-7-glycosides (Grayer et al. 2000). *C*-glycosides on the other hand, are found exclusively as the 6- and 8-*C* conjugates (Cuyckens and Claeys 2004). The molecular ion in both PI and NI loses a water molecule. The resulting fragment is of significantly higher intensity for the 8-C glycans. Water loss occurs between the 2”-OH group of the sugar and either 5- or 7-OH groups of the aglycone and the process is facilitated by H-bonding between these groups. Glycans linked to C-6 have two neighbouring hydroxyl groups on both 5- and 7- position as opposed to one hydroxyl group on 7- position for the C-8 glycan. This means better opportunity for forming H-bonds for the 6- isomer and consequently higher chance of losing a water molecule (Li et al. 1992).

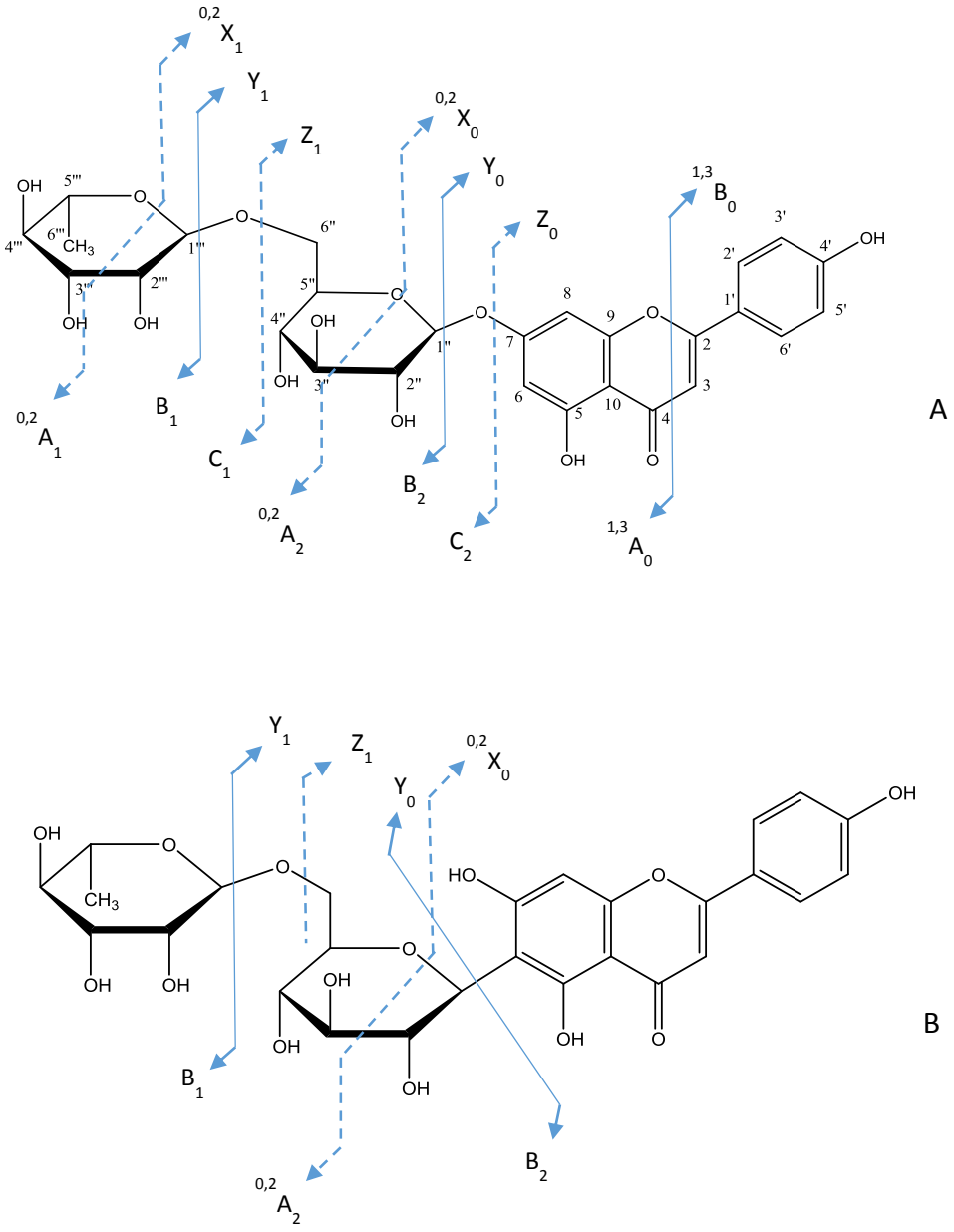

Figure 35 Nomenclature of fragments for flavonoid-O-glycosides (A) and flavonoid-C,O- and C-glycosides (B). Reproduced based on (Domon and Costello 1988; Ma et al. 1997; Vukics and Guttman 2010).

The type of the sugar moiety linked to the aglycone in C-glycosides can be identified by the distinctive ^{ij}X ions resulting from cross-ring bond cleavage. Figure 36 illustrates the fragments obtained for both hexoses and pentoses (Cuyckens and Claeys 2004; Marston and Hostettmann 2006).

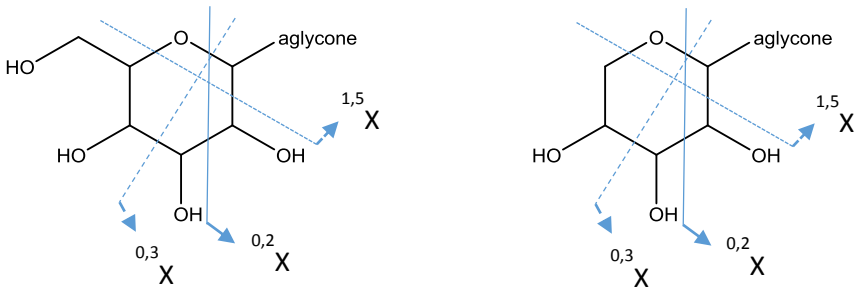

Hexose
^{0,2}X: [M±H – 120]
^{0,3}X: [M±H – 90]
^{0,5}X: [M±H – 134]

Pentose
^{0,2}X: [M±H – 90]
^{0,3}X: [M±H – 60]
^{0,5}X: [M±H – 104]

Figure 36 Fragment ions produced for hexoses and pentoses from cross-ring cleavage. Reproduced from (Cuyckens and Claeys 2004).

3.1.5.5. Nuclear magnetic resonance (NMR) spectroscopy

Despite the high sensitivity of MS and its ease of use, it is uncapable of providing the complete structural analysis of phenolic compounds. The potential of NMR as a powerful technique and a complementary tool appears in the possibility of complete structural identification utilising both 1D and 2D techniques including ^{1}H NMR, ^{13}C NMR, ^{1}H-^{1}H COSY, ^{1}H-^{13}C HSQC and HMBC. A range of deuterated solvents could be used provided the solubility, stability and ease of retrieval of the compound from it. Drawbacks of using NMR spectroscopy is its limited sensitivity and the requirement of relatively large quantities of the compound (Fossen and Andersen 2006; Robards 2003).

3.2. Methods

3.2.1. LC-MS analysis of bluebell phenolics

3.2.1.1. Preparation of methanolic extracts, acids and alkaline hydrolysates

Freeze-dried and powdered flowers, scapes and leaves collected in 15/05/2014 (3.0 g) each were extracted with MeOH (300 mL) by shaking for 2 hr. the extracts were filtered and the solvent removed on a rotary evaporator. The crude dry residues were re-dissolved in a 6 mL water containing about 10% MeOH. Each solution was divided into three 2 mL aliquots to be used for preparing the methanolic extract and for acid and alkaline hydrolysis as follows:

The methanolic extract: The first aliquot was centrifuged briefly for 3 min on 6000 rpm (technico Mini) then passed through a Sep-Pak C_{18} (1 mL) cartridge. The unbound material were washed off with an aqueous solution of 1% acetic acid and the bound part was eluted with 2 mL MeOH. This was labelled as the flower, scape or leaves extract.

The acid hydrolysate: The second aliquot was used to prepare the acid hydrolysate by adding 5 mL of 4 M HCl prepared in 50 % MeOH in water and heated for 4 hr on 95 ^{o}C. MeOH was removed from the reaction product by evaporation under vacuum, the pH of the remaining aqueous mixture was adjusted to 4 – 6 and the mixture was put through a Sep-Pak C_{18} cartridge as with the first aliquot.

The alkaline hydrolysate: For alkaline hydrolysis, 10 mL of 1 M NaOH was added to the third aliquot and the reaction mixture was stirred in the dark for 4 hr with continuous bubbling of N_2 gas through. At the end of the reaction, the pH of the mixture was adjusted to slightly acidic (4 – 6) and passed through Sep-Pak cartridges as before.

3.2.1.2. LC –MS analysis[1]

HPLC-MS analysis was performed on a Thermo Finnigan LC-MS system (Thermo Electron Corp., Waltham, MA, USA) utilising ESI source and a Finnigan LTQ linear ion trap and Finnigan Surveyor PDA Plus detector. The column used in the analysis was C18 Nova-Pak (Waters) (3.9 mm × 100 mm i.d., 4 µm). The temperature of the auto sampler tray was preserved at 5 ^{o}C while the temperature of the column at 30 ^{o}C. The PDA detector was set to the range 240 – 400 nm. A flow rate of 1 mL/min was applied with 100 µL/min sent to the

[1] Analysis undertaken by Dr Barbara Hauck, Aberystwyth University in collaboration.

mass spectrometer.

Gradient elution was applied in the separation and the solvent system was comprised of Water (A) and methanol (B) both acidified with 0.1% v/v formic acid. The gradient applied was 5 – 60% B in 65 min.

Mass spectra were acquired in negative and positive ionisation mode with the following parameters: nitrogen sheath gas 30 arbitrary units, nitrogen auxiliary gas 15 arbitrary units and capillary temperature 320 °C. Spray voltage was 4.0 kV in negative ionisation mode and 4.8kV in positive ionisation mode, capillary voltage -1 V and 45 V, respectively, and tube lens offset -68 V and 110 V. MS/MS fragmentation was carried out at normalised collision energy of 35 % and isolation width 2.0 (*m/z*). For MS^n of aglycone cores and flavonoid standards, collision energy was set to 70%.

3.2.2. Isolation of secondary metabolites from bluebell flowers

3.2.2.1. Preparation of the bluebell flowers extract

Dried bluebell flowers (124 g) were extracted with MeOH (2.5 L) by soaking overnight and occasional stirring. The extraction was repeated two more times. The extracts were combined and dried down using a rotary evaporator at temperatures below 40 ^oC. The purple coloured residue was dissolved in water and adsorbed onto 150 mL of HP20 gel previously activated by stirring with MeOH followed by water each for 1 hr. The HP20 gel was separated from the unbound part and washed with deionised water. Then methanol was used to elute the flower extract which was collected and dried down giving a dark purple-coloured powder (11.13 g).

3.2.2.2. Fractionation of the flower extract

A total of (9 g) of the MeOH extract was fractionated. Portions of (500 mg) of the pigment were adsorbed on (2 mL) of silica and dry loaded onto a C18 column and flash chromatography carried out using the following solvent system: A: MeCN and B: H_2O both acidified with 0.1 % formic acid (FA). The method started with initial 2 min hold at 100 % B, then 100 - 86 % B (2 min), 86 – 80 % B (60 min), 80 – 62 % B (11 min) and held at 62 % B for 5 min. The following fractions were considered for further purification: Fr 1 (550 mg, t_R 8 min), Fr 2 (625 mg, t_R 15 min) and Fr 3 (4500 mg, t_R 75 min) were further investigated.

Fr 1 was dissolved in 10 mL de-ionised water and injected in 2 mL portions onto C18 column. Gradient elution was applied using A: MeCN and B: H_2O both acidified with 0.1% FA starting from 100% B for 2 min then 100 – 75 % B in 50 min. Two fractions Fr 1,1 (26 mg, t_R 24 min)

and Fr 1,2 (47 mg, t_R 33 min) were subjected to further purification.

Fr 1,1 was put through FC with gradient elution as follows: Solvents A: MeCN and B: H_2O both acidified with 0.1% FA starting from 100% B for 2 min then 100 – 97% B in 6 min. Compound DR1 (6.5 mg) was isolated at t_R = 20 min.

Physical appearance: white powder

Mass: HR-FTMS-ESI $[M-H]^-$ gave m/z 445.135 $C_{19}H_{25}O_{12}$ requires 445.135

^1H NMR δ_H ppm (400 MHz, MeOD): 7.42 (1 H, t, *J* 9.9), 7.32 (1 H, t, *J* 7.4), 7.25 (1 H, d, *J* 7.2), 4.93 (1 H, d, *J* 11.5), 4.68 (1 H, d, *J* 11.5), 4.61 (1 H, d, *J* 7.6), 4.57 (1 H, d, *J* 7.6), 3.89 (1 H, dd, *J* 12.0, 1.7), 3.69 (1 H, dd, *J* 12.0, 6.1), 3.68 (1 H, d, *J* 10.6), 3.58 (1 H, t, *J* 8.8), 3.50 (1 H, t, *J* 9.6), 3.49 (1 H, t, *J* 7.6), 3.39 (1 H, t, *J* 9.3), 3.36 (1 H, t, *J* 8.9), 3.30 (1 H, t, *J* 8.9), 3.29 (1 H, m)

^{13}C NMR δ_C ppm (101 MHz, MeOD): 173.5, 138.9, 129.3, 129.0, 128.6, 84.2, 77.8, 77.7, 77.2, 76.9, 75.8, 73.3, 71.9, 71.4, 62.7.

Fr 1,2 was also subjected to FC using the following gradient: Solvents A: MeCN and B: H_2O both acidified with 0.1% FA starting from 100% B for 2 min then 100 – 85% B in 44 min and held for 16 min. Fr 121 (25 mg, t_R 46 min) was collected and further fractionated with C_{18} RP preparative TLC using 15% MeCN in water and two compounds (DR2 and DR3) were isolated with the following characteristics:

DR2 (3.8 mg) was separated at R_f = 0.32.

Physical appearance: white powder

Mass: HR-FTMS-ESI $[M-H]^-$ gave m/z 459.150 $C_{20}H_{27}O_{12}$ requires 459.150.

^1H NMR δ_H ppm (500 MHz, MeOD): 7.25 (2 H, m), 7.24 (2 H, m), 7.18 (1 H, m), 4.60 (1 H, d, *J* 7.9), 4.44 (1 H, d, *J* 7.6), 4.05 (1 H, m), 3.85 (1 H, dd, *J* 12.1, 2.2), 3.79 (1 H, t, *J* 9.7), 3.69 (1 H, m), 3.67 (1 H, m), 3.56 (1 H, t, *J* 8.6), 3.55 (1 H, t, *J* 9.7), 3.41 (1 H, t, *J* 8.9), 3.38 (1 H, t, *J* 8.6), 3.34 (1 H, t, *J* 8.9), 3.29 (1 H, t, *J* 8.0), 3.26 (1 H, m), 2.88 (2 H, t, *J* 7.5).

^{13}C NMR δ_C ppm (126 MHz, MeOD): 171.2, 139.9, 130.1, 129.3, 127.2, 105.5, 103.0, 84.5, 77.5, 76.9, 76.9, 75.6, 73.1, 71.7, 71.2, 62.5, 49.0, 37.2.

DR3 (3.1 mg) isolated with R_f = 0.42.

Physical appearance: yellow powder

Mass: HR-FTMS-ESI $[M-H]^-$ gave m/z 901.225 $C_{38}H_{45}O_{25}$ requires 901.225

^1H NMR δ_H ppm (400 MHz, Pyridine-d5 (500 µL) + MeOD (100 µL)): 8.03 (2 H, d, *J* 8.9), 7.29

(2 H, d, *J* 8.9), 7.23 (1 H, d, *J* 2.5), 7.02 (1 H, d, *J* 2.5), 6.89 (1 H, s), 5.92 (1 H, d, *J* 6.6), 5.29 (1 H, d, *J* 7.9), 4.86 (1 H, d, *J* 7.9), 4.82 (1 H, d, *J* 7.5), 4.67 (1 H, d, *J* 9.1), 4.53 (1 H, dd, *J* 11.2, 2.2), 4.45 (1 H, d, *J* 3.1), 4.43 (2 H, s, *J* 6.2), 4.42 (1 H, d, *J* 1.6), 4.40 (1 H, d, *J* 3.3), 4.21 (2 H, ddd, *J* 17.8, 10.1, 6.8), 4.18 (2 H, t, *J* 9.4), 4.13 (1 H, s), 4.10 (1 H, d, *J* 4.0), 4.06 (2 H, dt, *J* 9.0, 6.1), 4.01 – 3.94 (1 H, m), 3.90 (1 H, d, *J* 8.2), 3.89 – 3.82 (2 H, m), 3.78 (1 H, s), 3.63 (1 H, t, *J* 11.0), 3.61 (1 H, d, *J* 9.5).

^{13}C NMR δ_C ppm (101 MHz, Pyridine-d5 (500 µL) + MeOD (100 µL)): 183.9, 174.3, 166.2, 164.8, 163.4, 163.1, 158.9, 130.0, 123.2, 117.6, 107.6, 106.6, 106.1, 104.8, 104.2, 102.0, 100.7, 96.5, 83.7, 79.1, 78.8, 78.6, 77.9, 77.8, 77.5, 76.7, 76.6, 75.2, 73.5, 72.2, 71.8, 71.6, 70.0, 65.3, 63.2.

Fr 2 was chromatographed applying a gradient elution with A: MeOH and B: H_2O acidified with 0.1% FA as follows: starting at 100% B for 4 min then 100 – 45% B in 20 min and held for 5 min and 45 – 0% in 9 min. DR4 (15 mg) was collected at t_R = 24 min.

Physical appearance: yellow powder

Mass: HR-FTMS-ESI $[M-H]^-$ gave m/z 739.171 $C_{32}H_{35}O_{20}$ requires 739.172

^{1}H NMR δ_H ppm (400 MHz, MeOD): 7.89 (2 H, d, *J* 8.5), 6.93 (2 H, d, *J* 8.5), 6.82 (1 H, d, *J* 1.3), 6.65 (1 H, s), 6.52 (1 H, d, *J* 1.3), 5.35 (1 H, d, *J* 7.0), 4.66 (1 H, d, *J* 7.5), 4.24 (1 H, d, *J* 7.5), 4.01 (1 H, d, *J* 9.5), 3.87 (1 H, t, *J* 7.4), 3.76 (1 H, t, *J* 8.7), 3.76(1 H, dd, *J* 10.0, 3.0), 3.73 (1 H, dd, *J* 12.0, 6.0), 3.67 (1 H, t, *J* 10.0), 3.65 (1 H, m), 3.45 (1 H, t, *J* 9.5), 3.45 (1 H, t, *J* 9.5), 3.40 (1 H, m), 3.28 (1 H, t, *J* 8.2), 3.25 (1 H, t, *J* 8.7), 3.15 (1 H, t, *J* 9.5), 3.07 (1 H, dd, *J* 12.0, 8.0).

^{13}C NMR δ_C ppm (101 MHz, MeOD): 184.1, 166.8, 165.7, 164.4, 162.9, 162.8, 158.9, 129.7, 123.1, 117.1, 107.2, 105.3, 105.2, 104.1, 101.4, 100.1, 96.0, 82.9, 77.6, 77.5, 77.1, 76.9, 75.8, 74.7, 72.7, 71.1, 70.8, 68.7, 66.9.

Fr 3 yielded a saponin which will be considered in more detail in (Chapter 4).

Figure 37 shows an outline for the main steps of the separation.

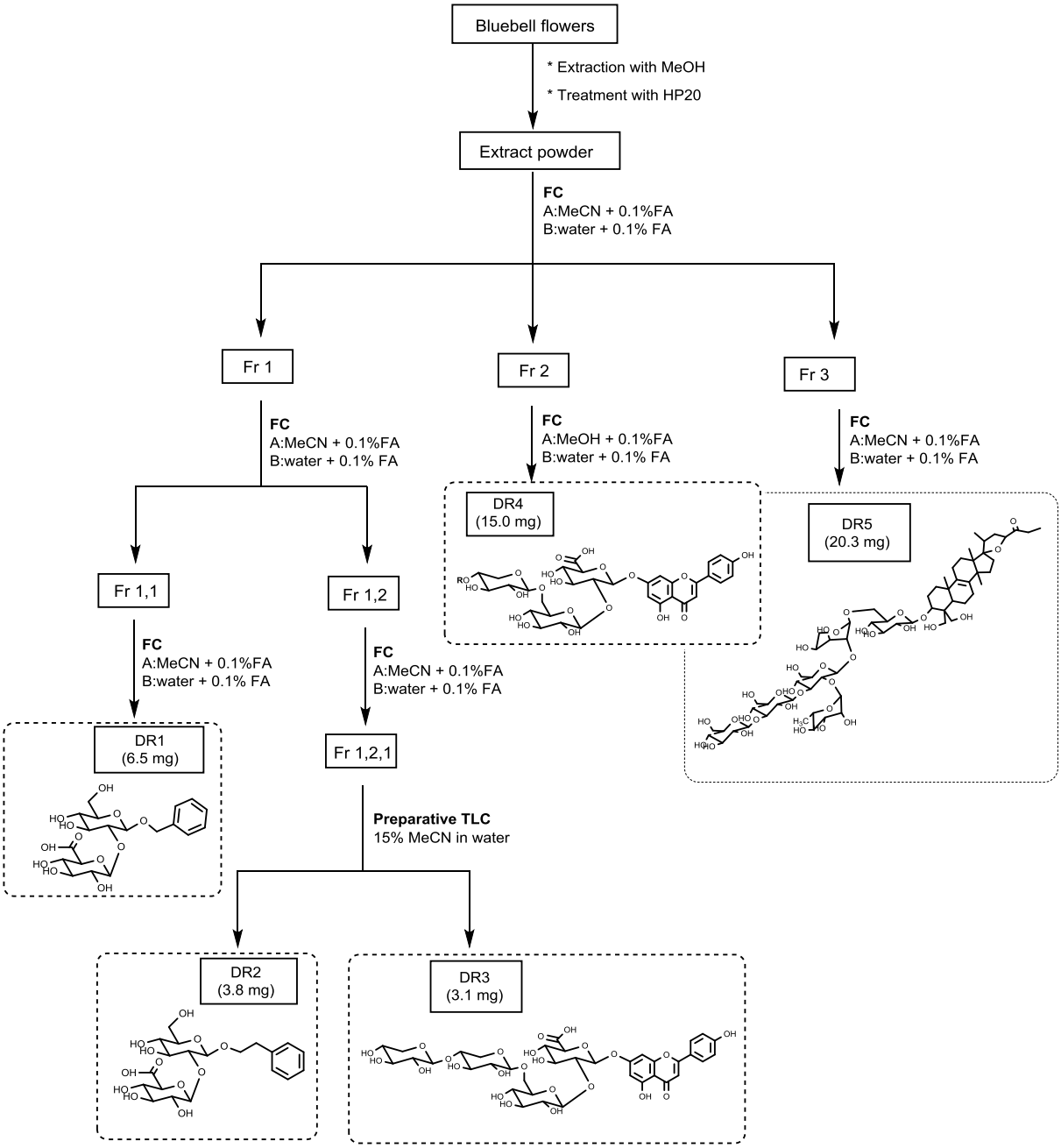

Figure 37 A diagram showing the main stages of the separation of metabolites from bluebell flowers. DR5 is a saponin for which detailed isolation and structural elucidation is covered in Chapter 4.

3.2.3. Seasonal variation of apigenin and *p*-coumaric acid

In order to quantify apigenin and *p*-coumaric acid in their unconjugated forms, the Methanolic extracts had to be hydrolysed and the resulting aglycones identified. This was achieved through the following steps:

3.2.3.1. Large-scale acid hydrolysis and separation of the aglycone

Dry bluebell flowers 30 g were extracted with acidified MeOH (0.5% HCl) and the extract was concentrated to approximately 200 mL. This was hydrolysed according to (GIUSTI and WROLSTAD 1996) using MeOH, H_2O and HCl in volume ratios (50: 33: 17). The mixture of the pigment extract and the acid was refluxed for (2 hr). After this time, the flask was allowed to cool down to RT, and then concentrated on a rotary evaporator. The remaining H_2O-acid solution was partitioned against EtOAc. The EtOAc part was dried down and fractionated using NP column chromatography.

3.2.3.2. Column chromatography of the EtOAc fraction

The EtOAc extract (approx. 1 g) was dry-loaded onto 80 mL silica in a 2.5 cm diameter column. A solvent system of MeOH: $CHCl_3$ was used starting from 100% $CHCl_3$ and increasing MeOH: $CHCl_3$ every 500 mL (0:100 – 8:92) with a final fraction of 100% MeOH. A total of 28 fractions 200 mL each were collected. Similar fractions were mixed together based on C_{18} RP TLC in 50% MeCN and the solvents removed on a rotary evaporator. The residues were then dissolved in a small volumes of $CHCl_3$ (ca. 5 mL) and the solution was let to stand. Shortly afterwards the formation of yellow precipitates was noticed which upon analysis showed relatively high purity. Separation of these precipitates yielded 4 compounds that were identified as follow:

Fraction 6 yielded *p*-Coumaric acid (1) (1.2 mg) with the following characteristics:

Physical appearance: yellow powder

^{1}H NMR δ_H ppm (400 MHz, MeOD): 7.62 (1 H, d, *J* 15.9), 7.47 (2 H, d, *J* 8.6), 6.82 (2 H, d, *J* 8.6), 6.30 (1 H, d, *J* 15.9).

^{13}C NMR δ_H ppm (101 MHz, MeOD): 169.5, 159.7, 145.1, 129.5, 125.8, 115.2, 114.2.

Fractions 7 – 9 gave apigenin (2) (38.5 mg)

Physical appearance: yellow powder

^{1}H NMR δ_H ppm (400 MHz, Pyridine-d5): 7.95 (2 H, d, *J* 8.7), 7.24 (2 H, d, *J* 8.5), 6.93 (1 H, s), 6.84 (1 H, d, *J* 2.0), 6.77 (1 H, d, *J* 2.0).

^{13}C NMR δ_H ppm (101 MHz, Pyridine-d5): 183.3, 166.4, 165.1, 163.7, 163.2, 159.0, 129.4, 122.8, 117.4, 105.5, 104.4, 100.5, 95.4.

From fractions 19 – 23, 7-*O*-(β-D-glucopyranoside methyl uronate) apigenin (3) (16 mg) was

obtained

Physical appearance: yellow powder

^{1}H NMR δ_H ppm (400 MHz, Pyridine-d5 (500 µL) + MeOD (100 µL)): 7.99 (2 H, d, J 8.8), 7.27 (2 H, d, *J* 8.8), 7.14 (1 H, d, *J* 2.2), 6.91 (1 H, s), 6.87 (1 H, d, *J* 2.2), 5.94 (1 H, d, *J* 7.4), 4.87 (1 H, d, *J* 9.6), 4.45 (1 H, t, *J* 9.2), 4.35 (1 H, t, *J* 8.9), 4.29 (1 H, dd, *J* 9.0, 7.5), 3.80 (3 H, s).

^{13}C NMR δ_H ppm (101 MHz, Pyridine-d5 (500 µL) + MeOD (100 µL)): 183.8, 171.0, 166.0, 164.4, 163.4, 163.2, 158.8, 129.9, 122.8, 117.6, 107.6, 104.8, 102.2, 101.3, 96.2, 77.9, 77.8, 75.1, 73.5, 52.6.

Fractions 26 – 28 gave 7-*O*-(β-D-glucopyranosideuronic acid) apigenin (4) (3.0 mg)

Physical appearance: yellow powder

^{1}H NMR δ_H ppm (400 MHz, Pyridine-d5 (500 µL) + MeOD (100 µL)): 7.92 (2 H, d, *J* 8.6), 7.24 (2 H, d, *J* 8.6), 7.20 (1 H, d, *J* 1.5), 6.92 (1 H, s), 6.91 (1 H, d, *J* 1.8), 6.05 (1 H, d, *J* 7.4), 4.99 (1 H, d, *J* 9.7), 4.67 (1 H, t, *J* 9.2), 4.50 (1 H, t, *J* 9.0), 4.43 (1 H, dd, *J* 9.1, 7.5)

^{13}C NMR δ_H ppm (101 MHz, Pyridine-d5 (500 µL) + MeOD (100 µL)): 183.5, 172.9, 165.7, 164.4, 163.3, 163.1, 158.6, 129.7, 122.9, 117.4, 107.4, 104.7, 102.2, 101.3, 96.1, 78.1, 75.1, 73.6.

3.2.3.3. Acid hydrolysis method optimisation

The hydrolysis method was optimised by following the changes in the amount of compounds 1 – 4 in dried bluebell flowers under different reaction conditions. Parameters considered for optimisation were: reaction temperature, reaction time, acid concentration and the ratio of MeOH in the acid solution. For the reaction temperature, hydrolysis was carried out at RT (22.5 ºC), 60, 80 and 100 ºC. Reaction time up to 5.5 h was considered. Hydrochloric acid concentrations ranging from 0.5 – 3.0 M were tested. The ratio of methanol added to the acid solution was also adjusted by experimenting with a range from 0 – 100% MeOH. Duplicate 20 mg freeze-dried and powdered bluebell flower samples were taken in 30 mL vials, 5 mL of the acid solution was added and the vials were capped and heated on a Techne DB-3 heat block. The reaction product was filtered and made up to 10 mL with 50% MeOH: water and 20 µL was injected for HPLC.

High reaction temperature was necessary for the hydrolysis to occur. For the hydrochloric acid, the analyte concentration was found to increase directly with the acid concentrations. However, at concentrations higher than 2 M a decrease was noticed which is most probably due to the

instability of the reaction products at such high acidity. The optimum ratio of MeOH in the acid solution was found to be 50 %. Applying the conditions above, it was found that a reaction time of 2 hr gives the most acceptable results.

3.2.3.4. Quantification of *p*-coumaric acid and apigenin in bluebell samples using HPLC-DAD

Freeze-dried and powdered samples of different parts of bluebell were used in this analysis. Samples were subjected to acid hydrolysis and analysed with HPLC using the procedure mentioned in (Total non-structural carbohydrates (TNC) by acid hydrolysis, p18). Calibration standards were *p*-coumaric acid (0.0015 – 0.1 mg. mL^{-1}), y= $4x10^{-4}x$, R^2=0.9998; apigenin (0.0015 – 0.1 mg. mL^{-1}), y= $7x10^{-4}x$, R^2=0.9998; Apigenin methyl glucoronate (0.0015 – 0.1 mg. mL^{-1}), y= $1.4x10^{-3}x$, R^2=0.9998; Apigenin methyl glucuronic acid (0.0004 – 0.03 mg. mL^{-1}), y= $1.4x10^{-3}x$, R^2=0.9975. *p*-Coumaric acid was quantified at 310 nm, apigenin and its two glycosylated conjugates at 335 nm. The calculated amounts were converted from mg. mL^{-1} to mg. g^{-1} DW basis using Equation (2).

For both methyl apigenin-7-O-*β*-D-glucuronate and apigenin-7-O-*β*-D-glucuronic acid, their values were corrected to give the corresponding equivalent amount of apigenin as follows:

$$C_{Apigenin}\ (mg.g^{-1}DW) = C_{Compound}\ (mg.g^{-1}DW) \times MWt_{Apigenin}/MWt_{Compound} \quad (7)$$

Where,

$MWt_{Apigenin}$ = 270.24 g. mol^{-1}

$MWt_{Compound}$ = 460.39 g. mol^{-1} for methyl apigenin-7-O-*β*-D-glucuronate or
446.36 g. mol^{-1} for apigenin-7-O-*β*-D-glucuronic acid

The values obtained were then summed up to give the total concentration of apigenin in the sample.

3.3. Results and Discussion

3.3.1. LC-MS analysis of bluebell flowers

HPLC-PDA coupled to ESI-MS analysis was used to study the phenolic profile of the flowers, leaves and scapes. Figure 38 shows the chromatograms obtained in the analysis. HPLC-PDA used to identify the class of the compounds present. In general, the phenolic acids, apigenin glycosides and their conjugates with *p*-coumaric acid were identified from their UV spectra (Figure 39). Further structural information was collected from the LC-MS and MS-MS analysis which included general scan events in the negative and positive modes in addition to a data-dependent scan whereby the most abundant ions where selected for MS^2 analysis. In addition to the UV spectra and MS data of the phenolic conjugates, comparison of aglycones produced from acid hydrolysis reactions such as *p*-coumaric acid, apigenin, luteolin, naringenin and eriodictyol with reference compounds in terms of UV spectra, t_R, Mwt and fragmentation as well as literature values were used to confirm their identification. Neutral mass losses were used for identification of the different moieties conjugated to the aglycones as follows:

42	Acetyl (in conjugation to hexoses giving rise to 204)
86	Malonyl
132	Pentose
146	Deoxyhexose (rhamnose)
162	Hexose
176	Glucuronic acid

However, the identification of the mass fragments was not always straight forward in particular with the fragment ions 162 and 146. Since these fragments could belong to either sugar moieties or the caffeate and *p*-coumarate moieties. Compounds containing these two fragments and undergoing alkaline hydrolysis clearly indicate that at least one of these fragments belong to the acid rather than a sugar. The apigenin conjugates at t_R 25.1 and 25.9 min and a number of other compounds are examples on such a tentative identification distinguished in Table 3 by light pink and light green shading when the data were inconclusive about the number of hexoses and rhamnose present respectively.

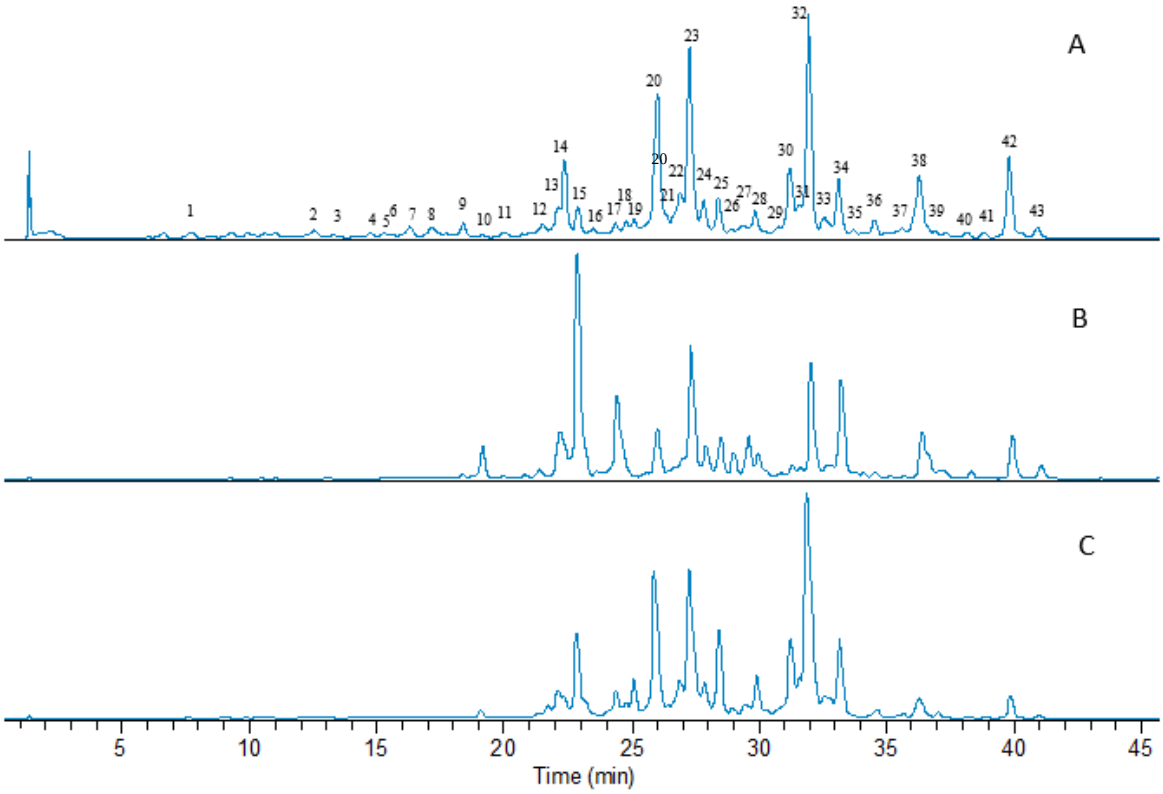

Figure 38 HPLC-PDA chromatograms of methanolic extracts of A, flowers; B, leaves and C, scapes at 340 nm.

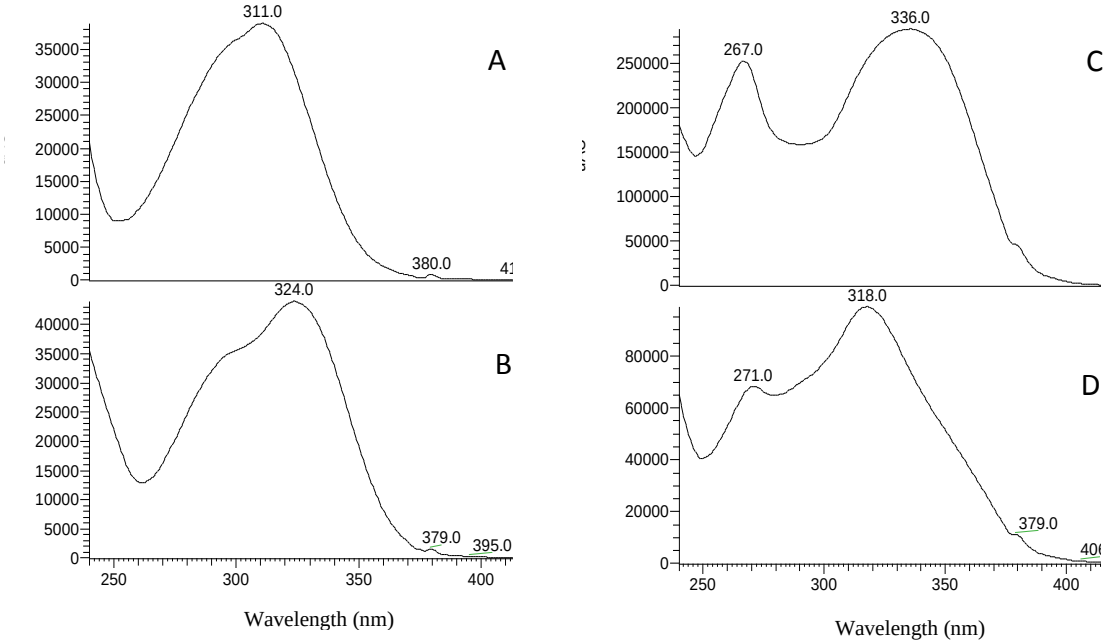

Figure 39 UV spectra used in classifying phenolic compounds in bluebell extracts. A, *p*-coumaric acid; B, ferulic acid; C, apigenin; D, flavonoid glycoside conjugated with *p*-coumaric acid.

Bluebell flowers and the upper portion of the scapes are characterised with a distinctive and intense blue-purple colour and the methanolic extract prepared from the flowers was also of dark blue-purple colour (()()()()()Figure 40 A and B). However, the analysis showed that the anthocyanins were of very little quantities. Investigating the HPLC chromatogram at 500–600 nm for anthocyanins showed only two tiny hints of a peak of which the one at t_R 29.3 min was tentatively identified as delphinidin-3-(6-*p*-coumarylglucoside)-5-(6-malonylglucoside) based on comparing its mass fragments in the positive mode with those reported by (Takeda et al. 1986) who had previously identified this compound in the flowers (Figure 4).

The following findings could be concluded from the HPLC-PDA-MS analysis:

- Hydroxyxinnamic acids are of little quantities compared to the flavonoid glycosides. The main acid present is *p*-coumaric acid followed by ferulic acid and they occur as conjugates with organic acids or sugars comprising most of the early eluting components in the HPLC chromatograms (Figure 38, peaks 1 – 9 and 11). Alternatively they found as conjugates with flavonoid glycosides.
- *O*-glycosylation is the major form of flavonoid glycoside found in all parts. However, the leaves and scapes show larger proportions of the *C*-glycosides compared to the flowers this is represented by the peaks 6, 9, 10, 12, 13 and 15 corresponding to Eriodictyol-*C*-hexoside-*C*-pentoside, apigenin-6-*C*-hexoside-8-*C*-pentoside, apigenin-6,8-di-*C*-hexoside and apigenin-6-*C*-pentosie-8-*C*-hexoside respectively. 15 appears to be the *C*-glycosides with highest abundant in leaves and scapes but to less extent in the flowers.
- Little diversity of the flavonoid aglycone moiety was found in the plant. Apigenin is by far the most abundant aglycone in addition to minor quantities of other flavonoid aglycones including luteolin and naringenin as *O*-glycosides, eriocictyol as *C*-glycosides.
- The number of sugar moieties attached to the flavonoid aglycones range from 2 – 4 including hexoses, pentoses, rhamnose and glucuronic acid. The different possibilities for the arrangement of these units and the additional incorporation of organic acid groups have given rise to a large number of conjugates for the same aglycone. *C*-glycosides are found to be rather limited in number with two sugars attached including only hexoses and pentose.
- Complete identification of the sugar moieties was not possible based on LC-MS analysis and they were tentatively reported as hexoses, pentoses, etc. The total assignment of these units require further work including isolation and NMR-based structural elucidation.

- Quantification of the flavonoids is not possible as such due to their structural complexity and diversity and the unavailability of commercial standards of these compounds. Acid hydrolysis is therefore, the strategy of choice for such a mixture.

The fact that bluebells produce mainly one type of aglycone can be viewed as an efficient utilisation of energy and resources by the plant. It is perhaps a means of economising on the use of energy otherwise required for the synthesis of multiple enzymes required for the production of different aglycones. The small amounts of anthocyanins used by the plant in producing such a rich and intense shade of colour also leads to the same conclusion. The plant therefore, appears to intelligently manipulate its limited chemicals such as apigenin glycosides and their conjugates with acids and use structural modifications by means of conjugation with acids, copigmentation with flavonoids and complexation with metal ions. Another bold feature of the plant is the high amount of glycosylation (the minimum number of sugars linked to any flavone being 2). This helps protect the cell from the toxic effect of the aglycone and at the same time ensures the successful trapping of the compound in the ionic and polar medium of the vacuole. In case of bluebells the sugar-rich nature of the plant would favour the accommodation of compounds with similar polarity. The flavonoid glycosides and their acid conjugates are further characterised with variations in nature and types of moieties, their linkage patterns and positions. These different forms can simply be intermediates or compounds undergoing further metabolism and eventually leading to other products, or they could be a successful implementation of a limited number of resources to fit different physiological functions.

A

B

()()()()()Figure 40 A, Bluebell flowers during anthesis; B, methanolic extract of the flowers after treatment with HP20.

Table 3 HPLC-PDA characteristics and LC-MS and MS-MS fragments in negative and positive modes used in the tentative identification of the phenolic compounds in the methanolic extract of bluebell flowers from 24/04/2014 and 15/05/2015. Analysis and peak identification performed by Dr. Barbara Hauck, Aberystwyth University.

Peak ID	t_R (min)	Spectral characteristics (nm)	MWt	MS^n fragments		Tentative compound identification	Present in		
				Negative ions	Positive ions		F[2]	L	S
Hydroxyxinnamic acids									
1b	7.7	272sh, 279, 287sh, 310sh	356	191, 209, 337		Coumaroyl glucarate			
2	12.3	ND	326	235, 265, 205, 163, 307, 119		Coumaroyl-hexoside			
3a	13.0	ND	518	193, 355, 149, 178, 134, 193, 235, 217		Feruloyl-dihexoside			
3b	13.0	ND	386	223, 208, 179, 164		Sinapoyl-hexoside			
4	14.6	ND	326	235, 265, 205, 307, 163, 119		Coumaroyl-hexoside			
5	15.1	ND	458	163, 325, 205, 119, 163, 205		Coumaroyl-pentosyl hexoside			
7a	16.3	311	338	173, 163		Coumaroylquinate			
7b	16.3	ND	472	163, 325, 205, 307, 119, 163, 205		Coumaroyl-hexosides-deoxy hexoside			
8a	16.8	ND	488	193, 355, 149, 178, 134, 235, 193					
8b	16.8	ND	502	193, 149, 355, 337, 149, 178, 134, 193, 235		Feruloyl-hexoside-deoxy hexoside			
9a	17.8	ND	386	223, 208, 179, 164		Sinapoyl-hexoside			
9d	18.4	301sh, 324	368	173, 193, 149, 134, 178		Feruloylquinate			
11	20.6	ND	502	355, 193, 149, 337, 193, 149, 134		Feruloyl-hexoside-deoxy hexoside			
Flavonoid-*C*-glycosides									

[2] F, flowers; L, leaves and S, scapes.

Peak ID	t_R (min)	Spectral characteristics (nm)	MWt	MS^n fragments		Tentative compound identification	Present in		
				Negative ions	Positive ions		F[2]	L	S
6	15.5	291, 329(sh)	582	461, 491, 401, 371, 563, 431, 473, 419, 521, 443		Eriodictyol-*C*-hexoside-*C*-pentoside			
9c	18.3	272, 335	594	473, 503, 353, 383, 575		Apigenin-6,8-di-*C*-hexoside			
10	19.1	ND	594	473, 503, 353, 383, 575		Apigenin-6,8-di-*C*-hexoside			
12a	21.4	ND	564	473, 503, 443, 545, 353, 383		Apigenin-6-*C*-pentoside-8-*C*-hexoside			
13a	22.1	266, 337	564	473, 443, 503, 545, 383, 353		Apigenin-6-*C*-pentoside-8-*C*-hexoside			
15c	22.9	267, 336	564	443, 473, 353, 545, 383, 503		Apigenin-6-*C*-hexoside -8-*C*-pentoside			
Flavonoid-*O*-glycosides									
7c	16.3	ND	714	519, 609, 285, 389, 285, 270/271, 447, 165, 195, 323, 221,150, 369,		Acylated luteolin-*O*-dihexoside			
9b	18.1	ND	610	447, 489, 285	449, 287	Luteolin-*O*-dihexoside			
12b	21.4	267, 336	902	631, 269, 883, 767, 839	609, 447, 271, 741	Apigenin-*O*-pentosyl-dihexosyl-hexoside uronic acid			
13b	22.1	266, 337	610	285, 447	449, 287	Luteolin-*O*-dihexoside			
14	22.3	267, 337	902	631, 269, 883, 767, 839	609, 741, 447, 271	Apigenin-*O*- pentosyl-dihexosyl-hexoside uronic acid			
15a	22.9	267, 336	580	285, 447, 417	449, 287	Luteolin-*O*-pentoside-*O*-hexoside			
15b	22.9	267, 336	756	285, 469, 621, 327	287, 463, 625	Luteolin-*O*- hexosyl-pentosyl-hexoside uronic acid			
16	23.4	266, 337	932	661, 913, 269, 797, 869	609, 447, 271, 771	Apigenin-*O*-trihexosyl-hexoside uronic acid			
17a	24.0		728			Naringenin-*O*-pentoside-dihexoside			
17b	24.3	267, 337	888	725, 269, 707, 431, 413, 593	595, 271, 727, 433, 565	Apigenin-*O*-pentoside-trihexoside			
17c	24.3	267, 337	742	609, 285, 447	611, 287, 449	Luteolin-*O*-dihexoside-pentoside			

Peak ID	t_R (min)	Spectral characteristics (nm)	MWt	MS^n fragments		Tentative compound identification	Present in		
				Negative ions	Positive ions		F^2	L	S
18a	24.7	ND	610	447, 285,		Luteolin-*O*-dihexoside			
18b	24.7	ND	858	813, 771, 753, 609, 285, 447	287, 611, 449	Luteolin-*O*-trihexodie-malonyl conjugate			
18c	24.8	267, 337	858	725, 269, 431, 707, 413, 593	595, 271, 727, 433	Apigenin-*O*-dipentoside-dihexoside			
18d	24.8	267, 337	770	269, 499, 635, 751, 427	609, 447, 271	Apigenin-*O*-dihexosyl-hexosyl uronic acid			
19a	25.1	268, 318	740	269, 469, 605, 721	609, 447, 271	Apigenin-*O*- hexosyl uronic acid-hexoside-pentoside			
19b	25.1	268, 318	1078	915, 807, 645, 645, 487, 427, 781, 269	917, 755, 447, 271, 447, 609	Apigenin-*O*-dihexoside- hexosyl uronic acid-coumaroyl-caffeoyl conjugate			
20a	26.0	267, 336	756	269, 431, 593, 413, 635		Apigenin-*O*-trihexoside			
20b	26.0	267, 337	740	269, 469, 605, 721	609, 447, 271	Apigenin-*O*-pentoside-hexoside-hexosyl uronic acid			
21a	26.4	ND	872	269, 725, 431, 413, 707, 751, 593		Apigenin-*O*-pentosyl-hexosyl acetate			
21b	26.4	ND	726	269, 431, 593, 413	271, 595, 433	Apigenin-*O*-pentoside-dihexoside			
22	26.9	267, 337	608	269	271, 447	Apigenin-*O*-hexoside- hexosyl uronic acid			
23a	27.3	267, 337	726	269, 431, 593, 413, 605	595, 271, 433	Apigenin-*O*-pentoside-dihexoside			
23b	27.4	ND	842	797, 755, 737, 269, 431, 593	271, 595, 433	Malonated apigenin-*O*-trihexoside			
24a	27.8	267, 335	594	269, 431	271, 433	Apigenin-*O*-dihexoside			
24b	27.8	267, 335	740	269, 431, 413, 593, 619	271, 595, 433	Apigenin-*O*-dihexoside-deoxyhexoside			
25a	28.4	271, 318 (broad)	1064	917, 899, 755, 269, 737, 431, 413, 593, 797, 545	903, 595, 433, 741, 579, 415	Apigenin-*O*-dihexoside-coumaroyl-caffeoyl conjugate			
25b	28.6	ND	594	447, 285		Luteolin-*O*-deoxy hexoside-*O*-hexoside			
26a	29.0	256, 267, 348	886	741, 783, 823, 609, 285, 447,	287, 611, 449, 563, 725	Acylated luteolin-O-pentoside-O-dihexoside			

Peak ID	t_R (min)	Spectral characteristics (nm)	MWt	MS^n fragments		Tentative compound identification	Present in		
				Negative ions	Positive ions		F[2]	L	S
26b	29.3	267, 327, 534	858		303, 551, 611	Delphinidin-3-(6-pcoumarylglucoside)-5-(6-malonylglucoside)			
26c	29.3	267, 327, 534	798	755, 737, 269, 431, 413	271, 595, 433	Apigenin-*O*-dihexoside-hexoside acetate			
27	29.6	255, 265, 348	652	609, 591, 447, 285	287, 449	Luteolin-*O*-hexoside-*O*-hexoside acetate			
28	29.8	266, 337	812	767, 707, 725, 269	271, 595, 433, 651, 489, 367, 447, 471	Apigenin-*O*-pentoside-*O*-dihexoside-malonyl conjugate			
29	30.7	ND	798	737, 755, 635, 269, 431	271, 637, 433	Apigenin-*O*-trihexoside-acetyl conjugate			
30	31.2	269, 318 (broad)	916	645, 427, 269, 487, 499, 781, 897	755, 447, 271, 609	Apigenin-hexosyl-hexoside uronic acid-coumaroyl conjugate			
31	31.6	267, 336	884	739, 781, 269, 821, 613, 469	609, 447, 271, 867	Acylated apigenin-*O*-pentosyl-hexosyl-hexoside uronic acid			
32a	31.9	267, 338	870	725, 767, 807, 707, 269, 431, 593, 413	271, 595, 433	Acylated apigenin-*O*-pentoside-dihexoside			
32b	31.9	ND	1064	917, 899, 755, 269, 737, 431, 413, 593, 797, 545		Apigenin-*O*-dihexoside-coumaroyl-caffeoyl conjugate			
33a	32.5	ND	650	269, 379	271, 447	Apigenin-*O*-hexosyl uronic acid-hexoside acetate			
33b	32.5	268, 320	902	755, 737, 269, 593, 575, 431, 413, 695	271, 433, 741, 595, 415, 885	Acylated apigenin-*O*-hexoside-deoxy hexoside			
34	33.1	267, 337	636	269, 593, 575, 431, 515, 413	271, 433	Apigenin-*O*-hexosyl-hexoside acetate			
35	33.7	267, 339	858	695, 269, 677, 401, 563	565, 271, 697, 403	Apigenin-*O*-dipentoside-dihexoside			
36a	34.5	268, 322 (broad)	726	269, 401, 563	271, 565, 403	Apigenin-*O*-pentoside-hexoside-caffeoyl conjugate			
36b	34.5	268, 322 (broad)	754	269, 483, 325, 265, 337, 619	271, 447, 609	Apigenin-*O*-hexoside-hexosie uronic acid-coumaroyl conjugate			

Peak ID	t_R (min)	Spectral characteristics (nm)	MWt	MS^n fragments		Tentative compound identification	Present in		
				Negative ions	Positive ions		F[2]	L	S
37a	35.7	268, 320	902	755, 737, (631), 269, 431, 593, 413, 635	271, 433, 595, 741, 579	Apigenin-tri-*O*-hexoside-coumaroyl conjugate			
37b	35.8	269, 321 (broad)	916	645, 487, 427, 269, 781, 897, 499	755, 447, 271, 609	Apigenin-*O*-dihexosyl-hexosyl uronic acid-coumaroyl conjugate			
38a	36.3	267, 338	696	269, 563, 401	565, 271, 403	Apigenin-*O*-hexoside-di-*O*-pentoside			
38b	36.6	269, 319	902	755, 737, 269, 593, 575, 431,	271, 741, 433, 579, 595	Apigenin-tri-*O*-hexoside-coumaroyl conjugate			
39a	36.9	270, 318 (broad)	1034	887, 869, 725, 269, 707, 401, 563		Apigenin-*O*-pentoside-di-O-hexoside-coumaroyl-caffeoyl conjugate			
39b	36.9	270, 318 (broad)	710	269, 401	565, 271, 403	Acylated apigenin-*O*-pentosyl-hexoside			
39c	37.3	267, 335	754	269	623, 271, 461	Acylated apigenin-*O*-pentoside-*O*-hexoside			
40a	38.2	267, 337	782	737, 677, 695, 269, 401, 563	271, 565, 403, 489	Apigenin-di-*O*-pentoside-*O*-hexoside-malonyl conjugate			
40b	38.2	267, 337	956	911, 767, 767, 809, 849, 269, 725, 707, 473, 635, 455, 593, 413, 575, 431	681, 519, 271, 939, 649, 433	Acylated-apigenin-*O*-pentoside-dihexoside-malonyl conjugate			
41a	38.8	268, 319 (broad)	754	269, 483, 325, 265, 337, 619	271, 447, 609	Apigenin-*O*-hexosyl-hexosyl uronic acid-coumaroyl conjugate			
41b	38.8	ND	768	707, 725, 605, 269, 401, 587, 545, 563	271, 607, 403	Apigenin-*O*-pentosyl-hexosyl-hexosylacetae			
42	39.8	267, 339	840	695, 737, 777, 269, 563, 401, 605, 545	271, 565, 403, 547	Acylated apigenin-di-*O*-pentoside-*O*-hexoside			
43	40.9	267, 336	606	269, 545, 563, 401	271, 403	Apigenin-*O*-pentoside-*O*-hexoside acetate			
Non-phenolic compounds									
1a	7.7	272sh, 279, 287sh	204	159, 116, 186	188, 146, 144	Tryptophan			

3.3.2. Secondary metabolites from bluebell flowers

Fractionation of the methanolic extract of bluebell flowers resulted in the isolation of 4 compounds which could be classified into two groups of secondary metabolites: phenylethanoids and flavonoid-*O*-glycosides. The structural elucidation was based on the use of 1D and 2D NMR and confirmed by LC-MS.

3.3.2.1. Phenylalkyl glycosides

Two phenylalkyl glycosides were isolated from the flowers Figure 41. The structure of these compounds comprised a glycan part which included a glucuronic acid unit bonded to the central glucose via a *β*-(1→2) glycosidic linkage. The difference between the two compounds arise in the aglycone part being based on either 2-phenylethanol or benzyl alcohol moieties. The two compounds were identified as (benzyl-O-β-D-glucopyranosyluronic acid-(1→2)-glucopyranoside (DR1) and 2-phenylethyl-O-β-D-glucopyranosyluronic acid-(1→2)-glucopyranoside (DR2) (Figure 41) based on NMR and LC-MS data as follows:

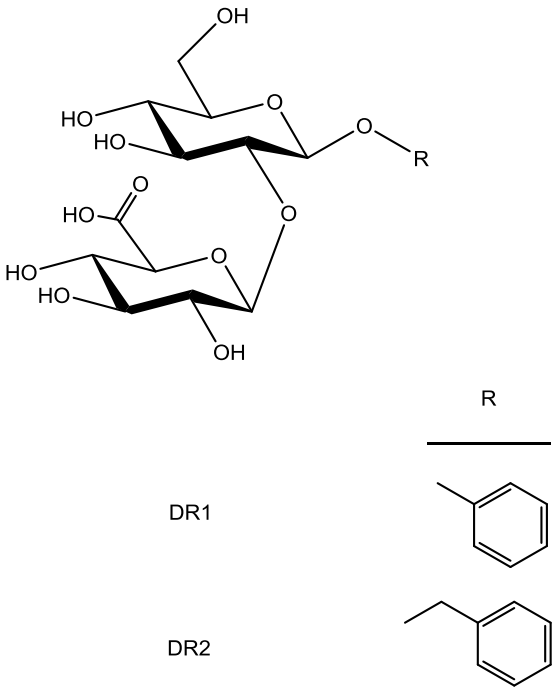

Figure 41 The chemical structure of compounds DR1 and DR2 isolated from bluebell flowers.

3.3.2.1.1. NMR spectroscopy

The structure of the compounds was identified using NMR spectroscopy (Figure 44 - Figure 49). Table 4 summarises ^{1}H and ^{13}C chemical shifts. ^{1}H NMR showed signals in the aromatic

region from 7.2 – 7.5 ppm corresponding to the phenyl ring protons. The rest of the chemical shifts were characteristic of glycosides with the anomeric protons at 4.5 and 4.6 ppm with *J* values of 7.5 Hz. Other glycosidic -CH-OH protons were in the range 3.3 – 4.0 ppm. The sequence of protons in the different moieties was established from ^{1}H-^{1}H COSY correlations. The different protons were linked to their corresponding carbon atoms using ^{1}H – ^{13}C HSQC correlation. HSQC showed the presence of 2 × -CH_2 groups in the molecule with one having higher δ_H than the other glycosidic -CH_2-OH. These two protons were identified as the H-7 protons of the aglycone based on their HMBC correlation with the anomeric C of glucose in addition to the aromatic carbons 1, 2 and 6. HSQC-TOCSY further backed this up by the fact that these two protons did not belong to any of the other spin systems. The second sugar was identified as glucuronic acid from HMBC correlation between its 4-H and 5-H with the –**C**OOH signal at 173 ppm. The relatively higher δ_C of glucose-C2 was taken as indication for the position of the linkage and was further confirmed by HMBC, the interglycosidic linkage was thus identified as β -(1→2). Figure 42 shows 2D correlations used to identify the linkage points between different moieties.

Table 4 1H and 13C NMR data for the isolated phenylalkyl glycosides DR1 and DR2 in MeOD.

Position	δ_H ppm (multiplicity, *J* Hz)		δ_C ppm	
	DR1	**DR2**	**DR1**	**DR2**
Aglycone				
1			138.9	139.9
2	7.42 (*d*, 7.4)	7.24 (*m*)	129.0	129.9
3	7.32 (*t*, 7.4)	7.26 (*m*)	129.3	129.0
4	7.25 (*d*, 7.3)	7.20 (*m*)	128.6	126.9
5	7.32 (*t*, 7.4)	7.26 (*m*)	129.3	129.0
6	7.42 (*d*, 9.9)	7.24 (*m*)	129.0	129.9
7	4.68 (*d*, 11.5), 4.93 (*d*, 11.5)	2.88 (*t*, 7.5)	71.9	36.9
8		3.71 (*m*), 4.07 (d*t*, 9.3, 7.5)		71.4
D-Glucose				
1	4.57 (*d*, 7.6)	4.46 (*d*, 7.6)	102.2	102.7

2	3.49 (*t*, 9.0)	3.39 (*t*, 8.3)	84.3	84.4
3	3.58 (*t*, 8.8)	3.56 (*t*, 9.1)	77.7	77.6
4	3.38 (*t*, 8.9)	3.34 (*t*, 9.9)	69.9	70.8
5	3.29 (*m*)	3.28 (*m*)	76.4	77.6
6	3.68 (*dd*, 12.0, 6.1), 3.88 (*dd,* 12.0, 1.7)	3.67 (*dd*, 12.1, 4.9), 3.85 (*dd,* 12.1, 2.2)	61.3	62.5
D-Glucuronic acid				
1	4.61 (*d*, 7.6)	4.60 (*d*, 7.9)	105.5	105.2
2	3.30 (*t*, 8.9)	3.29 (*t*, 8.7)	75.8	75.6
3	3.39 (*t*, 9.3)	3.42 (*t*, 9.2)	77.2	76.9
4	3.50 (*t*, 9.6)	3.55 (*t*, 9.1)	73.3	73.1
5	3.68 (*d*, 10.6)	3.79 (*d*, 9.7)	76.8	76.9
6			173.5	171.2

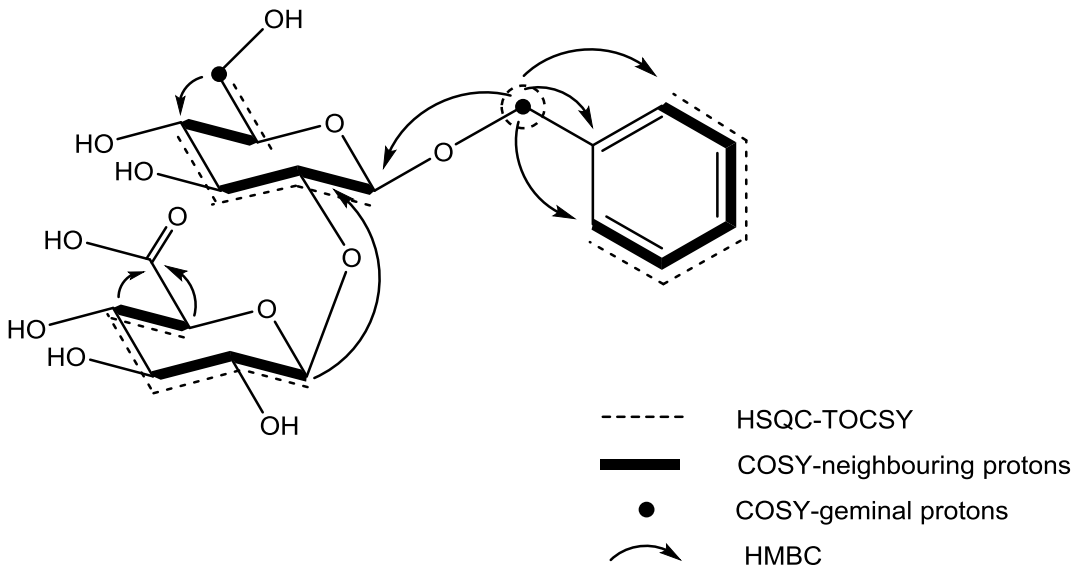

Figure 42 Some HSQC-TOCSY, COSY and HMBC correlations used in the structural analysis of DR1.

Similarly, compound DR2 was characterised using NMR spectroscopy (Figure 50 - Figure 56) for which the ^{1}H and ^{13}C chemical shifts are listed in Table 4 The protons on C7 of the aglycone were detected as a triplet in ^{1}H NMR at 2.88 ppm upfield from the glycosidic signals and correlated to the carbon signal at 36.9 ppm in DEPTQ. The second pair of protons on C8 of the aglycone showed two signals in ^{1}H NMR which appeared relatively upfield compared to the CH_2 group in DR1. This could be attributed to the decreased de-shielding effects by the electron withdrawing aromatic ring provided by the separation by an extra CH_2 group in DR2 compared to DR1.

The values of the coupling constants *J* reported in Table 5 were calculated from 2D cross peaks for the signals in the crowded regions. Both compounds DR1 and DR2 contained noticeable amounts of impurities as could be seen from their ^{1}H and ^{13}C NMR spectra. However, it was possible to identify these extra signals as they did not show any correlation to the other signals in any of the 2D NMR experiments. They also showed integrations that did not match those from the rest of the signals in ^{1}H NMR (Figure 54 shows an example). Furthermore, the structures characterised from NMR were confirmed by the results from MS analyses.

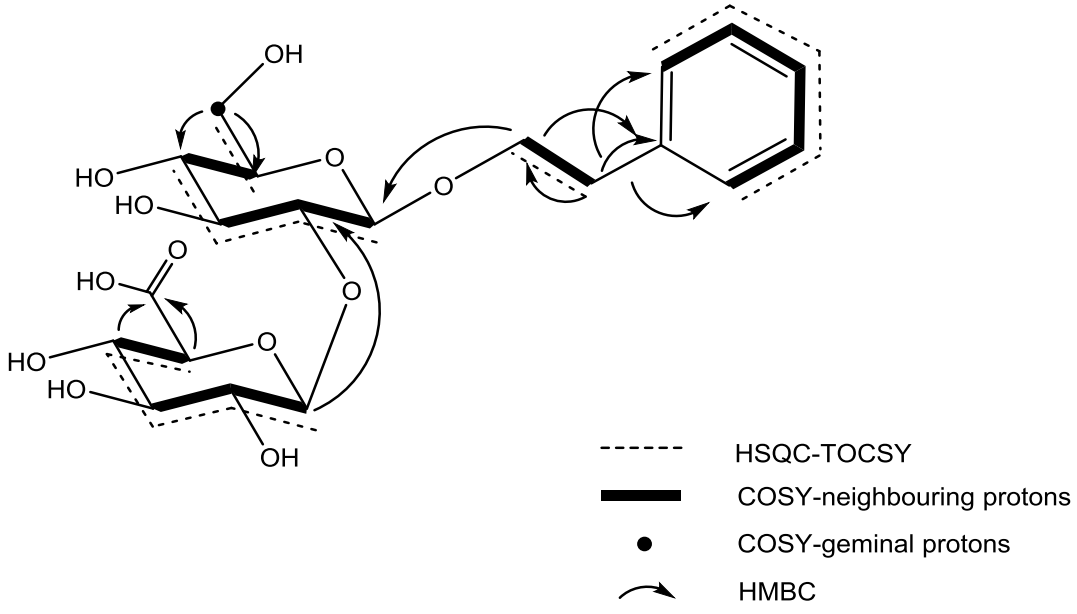

Figure 43 Some HSQC-TOCSY, COSY and HMBC correlations used in the structural analysis of DR2.

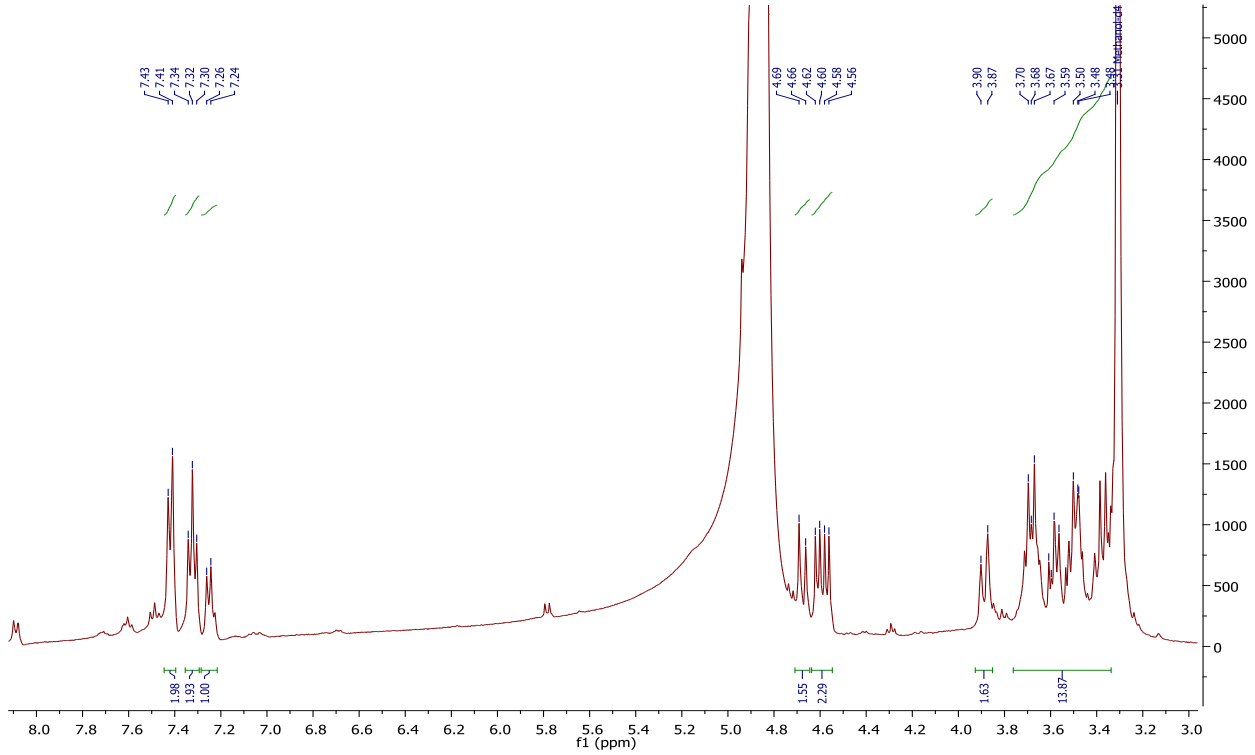

Figure 44 ^{1}H NMR of DR1 in MeOD.

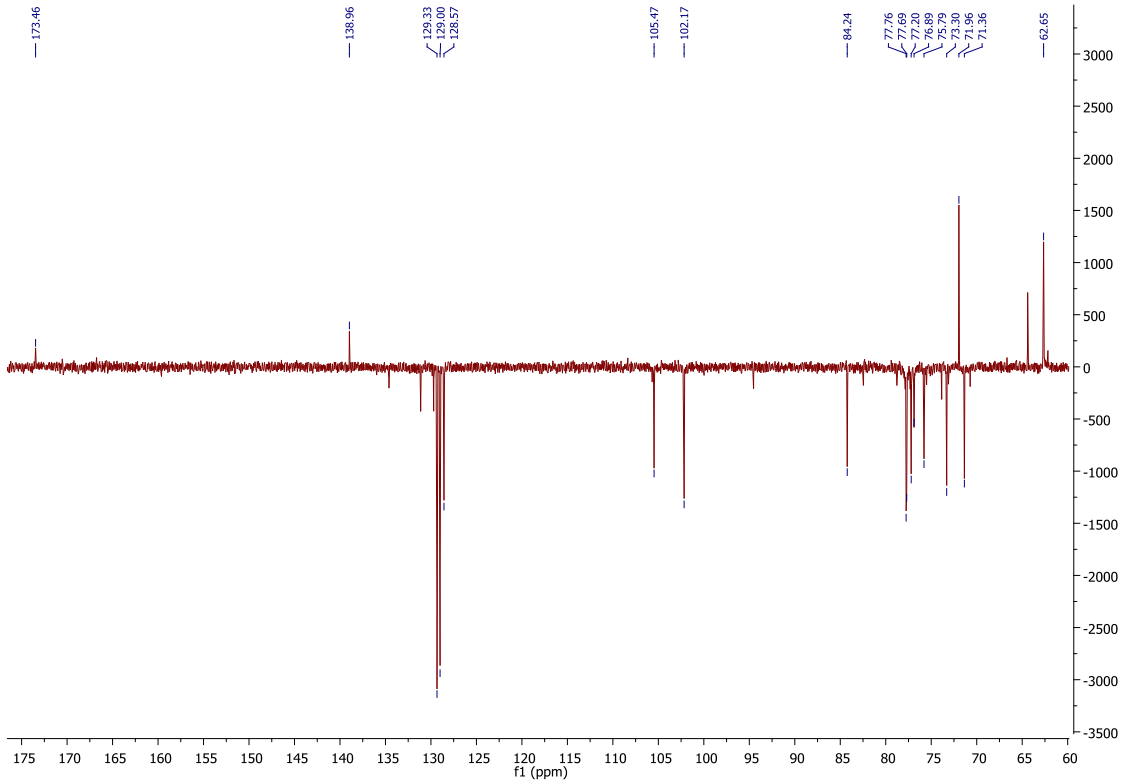

Figure 45 DEPTQ of DR1 in MeOD.

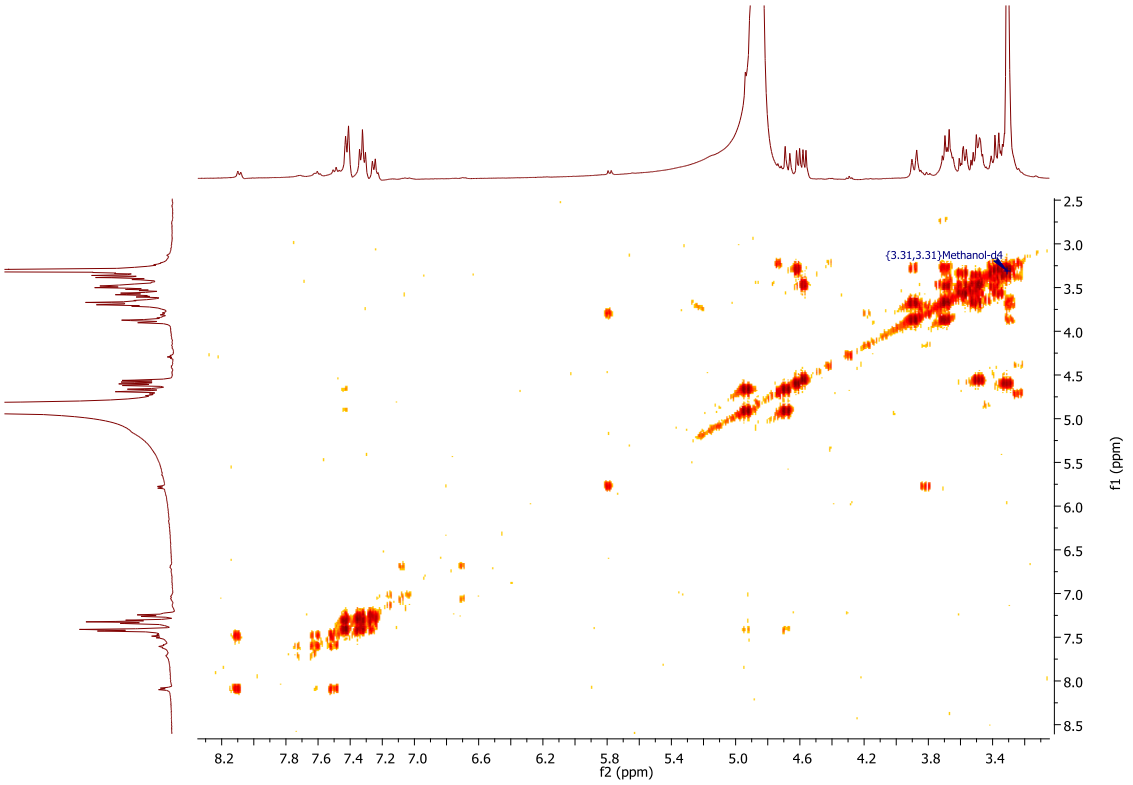

Figure 46 ^{1}H-^{1}H COSY of DR1 in MeOD.

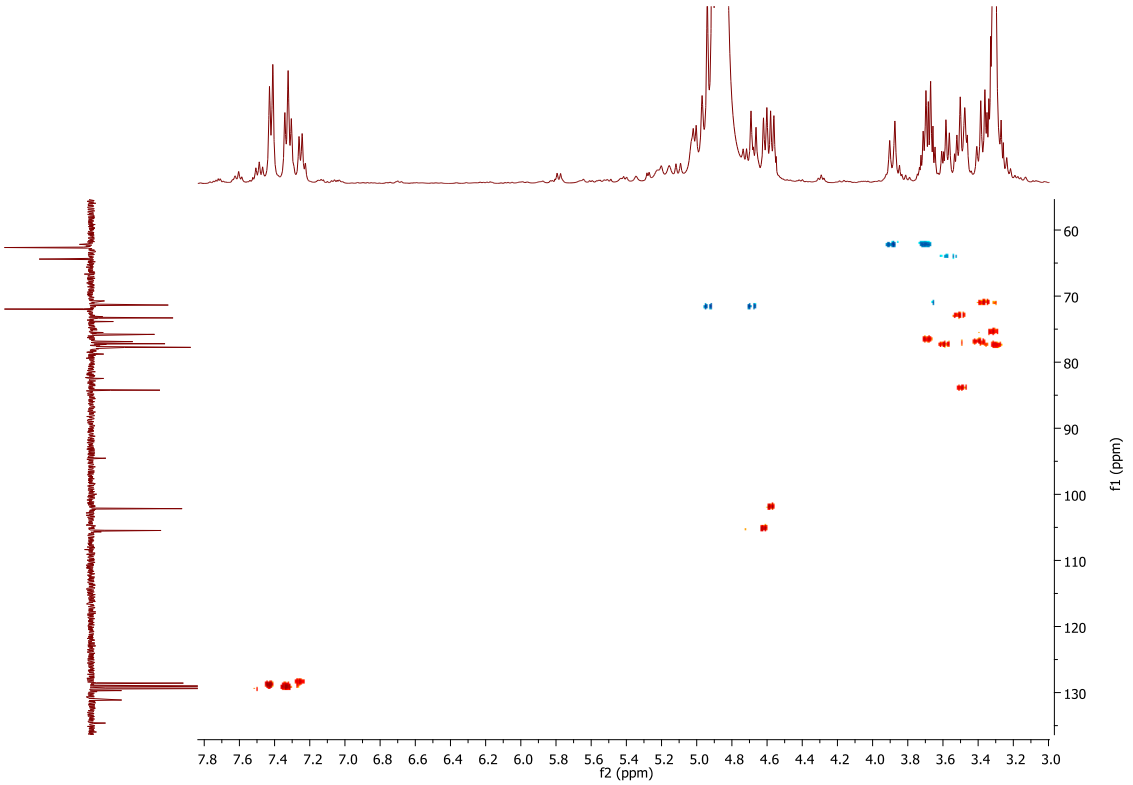

Figure 47 ^{1}H-^{13}C HSQC of DR1 in MeOD.

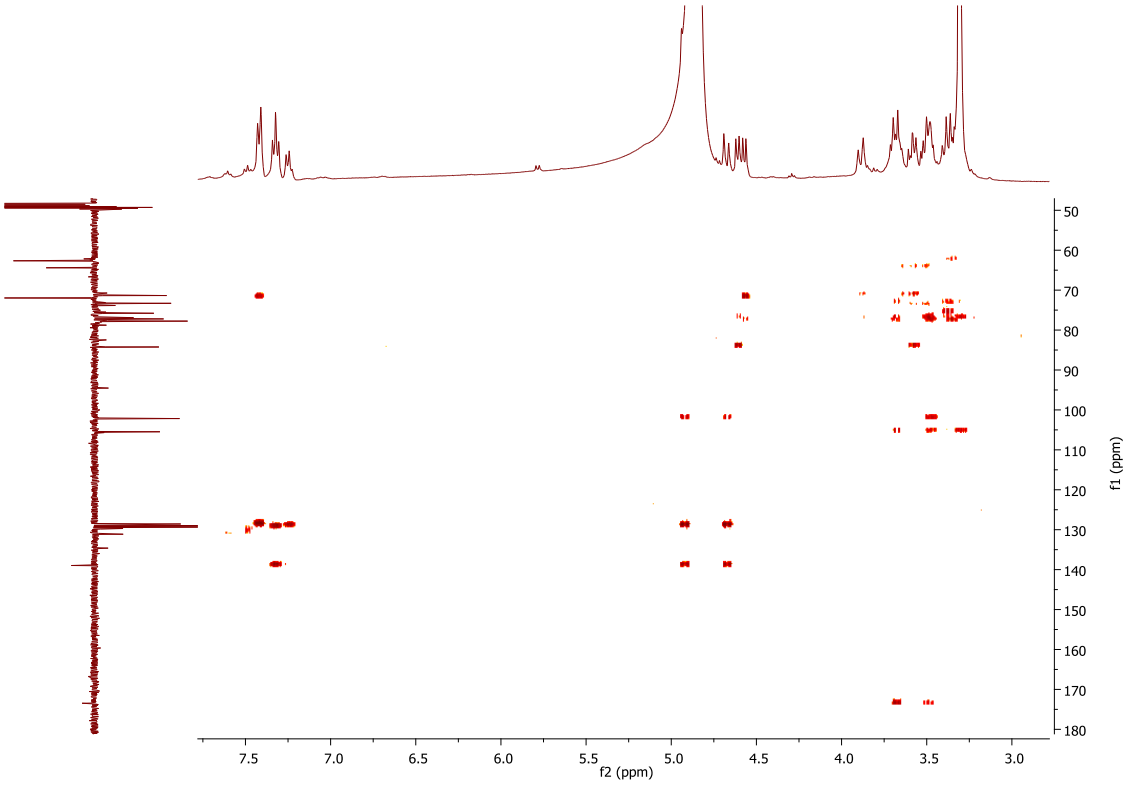

Figure 48 ^{1}H-^{13}C HMBC of DR1 in MeOD.

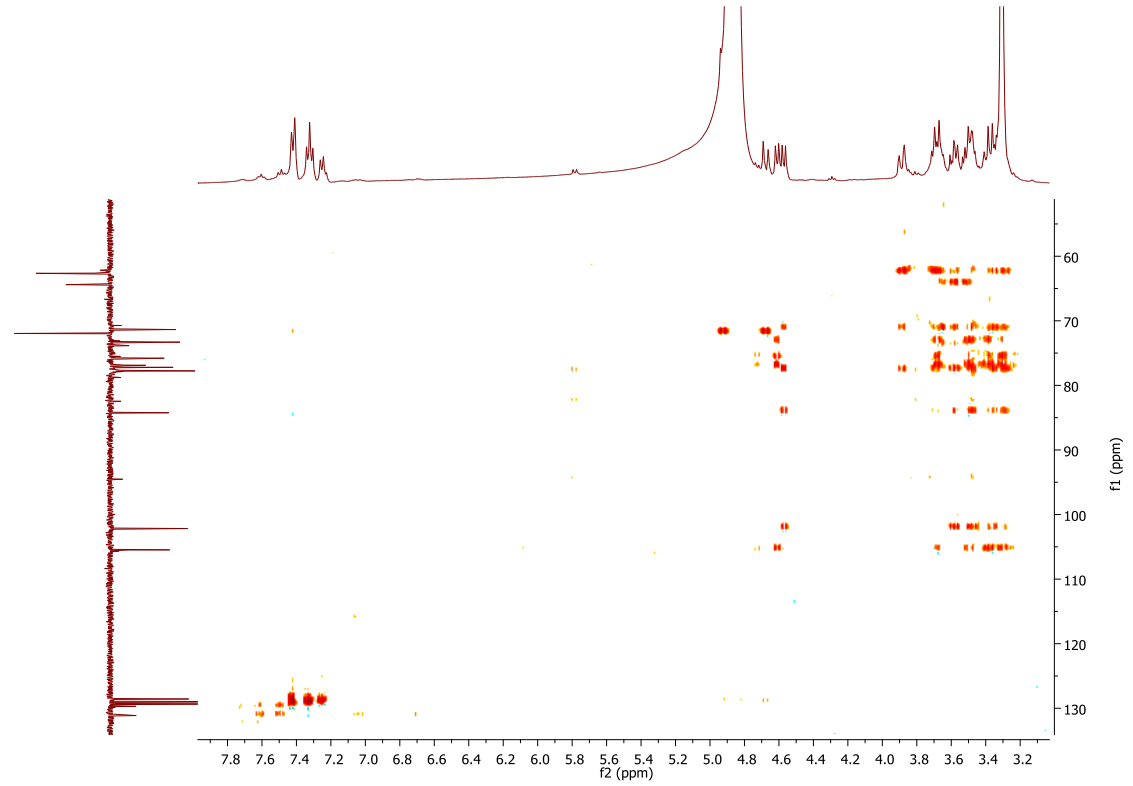

Figure 49 HSQC-TOCSY of DR1 in MeOD

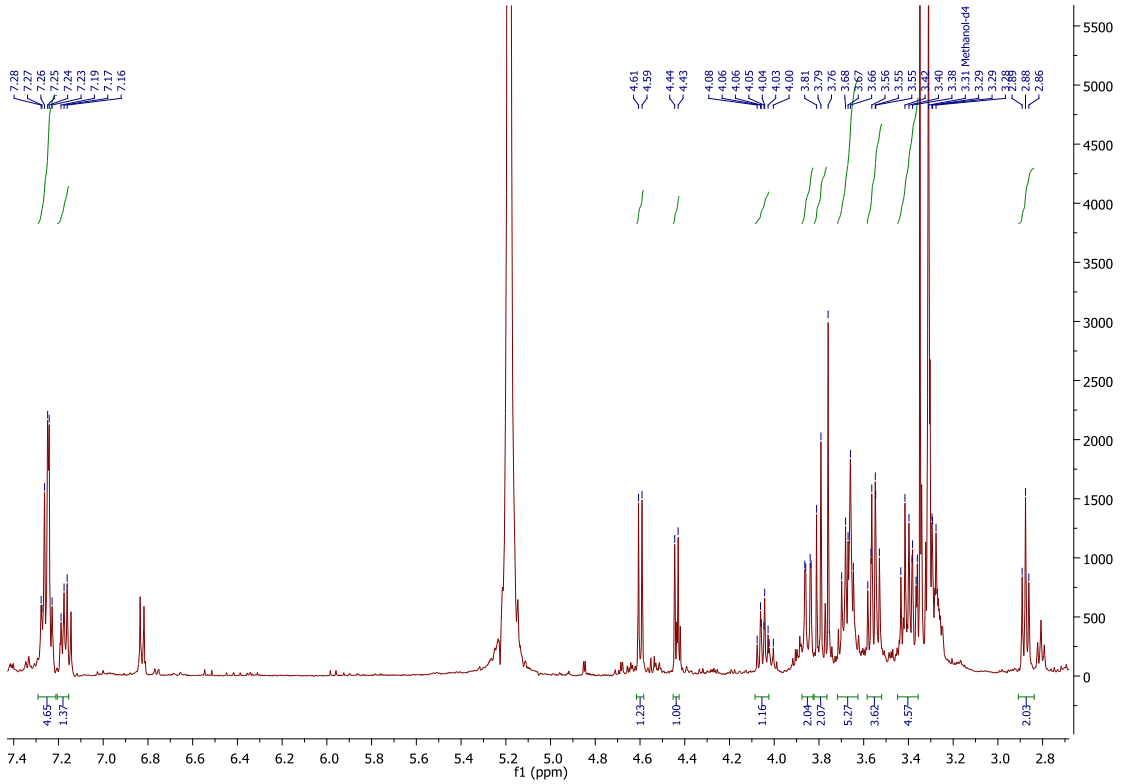

Figure 50 ^{1}H NMR of 105-5-2 in MeOD.

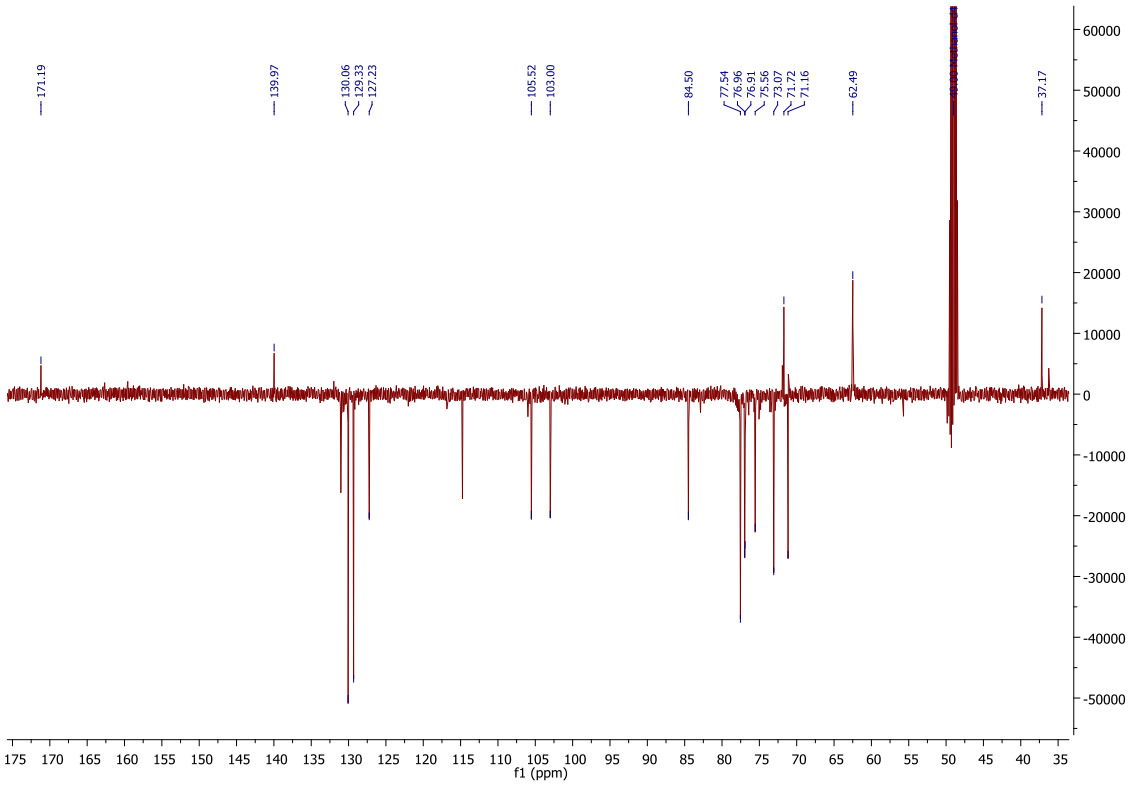

Figure 51 DEPTQ of DR2 in MeOD.

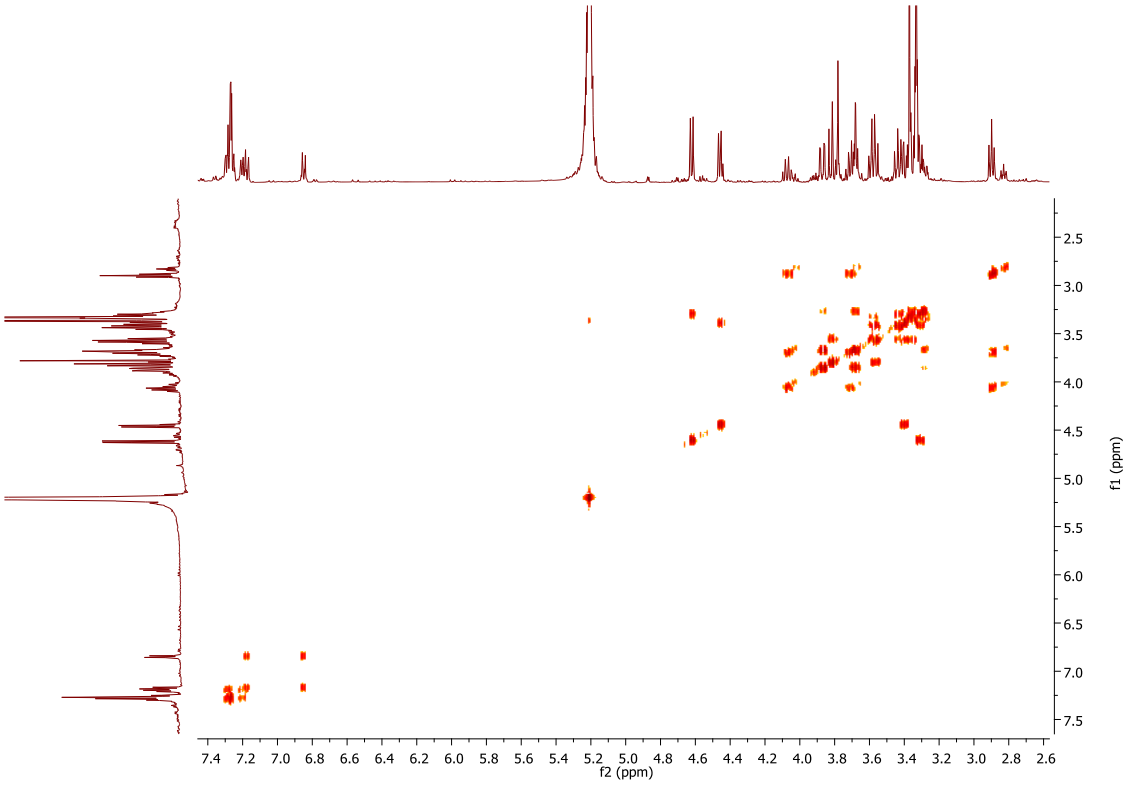

Figure 52 ^{1}H-^{1}H COSY of DR2 in MeOD.

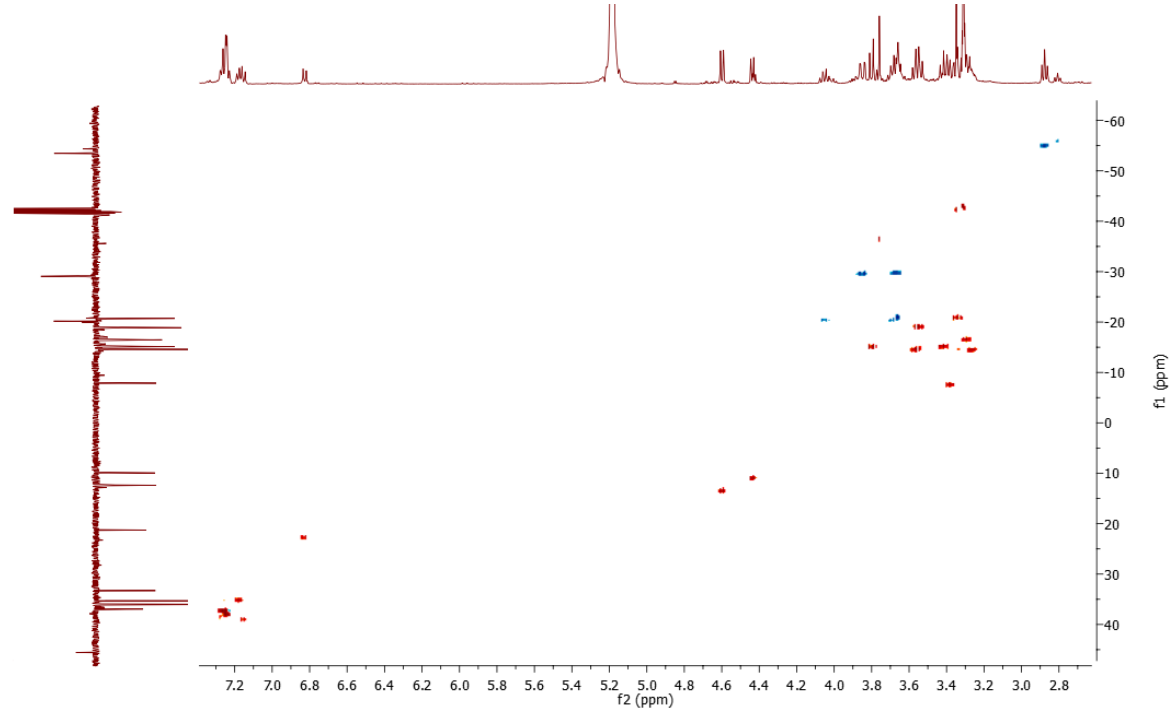

Figure 53 ^{1}H-^{13}C HSQC of DR2 in MeOD.

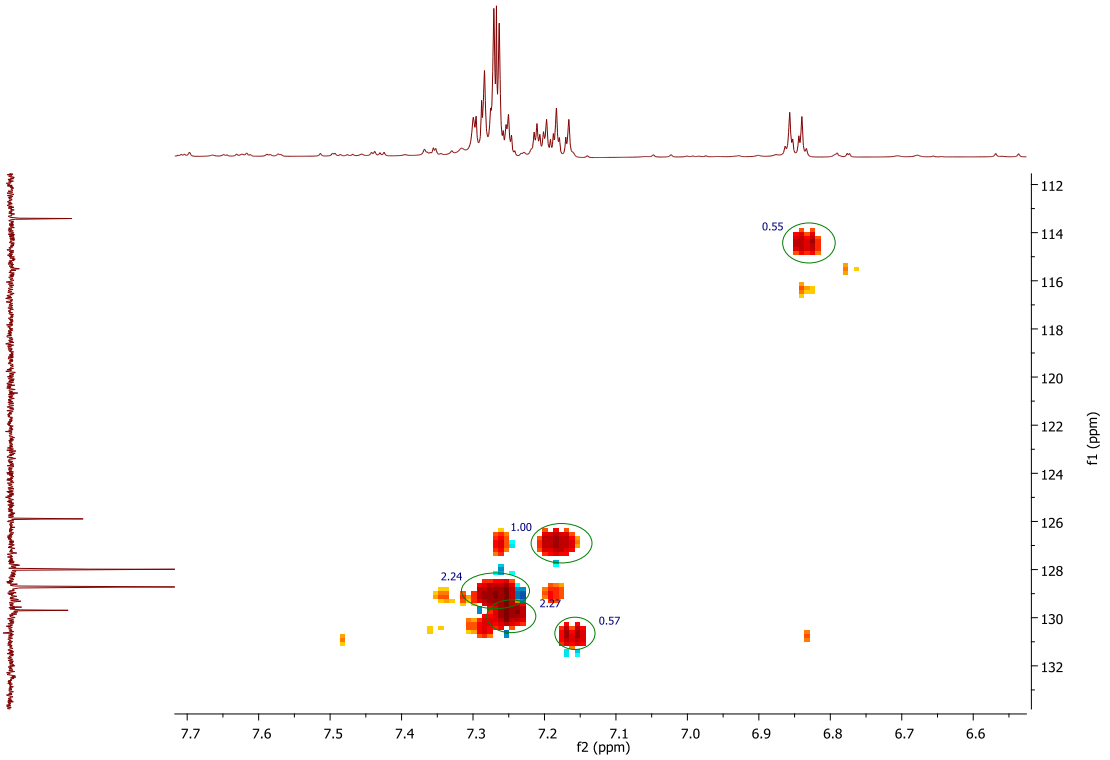

Figure 54 integration of the cross peaks in HSQC of DR2. Unrelated signals show much lower integrations compared to the rest of the protons (e.g. the signal at 6.82,114.3 ppm).

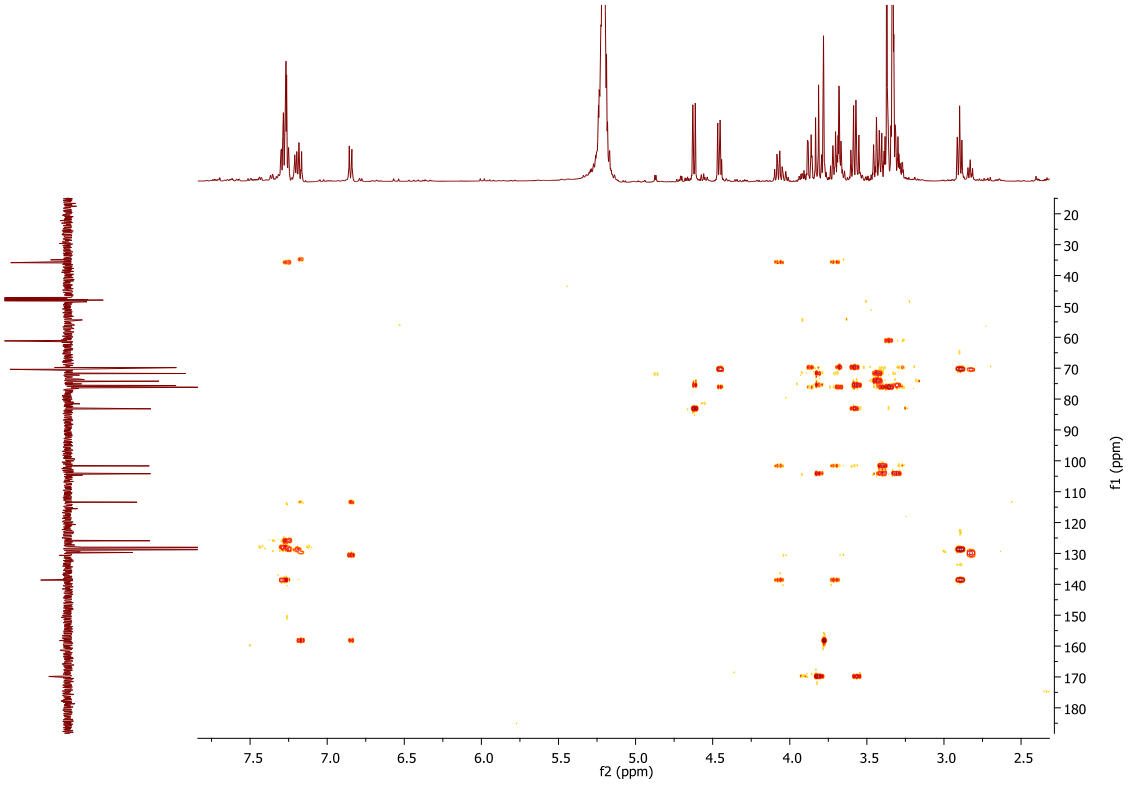

Figure 55 ^{1}H-^{13}C HMBC of DR2 in MeOD.

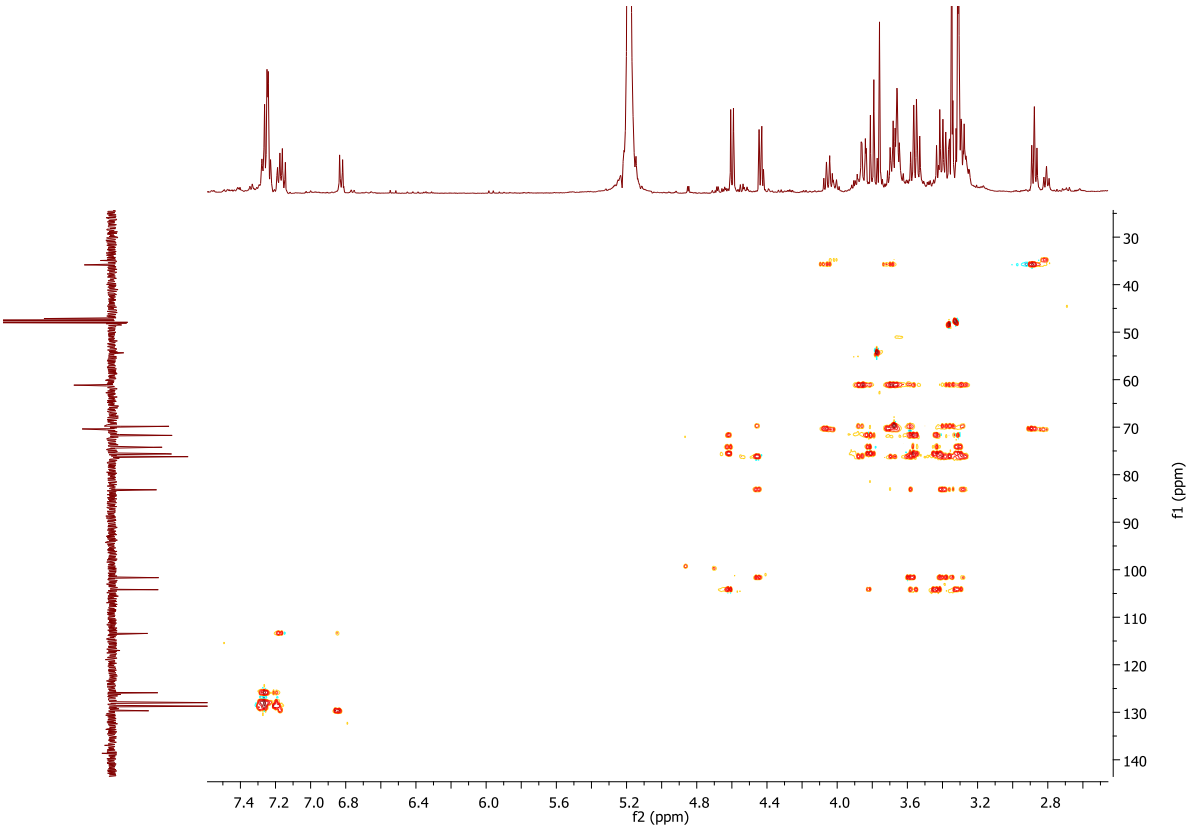

Figure 56 HSQC-TOCSY of DR2 in MeOD.

3.3.2.1.2. LC-ESI-MS

High resolution MS for DR1 in the negative mode gave 445.135 (Figure 125) which corresponds to the molecular formula $C_{19}H_{25}O_{12}$. DR2 gave 459.150 (Figure 126) corresponding to the molecular formula $C_{20}H_{27}O_{12}$.

MS and MS^2 were run in both negative and positive modes (Figure 58). In the negative mode experiment, the deprotonated molecular ion $[M - H]^-$ at *m/z* 445 gave daughter ions at *m/z* 427, 385, 269, 175 and 161. Table 5 lists the fragments obtained in both modes *m/z* 269 represent Y_1 (the loss of glucuronic acid from the molecular ion), while and the last two fragments can be attributed to deprotonated gluronoic B_1 acid and glucose units B_2 respectively. The glycan part Y_0 gave a signal with a low intensity at m/z 339.

The positive mode experiment showed the protonated molecular ion $[M + H]^+$ at *m/z* 447 and its sodium adduct in addition to a fragment at m/z 339 for Y_0. Only one fragment was seen at m/z 293 in MS^2 corresponding to the sodium adduct of Y_1.

ESI-MS analysis for DR2 showed a similar fragmentation pattern to DR1 with a difference of 14 mass units corresponding to the extra CH_2 for the fragments containing the aglycone (Figure 59). Fragments that were not detected for this compound included Y_1 in the negative mode and the molecular ion in the positive mode.

The proposed fragmentation is presented in Figure 57 on compound DR2.

Table 5 Fragments in negative and positive mode for compounds DR1 and DR2. * refers to a low-intensity signal.

	DR1	DR2
Negative mode fragments		
Molecular ion $[M-H]^-$	445	459
Loss of water	427	441
Unidentified loss	385	399
The glycan part	339*	339*
Loss of glucuronic acid (Y_1)	269	
Glucuronic acid	175	175
Glucose	161	161
Positive mode fragments		
Molecular ion $[M+H]^+$	447	
Molecular ion + sodium $[M+Na]^+$	465	483
The glycan part	339	339
Loss of glucuronic acid (Y_1) + sodium	293	307

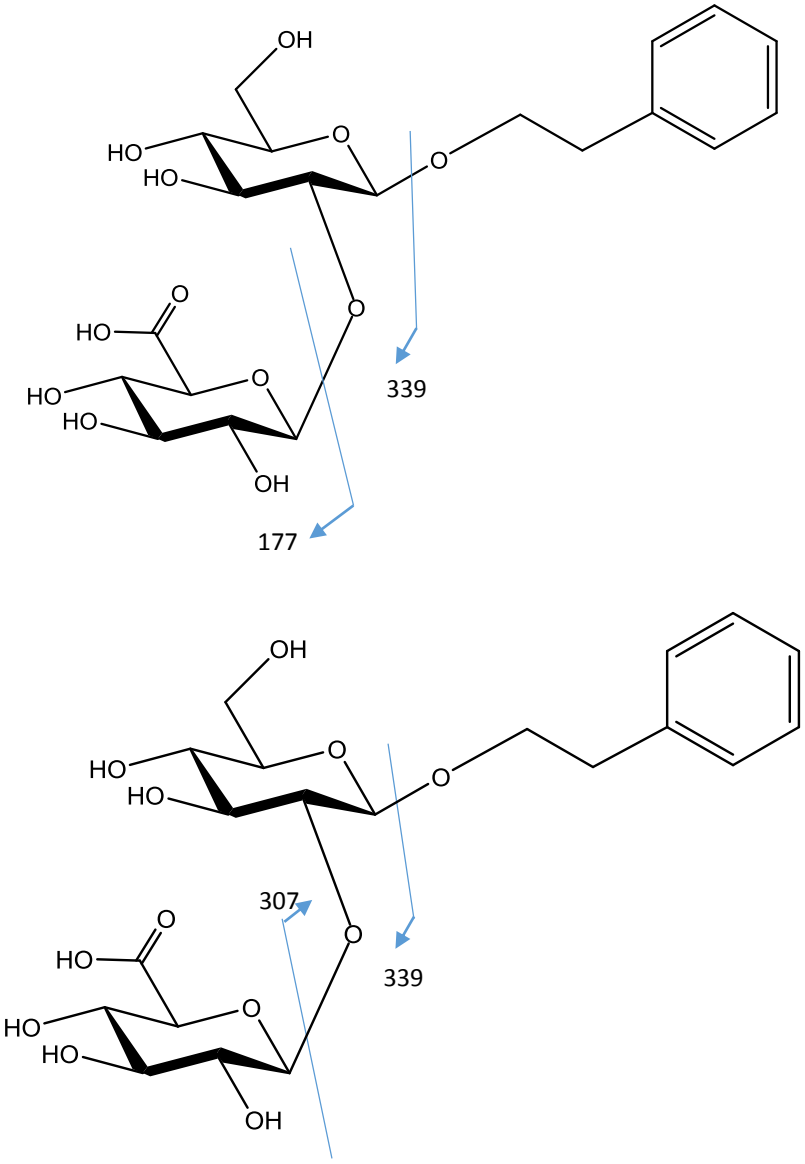

Figure 57 ESI-MS^2 fragmentation of the isolated phenylalkyl glycosides as exemplified by compound DR2 in A: negative and B: positive ionisation modes.

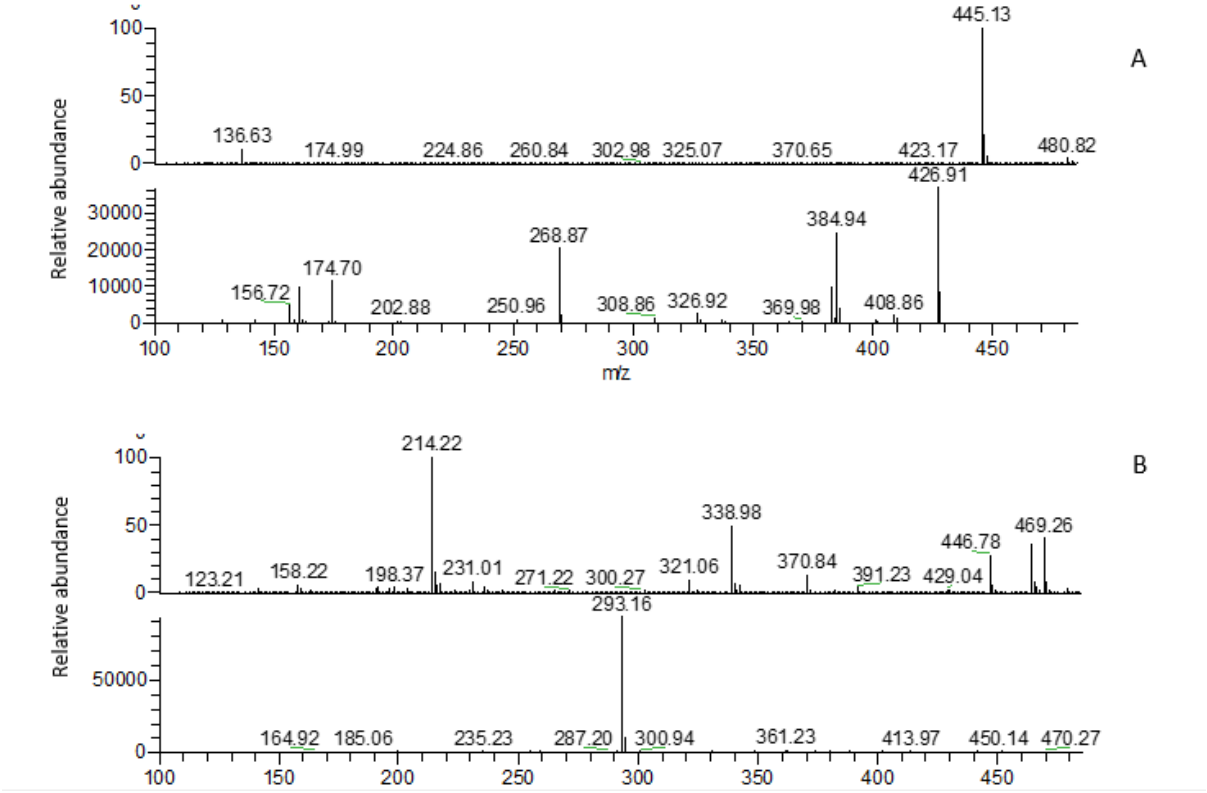

Figure 58 LC-MS and MS^2 of DR1 in A, negative and B, positive ion modes.

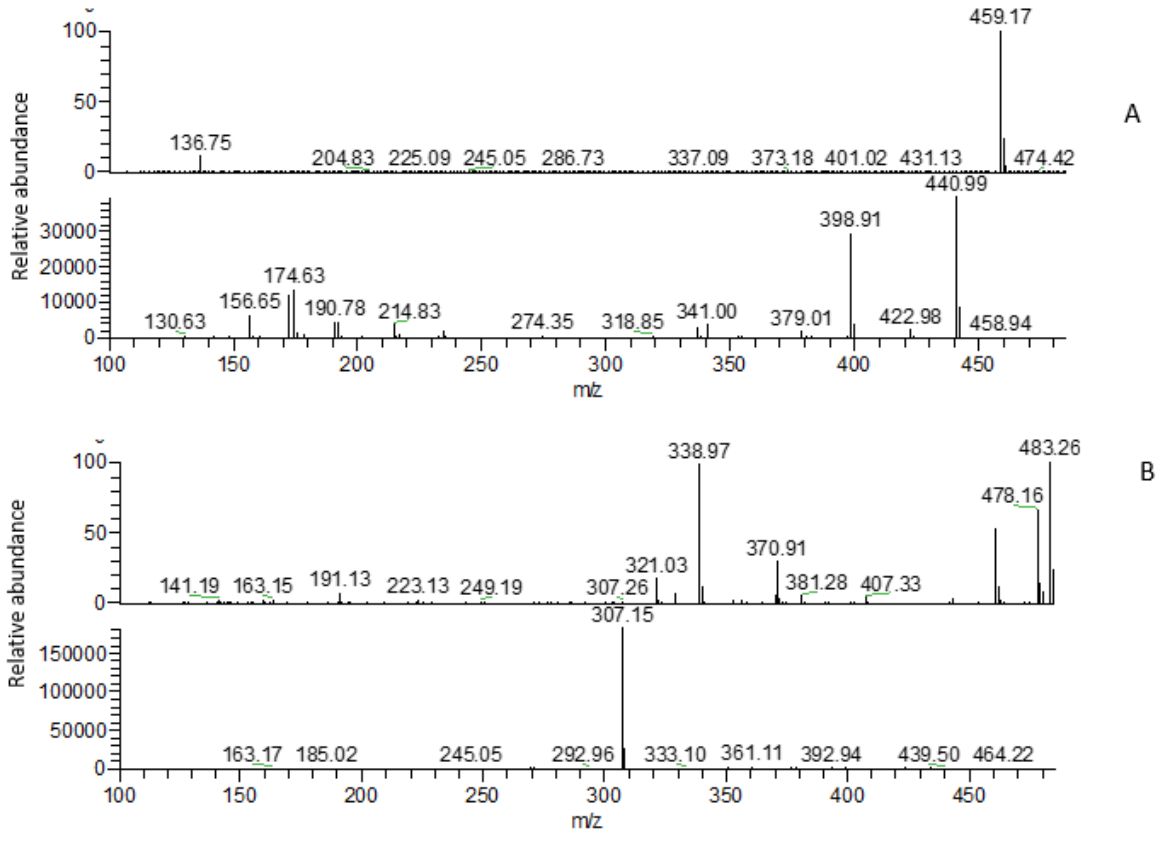

Figure 59 LC-MS and MS^2 of DR2 in A, negative and B, positive ion modes.

3.3.2.2. Flavonoid-*O*-glycosides

Two flavonoid-*O*-glycosides (Figure 60) were isolated from bluebell flowers. The flavone aglycone in both compounds was found to be apigenin linked to the glycan chain via an *O*-glycosidic linakge on C-7. The glycan chain is made up of a series of 4 or 3 interlinked sugar units including glucuronic acid, glucose, and xylose. The structures of these compounds were elucidated using 1D and 2D NMR spectroscopy and LC-ESI-MS. The compounds were identified as 7-[*O*-*β*-D-glucopuranosyl-(1→3)-*O*-*β*-D-xylopyranosyl-(1→6)-*O*-*β*-D-glucopyranosyl-(1→2)-*O*-*β*-D-glucopyranosideuronic acid-(1→)]-apigenin (DR3) and 7-[*O*-*β*-D-xylopyranosyl-(1→6)-*O*-*β*-D-glucopyranosyl-(1→2)-*O*-*β*-D-glucopyranosideuronic acid-(1→)]-apigenin (DR4)

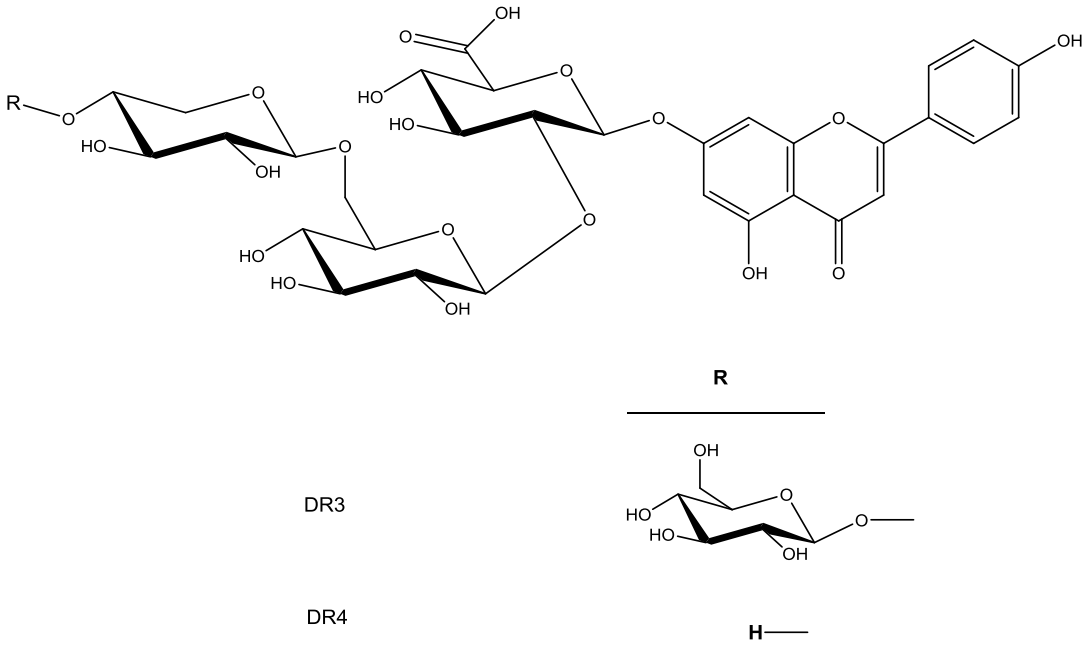

Figure 60 The structure of compounds DR3 and DR4 isolated from bluebell flowers.

3.3.2.2.1. NMR spectroscopy

^{1}H and ^{13}C NMR data used for the structural identification of the two compounds are listed in Table 6. Compound DR3 yielded the spectra presented in (Figure 62 - Figure 67). ^{1}H NMR showed the presence of two types of protons in the molecule: aromatic protons in the region 6 - 8 ppm corresponding to the aglycone apigenin, and typical glycosidic signals that were distributed into two regions namely anomeric protons in the range 4 – 5.5 ppm and the rest of the glycosides –CHOH protons between 3 - 4 ppm. The chemical shifts in the aromatic region were comprised of two doublets with *J* values above 8 Hz, each integrated to 2H corresponding to *o*- or *p*- arrangement of the protons. Two doublets with smaller *J* values of 1 – 2.5 Hz that

indicated *m*- arrangement of the aromatic protons and each integrating to 1H, and finally a singlet signal that integrated to 1H. DEPTQ showed the glycosidic carbons differentiated into methylene and methyne. It further distinguished the anomeric methyne carbons from the other glycosidic -CHOH signals. The aromatic protons were distributed in the range 90 - 130 ppm. Additionally, several quaternary carbons were found between 150 – 185 ppm. The carbon signals were assigned to their corresponding protons from HSQC cross peaks. The quaternary carbons were characterised from correlation with their neighbouring protons in HMBC. The proton sequence was established from $^{1}H - {}^{1}H$ COSY correlations and further confirmed form HSQC-TOCSY. The point of attach of the glycan chain to the aglycone was characterised from HMBC correlation between the anomeric proton of glucuronic acid and C-7 of the aglycone. Points of attach between the sugar moieties were often of higher δ_H and/or δ_C than the common chemical shift for their non-bonded counterparts. The interglycosidic linkages were further confirmed from HMBC correlations.

Compound DR4 showed NMR spectra that largely resembled those of DR3 (Figure 68 - Figure 73). However, the fact that it contained one sugar moiety less was readily detectable from their ^{1}H, ^{13}C NMR, and the rest of the 2D spectra.

Despite the overlap of the glycosidic signals it was possible to identify the configuration of the sugars utilising their 2D cross peaks. Therefore, *J* values listed in table 5 - except for the clearly resolved signals- are approximate measurements of the true values.

Figure 61 illustrates HSQC-TOCSY, COSY and some of the HMBC correlations used in the identification of the different moieties and their points of attach.

Table 6 1H and 13C NMR data for compounds DR3 and DR4. a: NMR in pyridine-D5 (500 µL) + MeOD (100 µL), b: NMR in MeOD.

Position	δ_H ppm (multiplicity, *J* Hz)		δ_C ppm	
	DR3[a]	**DR4[b]**	**DR3[a]**	**DR4[b]**
Aglycone				
1				
2			164.9	166.8
3	6.0 (*s*)	6.66 (*s*)	103.5	104.1
4			182.6	184.1
5			157.6	159.0

Position	δ_H ppm (multiplicity, *J* Hz)		δ_C ppm	
	DR3[a]	**DR4[b]**	**DR3[a]**	**DR4[b]**
6	6.40 (*d*, 2.5)	6.82 (*d*, 1.3)	95.3	96.0
7			163.5	164.4
8	6.23 (*d*, 2.5)	6.52 (*d*, 1.3)	100.8	101.4
9			161.9	162.8
10			106.3	107.2
1’			121.9	123.1
2’	7.04 (*d*, 8.8)	7.89 (*d*, 8.5)	128.8	129.7
3’	6.41 (*d*, 8.9)	6.93 (*d*, 8.5)	116.4	117.1
4’			161.9	162.9
5’	6.41 (*d*, 8.9)	6.93 (*d*, 8.5)	116.4	117.1
6’	7.04 (*d*, 8.8)	7.89 (*d*, 8.8)	128.8	129.7
D-Glucuronic acid				
1	5.19 (*d*, 7.5)	5.35 (*d*, 6.7)	99.5	100.1
2	3.64 (*t*, 8.3)	3.83 (*dd*, 7.4, 8.6)	82.5	82.9
3	3.73 (*t*, 8.8)	3.76 (*t*, 8.7)	76.2	77.7
4	3.81 (*t*, 9.0)	3.67 (*t*, 9.8)	72.3	72.7
5	4.04 (*d*, 9.3)	4.04 (*d*, 9.7)	76.6	76.4
6			173.0	174.2
D-Glucose 1				
1	4.54 (*d*, 7.6)	4.66 (*d*, 7.5)	105.3	105.3
2	3.17 (*t*, 8.9)	3.25 (*t*, 8.7)	75.3	75.8
3	3.18 (*t*, 8.6)	3.40 (*t*, 9.5)	76.5	77.6
4	3.39 (*t*, 9.6)	3.45 (*t*, 9.5)	70.36	70.8
5	3.35 (*m*)	3.40 (*t,* 9.0)	77.56	76.9
6	3.42 (*m*), 3.81 (*m*)	3.66 (*m*), 3.72 (*m*)	68.8	68.7
D-Xylose				
1	4.03 (*d*, 7.5)	4.24 (*d*, 7.5)	104.9	105.2

Position	δ_H ppm (multiplicity, *J* Hz)		δ_C ppm	
	DR3[a]	**DR4[b]**	**DR3[a]**	**DR4[b]**
2	3.14 (*m*)	3.15 (*t,* 9.5)	73.9	74.7
3	3.29 (*t*, 9.0)	3.28 (*t*, 8.2)	75.4	77.5
4	3.43 (*t*, 9.4)	3.40 (*t*, m)	77.4	71.1
5	2.77 (*m*),	3.07 (*m*),	64.1	66.9
	3.56 (*m*)	3.73 (*m*)		
D-Glucose 2				
1	4.11 (*d*, 7.7)		102.9	
2	3.13 (*m*)		73.9	
3	3.33 (*t*, 9.4)		77.4	
4	3.29 (*t*, 8.9)		70.9	
5	3.12 (*t,* 8.6)		77.8	
6	3.43 (*m*),		61.9	
	3.66 (*m*)			

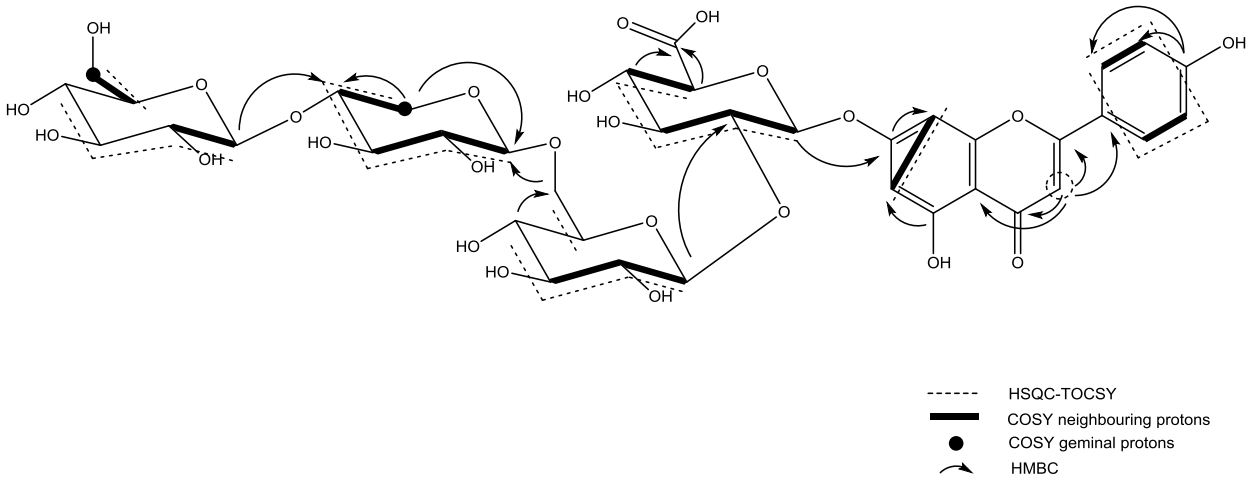

Figure 61 2D NMR correlations including HSQC-TOCSY, COSY and some HMBC correlations used in the structural identification of the isolated flavonoid-*O*-glycosides as exemplified by compound DR3.

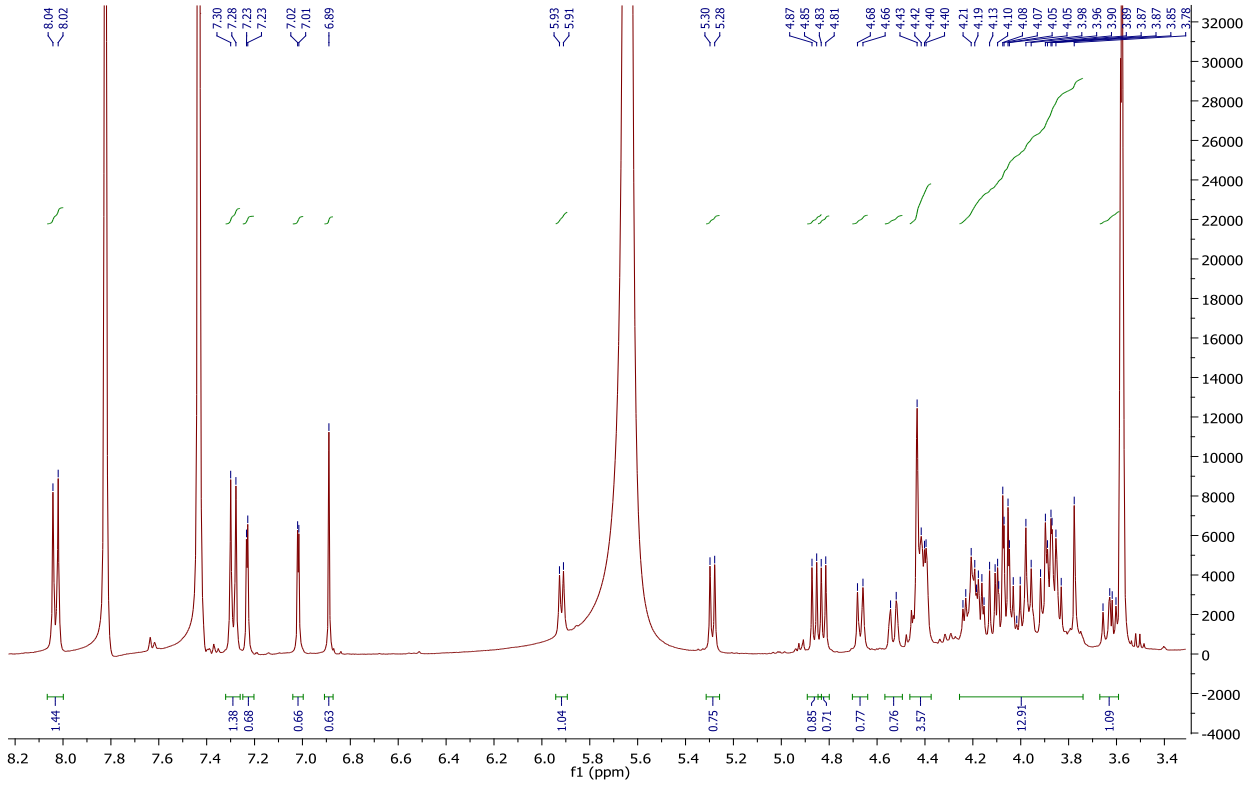

Figure 62 ^{1}H NMR of DR3 in pyridine-D5 (500 µL) + MeOD (100 µL).

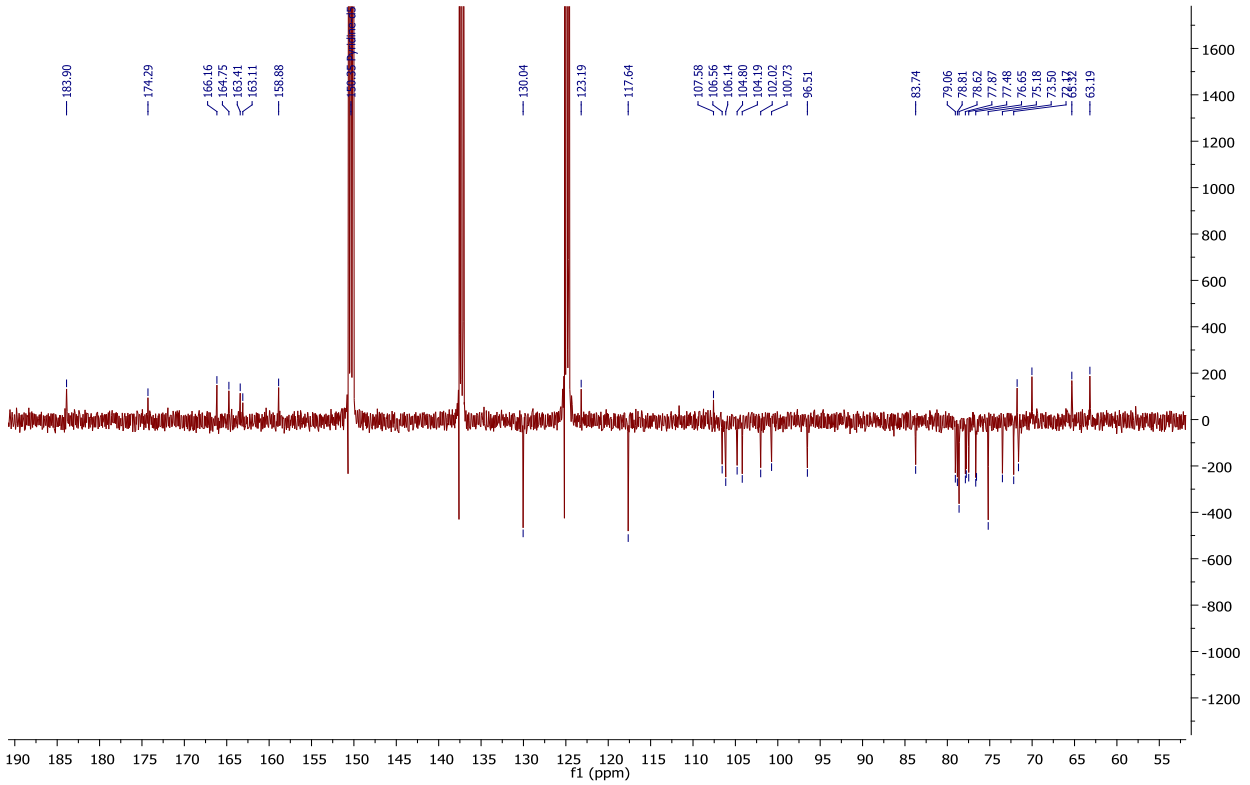

Figure 63 DEPTQ of DR3 in pyridine-D5 (500 µL) + MeOD (100 µL).

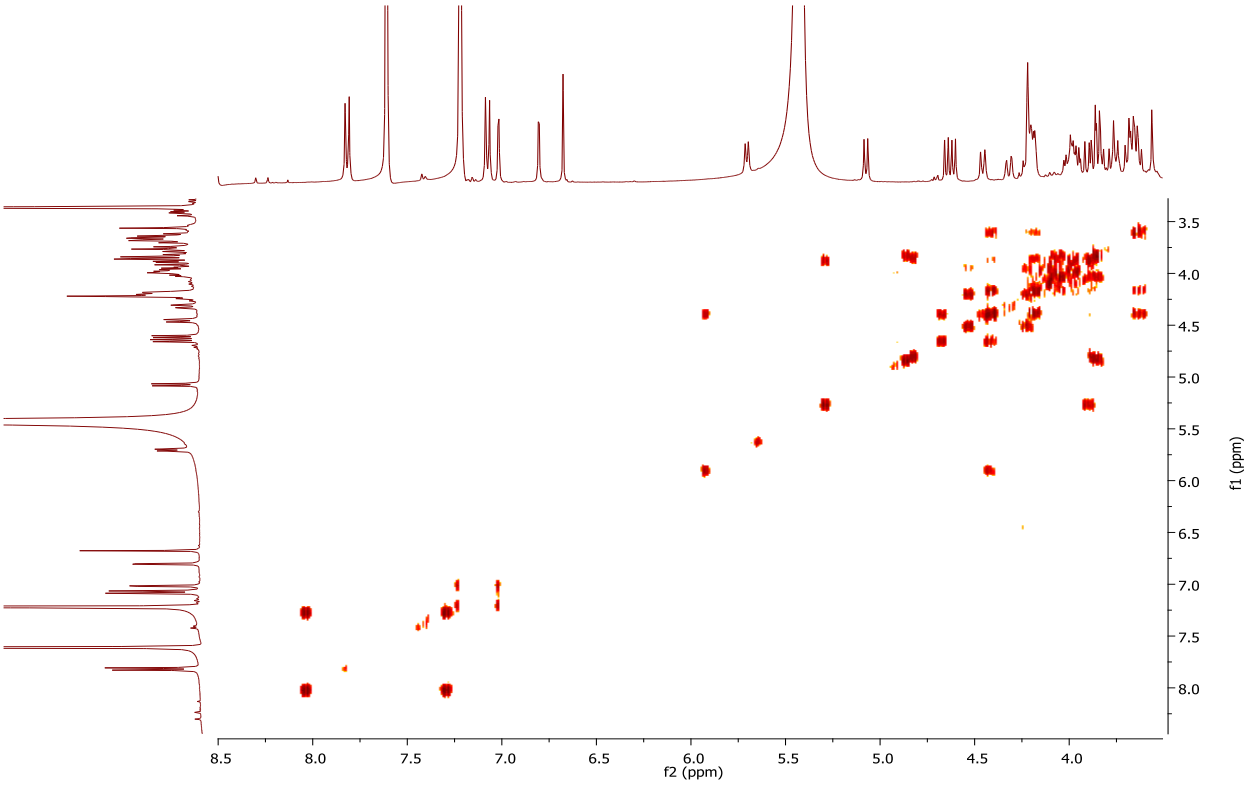

Figure 64 ^{1}H-^{1}H COSY of DR3 in pyridine-D5 (500 µL) + MeOD (100 µL).

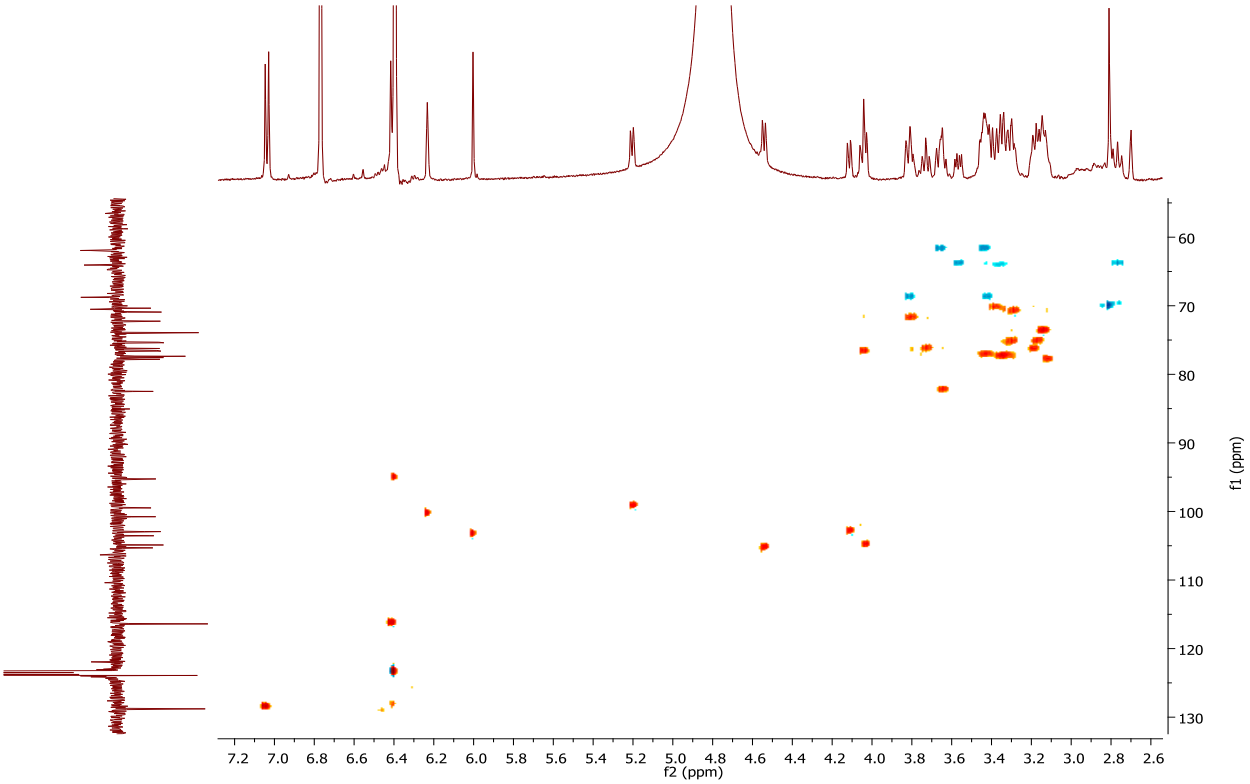

Figure 65 ^{1}H-^{13}C HSQC of DR3 in pyridine-D5 (500 µL) + MeOD (100 µL).

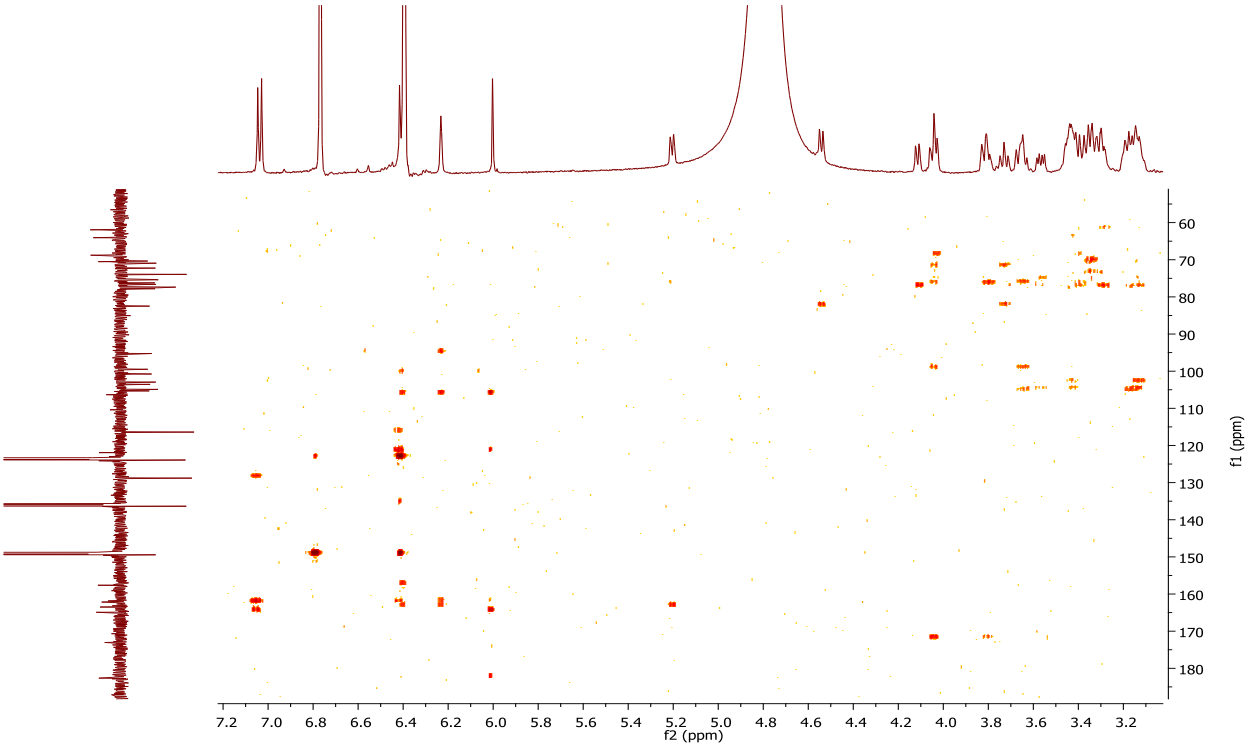

Figure 66 ^{1}H-^{13}C HMBC of DR3 in pyridine-D5 (500 µL) + MeOD (100 µL).

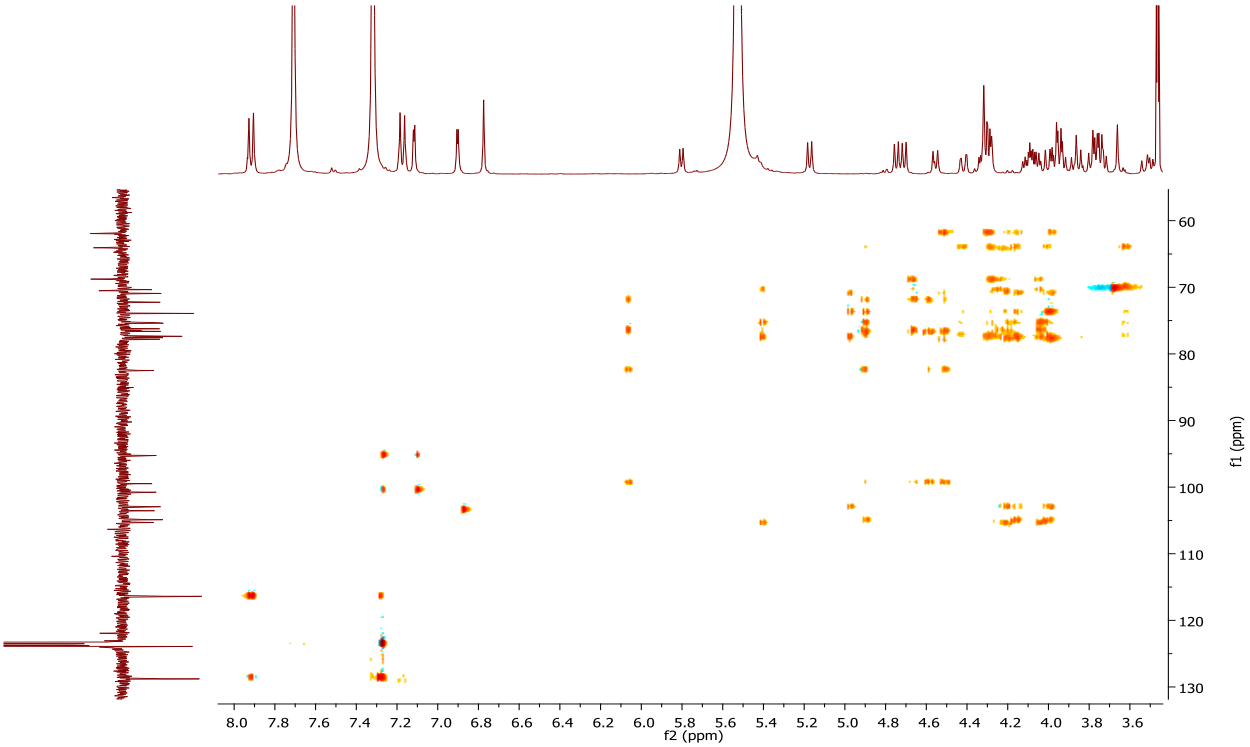

Figure 67 HSQC-TOCSY of DR3 in pyridine-D5 (500 µL) + MeOD (100 µL).

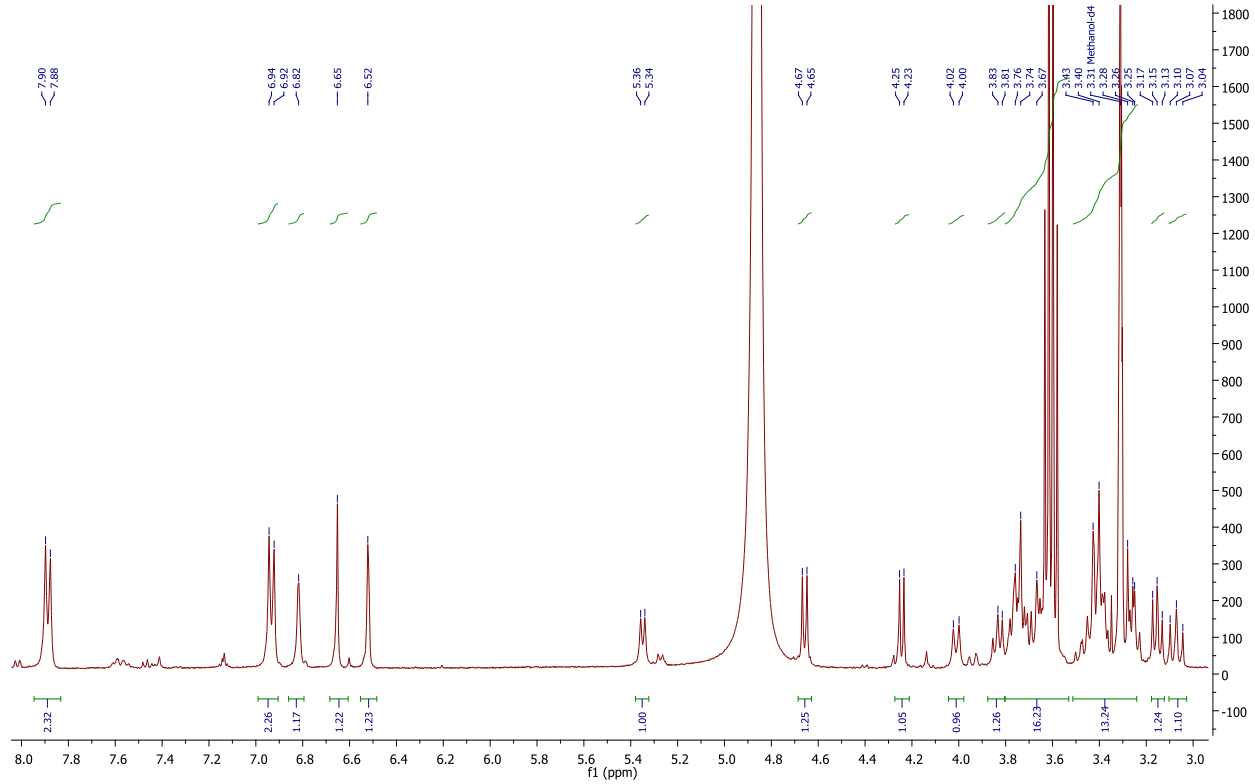

Figure 68 ^{1}H NMR of DR4 in pyridine-D5.

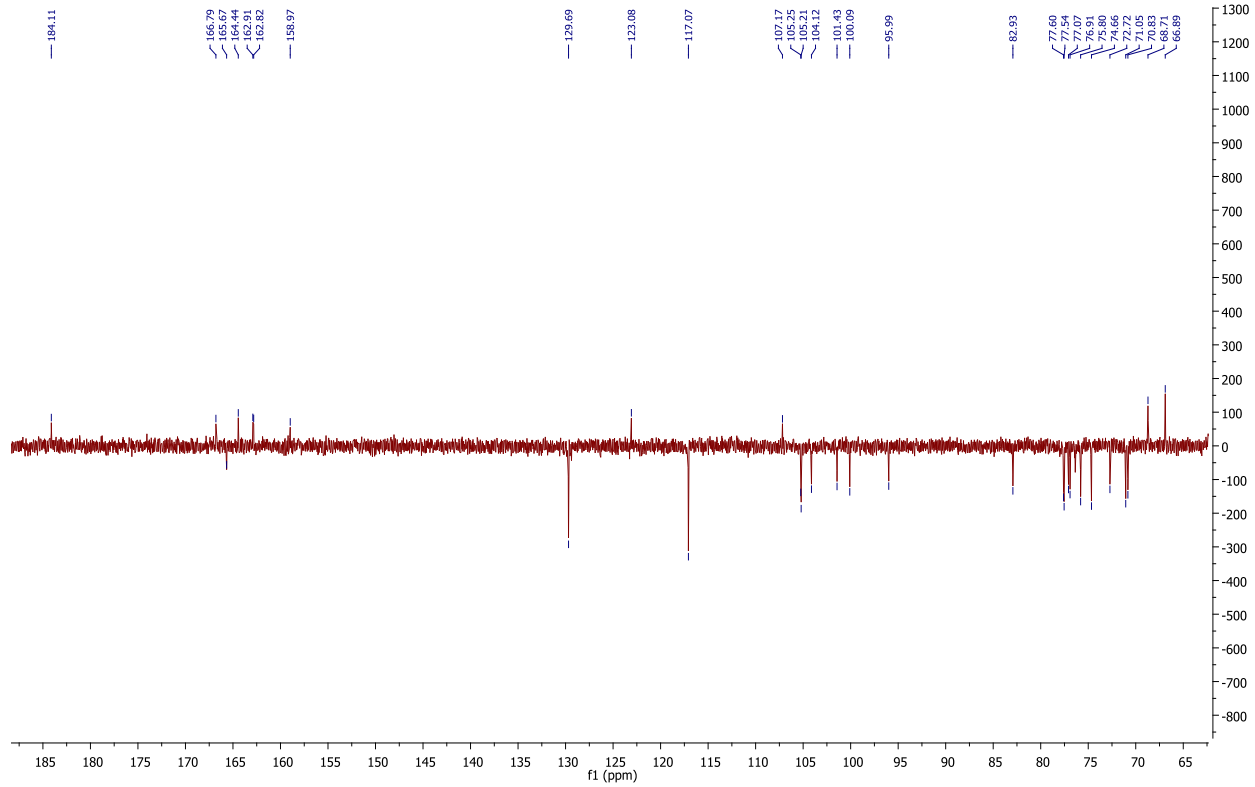

Figure 69 DEPTQ of DR4 in pyridine-D5.

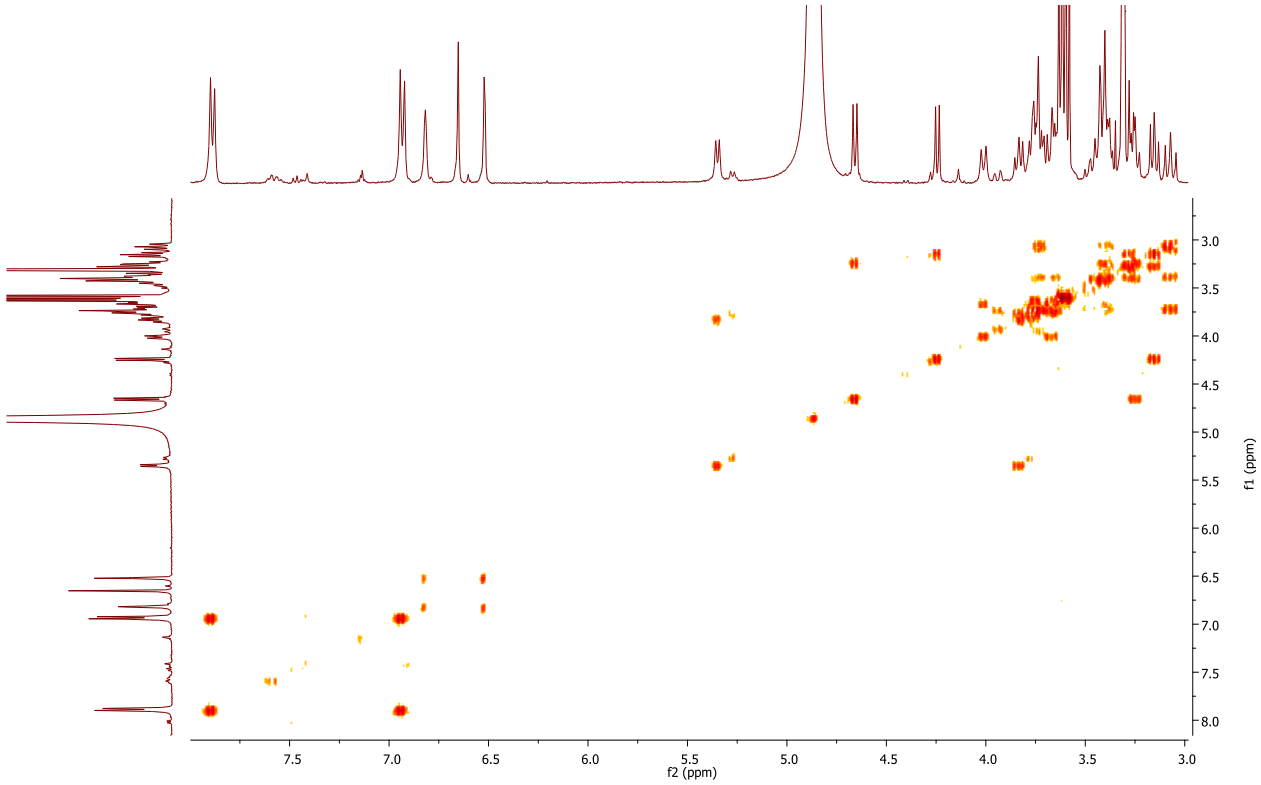

Figure 70 ^{1}H-^{1}H COSY of DR4 in pyridine-D5.

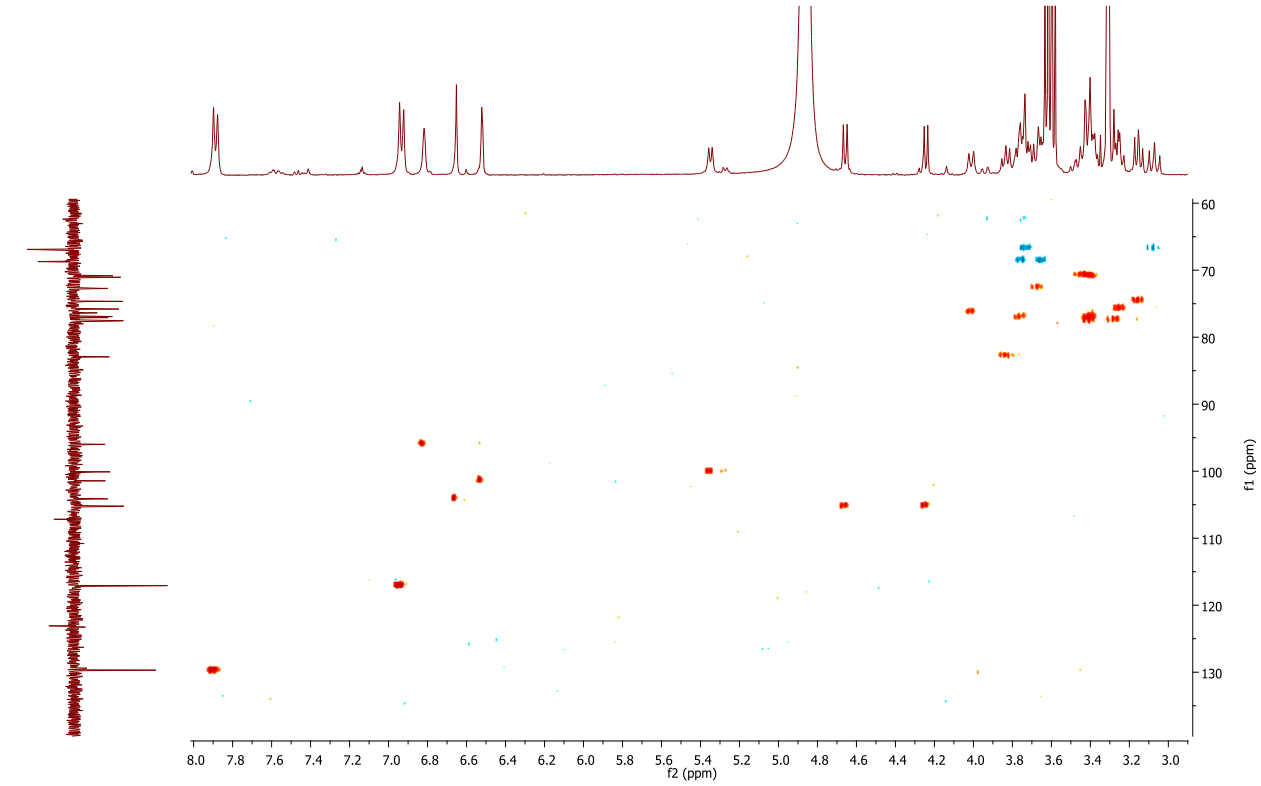

Figure 71 ^{1}H-^{13}C HSQC of DR4 in pyridine-D5.

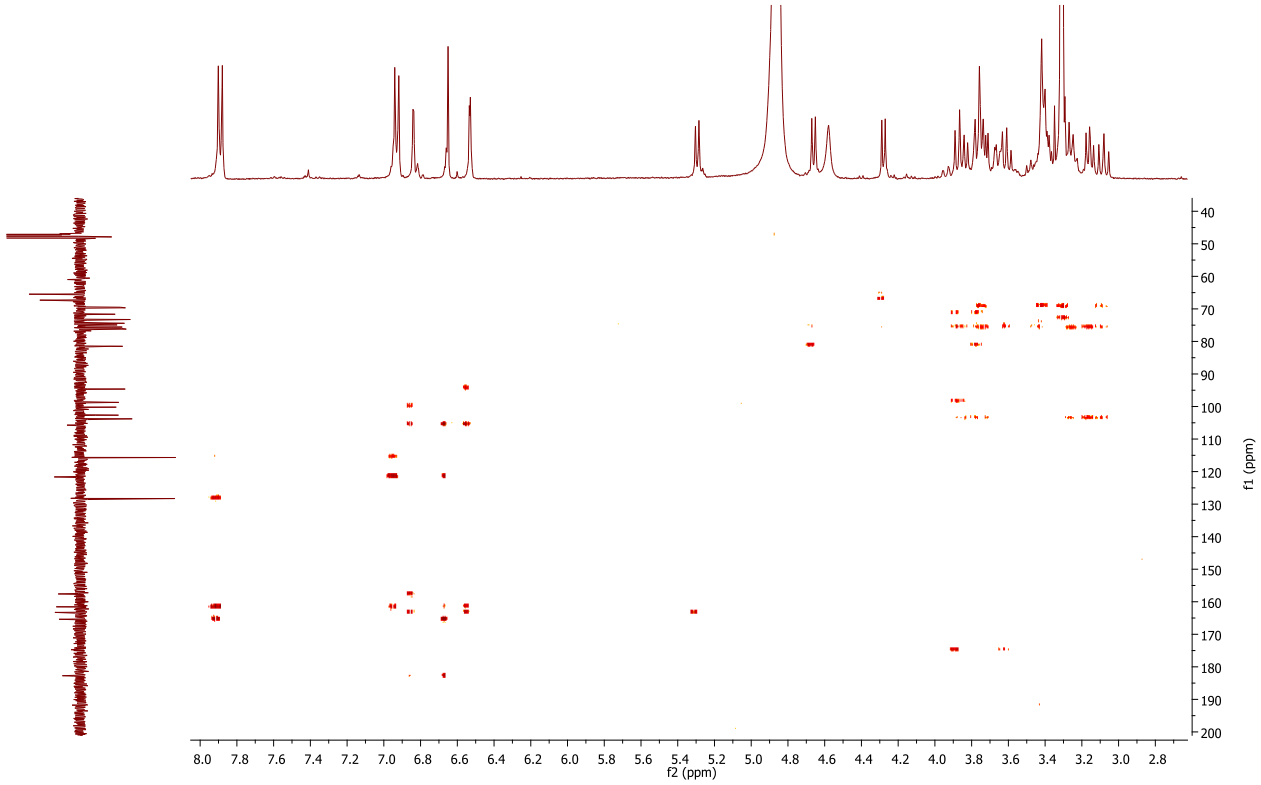

Figure 72 ^{1}H-^{13}C HMBC of DR4 in pyridine-D5.

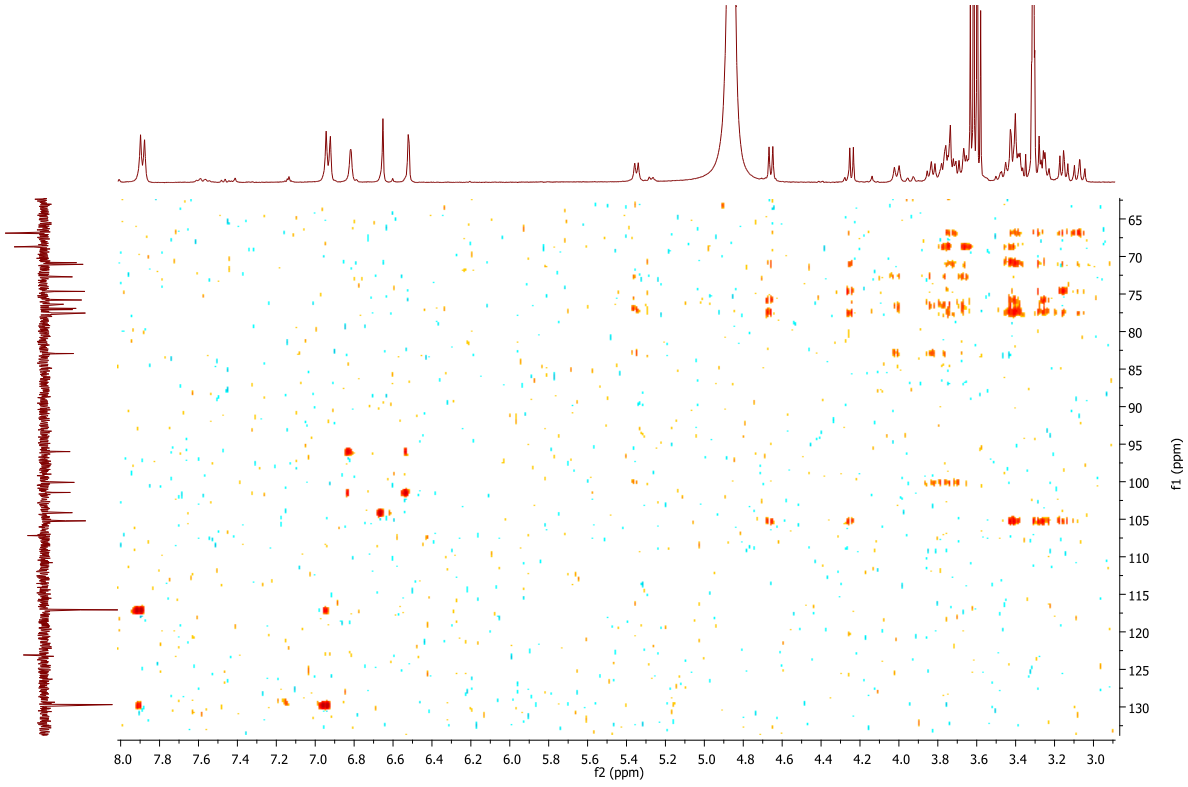

Figure 73 HSQC-TOCSY of DR4 in pyridine-D5.

3.3.2.2.2. LC-ESI-MS

The structure identified from NMR was further confirmed from the molecular mass obtained using high resolution mass in the negative ion mode which gave m/z 901.225 for DR3 with the molecular formula $C_{38}H_{45}O_{25}$ and for DR4 m/z 739.171 corresponding to the molecular formula $C_{32}H_{35}O_{20}$ (Figure 127 and Figure 128).

LC-MS and MS^2 in negative and positive ion modes were applied to the isolated compounds, the different fragment observed in both negative and positive modes are listed in Table 7. In the negative mode, the molecular mass, mass of the aglycone and the glycan chain could be identified in addition to two other fragments corresponding to loss of a water molecule and the loss of water and COOH (Figure 74 A). The positive mode fragmentation Figure 74 B gives valuable information in addition to the molecular mass and the aglycone part about the type of the sugar moieties present and their sequence in the glycan chain. For compound DR3 with $[M+H]^+$ of 903, the loss 162 mass units followed by 132, 162 and 176 is in agreement with the structure identified from NMR assignment containing a glycan sequence of a hexose, a pentose, a hexose and a glucuronic acid starting from the farther end from the aglycone.

Compound DR4 showed a very similar fragmentation to compound DR3 in both negative and positive modes, with a difference of 162 mass units (Figure 76). The mass fragment corresponding to the loss of the terminal hexose Y3 was missing for this compound indicating the presence of only three sugars in the glycan part of the molecule.

Table 7 Fragments in negative and positive mode for compounds DR3 and DR4.

	DR3	DR4
Negative mode fragments		
Molecular ion $[M-H]^-$	901	739
Loss of water	883	721
Loss of water and CO_2	839	677*
The glycan part	631	469
The aglycone (Y_0)	269	269
Positive mode fragments		
Molecular ion $[M+H]^+$	903	741
Y_3	741	n.a.
Y_2	609	609
Y_1	447	447
The aglycone (Y0)	271	271

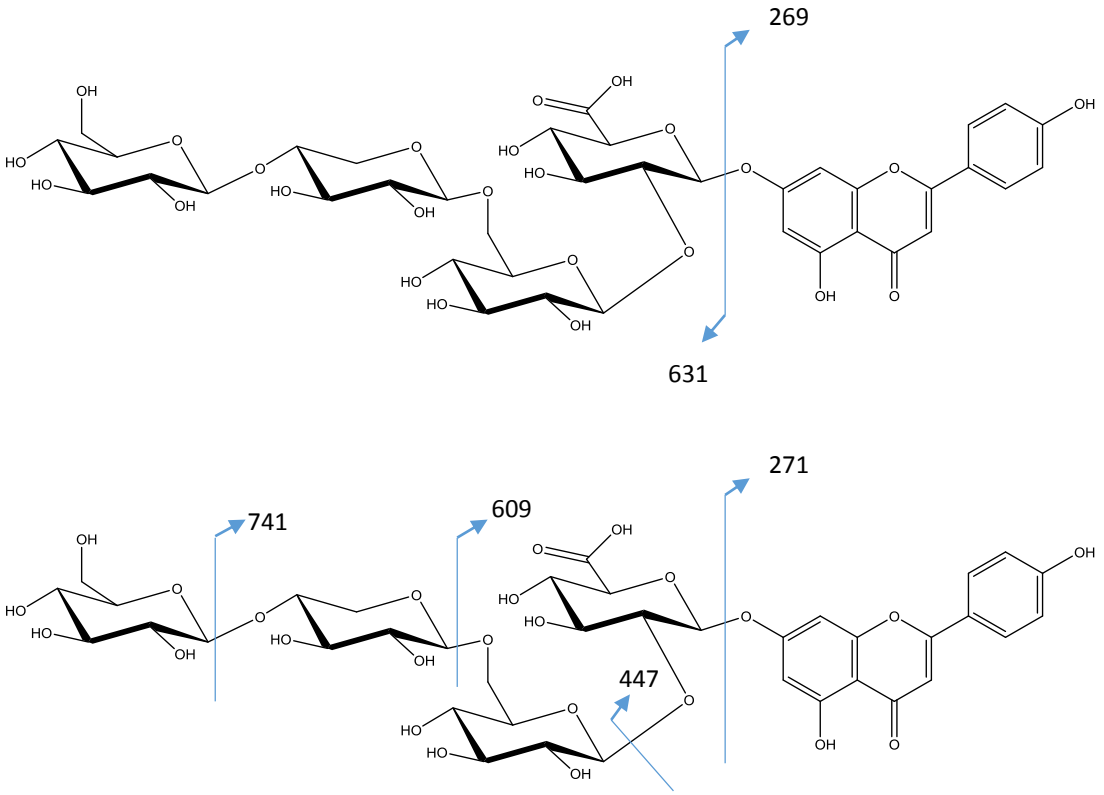

Figure 74 Fragmentation pattern for the isolated flavonoid-*O*-glycosides as exemplified by compound DR3 in A: Negative and B: positive ionisation modes.

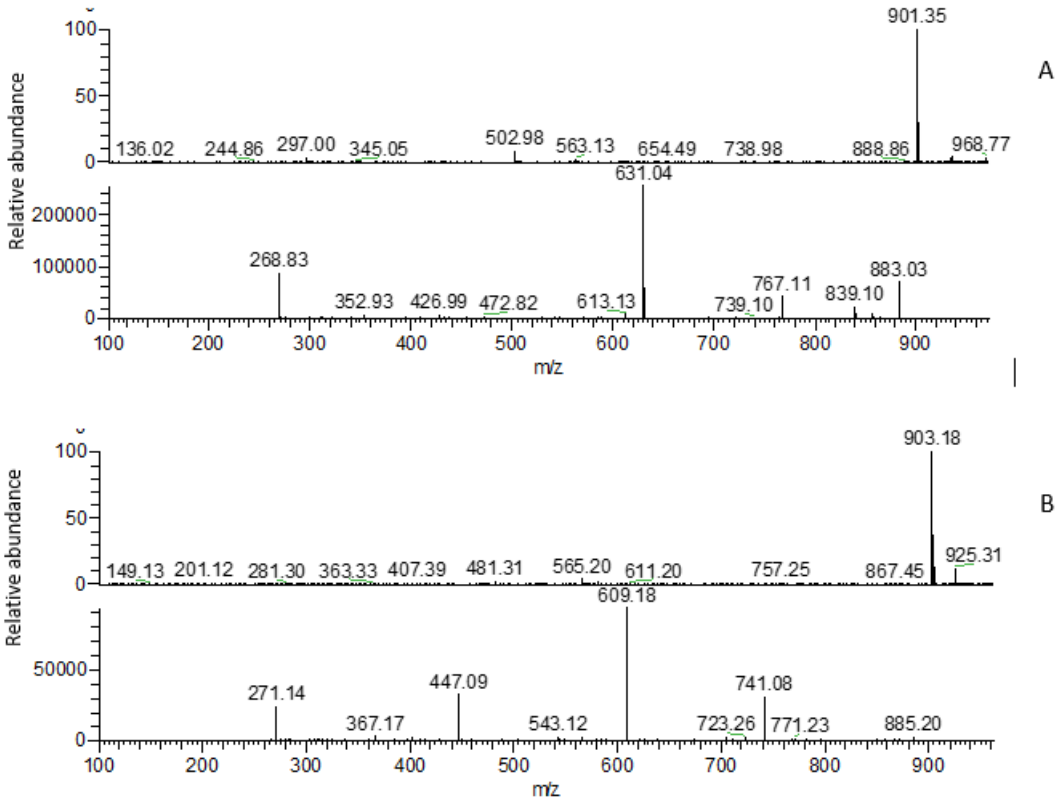

Figure 75 LC-MS and MS2 of DR3 in A, negative and B, positive ion modes.

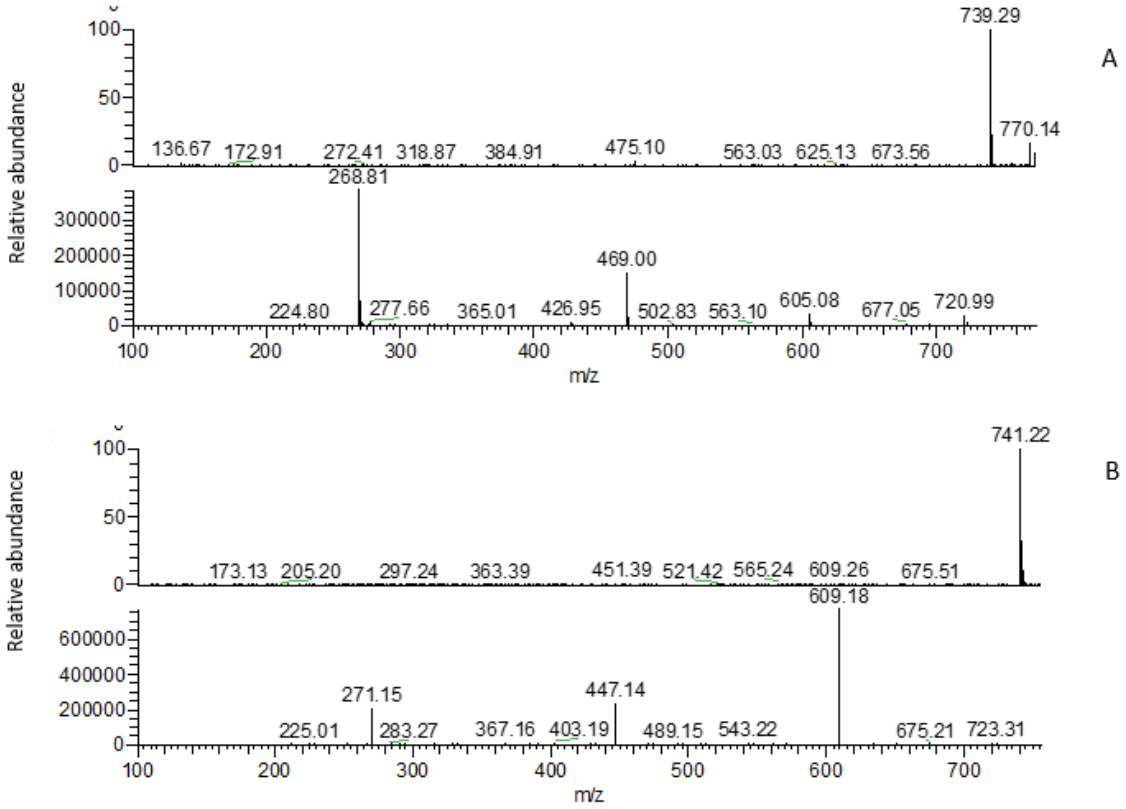

Figure 76 LC-MS and MS2 of DR4 in A, negative and B, positive ion modes.

3.3.3. Seasonal variation of *p*-coumaric acid and apigenin

3.3.3.1. Acid hydrolysis and product identification

Acid hydrolysis was employed in the quantification of hydroxycinnamic acids and flavonoids as it largely simplifies the chemical profile and subsequently the quantification of the target compounds in the plant. Comparison of HPLC chromatograms of the hydrolysis products of the different plant parts (Figure 77) with their methanolic extracts. Figure 38 shows the extent to which acid hydrolysis can facilitate the quantification of the aglycones by limiting the chemical composition to only few components.

There are however some draw backs for the use of acid hydrolysis which include underestimations due to the presence of the acid-resistant *C*-glycosides and decomposition of aglycones under the reaction conditions of high temperature and acidity. Also the possibility of side reactions and polymerisation can add to the uncertainties in the analysis.

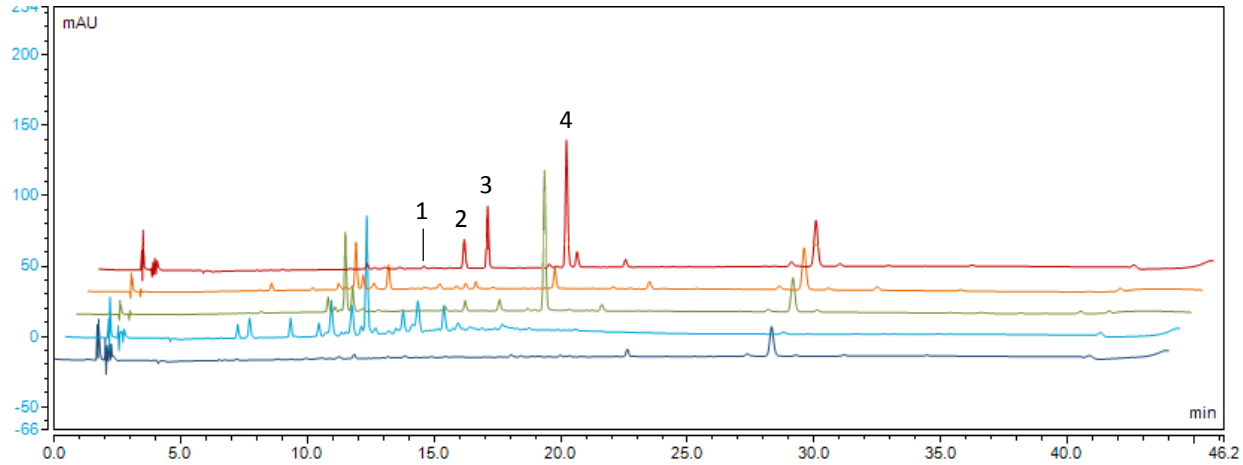

Figure 77 HPLC chromatogram for acid hydrolysis mixture of different parts of bluebell plants. 1: *p*-coumaric acid, 2: apigenin, 3: 7-*O*-(*β*-D-glucopyranoside methyl uronate) apigenin, and 4: 7-*O*-(*β*-D-glucopyranosideuronic acid) apigenin at 335 nm.

It was therefore necessary to identify the products of the hydrolysis reaction. Bluebell flowers were chosen at this stage due to the visual indication of the presence of flavonoids especially during anthesis. After hydrolysis of the flower extract, the less polar de-glycosylated compounds were extracted into ethyl acetate and four compounds were isolated from this fraction. Data combined from ^{1}H NMR, ^{13}C NMR, COSY, HSQC, HMBC and HSQC-TOCSY were used in the complete structural elucidation of the isolated compounds (Figure 129 - Figure 150). Compound 1 was identified as *p*-coumaric acid from NMR data and also from comparing t_R and UV spectrum with a standard compound. NMR data were in good agreement with previously reported values (Swislocka et al. 2012). The structure of compounds 2, 3 and 4 were identified based on their NMR data and the results showed good agreement with literature values (Švehlíková et al. 2004). Table 8 and Table 9 show ^{1}H and ^{13}C NMR values for the isolated compounds respectively.

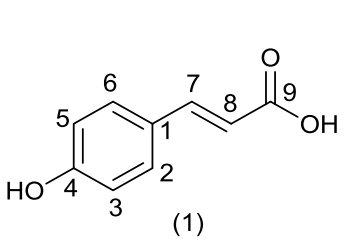

(1)

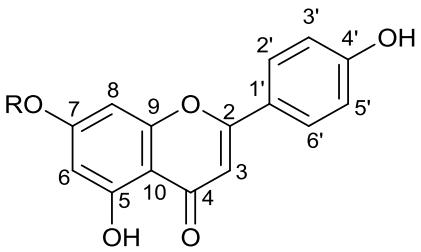

(2) R = H
(3) R = *β*-D-glucopyranoside methyl uronate
(4) R = *β*-D-glucopyranosideuronic acid

Figure 78 Phenolic compounds isolated after acid hydrolysis of bluebell pigment extract.

Table 8 ^{1}H NMR data of compounds 1, 2, 3 and 4.

a: NMR was taken in MeOD; b: NMR in 500 µL pyridine-D_5 + 100 µL MeOD.

Position	δ_H ppm (multiplicity, *J* Hz)			
	1[a]	**2**[a]	**3**[b]	**4**[b]
Aglycone				
1				
2	7.47 (d, 8.6)			
3	6.82 (d, 8.6)	6.89 (s)	6.66 (s)	6.81 (s)
4				
5	6.82 (d, 8.6)			
6	7.49 (d, 8.6)	6.73 (d, 2.0)	6.89 (d, 2.16)	7.09 (d, 1.75)
7	7.62 (d, 15.9)			
8	6.30 (d, 15.9)	6.81 (d, 2.0)	6.62 (d, 2.16)	6.80 (d, 1.8)
9				
10				
1’				
2’		7.91 (d, 8.7)	7.74 (d, 8.87	7.81 (d, 8.6)
3’		7.20 (d, 8.5)	7.02 (d, 8.74)	7.13 (d, 8.6)
4’				
5’		7.20 (d, 8.5)	7.02 (d, 8.74	7.13 (d, 8.6)
6’		7.91 (d, 8.7)	7.74 (d, 8.87)	7.81 (d, 8.6)
D-glucuronic				
acid				
1”			5.69 (d, 7.43)	5.94 (d, 7.45)
2”			4.04 (dd, 7.56, 8.90)	4.31 (dd, 7.47, 9.12)
3”			4.10 (t, 8.90)	4.39 (t, 8.97)
4”			4.20 (t, 9.22)	4.56 (t, 9.24)
5”			4.62 (d, 9.65)	4.88 (d, 9.69)
6”				
-OCH_3			3.55 (s)	

Table 9 ^{13}C NMR data of compounds1, 2, 3 and 4.

a: NMR was taken in MeOD; b: NMR in 500 µL pyridine-D5 + 100 µL MeOD.

Position	δ_C ppm			
	1[a]	**2**[a]	**3**[b]	**4**[b]
Aglycone				
1	125.8			
2	129.7	164.3	164.6	164.7
3	114.2	103.7	103.5	103.7
4	159.7	182.5	182.4	182.4
5	114.2	162.9	157.4	157.6
6	129.7	99.8	94.9	95.0
7	145.1	165.7	163.0	163.4
8	115.2	94.6	99.9	100.2
9	169.5	158.3	161.8	162.0
10		104.8	106.2	106.3
1’		122.1	121.4	121.8
2’		128.7	128.5	128.6
3’		116.6	116.2	116.3
4’		162.5	162.0	162.2
5’		116.6	116.2	116.3
6’		128.7	128.5	128.6
D-glucuronic acid				
1”			100.8	101.2
2”			73.7	74.0
3”			76.5	77.1
4”			72.1	72.5
5”			76.4	77.1
6”			169.6	171.9
-OCH_3			51.2	

3.3.3.2. Quantification of apigenin and *p*-coumaric acid

At the start of growth in March, 2014 when the above ground organs were comprised solely of the leaves and the flower primers encapsulated inside them, both parts were found to contain appreciable amounts of apigenin of approximately 2 – 3 mg. g^{-1} DW . The leaves content increased up to 6 mg. g^{-1} DW during the rapid shoot growth in April (see Figure 15 for the phenological stages), then remained relatively constant over the following month. A slight decrease was noticed in the leaves during anthesis from mid– end of May. Leaf senescence was accompanied by an increase in apigenin content per dry weight, which could be attributed in part to the decrease in tissue content of other components such as carbohydrates (Figure 19) which are being catabolised or mobilised at this stage leaving behind the flavonoids in the aging leaves. Apigenin content in the scapes started low in the first week of their emergence in April then increased to 16 mg. g^{-1} DW during anthesis to drop again with the start of senescence. The flower content also increased with the plant growth reaching over 11 mg. g^{-1} DW at the start of anthesis in the first week of May. The high values were maintained up until the end of anthesis, after which it dropped to 1.5 – 2.5 mg. g^{-1} DW during fruiting and seed formation. Figure 79 shows the seasonal changes in the concentration of apigenin in the different parts for the growth season in 2014.

None of the underground organs showed concentrations any close to that of the above ground parts throughout the growth season. The root's content of apigenin averaged around 0.05 – 0.1 mg. g^{-1} DW, while the bulbs contained relatively higher contents ranging from 0.15 – 0.25 mg. g^{-1} DW. However, the chromatogram of the bulbs showed several other unidentified peaks at 335 nm with earlier elution than apigenin and its two other glycosylated conjugates. This can indicate that these compounds are of higher polarity and/or lower molecular weight. Allocation of secondary metabolites can vary between the different organs and even within the same organ based on their function and importance to the plant (Bazzaz 1997). The preferential distribution of apigenin to the above ground organs can be explained with regard to the role of flavonoids in protection against UV radiation, herbivorous predators, insects and parasites and as visual signal to attract potential pollinating insects. Since flavones contribute to flower colour production through co-pigmentation with anthocyanins (Miller et al. 2011). The significant increase of apigenin content in both flowers and scapes during anthesis is probably due to the high demand of flavonoids for optimal display of coloration in these two parts during this crucial period to attract pollinators and ensure seed formation. The common pollinators of

British bluebells are reported to be bumble bees and hoverflies (Rix 2004). In fact, most of flowers pollinated by bees are in general either blue or yellow in colour (Miller et al. 2011).

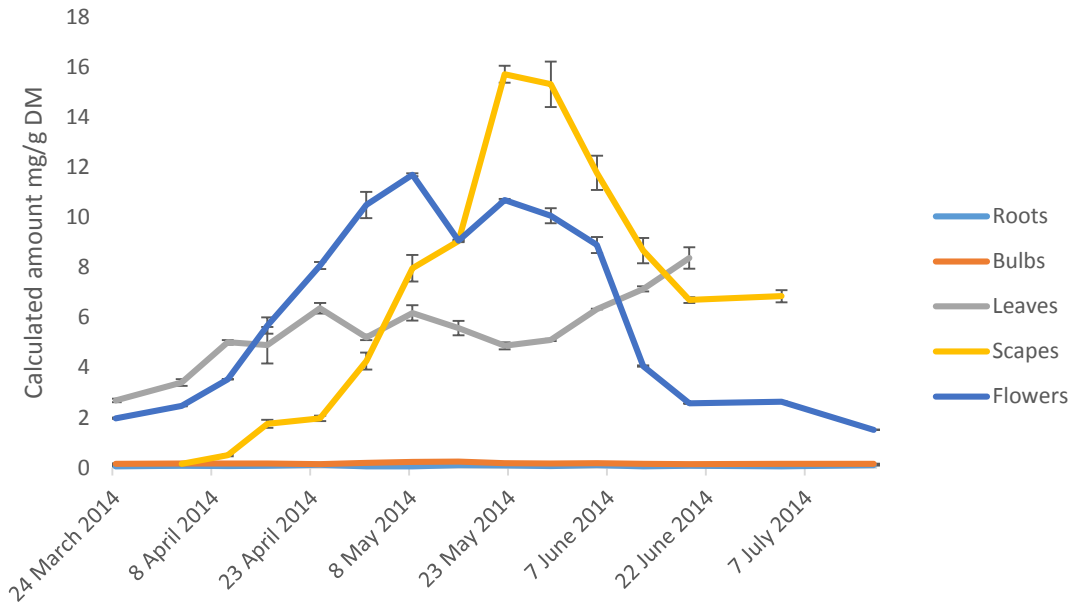

Figure 79 Seasonal variation of apigenin in different parts of bluebell.

Quantification of *p*-coumaric acid, showed that this phenolic acid is distributed mainly in the flowers with concentrations reaching up to 0.5 mg. g^{-1} DW during anthesis. The content of the other plant parts didn't exceed 0.1 mg. g^{-1} DW with the scapes showing higher concentrations compared to the other parts in particular during anthesis Figure 80. This could be due to that scapes exhibit a purple colouration at their upper portion similar to the flowers. *p*-Coumaric acid is not the only phenolic acid present in bluebells as LC-MS analysis Table 3 showed the occurrence of ferulic and sinapic acids in the plant.

The high concentration of *p*-coumaric acid in the flowers and to less extent in the scapes and in particular during anthesis can be taken as a clue for the participation of this compound in the visual attraction and colour development. *p*-Coumaric acid is reported to occur in conjugation to the anthocyanin in bluebell flower along with malonic acid (Takeda et al. 1986). Additionally, and as is shown from LC-MS analysis (Table 3), *p*-coumaric acid is also found in conjugation to several other flavonoid-*O*-glycosides.

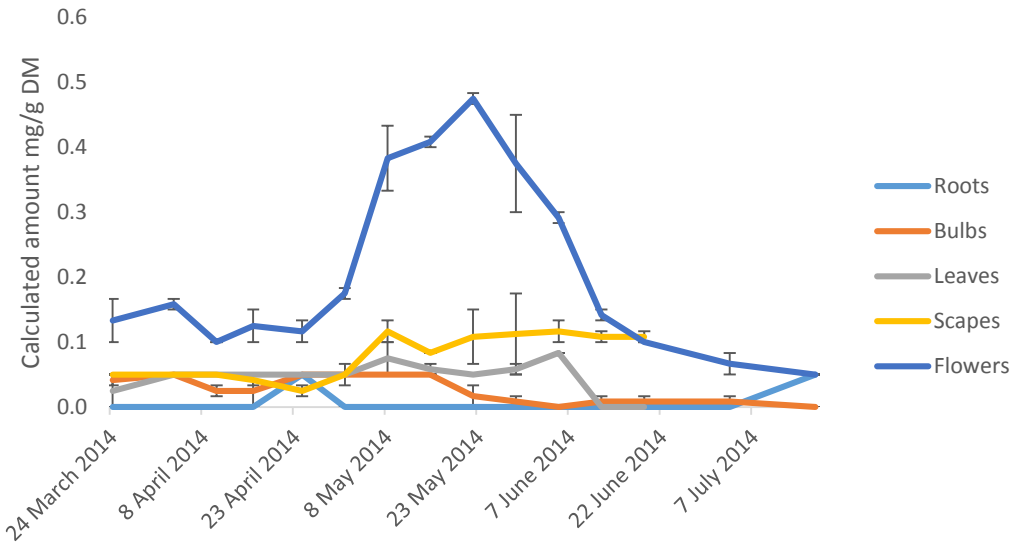

Figure 80 Seasonal variation of *p*-coumaric acid in different parts of bluebell.

It can be noticed from both graphs for apigenin and *p*-coumaric acid that- unlike non-structural carbohydrates that drop in content to values close to zero- the leaves and scapes were found to preserve a considerable amount of both phenolic aglycones during the last weeks of their life. Therefore, shedding of the dead tissues from the leaves and scapes might result in the addition of these compounds to the surrounding soil. However, it wasn't possible to indicate any presence of apigenin or *p*-coumaric acid by HPLC analysis of water, methanolic and aqueous methanolic extracts of soil sample taken from the same period. This could be explained in the light of the possible bacterial action in the soil that can degrades these compounds into phenols, phenolic acids and carboxylic acids. Flavonoids in soil face microbial degradation resulting in cleavage of ring C and the release of ring A as phloroglucinol and ring B in the form of the hydroxycinnamic acid originally incorporated in the molecule which in the case of apigenin is *p*-coumaric acid. The released compounds will get exposed to different microbial enzymes resulting in side-chain shortening ring cleavage and eventually producing aliphatic compounds and CO_2 (Cesco et al. 2012; Rao and Cooper 1994). The transfer of these compounds to the plant's surrounding will extend the ecological function of bluebell phenolics beyond defence and attraction into symbiosis, allelopathy and contribution to mineral uptake.

Chapter 4: Saponins

4.1. Introduction

Saponins are secondary metabolites widely distributed in plants. Their basic skeleton comprises a non-polar triterpenoid or steroid part and a polar glycosidic part. The presence of the two polar and non-polar parts within the same molecule provides these compounds with their soap-like properties in water and aqueous solutions (Haralampidis et al. 2002; Hostettmann and Marston 2005b). Saponins are stored in cell vacuoles, but other cellular locations such as mitochondria and the chloroplasts have also been reported to contain them (Hostettmann and Marston 2005b; Kesselmeier and Urban 1983). Although saponins are mainly found in angiospermous plant, there are also reports of these compounds in ferns and marine organisms (Hanuš et al. 2003; Mackie et al. 1977).

Saponins are classified broadly based on their aglycone into steroids and triterpenoids (Figure 81). Nitrogen-containing aglycones are put in a third class and referred to as steroidal alkaloids.

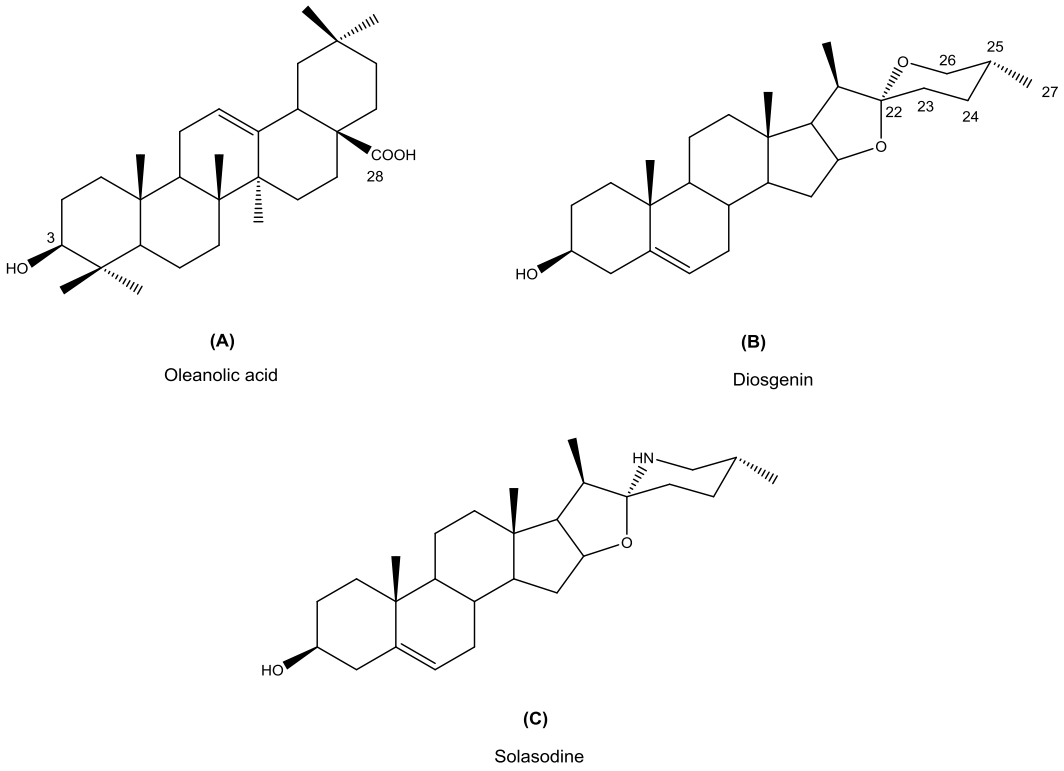

Figure 81 Examples on the main classes of saponin aglycones: A, triterpene; B, steroid and C, steroid alkaloid.

Saponins are also classified based on the number of glycan residues into monodesmosidic saponins where one glycan chain is attached via an ether linkage to the hydroxyl group on C-3, didesmosidic where a second glycan chain is linked via an ester bond to the -COOH group on C-28. Tridesmosidic saponins containing three glycan residues are rarely found. The glycan chains can be linear or branched often containing 2 – 5 sugar units with glucose, galactose, arabinose, xylose, rhamnose and glucuronic acid being the most common. Additional structural diversity can arise from the presence of other functional groups in the molecule mainly being –OH, -CO, -COOH and aromatic and aliphatic carboxylic acids ((Augustin et al. 2011; Haralampidis et al. 2002; Hostettmann and Marston 2005b; Hostettmann and Marston 2005b; Sparg et al. 2004; Vincken et al. 2007).

4.1.1. Biosynthesis

Both steroids and triterpenes share a basic skeleton made up of 6 isoprene units. They are biosynthesised from squalene via cyclisation of oxidosqualene (squalene-2,3-epoxide). Cyclisation of the chair-chair-chair conformation results in the formation of a tetracyclic cation which gives the C_{30} pentacyclic triterpene (β-amyrin). Conversely, the cyclisation of a chair-boat-chair form of oxidosqualene results in the formation of the C_{27} steroids lanosterol and cycloartenol as the end products after several rearrangements of the tetracyclic carbon cation. Figure 82 shows a simplified schematic diagram of the biosynthetic pathways leading to triterpenoids and steroids (Augustin et al. 2011; Hostettmann and Marston 2005b; Hostettmann and Marston 2005b; Vincken et al. 2007).

Glycosylation of the produced aglycone is the final step in the biosynthesis and occurs by the action of uridin diphosphate glycosyl-trasferases which adds sugar units to the C-3 hydroxy group in a stepwise manner. However, a complete glycan chain is added when glycosylation is at a carboxy group (Haralampidis et al. 2002; Hostettmann and Marston 2005a; Vincken et al. 2007).

4.1.2. Biological activities of saponins

Despite their low toxicity to mammals, saponins are known to be toxic to most cold-blooded species. They have long been known for their poisonous effects to fish and snails (Francis et al. 2002; Neuwinger 2004). They also confer insecticidal properties due to their anti-feeding and growth-regulating characteristics on harmful insects (Chaieb 2010; Goławska et al. 2008). Saponins are known for their haemolytic action on mammalian erythrocytes. This is an example of the membrane-disrupting activities cause by these compounds. The presence and

distribution of sterols in the membrane is the main factor in this phenomenon. Saponins interact with these steroids and as a result the aglycone part is integrated into the membrane leading to membrane curvature and the formation of pores (Augustin et al. 2011; Lacaille-Dubois and Wagner 1996; Milgate and Roberts 1995). Saponins are reported to possess antiviral activity (He et al. 2005; Simões et al. 1999), cancer-preventing activities including cytotoxicity and anti-tumour promoting effects (Kuroda et al. 2004; Lacaille-Dubois and Wagner 1996; Lee et al. 2002; Man et al. 2010). They are also known for their anti-inflammatory (Tapondjou et al. 2008), anti-fungal (Coleman et al. 2010; Zhang et al. 2005) and anti-microbial effects (Saleem et al. 2010).

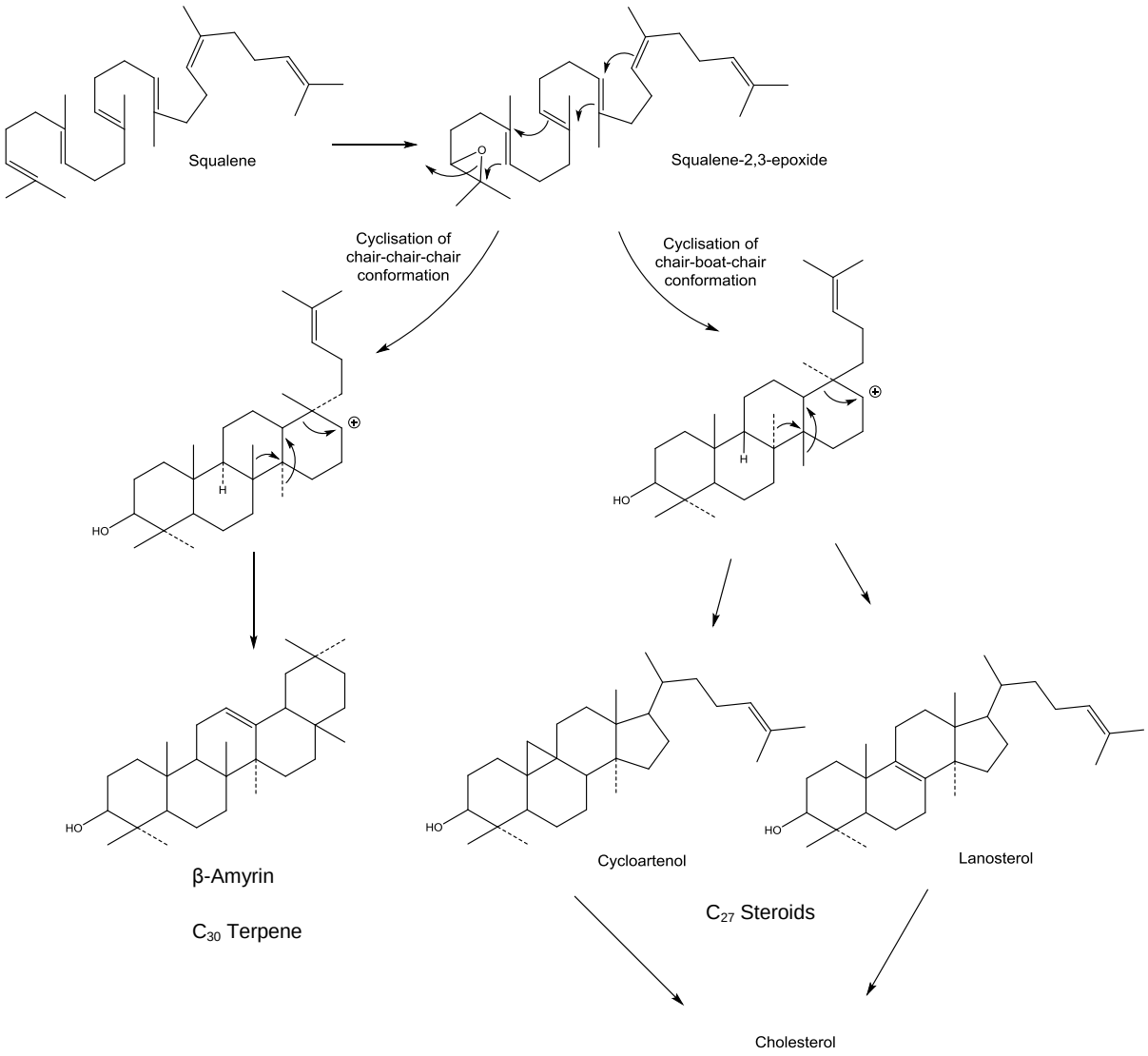

Figure 82 Biosynthesis of terpenes and steroids from squalene.

4.1.3. Ecological significance of saponins

The biological activity of saponins has enabled them to contribute to plant's defence against biotic stress factors including different pathogens and herbivores. The localisation of the saponins and their hydrolysing enzymes in the cell is disturbed upon fungal infection leading to the release of the bioactive form of these compounds (Osbourn 1996). Saponins exhibit insecticidal properties as a result of their toxicity on insects feeding on the plant, leading to increased mortality, decreased weight and low development and reproduction rates (De Geyter et al. 2007). Larval herbivory on alfalfa leaves was found to result in an increase in the total saponin content which indicates their involvement in the response mechanism (Agrell et al. 2003). In addition to contributing to plant defence, saponins are also involved in symbiosis with nitrogen-fixing rhizobia and mycorrhizal fungi necessary for nutrient uptake (Szakiel et al. 2011b).

Saponins also contribute to the plant's response to abiotic stress. High UV-B radiation levels was found to increase the content of saponins and flavonoids in leaves of *Centella asiatica* (Müller et al. 2013). Conversely, water and salinity stress was found to decrease saponin content and increase phenolics in quinoa plants (Gómez-Caravaca et al. 2012). Environmental conditions of light and temperature also affect plant saponin levels (Szakiel et al. 2011a).

Saponins can exert allelopathic effects through inhibiting growth of other plants. Alfalfa saponins, which comprise a range of structurally varying aglycones in addition to differences in glycosylation patterns, are found to inhibit the growth of wheat seedling shoots and roots. They were also found to be toxic and causing growth reduction of cotton, barnyard grass and wheat (Oleszek et al. 1999; Oleszek 1993).

4.1.4. Metabolomics and multivariate analysis

In order to investigate the seasonal changes in chemistry of the overall bluebell secondary metabolites, metabolomics was used as a comprehensive approach utilising high resolution MS and multivariate data analysis (MVA).

Metabolomics aim at the complete quantitative investigation of a broad range of metabolites in a given biological sample. Since metabolites exist in enormous numbers and often of widely varying physio-chemical nature and concentration levels, their complete study is a challenging task requiring instrumentation with high sensitivity, reproducibility and the ability to discriminate between these metabolites (Dettmer et al. 2007; Roessner and Bowne 2009). A

number of techniques have been utilised in the analysis of metabolites in varying tissues and organisms of which LC -MS, GC-MS, NMR, capillary electrophoresis (CE) and FT-IR are the most common examples (Roessner and Beckles 2009). The chromatograms and spectra obtained by application of these techniques usually contain a large amount of data, a matter that necessitate the use of MVA to draw useful biological conclusions from the results. The raw data should first be processed. In an LC-MS analysis, this would involve peak detection, peak deconvolution, isotope grouping, noise removal and peak alignment to correct deviations in retention time. This can be performed using MZmine software for mass spectroscopy data analysis. This software can additionally perform clustering and produce a heatmap plot for the resulting peak list (Dettmer et al. 2007; Villas-Boas et al. 2007; Worley and Powers 2013). Following data analysis, dereplication is performed in an attempt to identify the metabolites by comparing the data with a relevant database (e.g., dictionary of natural product (DNP), MarineLit, etc.) which produces a table including peak IDs, their m/z, t_R and molecular formula within a given t_R and mass tolerance (Abdelmohsen et al. 2014; Tawfike et al. 2013; Wishart et al. 2009). Statistical multivariate analysis of the data involves the application of chemoinformatics principles to the metabolomics data (Kettaneh et al. 2005; Wold et al. 2001). The main strategies involved in MVA are the principal component analysis (PCA) and partial least square projection to latent structures (PLS) (alternatively, orthogonal partial least square projection to latent structures differential analysis (OPLS-DA)) (Worley and Powers 2013). PCA is an effective means of unbiased reduction of dimensionality that reveals group or cluster structures where variability between groups is sufficiently higher than within groups. PLS algorithm allows to further expose separations between groups. The application of PCA gives unbiased initial conclusion about the data which could be further confirmed with PLS plots. The results of either PCA or PLS is in the form of score and loading plots. Score plots reveal correlations between the samples, observations or experimental conditions revealing groups, trends or outliers. While loading plots reveal the trends in the variables, peaks or masses resulting in the variations between the samples (Worley and Powers 2013). Figure 83 shows an outline of the main steps in a metabolomics analysis for a plant sample.

The application of metabolomics to the ecology has been given the term ecometabolomics. This involves studying the influence of abiotic factors such as temperature stress, draught, salinity and the availability of nutrients as well as biotic factors such as the effect of fungi, bacteria and viruses, insects and animals on the metabolic profile. The holistic approach of metabolomics is of higher adequacy in presenting snapshots of the metabolites under the

experimental (controlled or field) conditions (Roessner and Beckles 2009; Sardans et al. 2011). Analysis of plant metabolomics has been widely applied in assigning phenotypes of genetically modified species. The application of metabolomics to drug discovery from natural products facilitates the process by speeding up the identification of the biologically active fractions or samples using natural product databases, given the previous isolation and identification of these compounds (Yuliana et al. 2011).

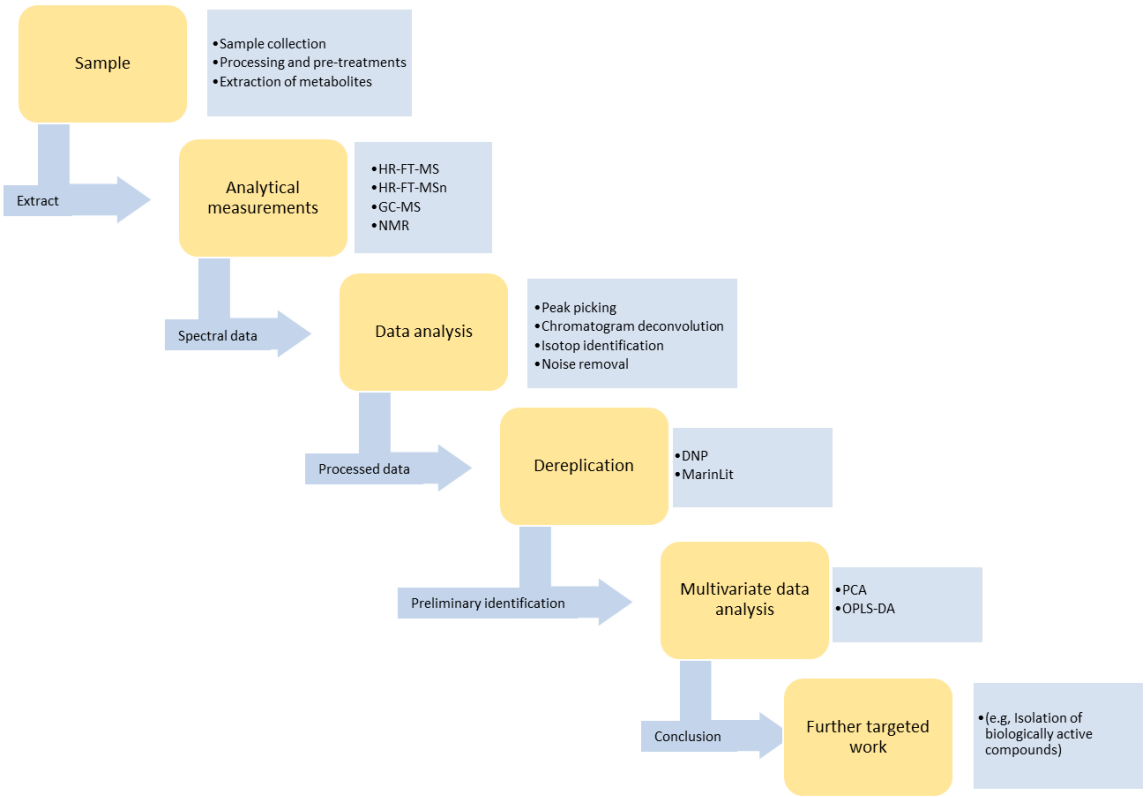

Figure 83 Diagram explaining the main steps in the metabolomics approach combined with multivariate analysis of the resulting data.

4.1.5. Analysis of plant saponins

4.1.5.1. Extraction

Extraction of saponins is usually performed using water or any of the low molecular weight alcohols from methanol to butanol. Extraction with alcohols is often preferred due to the ease of removal of these solvent as they result in less foaming of saponins compared to when water is used. Solvent extraction requires large quantities of solvents and long extraction time. Applying heat, mechanical stirring and shaking is sometimes used in order to facilitate the process. Green extraction techniques such as microwave and ultrasound- assisted extraction are gaining popularity in saponin extraction. These methods feature shorter extraction time, higher efficiency and the use of significantly lower solvent volumes (Cheok et al. 2014; Kerem et al. 2005; Rocher 1969).

4.1.5.2. Chromatography

Crude mixtures of saponin extracts are often subjected to several chromatographic separations utilising various stationary phases. This includes initial fractionation on Sephadex LH-20 or Diaion HP-20 beds, followed by chromatography on either NP-silica or C18 columns. The isolation of saponins is complicated by the presence of large number of these compounds in the same plant with very little structural variations. Added to this is their high polarity and lack of chromophores. Therefore, several consecutive chromatographic separations might be required. HPLC both on the analytical and preparative scale can provide better separation of saponins combined with high sensitivity, speed and the possibility of using various stationary phases (Kuroda et al. 2004; Mahato et al. 1982; Oleszek and Bialy 2006; Oleszek 2002).

4.1.5.3. Structural elucidation

The structural identification of saponins follow the same procedure for phenolics, which in summary involves the use of extensive spectrometric techniques including MS and MS/MS in addition to 1D and 2D NMR experiments. The difficulties caused by the presence of the oligomeric sugar chains can be circumvented by the use of hydrolytic techniques using either acid, alkali or enzymes. The cleaved sugar units can then be identified either by TLC with reference compounds or using GC-MS after derivatisation to more volatile forms. It should be noted however, that hydrolysis conditions might sometimes lead to partial decomposition of the aglycone (Domon and Hostettmann 1984; Mahato et al. 1982; Ori et al. 2003).

4.2. Methods

4.2.1. Metabolomics approach for bluebell saponin and general metabolite analysis

Preparation of samples

Samples used in this study were from March 2014 until the end of the of the above ground stage of the plant's life in July followed by the subterranean phase (end of July- October) and also three samples from the time of shoot emergence and re-growth in the following season (Table 10).

Freeze-dried and powdered plant tissues (100 mg) were extracted with MeOH on a 10 mg dry weight to 1 mL of solvent ratio. The samples were shaken at 250 rpm for 30 min. After this period, the samples were centrifuged for 30 min at 5000 rpm and the clear supernatant was separated and the solvent was evaporated.

Aliquots of 1 mg of the dried extracts were transferred into GC vials and dissolved in 1 mL of MeOH and submitted for LC-MS analysis.

LC-MS analysis

MS data was acquired in both positive and negative modes using a Dionex UltiMate3000 ThermoScientific HPLC system coupled to a Finningan LTQ high resolution ESI-MS. The samples were eluted through a C_{18} column (ACE) with a length of 75 mm, i.d. of 3.0 mm and particle size 5 µm. Using a mobile phase of water containing 0.1% formic acid (solvent A) and acetonitrile (solvent B), flow rate of 300 µL/min. Gradient elution was applied starting with 10% B for 5 min, then increased to 100% B over 30 min and held for another 5 mins then decreased to 10% B over 1 min. The column was then equilibrated with 10% B for 4 min until end of the run.

Fragmentation was performed for a number of samples on a Finnigan Surveyor system coupled to a Thermo-Finnigan LTQ Orbitrap (Thermo Scientific, Germany).

Data processing and statistical analysis

The spectral data obtained from the first stage LC-MS analysis were processed using Mzmine 2.17. The output data was then cleaned up using an excel macro where the data obtained in

positive and negative modes were combined, solvent-related peaks were removed and the results were compared with NPD database to facilitate the identification of any previously known metabolites. Multivariate analysis was performed using SIMCA-P v 13 for data analysis and recognition of patterns and outliers.

Table 10 The seasonal bluebell samples used in the metabolomics study.

Sampling date	Bulbs	Leaves	Scapes	Shoots	Flowers
24 March 2014	1			30	
03 April 2014	2	16	22		34
16 April 2014	3	17	23		35
01 May 2014	4	18	24		36
15 May 2014	5	19	25		37
29 May 2014	6	20	26		38
12 June 2014	7	21	27		39
03 July 2014	8		28		40
17 July 2014	9		29		41
30 July 2014	10				
13 August 2014	11				
29 October 2014	12				
09 February 2015	13			31	
04 March 2015	14			32	
16 March 2015	15			33	

4.2.2. Bluebell flower saponin

4.2.2.1. Extraction

Bluebell flowers were extracted with MeOH as stated in (Preparation of the bluebell flowers extract, p 74).

4.2.2.2. Chromatographic separation

From Fr 3, 300 mg was taken and dissolved in 6 mL de-ionised water and 1 mL portions were injected onto a C18 column. Gradient elution was applied using a solvent system of A: MeCN and B: H_2O both acidified with 0.1% FA starting from 100% B for 2 min then 100 – 70% B in 1.5 then 70 – 62% in 30 min. DR5 (20.3 mg) was collected as a white powder at t_R = 11.0 min. the structure was determined using NMR and MS. Figure 37 shows a diagram of the separation.

Physical appearance: white powder

Mass: HR-FTMS-ESI $[M+formate]^-$ gave m/z 1445.64 $C_{64}H_{103}O_{33}+HCO_2$ requires 1445.64 and $[M-H]^-$ gave m/z 1399.64 $C_{64}H_{103}O_{33}$ requires 1339.64.

^1H NMR δ_H ppm (400 MHz, Pyridine-d5): 6.25 (8 H, s), 5.27 (10 H, d, J 3.0), 4.63 (37 H, dd, J 9.2, 3.9), 4.58 – 4.41 (42 H, m), 4.35 (19 H, s), 4.28 (16 H, s), 4.23 – 4.10 (59 H, m), 4.06 (27 H, dd, J 15.4, 7.0), 4.03 – 3.87 (59 H, m), 3.82 – 3.74 (12 H, m), 3.59 (11 H, d, J 8.6), 2.52 (13 H, dd, J 7.3, 2.7), 2.47 – 2.32 (16 H, m), 2.16 (37 H, dd, J 24.0, 11.6), 2.09 – 1.92 (33 H, m), 1.74 (34 H, d, J 6.0), 1.64 (20 H, d, J 19.3), 1.54 (8 H, d, J 10.7), 1.47 (28 H, s), 1.32 (29 H, d, J 9.1), 1.09 – 0.96 (59 H, m), 0.92 (32 H, s).

^{13}C NMR δ_C ppm (101 MHz, Pyridine-d5): 212.6, 135.5, 134.9, 123.9, 105.5, 105.3, 103.9, 102.5, 102.0, 101.0, 97.1, 89.3, 88.1, 82.1, 81.6, 78.6, 78.2, 78.2, 78.0, 77.8, 77.6, 76.7, 75.4, 75.4, 75.2, 74.2, 73.7, 72.7, 72.6, 72.2, 71.6, 69.8, 69.7, 69.2, 68.6, 66.8, 62.7, 62.7, 62.4, 62.1, 61.8, 61.0, 50.9, 48.9, 48.2, 43.8, 43.5, 39.8, 36.9, 36.7, 35.8, 32.4, 32.2, 27.3, 26.6, 26.3, 25.4, 21.2, 19.7, 19.4, 18.8, 18.7, 17.3, 7.7.

4.2.2.3. Acid hydrolysis and GC-MS analysis

The isolated saponin was subjected to acid hydrolysis as follows:

2 × 0.1 mg aliquots of the compound were taken in GC-MS vials. To one of the vials, 100 µL of 2 M HCl was added and to the second 100 µL of 2 M HCl prepared in 50% aqueous MeOH. Both vials were heated on 90 ºC for 45 min, then dried down at 45 ºC under a stream of N_2. Once dry, the samples - along with a range of sugar standards - were converted to their oxi-trimethylsilyl derivatives for GC-MS analysis following the protocol used for mono- and disaccharides (GC-MS analysis of mono- and disaccharides, p 27).

4.2.3. Biological assays

4.2.3.1. Alamar blue assay to determine drug sensitivity of African trypanosomes in vitro[3]

The antitrypanosomal activity of the saponin DR5 was tested against the blood stream form of the Trypanosoma brucei (S427) using a modification of the microplate Alamar blue assay. The compounds were prepared as 10 mg/mL stock solutions in 100% DMSO. The 200 µg/ml test

[3] Biological activity tests against *T. brucei* and *M. marinum* were undertaken by Carol Clements. Strathclyde Institute of Pharmacy and Biomedical Sciences in collaboration.

solution was prepared by adding 4 µl of (10 mg/ml) stock solution to 196 µl HM1-9 medium (%10 FCS). Hundred microliters of the test solution were pipetted in duplicate into the first column of a 96-well microplates and the serial 1:1 dilutions was carried out from column 2 to 11. DMSO at a concentration range of 0.001–1% and suramin over a concentration range of 0.008–1 µM were included as negative and positive controls. A sterility check was conducted by using 90µl of the diluted bacterial inoculum to all the assay plates with the exception of well A1. The microplates were incubated at 37 ºC in a humidified 5% CO_2 atmosphere for 48 hours. Thereafter, 10% alamar blue™ was added to each well and the microplates were incubated for a further 20 hours. Fluorescence was determined using a microplate fluorometer at an excitation wavelength of 560 nm and an emission wavelength of 590 nm. Percentages of control values were calculated and the MIC was determined as the lowest compound concentration with <5 % of the control values.

4.2.3.2. Antimicrobial assay - M. marinum ATCC.BAA535

A modification of the microplate Alamar blue method for susceptibility testing of fast growing species of *Mycobacterium* was used. *Mycobacterium marinum* ATCC.BAA535 from the thawed stock cryoculture was streaked onto Columbia (5% horse blood) agar slopes and incubated at 31 ºC for 5 days. A loopful of the culture was then transferred into 10 mL of sterile 0.9% NaCl containing glass beads. The suspension was mixed and allowed to settle. 1 mL of the supernatant was added to 10 mL sterile MHB (Mueller Hinton broth) saline that had been used to zero the turbidity meter. The turbidity of the solution was adjusted to be the same as a 0.5 McFarland standard. A few drops of Tween 80 0.02% were filter sterilized and added to homogenise the suspension. This was then shaken and the inoculum diluted 1 in 10 with Mueller Hinton Broth for use in the assay. Samples were dissolved in a sufficient quantity of DMSO to reach a concentration of 10 mg/mL or 1 mg/100 µL. For the initial screen, the 10 mg/mL stock solutions of the samples were diluted to 1000 µg/mL using MHB. Twenty microlitres of each extract were placed in each well and 80 µL of MHB was added. DMSO was added as the negative control at a concentration range of 1 to 0.002% and gentamycin as positive control at a range of 100 to 0.78 µg/mL. One hundred microlitres of the bacterial suspension were added to the wells. The plates were sealed and incubated at 31 ºC for 5 days before the addition of 10 µl of Alamar blue. The plates were again sealed and incubated at the same temperature for 24 hours after which fluorescence was determined using the Wallac Victor microplate reader in fluorescence mode (Excitation 530 nm; Emission 590 nm). The results were calculated as percentages.

The same method was used for *Klebsiella pneumonia* (strains ATCC 13883 and BAA 2146) and *Methicillin resistant staphylococcus aureus* (MRSA) (strains 16 and 106) except that a loopful of each bacterial strain was streaked on to individual Columbia 5% horse blood agar slopes and were incubated at 37 ºC for 20 hours.

4.2.3.3. Antifungal assay[4]

Five strains of *C. albicans* harbouring a range of *ERG3* and *ERG11* mutations (Table 6.19), and representing different anti-fungal resistance spectra were selected to analyse the potential toxic properties of these compounds. The 5 strains were SC514 (wild type), CA12, CA488, CA490 and CA1008. A description of the mutations present in each strain is detailed in Table 1. All *C. albicans* strains were cultured on YPD (1% yeast extract, 2% peptone, and 1% dextrose) agar plates at 30°C. For routine growth, yeast strains were grown with rotary shaking at 37°C in RPMI-1640 + 2% glucose media.

Table 11 *Candida albicans* strains.

Strain	*ERG3* Mutation	*ERG11* Mutation
SC514	-	-
CA12	W332R	-
CA488	H243N; T330A; A351V	D225G; E266D; E391G; V488I
CA490	D147G; T330A; A351V	F72S; T229A; E266D; N440S; V488I; R523G
CA1008	K97E; L193P; V237A; A351V; A353T	E266D

The plated cultures of *C. albicans* were grown for 24 hours at 30°C. Isolated colonies were then selected from this plated culture, transferred to 0.85% Saline and cell density determined by haemocytometer counts. Cell suspensions at a density of 1.5 x 10^3 cells/mL were prepared in RPMI-1640 media, and 100µL of inoculate transferred to each well of 96 well flat-bottomed plate. Working stocks of the compounds were prepared in RPMI-1640 media at concentrations of 40 µg/mL and 80 µg/mL and 100 uL added to each of triplicate wells to give final concentrations of 20 µg/mL and 40 µg/ml, respectively. Thus, each plate consisted of a specific yeast strain with each compound assessed in triplicate. Plates were incubated with shaking at

[4] Undertaken by Prof. Steve Kelly's Group, University of Swansea in collaboration.

37 °C for 24 hours and then the cell growth assessed by microscopy with a 10x objective. The experiments were performed in duplicate.

4.2.3.4. Pesticidal assays[5]

4.2.3.4.1. Fungicide assays

The compounds were evaluated in mycelial growth tests in artificial media against *Pythium dissimile*, *Alternaria solani*, *Botryotinia fuckeliana* and *Gibberella zeae*, at rates of 20ppm.

Test species	Media	Rate (ppm)
Pythium dissimile	Semi-solid	20
Alternaria solani	Semi-solid	20
Botryotinia fuckeliana (Botrytis cinerea)	Semi-solid	20
Gibberella zeae (Fuscarium graminearum)	Semi-solid	20

The compounds were also evaluated against several pathogens on leaf-piece assays at the rate of 100 ppm for *Uromyces viciae-fabae* on bean and *Zymoseptoria tritici* on wheat, and at the rate of 200 ppm for *Phytophthora infestans* on tomato. The compounds were applied prior to inoculation with the pathogens.

Test species	Host	Rate (ppm)
Zymoseptoria tritici	Wheat	100
Phytophthora infestans	Tomato	200
Uromyces viciae-fabae	Bean	100

Mycelial growth or disease inhibition was assessed visually and scored using a 3 band system (0, 55 and 99 where 99 = total inhibition of hyphal growth/disease development, 55 = partial inhibition, 0 = no inhibition), 4-14d after inoculation depending on the assay.

4.2.3.4.2. Herbicide assays

The compounds were tested for herbicidal activity against *Arabidopsis thaliana* at 10 ppm and *Poa annua* at 32ppm. Test plates were stored for seven days in a controlled environment cabinet. They were scored as 0 or 99, where 99 = significant herbicidal effect, and 0 = no effect.

[5] Undertaken by Dr Diane Irvin, Syngenta, UK.

Test species	Treatment timing	Rate (ppm)
Arabidopsis thaliana	Pre-emergence	10
Poa annua	Pre-emergence	32

4.2.3.4.3. Insecticide assays

The compounds were tested for activity against an aphid species at 1000 ppm on a leaf-piece based assay, and against *Plutella xylostella* and *Diabrotica balteata* at 500 ppm in artificial diet assays. Chemicals were applied to feeding aphids, or prior to infestation with *P. xylostella* and *D. balteata* larvae. Mortality was assessed relative to control wells using a 2 band system (0 or 99 where 99 = significant mortality, 0 = no effect), 3-6 days after the treatments depending on the assay.

Test species	Treatment type	Media	Rate (ppm)
Aphid species	Feeding/contact	Leaf disc	1000
Plutella xylostella	Feeding/contact	Artificial diet	500
Diabrotica balteata	Feeding/contact	Artificial diet	500

Positive controls: In addition to the test compounds, positive control compounds were included in each test: azoxystrobin and prochloraz for fungicide assays, thiamethoxam and indoxacarb for insecticide assays and norflurazon for herbicide assays. For all screens, data were recorded for replicates and averaged.

4.2.3.5. Anti-schistosomal activity of DR5 and crude saponin extracts

Samples and extracts

The flower saponin (DR5) and bluebell seed extracts were tested. The seed extracts were prepared as follows:

Bluebell seeds were collected in July, 2013 and 2014. The seeds were flaked using the (Eschenfelder Seed and Grain Flaker 1200) then de-fatted by stirring overnight with *n*-hexane at 1 mg seed/5 mL solvent ratio. Solvent extraction was repeated two more times to ensure maximum removal of the non-polar constituents. The solvent was filtered off and the residue was left to dry on a tray in the fume hood. The dried seed residue was then extracted with MeOH using the same solvent ratio and extraction times as with *n*-hexane. At the end of the

extraction process, the MeOH extracts were pooled together and the solvent was removed using a rotary evaporator at < 40 ^{o}C. The dried MeOH extract obtained at this stage was suspended in water (500 mL) and extracted three time with an equal volume of 1-butanol (1-BuOH). At the end of this stage, both the aqueous and 1-BuOH layers were dried down and obtained powder was labelled as crude water and 1-BuOH extracts respectively. Figure 84 outlines a summary for the extraction process. It should be noted that the two seed batches were extracted separately each after their harvest and the dried extracts were stored at room temperature until their submission for the test at the end of July 2014. The samples submitted for the test are listed below:

Compound/fraction	Details
DR5	Saponin isolated from bluebell flowers
DR6	1-BuOH seed extract from 2013
DR7	1-BuOH seed extract from 2014
DR8	Water extract of seed from 2014

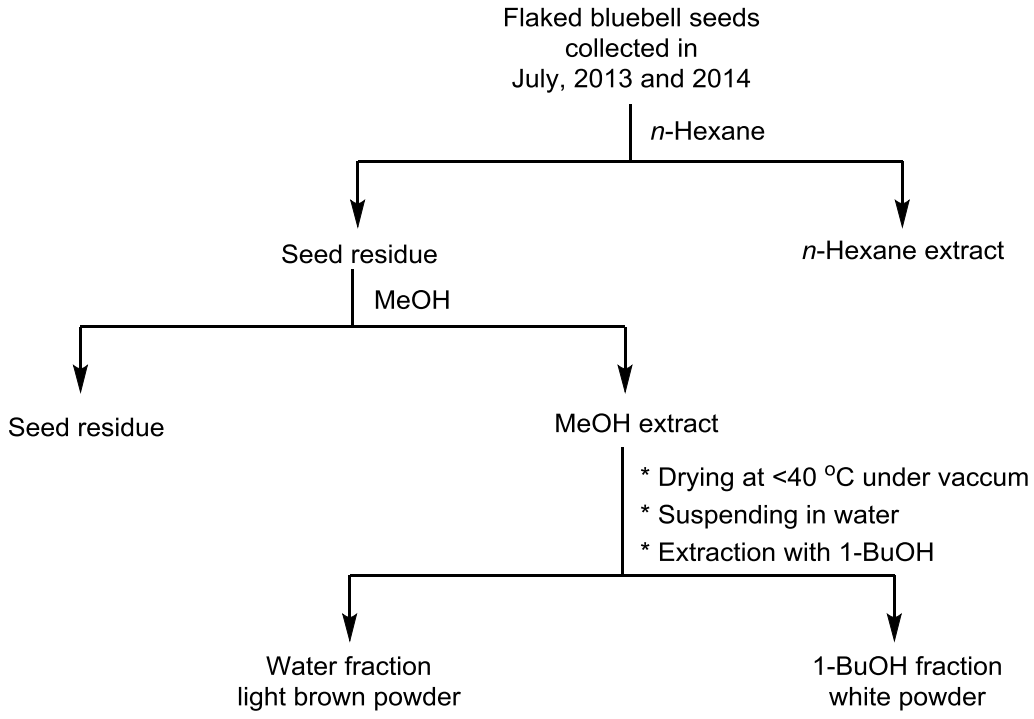

Figure 84 Diagram showing the main steps in preparing bluebell seed extracts for the anti-schistosomal activity test.

Anti-schistosomal screening[6]

Cercaria from *Schistosoma mansoni* were shed from *Biomphalaria* snails upon exposure to light and were subsequently transformed mechanically to obtain schistomsomula. Solutions of the test compounds were dissolved in DMSO to obtain a working concentration of 1.6 mM and added to a stock plate. Basch culture media (80 µL) and approximately 120 schistosomula were pipetted into a 384 well plate (known as the master plate), and compounds were transferred from the stock plate to the master plate using the Biomek platform (Beckman Coulter) to give a final concentration of 10µM within each well. On each plate two controls were used- Auranoufin which completely kills the parasite (positive control) and DMSO (negative control). Each plate also contained the currently used drug for treating the disease- Praziquantel. All control compounds were run at a concentration of 10µM. The plates were then incubated at 37oC for 72 hours in an incubator containing 5% CO2 after which the Biomek platform was used to re-suspend the schistosomula mixture. The 384 well plate was then imaged for both phenotype and motility using the Molecular Devices ImageExpress XL microscope. Phenotype was imaged at 10x objective in four well locations and combined into one image tile. Motility was imaged at 10x objective over six seconds, five times and displayed as a video.

The data generated from the images were analysed using Pipeline pilot to quantify the effect of the test compounds in comparison to the control compounds. Any compound that falls within the 'hit' area has had an effect on both motility and phenotype of the parasites within the Schistosomula life cycle stage of the parasite.

[6] Undertaken by Prof Karl Hoffman and Dr Helen Whiteland, IBERS, Aberystwyth University. Funded by National Research Network.

4.3. Results and Discussion

4.3.1. Metabolomics in investigating bluebell saponins and general metabolite profiling

Data obtained from the Orbitrap mass spectrometer in positive and negative modes were processed using Mzmine 2.17 software which works on peak picking, deconvolution and alignment also de-isotoping and gap filling to ensure that all the spectra are comparable. Afterwards, the resulting data were exported to a csv file where a macro was used to combine the positive and negative mode data for further statistical analysis using SIMCA-P. Dereplication was performed by comparing the data to the DNP database to find probable hits and identify some of the compounds based on their elemental composition and mass data. According to this, most of the hits above Mwt of 1000 were saponins and occasionally flavonoid glycosides. Table 12 shows some of these compounds. Based on dereplication results and previous experience with chromatography and isolation of saponins, it was assumed that compounds with MWt ranging from 1000 – 1500 Da and eluting between t_R 10 – 18 min were saponins and this assumption was used later in investigating these compounds quantitatively.

Table 12 Some example DNP matches for bluebell components using dereplication and metabolite profiling.

Polarity	m/z	Rt	MW	Name	Formula	Source
N	1029.565	26.34	1030.572	12-Oleanene-3,16,28-triol; (3,16)-fo	C52H86O20	Constit. of Androsace septentrional
N	1031.544	22.01	1032.552	Furost-20(22)-ene-3,26-diol; (3,5,25	C51H84O21	Constit. of Tribulus terrestris
N	1051.582	38.38	1052.59	3,8,12,14,17-Pentahydroxypregn-5-e	C55H88O19	Constit. of Cynanchum wilfordi
P	1093.543	12.1	1092.536	2,3,20,23-Tetrahydroxy-12-ursen-28	C52H84O24	Constit. of Tupidanthus calyptratus
P	1121.537	15.32	1120.53	3,16-Dihydroxy-12-oleanene-23,28-(	C53H84O25	Constit. of Saponaria officinalis
P	1121.539	14.47	1120.532	3,16-Dihydroxy-12-oleanene-23,28-(	C53H84O25	Constit. of Saponaria officinalis
N	1151.512	11.31	1152.519	2,3,16,24,30-Pentahydroxy-12-olear	C53H84O27	Constit. of Cassia angustifolia
N	1281.575	15.65	1282.582	3,16-Dihydroxy-12-oleanene-23,28-(	C59H94O30	Constit. of Saponaria officinalis

Multivariate statistical data analysis was performed for the LC-MS spectral results and the outputs were presented as PCA and OPLS-DA plots with each producing score and loading plots. PCA score plots (Figure 85 A) showed the bulb samples clustered away from all the other plant parts which appeared to share greater similarities to be clustered together. This showed the uniqueness of bulb metabolites compared to the rest of the plant parts. Bulb samples with the highest variability included samples from March – start of May and July. PCA loading plot (Figure 85 B) which aims to reveal the variables responsible for grouping the samples in

the score plot, showed that two bulb metabolites (MWt 470 and 456) were responsible for the greatest part of the variability of the first bulb samples and a range of metabolites of MWt 472, 643, 467, 599, 511, 555 for bulb samples in July in addition to a range of other metabolites with values included in Figure 85 B. Taking into account the variations within groups, OPLS-DA further confirmed these results for both the scores and the loadings (Figure 86). The heatmap (Figure 87) shows the raw scores of each peak measurement presented as a z-score by subtracting the score value from the mean of that score then dividing by the standard deviation. It shows the different distribution of metabolites between the below and above-ground parts with the leaves, scapes, shoots and flowers showing scores above the average for more polar metabolites versus less polar ones in the bulbs. Amongst the flower sequence of samples, the start of fruiting (sample 38) showed a distinct pattern with higher quantities and diversity of metabolites.

Based on their MS^3 data, it was possible to identify the two bulb metabolites of MWt 470 and 456 Da as norlanostane-based steroidal aglycones (Figure 88). The proposed structures were backed by the presence of close structurally related aglycones in previous reports from the hyacinthoideae (Adinolfi et al. 1987; Mulholland et al. 2013; Parrilli et al. 1980). Although it was possible to propose a structure for the first two bulb metabolites, further work is needed before stating much about most of the others.

4.3.2. The seasonal variation of saponins

By summing up the peak areas lying within the criteria of MWt 1000 – 1500 Da and t_R 10 – 18 min, it was possible to compare the different plant parts with regards to their saponin contents. Since, the amount of the methanolic extracts of the samples varied between the different plant parts and within the same part at different times, the total peak areas were multiplied by the percentage of extract obtained from a unit dry weight of the plant part as follows:

$$C_{\,Saponin} = Peak\ area\ \times \frac{Wt_{MeOH\ ext.}}{DW} \times 100 \qquad (8)$$

Where,

$C_{\,saponin}$ = Saponin content in a particular plan part at any sampling occasion

Peak area = The sum of all peak areas within MWt (1000 – 1500 Da) and t_R 10-18 min

$Wt_{\,MeOH\ ext}$ = The dry weight of the methanolic extract

DW = The dry weight of the plant part used in the analysis

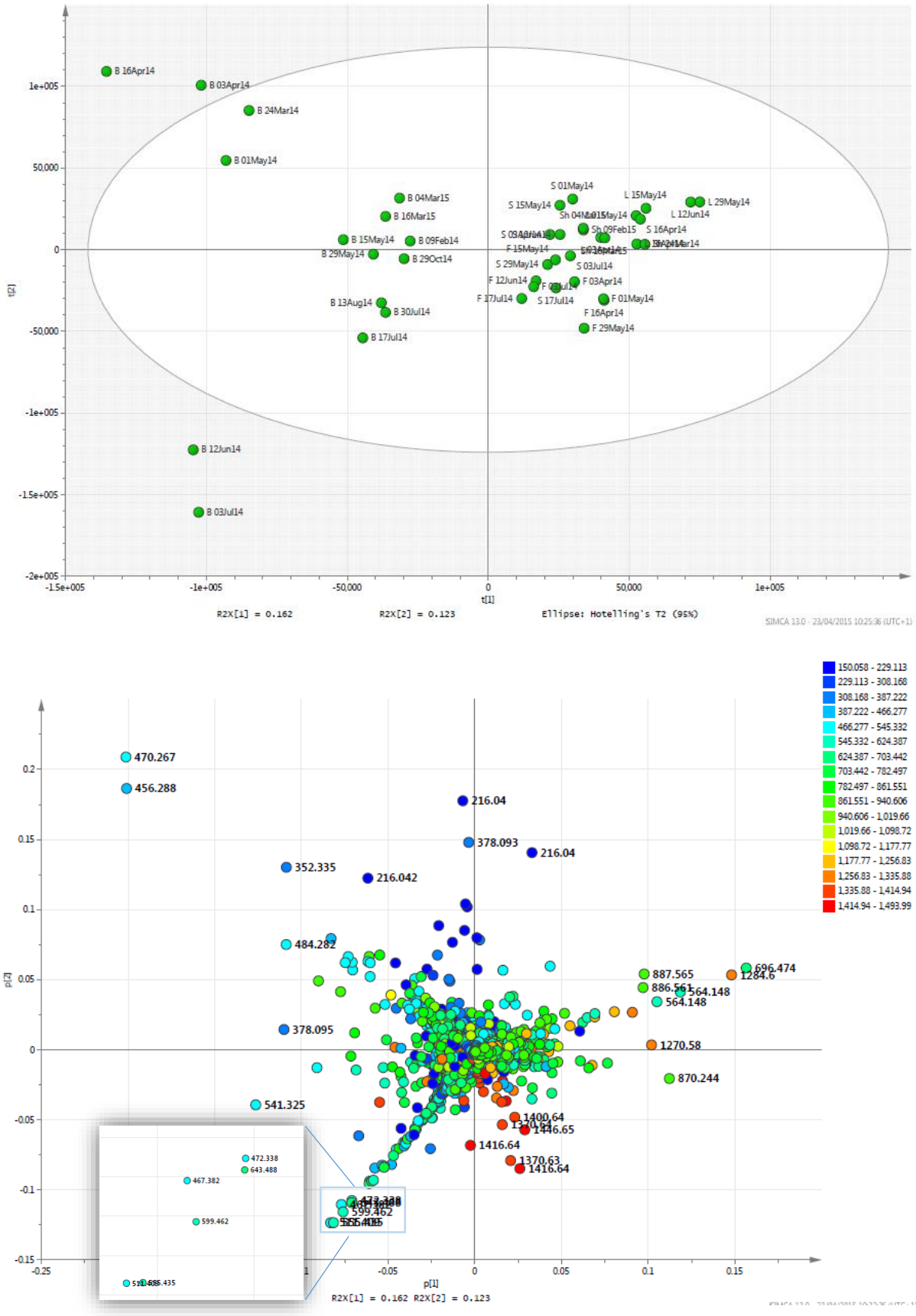

Figure 85 Principal component analysis of bluebell metabolites, (A): score plot. Sample names include first letter of the plant part B: bulbs, L: leaves, S: scapes, Sh: shoots and F: flowers followed by sampling date. (B): loading plot. Some of the outlier values are shown.

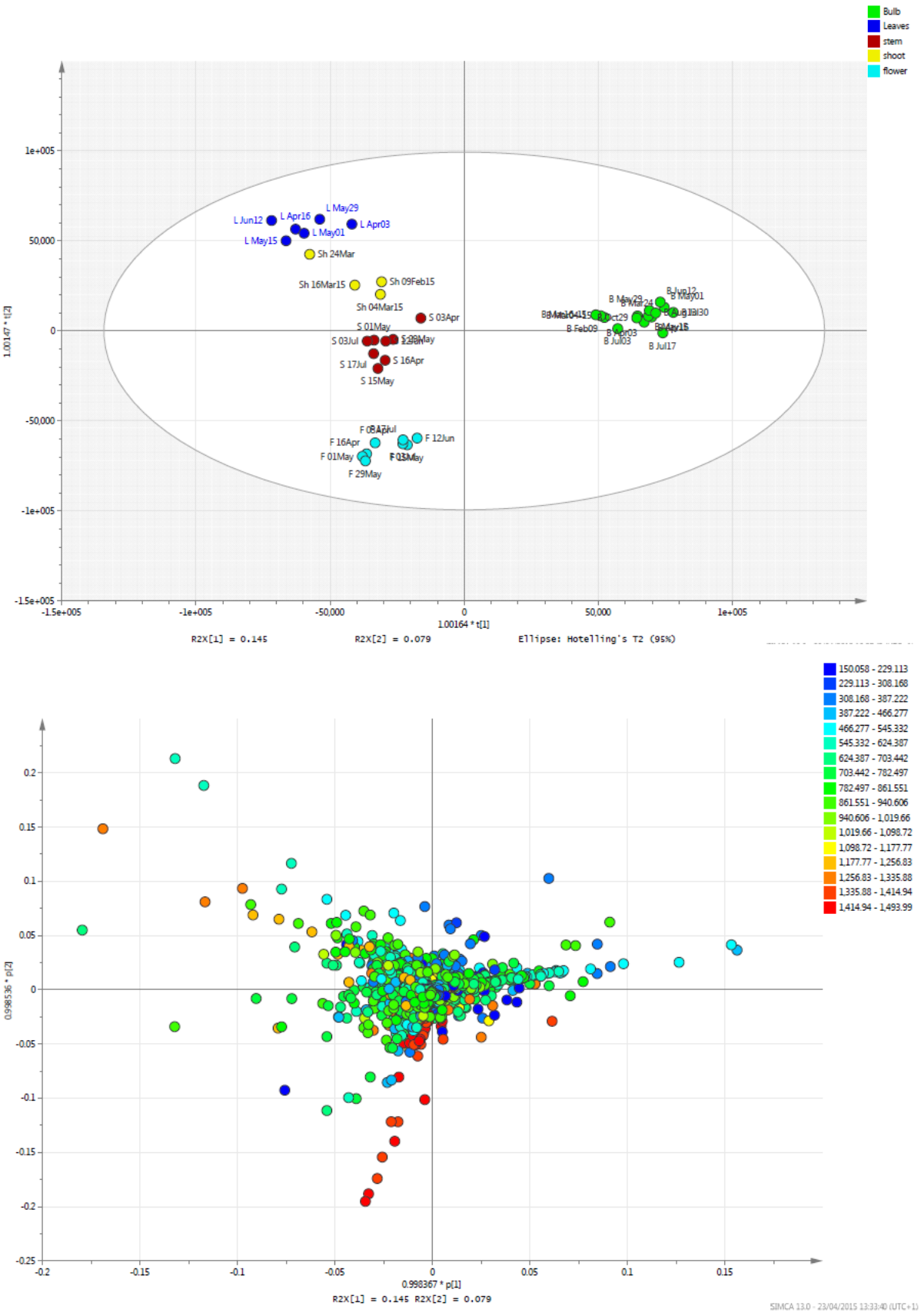

Figure 86 OPLS-DA analysis of bluebell metabolites, (A): score plot coloured according to classes. (B): loading plot.

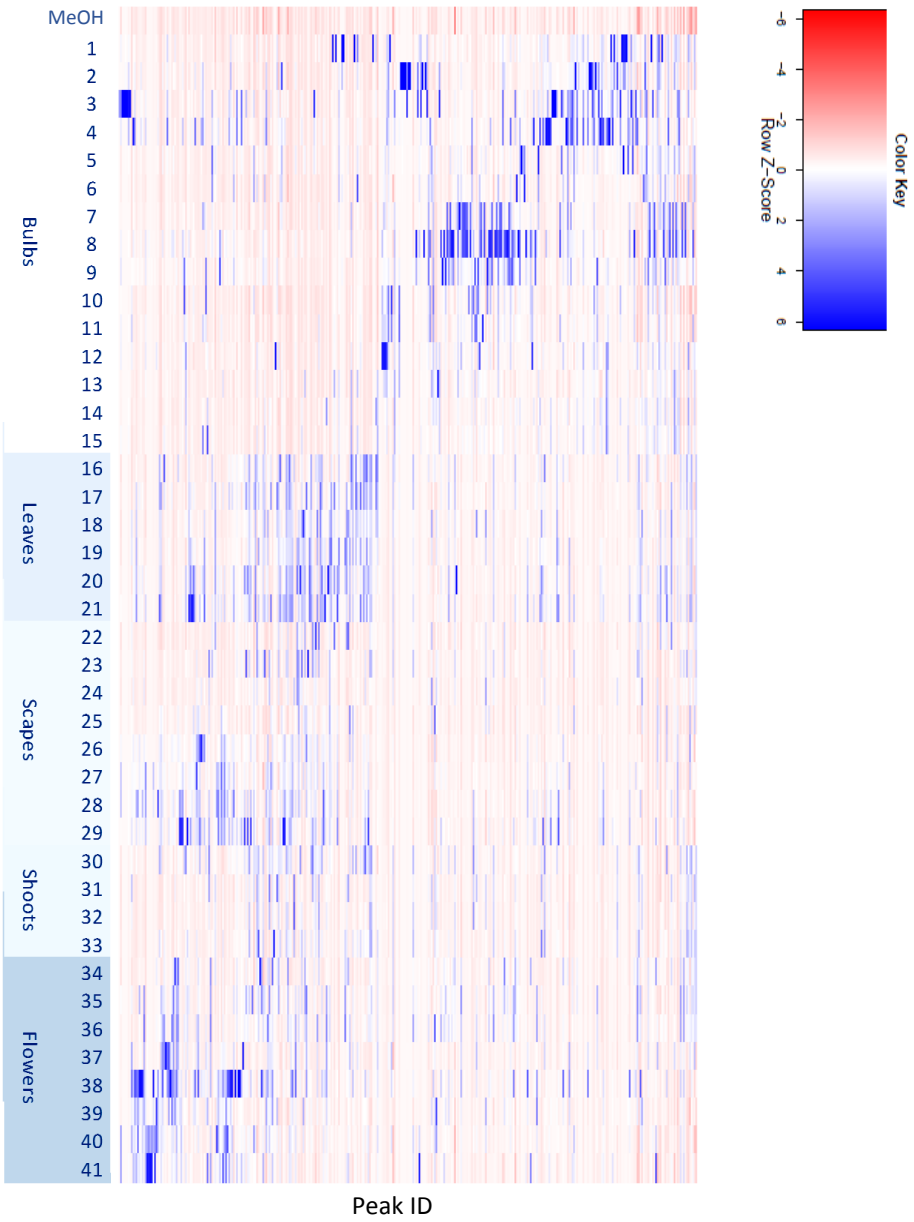

Figure 87 Heatmap showing peak IDs for the analysed samples. Selected TIC chromatograms for the different plant parts.

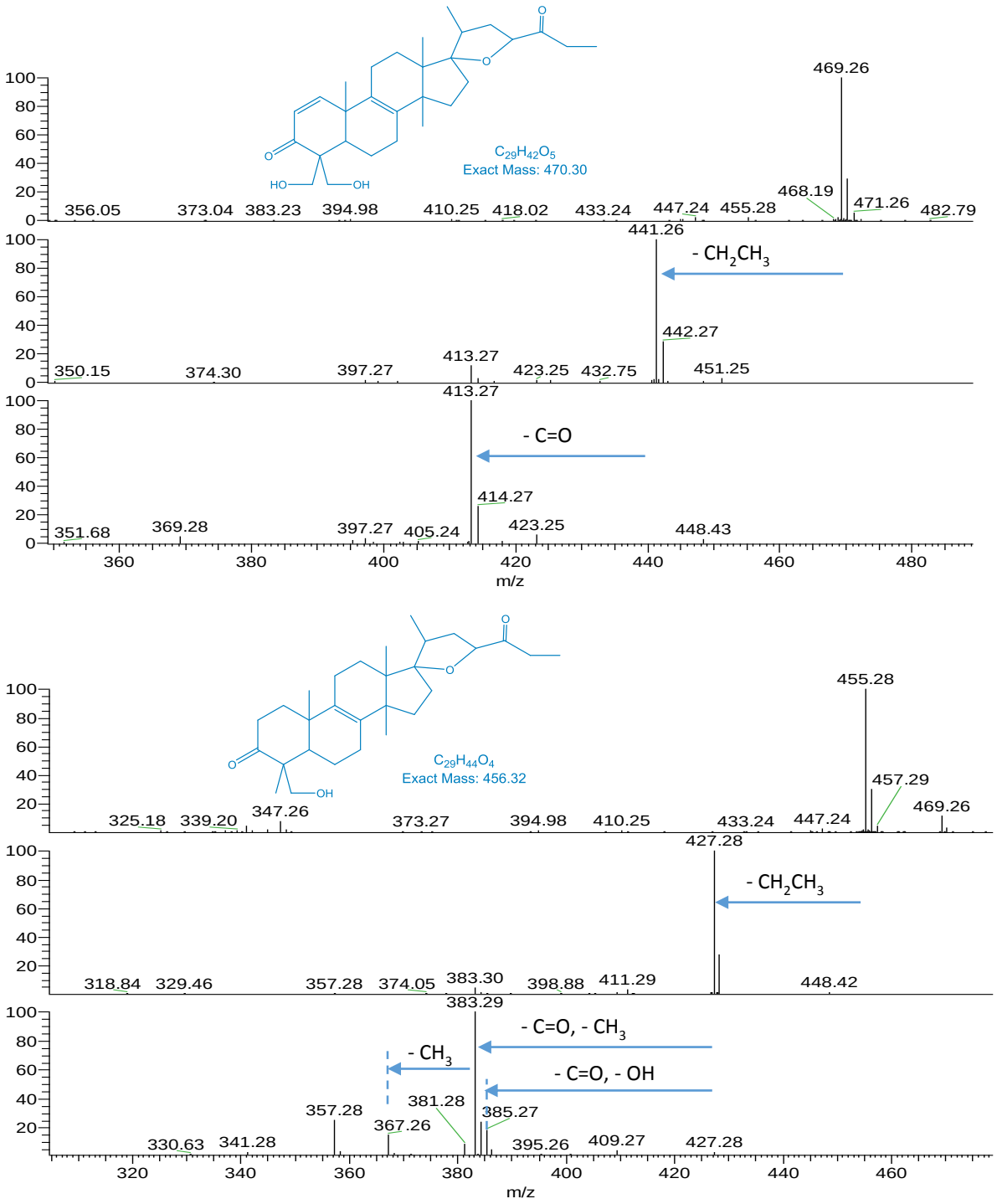

Figure 88 Structure of two bulb metabolites with m/z 469.26 and 455.28 based on their MS^3 fragments

Applying the previous equation, the analysis revealed useful information including ratios and relative contents of saponins in different parts as well as their variation trends throughout the season (Figure 89). All the above-ground parts showed relatively high and comparable content at the start of plant growth until mid-April. Soon afterwards, the different parts started to differentiate with regards to their content of saponins. Both the leaves and scapes contents started to fall with the decrease being more remarkable in the scapes. The flowers on the other

hand, maintained a comparably higher saponin levels although a slight downwards trend could be seen over time with seed formation at the end resulting in a significant decrease in saponin contents. The bulbs were the organs with the least content of saponin, as the highest content in the bulbs didn't exceed 20% of the content in the other parts. The maximum value in this part was in March-April during shoot growth, then it dropped from mid-April and reached a minimum at anthesis. Bulb saponin contents remained low until the end of the above ground growth and dormancy then started to build up gradually in preparation for the next growth phase.

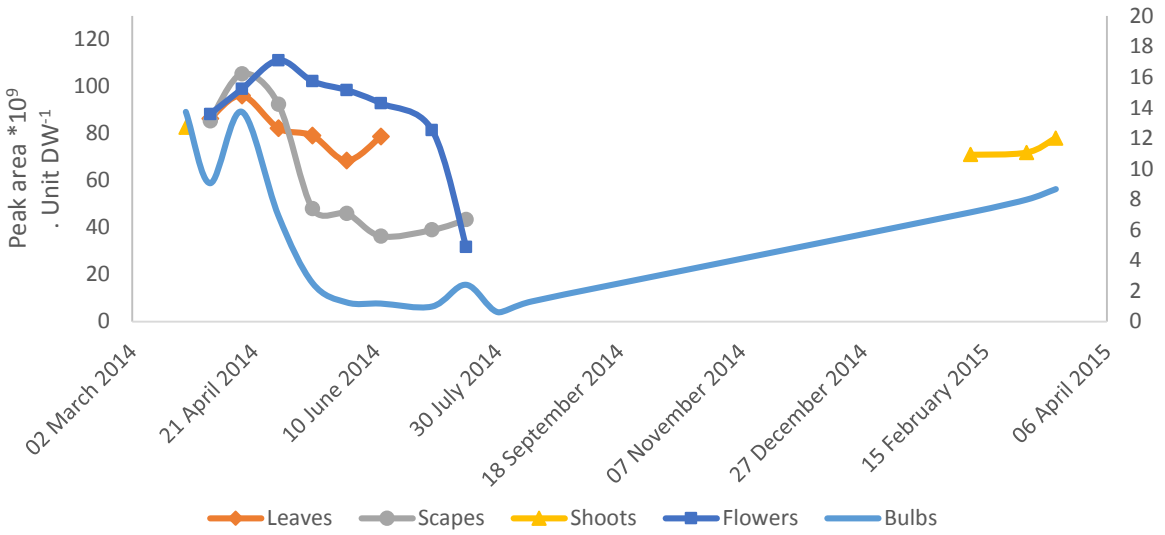

Figure 89 The seasonal change in saponins in different parts of bluebells. Values represent peak areas per unit dry weight of the plant part. Values on the secondary axis represent bulbs saponin contents.

Transformations between the different phenological stages were characterised with distinct changes in saponin contents. For instance, the start of growth represented by first few bulb samples, shoots, early leaf, scape and flower samples were often of higher saponins contents. Bluebells require arbuscular mycorrhizal (AM) fungi for phosphorous uptake. Colonisation of bluebell roots with AM was found to be high from October - mid March during shoot emergence and the underground stage of growth (Merryweather and Fitter 1995b). This might influence the production of saponins at the early growth stages as symbiotic AM fungi are reported to affect the content (quantitatively and qualitatively) of a number of plant secondary metabolites including saponins (Szakiel et al. 2011b). Fruiting (sample 38) was characterised with the appearance of a large number of various compounds of which some decreased through

seed formation. Table 13 lists some of the saponins that were possible to identify from their LC-MS data. The list includes the compounds that were of relatively higher abundance and their retention behaviour allowed enough resolution for their MS peaks to be used in the identification. Undoubtedly, the actual number of saponins is much higher and different aglycones might be incorporated in the structure. Compound 4 in Table 13, for example, is present mainly in the flowers, but was also found in the last scape sample and in the bulbs in mid-July. This can suggest that the fate of flower saponins towards the end of the above-ground stage is to be either partially incorporated into the seeds, or recycled into the bulbs. This hypothesis is supported by an increase in bulb saponin content in mid-July concurrent with the end of the above-ground growth stage (Figure 89). This stage in the bulbs was also characterised by the accumulation of metabolites from t_R 21 – 30 min with m/z mostly in the range 250-400 (chromatograms 7-10 Figure 90) which could be products of recycling and breakdown of metabolites from the above-ground parts.

The bulbs show a distinctive profile compared to the other parts characterised by the presence of different metabolites in the t_R range 28.5- 40 min compared to the other parts (Figure 90 - Figure 94) with m/z mostly between 400 – 500. The most significant of which are the two peaks at 31.7 and 31.9 min with m/z 469.26 and 455.28 respectively for the steroidal aglycones. Applying equation (8) to their peak areas showed that these two compounds follow a similar trend to bulb saponins and they even exist in comparable amounts (Figure 95). Based on their structure and seasonal pattern, these compounds could possibly be biosynthetic precursors in the bulbs to produce saponins for the early emerging shoots which diminish in quantity when the latter become photosynthetically competent and capable of producing their metabolites independent from the support of bulbs.

The metabolomics profile of the above ground parts was characterised by the presence of higher ratios of the early-medium eluting, low Mwt or higher polarity, high Mwt compounds which could be concluded from the heatmap (Figure 87) as well as their LC-MS chromatogram (Figure 91 - Figure 94). The shoots, representing the early stages of above-ground growth when it wasn't possible to separate to leaves, scapes and flowers, showed a profile intermediate between that of the leaves and scapes. The flowers showed higher quantity of metabolites between t_R 5 – 18 min mostly due to flavonoid glycosides and saponins.

Table 13 Bluebell saponins identified based on their LC-MS data with their tentative identification and allocation in the plant. The identity of the first four sugars linked to the aglycone were assumed to be rham-glc-arab-glc similar to DR5.

No.	t_R	m/z	MS/MS	Tentative ID	Allocation to plant part
1	**11.73**	- 1299.59		Hex-glc-(rham)- ara-glc-Aglycone (490, maybe 27C with OH on C-24)	Mainly in fruits and seeds, a little in bulbs around dormancy and traces in some other parts
		+ 1255.60	1093.54, 1109.54, 947.49, 785.43, 653.39, 491.34		
2	**11.97**	- 1299.59		Hex-hex- glc-ara-glc-Aglycone	Mainly in fruits (sample 38), a little in scapes after fruiting
		+ 1255.60	1093.54, 931.49, 637.40, 745.34, 457.33, 330.26		
3	**15.26**	- 1445.64, 1399.64		Glc-glc-glc-(rham)-ara-glc-Aglycone **DR5**	Second most abundant saponin in flowers. Also present in scapes and in bulbs during the subterranean stage.
		+ 1401.65	1255.60, 1239.60, 1093.54, 1077.55, 931.49, 915.50, 769.44, 637.40, 475.34, 457.33		
4	**15.5**	- 1415.63, 1369.63		Pent-hex-glc-(rham)-ara-glc-Aglycone	Samples 8 and 9 (bulbs before dormancy), 29 and flowers-seeds
		+ 1371.64	1239.60, 1077.55, 931.49, 769.44, 637.40, 475.34		
5	**15.76**	- 1283.59		Hex-glc-(rham)- ara-glc-Aglycone	Most abundant saponin in all parts
		+ 1239.60	1093.54, 1077.55, 931.49, 783.45(glycan), 769.44, 637.40(glc.agly), 621.40(Glc.agly-H2O), 475.34(agly), 457.33(agly-H2O)		
6	**16.20**	- 1121.54	771.59, 489.28, 374.25	Rham-glc-ara-glc-Aglycone	Bulbs (max in 3, 4), 29, 38 and 41. In addition to traces in other parts
		+ 1077.55	931.49, 637.40, 745.34, 457.33, 330.26		
7	**16.20**	- 1107		Pentose-glc-ara-glc-Aglycone	Bulbs (max in 3, 4), 29, 38 and 41. In addition to traces in other parts
		+ 1063	931.49, 637.40, 745.34, 457.33, 330.26		

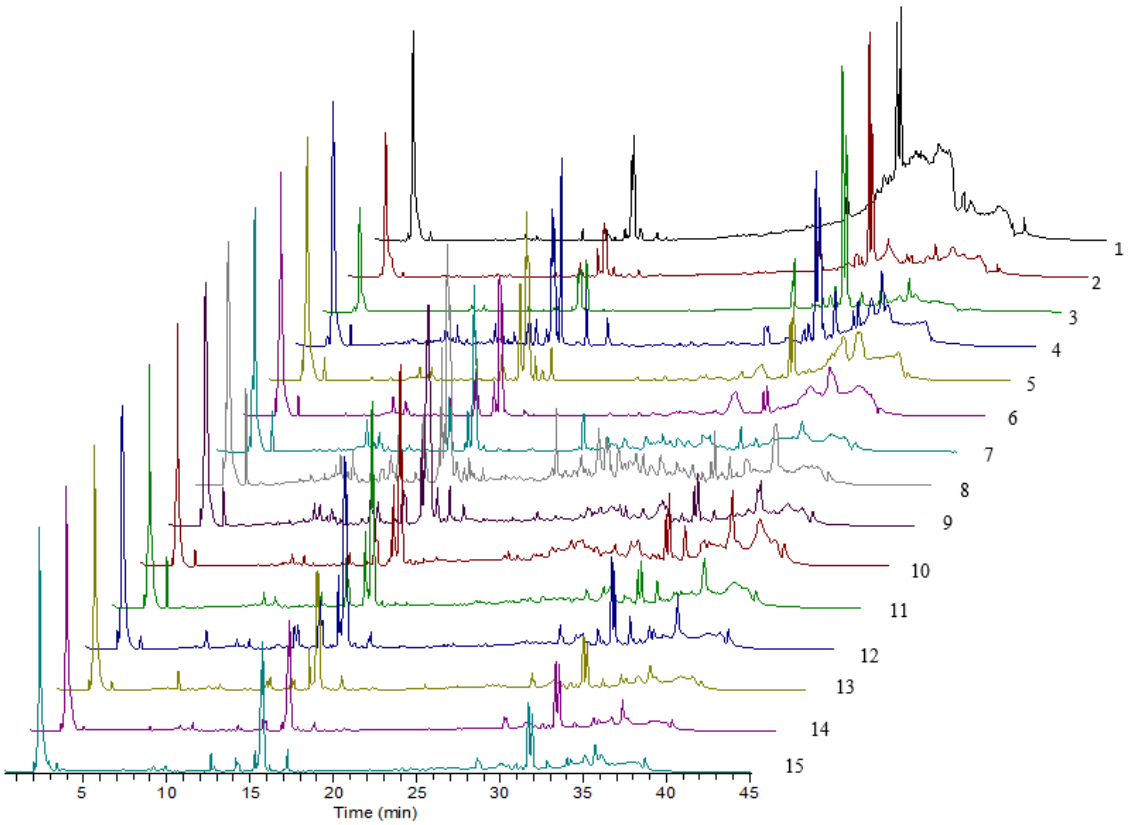

Figure 90 LC-MS chromatograms of bluebell bulb samples collected in 2014-2015. Frequency of sampling and collection dates are listed in (Table 10).

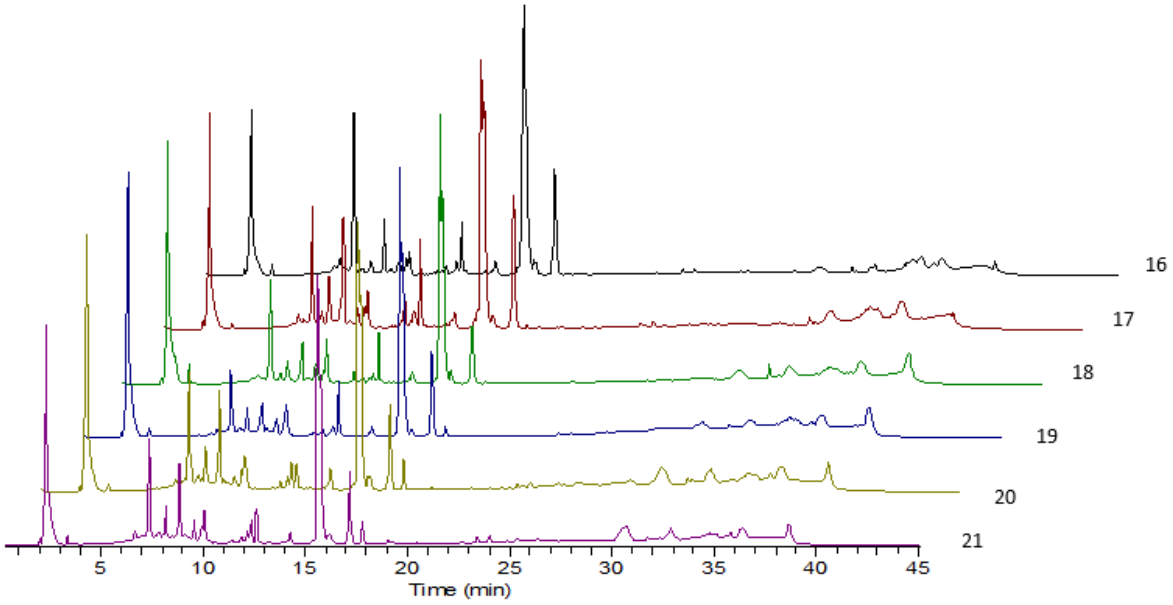

Figure 91 LC-MS chromatograms of bluebell leaf samples collected in 2014. Frequency of sampling and collection dates are listed in (Table 10).

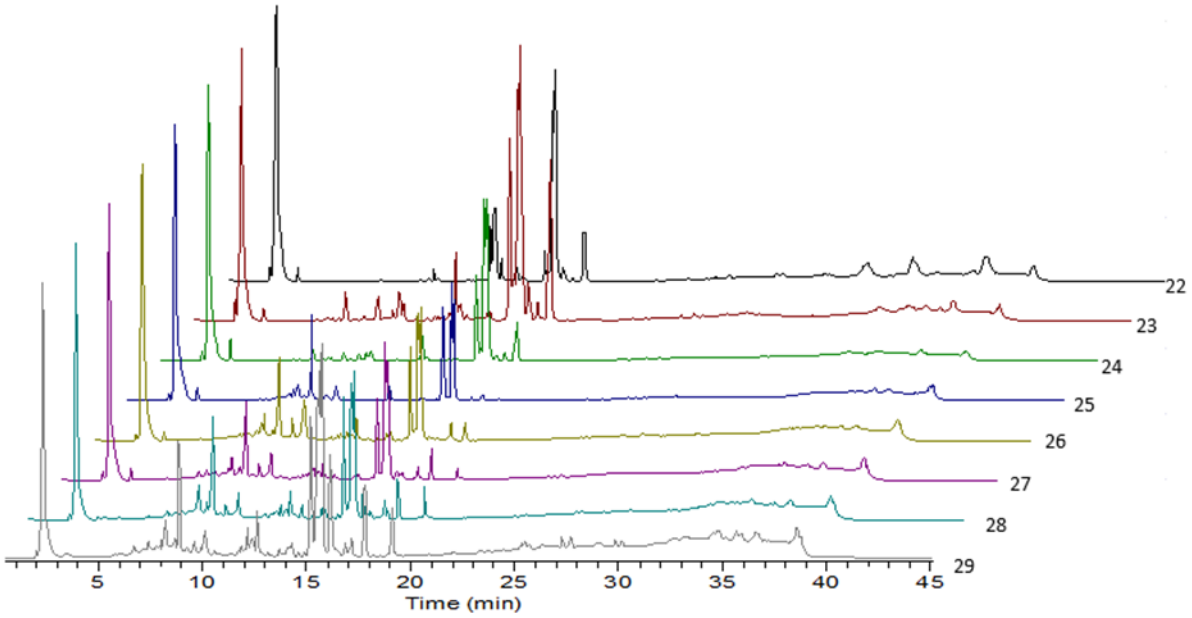

Figure 92 LC-MS chromatograms of bluebell scape samples collected in 2014. Frequency of sampling and collection dates are listed in (Table 10).

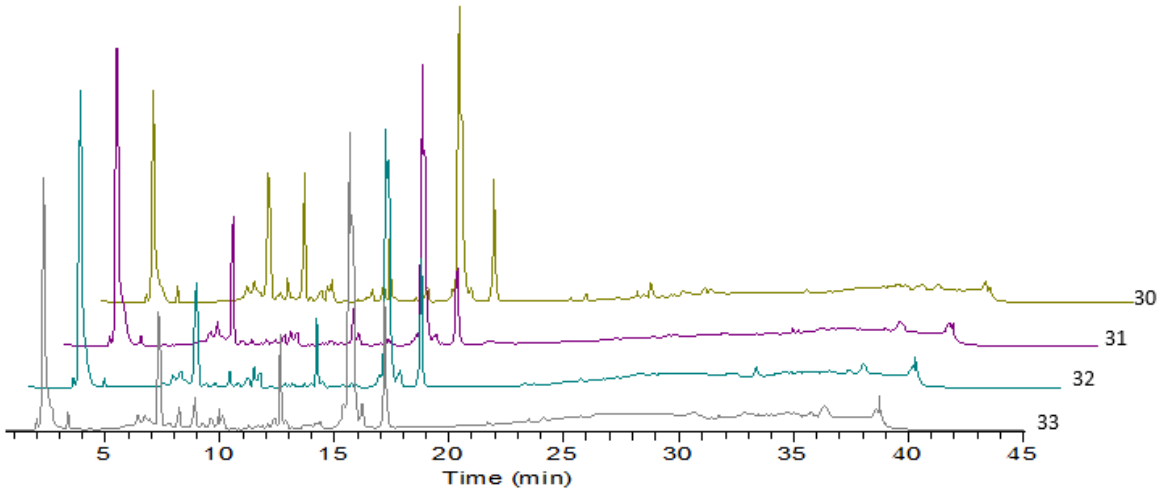

Figure 93 LC-MS chromatograms of bluebell shoot samples collected in 2014-2015. Frequency of sampling and collection dates are listed in (Table 10).

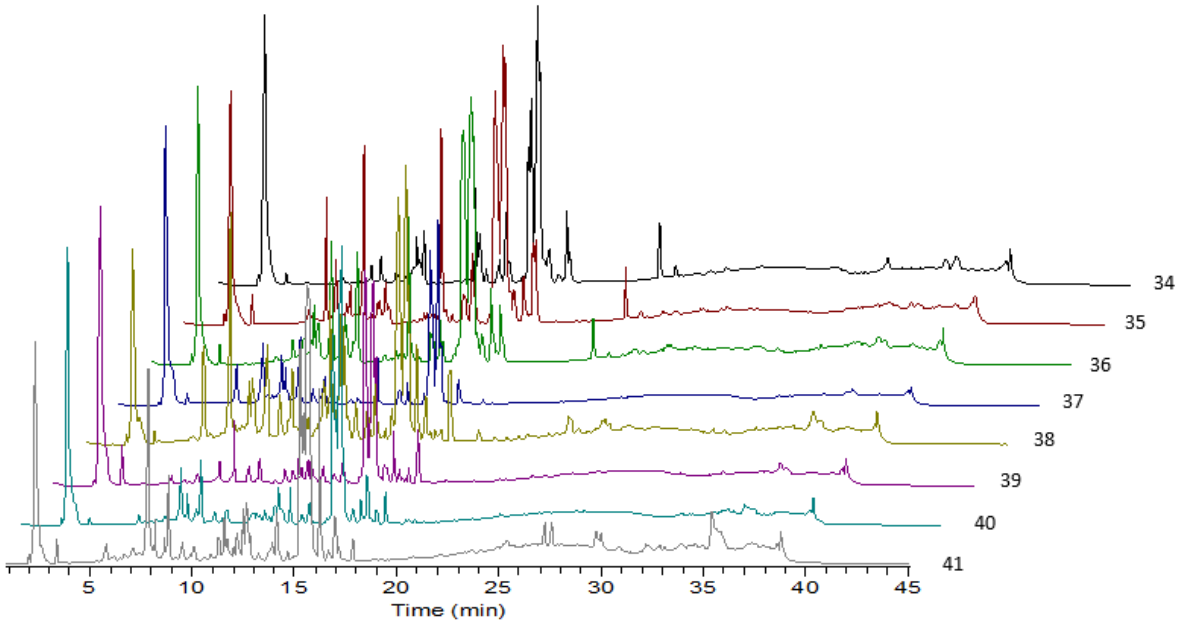

Figure 94 LC-MS chromatograms of bluebell bulb samples collected in 2014. Frequency of sampling and collection dates are listed in (Table 10).

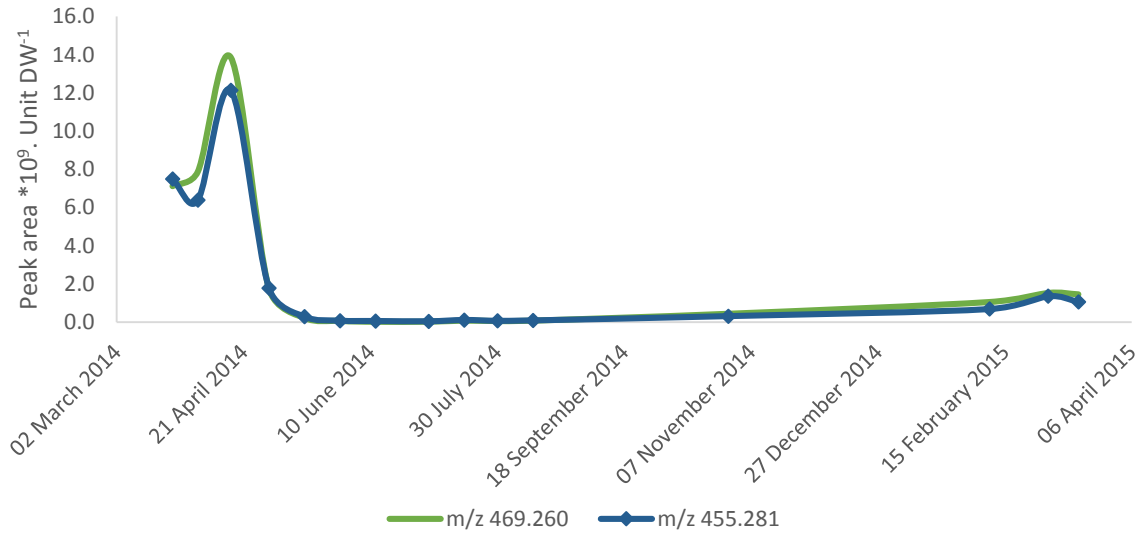

Figure 95 The seasonal change in two metabolites of bluebell bulbs.

4.3.3. Structural elucidation of the main flower saponin

Based on their weight ratios, saponins seem to comprise a larger proportion of the flower extract compared to the phenolics. Fr3 from the flower extract which was mainly saponins made up 50% of the total amount of the extract weight (see: Fractionation of the flower extract, p74). According to NMR of subfactions collected from FC of the flower methanolic extract, these compounds appear to be mostly of similar structural backbones with differences in the sugar moieties in the glycan part. The high glycosylation and their presence in large numbers with only small structural differences made the isolation and purification of saponins a challenging task. Nevertheless, it was possible to isolate a saponin from bluebell flowers with good purity. The structure was characterised using NMR, HR-ESI-MS and GC-MS analysis of the sugars released from acid hydrolysis of the compound. Figure 96 shows the structure of the isolated norlanostane-type steroidal saponin identified as 3*β*-(*O*-*β*-D-glucopyranosyl-(1→3)-*O*- *β*-D-glucopyranosyl-(1→3)-[*α*-L-rhamnopyranosyl-(1→2)]-*O*-*β*-D-glucopyranosyl-(1→2)-*O*-*α*-L-arabinopyranosyl-(1→6)-*O*-*β*-D-glucopyranosyl)oxy-17,23-epoxy-28,29-dihydroxy-27-norlanost-8-en-24-one.

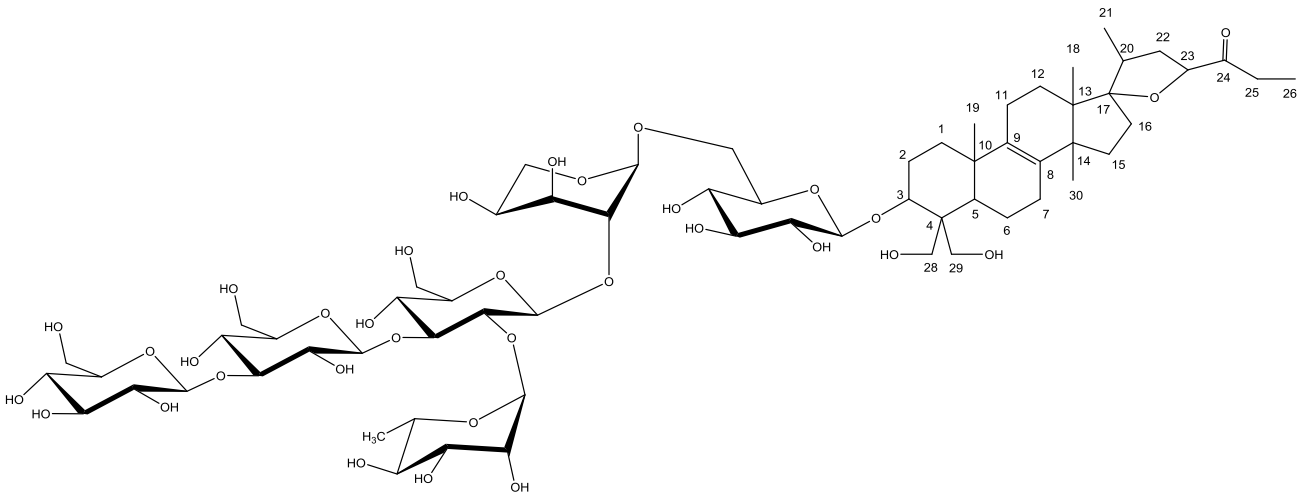

Figure 96 Chemical structure of the saponin DR5 isolated from bluebell flowers.

4.3.3.1. NMR spectroscopy

^{1}H NMR of this compound showed a large number of signals distributed mainly on two regions of the spectrum: the signals from 0.75 – 2.65 ppm belonging to the aglycone and signals from 3.5 – 6.5 ppm attributed to the glycosidic part. The 2D correlation of these proton shifts with the relevant carbon signals in HSQC made the distribution of these groups even clearer. In the

first region, a number of chemical shifts were readily identifiable as CH_3-group signals by their relatively high intensity, multiplicities and negative orientation in DEPTQ. These included the singlet signals of C-18, 19 and 32, a doublet for C-21 and a triplet for C-26. Although the rest of the signals in this region were more overlapped in ^{1}H NMR, their separation in DEPTQ and consequently in HSQC allowed their identification. The arrangement of atoms and their linkages in the aglycone were identified combining the information from COSY, HMBC, and HSQC-TOCSY. Table 14 lists ^{1}H and ^{13}C NMR data and Figure 97 shows a schematic summary of 2D correlations utilised in the structural elucidation drawn based on the spectra in (Figure 98 - Figure 103).

The presence of six sugars could be identified from their anomeric signals count in HSQC. In most cases, except when the proton shifts are well resolved, *J* values were calculated from 2D cross peak. Accordingly, four of the anomeric protons showed *J* vales of 6.9 – 8.2 Hz were later identified as glucose. Arabinose with a small doublet of 3.1 Hz and finally rhamnose being the most downfield signal with a broad singlet proton (br s) signal. Therefore, the anomeric configurations were identified as β for the glucose units and α for arabinose and rhamnose.

Starting from the anomeric protons, the neighbouring protons were identified from COSY. Protons and carbons belonging to the same sugar where identified from HSQC-TOCSY and confirmed by HMBC. The higher ^{13}C chemical shifts of the C atoms involved in *O*-glycosidic bond formation helped in the initial identification of the interglycosidic linkages (points of branching). This involved C-6 of glucose1, C-2 of arabinose and C-3 of both glucose2 and glucose 3.

Arabinose was identified as a six-membered pyranose rather than a five-membered furanose ring conformer. This was based on the presence of HMBC correlations between the anomeric CH and the CH_2 group, such correlation indicates the proximity of these two groups and would not have existed in a furanose ring. Also the ^{13}C chemical shift values were in agreement with arabinopyranose rather than arabinofuranose as reported by (Adinolfi et al. 1984) where the latter showed higher ^{13}C values typical to furanose rings in particular with C-4 being higher than 80 ppm.

Some of the common sugars found in saponins are D-glucose, D-galactose, L-arabinose, L-rhamnose, D-xylose and D-glucuronic and D-galacturonic acids in addition to other less common one. The fact that the opposite enantiomers of these sugars are not detected in plants has been taken as a clue in identifying their configurations (Massiot and Lavaud 1995).

Arabinose however, is an exception since it can occur in both D- and L- isomers in plants (Bhat et al. 2005). Distinguishing the D- and L-arabinopyranose isomers has been achieved using ^{1}H and ^{13}C NMR as the different isomers show different ^{13}C chemical shifts and coupling constants of the anomeric protons (Ishii et al. 1981). Chemical shifts and coupling values of the arabinose moiety in the isolated saponin showed closeness to the L- isomers reported in the paper rather than the D-isomer. Additionally, saponins from members of the hyacinthoideae subfamily reviewed by (Mulholland et al. 2013) usually contain the same arrangement of the 3 - 4 first sugars in the oligosaccharide chain including L-arabinose. Based on the above, the identified sugars were assigned as D-glucose, L-rhamnose and L-arabinose. It has been indicated that *O*-glycosylation at C-2 of L-arabinopyranose favours the $^{1}C_4$ conformation to reduce steric effect caused by the substituent (Ishii et al. 1981).

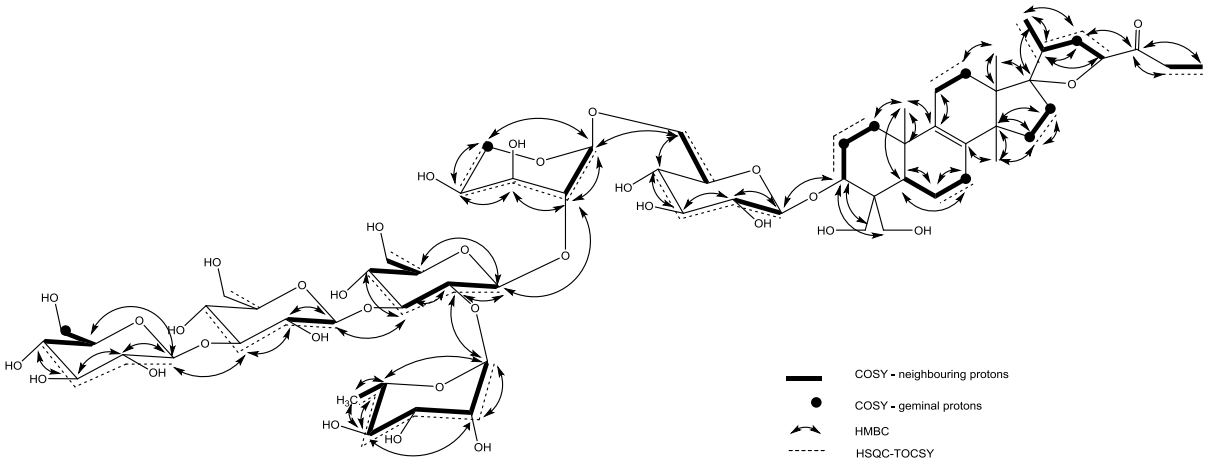

Figure 97 NMR correlations including COSY, HMBC and HSQC-TOCSY used in the structural identification of DR5.

Table 14 ^{1}H and ^{13}C NMR data for DR5 in pyridine-D_5. *: *J* values are calculated from 2D NMR cross peaks.

Position	δ_H ppm (multiplicity, *J* Hz)*	δ_C ppm
Aglycone		
1	1.27 (*t*, 12.7), 1.75 (*t*, 12.0)	35.8
2	2.13 (*dd*, 5.0, 13.0), 2.39 (*dd*, 5.0, 13.0)	27.3
3	4.50 (*d*-like, 13.0)	82.1
4	-	48.2
5	2.19 (*m*)	43.5
6	1.75 (*m*), 2.15 (*m*)	18.7
7	2.0 (*m*), 2.19 (*m*)	26.6

Position	δ_H ppm (multiplicity, *J* Hz)*	δ_C ppm
8	-	135.5
9	-	134.9
10	-	36.9
11	2.0 (*m*), 2.19 (*m*)	21.2
12	1.45 (*m*), 2.43 (*m*)	25.4
13	-	48.9
14	-	50.9
15	1.33 (*m*), 1.65 (*m*)	32.2
16	1.59 (*m*), 2.16 (*m*)	39.8
17	-	97.1
18	0.92 (*s*)	19.4
19	1.05 (*s*)	19.7
20	2.03 (*m*)	43.8
21	1.02 (*d*, 7.2)	17.3
22	1.76 (*m*), 1.98 (*m*)	36.7
23	4.64 (*t*, 8.5)	81.6
24	-	212.6
25	2.54 (*dq*, 2.9, 7.2)	32.4
26	1.03 (*t*, 7.1)	7.7
28	3.90 (*m*), 4.62 (*d*, 12.5)	62.7
29	4.37 (*d*, 12.0), 4.93 (*d*, 12.9)	61.0
30	1.47 (*s*)	26.3
D-Glucose 1		
1	5.13 (*d*, 8.0)	105.5
2	3.99 (*t*, 8.6)	75.4
3	4.05 (*t*, 10.0)	78.2
4	4.16 (*t*, 10.0)	72.7
5	3.78 (*m*)	75.4
6	4.17 (*m*), 4.44 (*dd*, 3.0, 12.0)	68.6
L-Arabinose		
1	5.27 (*d*, 3.1)	101.0
2	4.65 (*m*)	77.8
3	4.66 (*m*)	71.6
4	4.55 (*m*)	66.7
5	3.93 (*m*), 4.35 (*m*)	62.7
D-Glucose 2		
1	5.14 (*d*, 6.9)	102.5
2	4.18 (*t*, 8.1)	76.7
3	4.06 (*t*, 11.2)	89.3

Position	δ_H ppm (multiplicity, *J* Hz)*	δ_C ppm
4	4.10 (*t*, 10.0)	69.2
5	3.58 (*m*)	77.6
6	4.11 (*m*), 4.20 (*m*)	61.8
L-Rhamnose		
1	6.25 (*br s*)	102.1
2	4.80 (*dd,* 1.9, 4.0)	72.2
3	4.63 (*dd*, 5.1, 10.3)	72.6
4	4.28 (*t*, 9.5)	74.2
5	4.89 (*d,* 9.2)	69.8
6	1.75 (*d*, 7.1)	18.8
D-Glucose 3		
1	5.01 (*d*, 7.19)	103.9
2	3.98 (*t*, 9.5)	73.7
3	4.16 (*t*, 10.0)	88.1
4	3.95 (*t*, 10.0)	69.7
5	3.93 (*m*)	78.0
6	4.14 (*m*), 4.44 (*dd*, 3.3, 10.5)	62.1
D-Glucose 4		
1	5.19 (*d*, 8.2)	105.3
2	4.06 (*t*, 9.3)	75.2
3	4.19 (*t*, 9.1)	78.2
4	4.15 (*t*, 10.0)	71.6
5	3.97 (m)	78.6
6	4.28 (*dd*, 6.0, 12.0), 4.52 (*dd*, 3.0, 12.0)	62.4

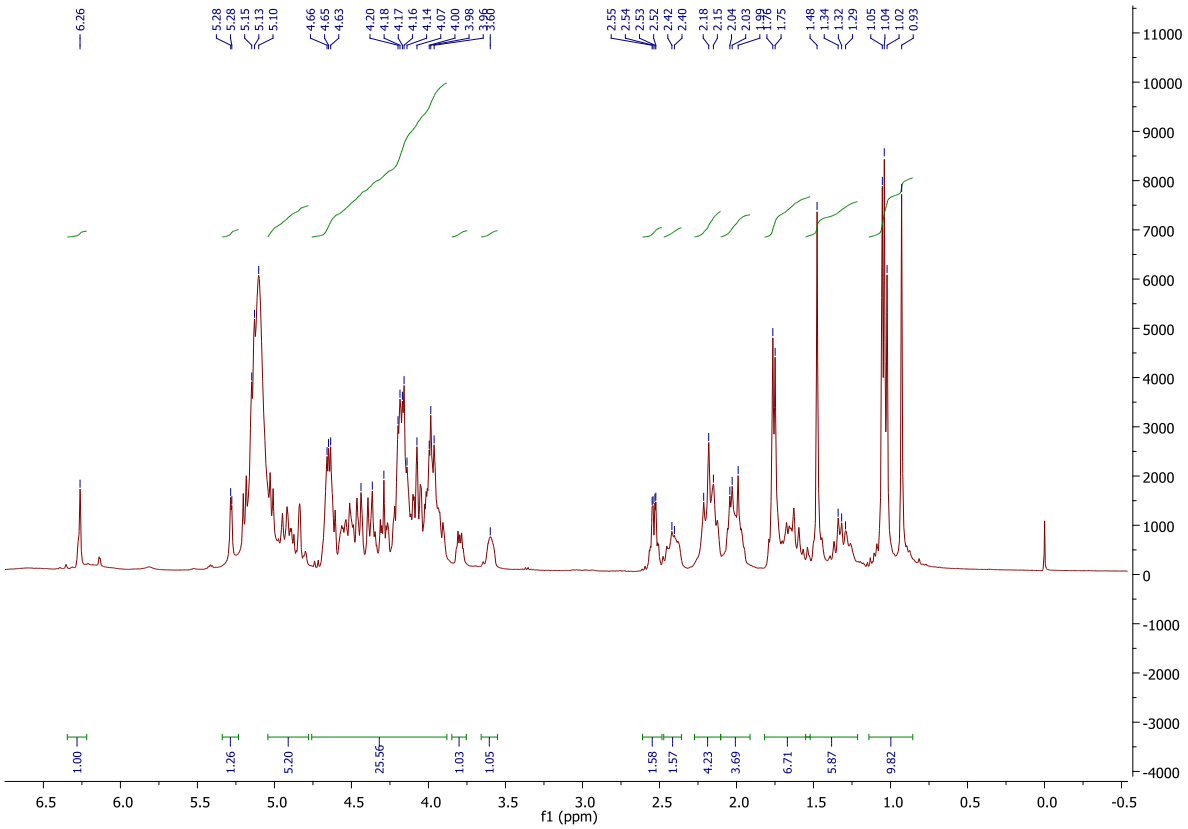

Figure 98 ^{1}H NMR of DR5 in pyridine-D_5.

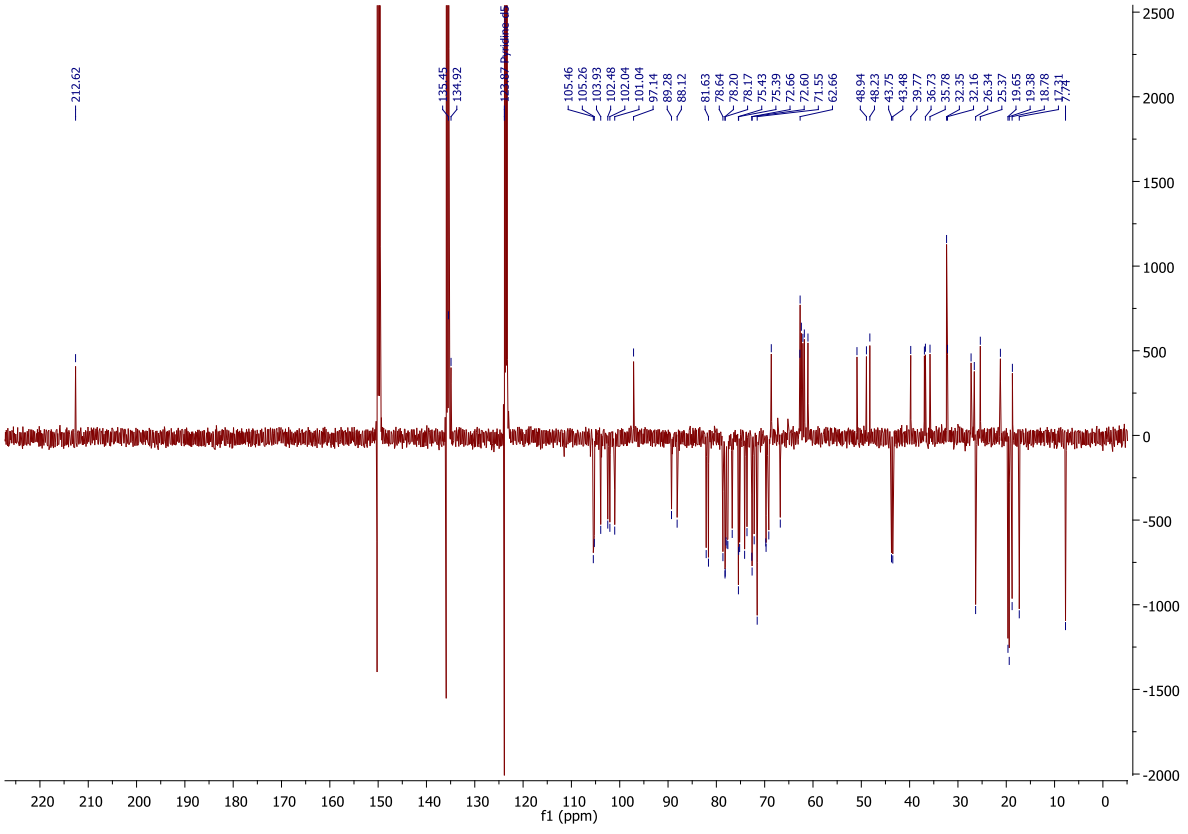

Figure 99 DEPTQ of DR5 in pyridine-D_5.

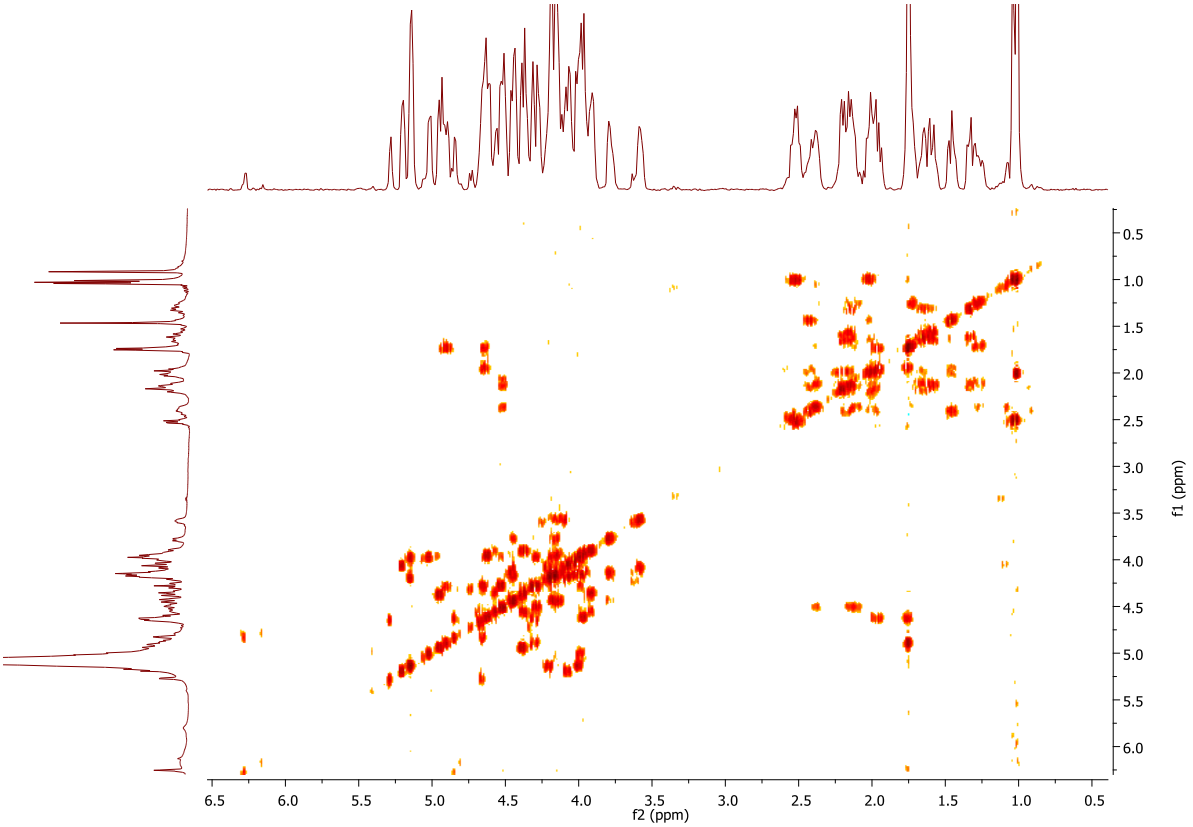

Figure 100 ^{1}H-^{1}H COSY of DR5 in pyridine-D_5.

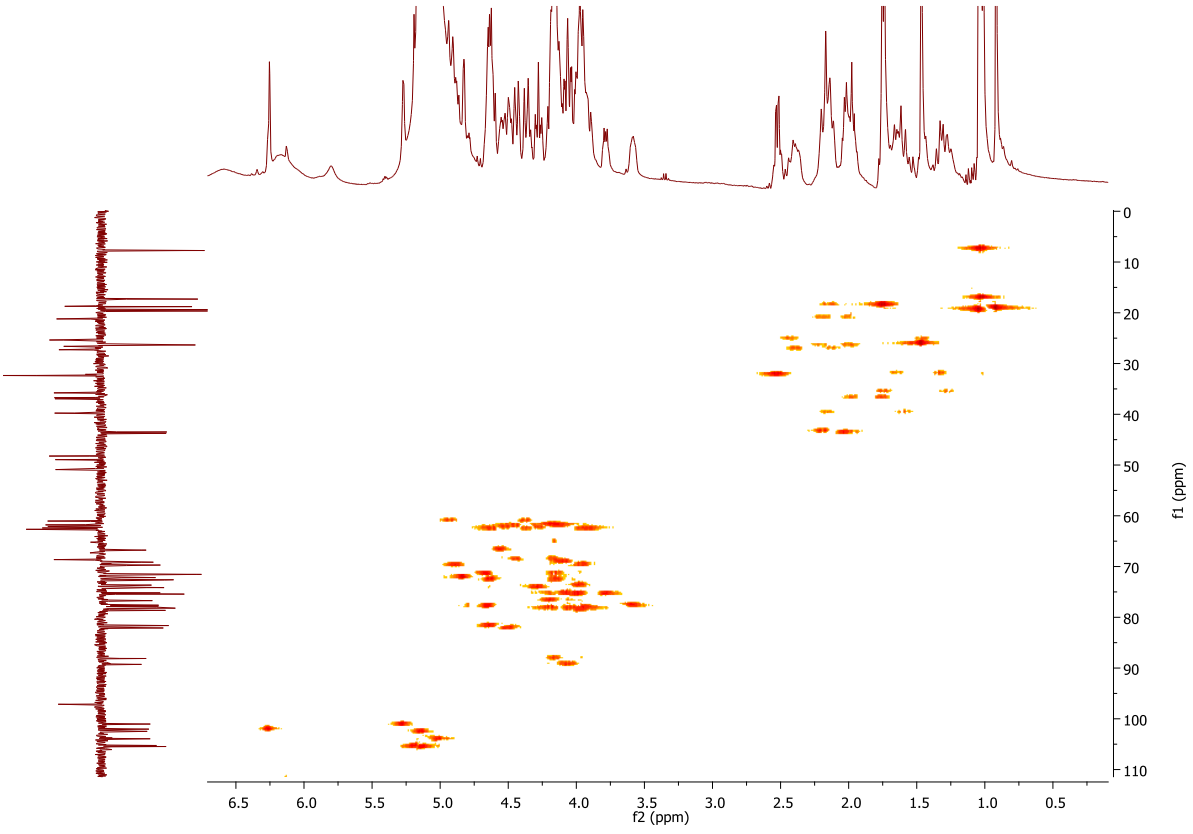

Figure 101 ^{1}H-^{13}C HSQC of DR5 in pyridine-D_5.

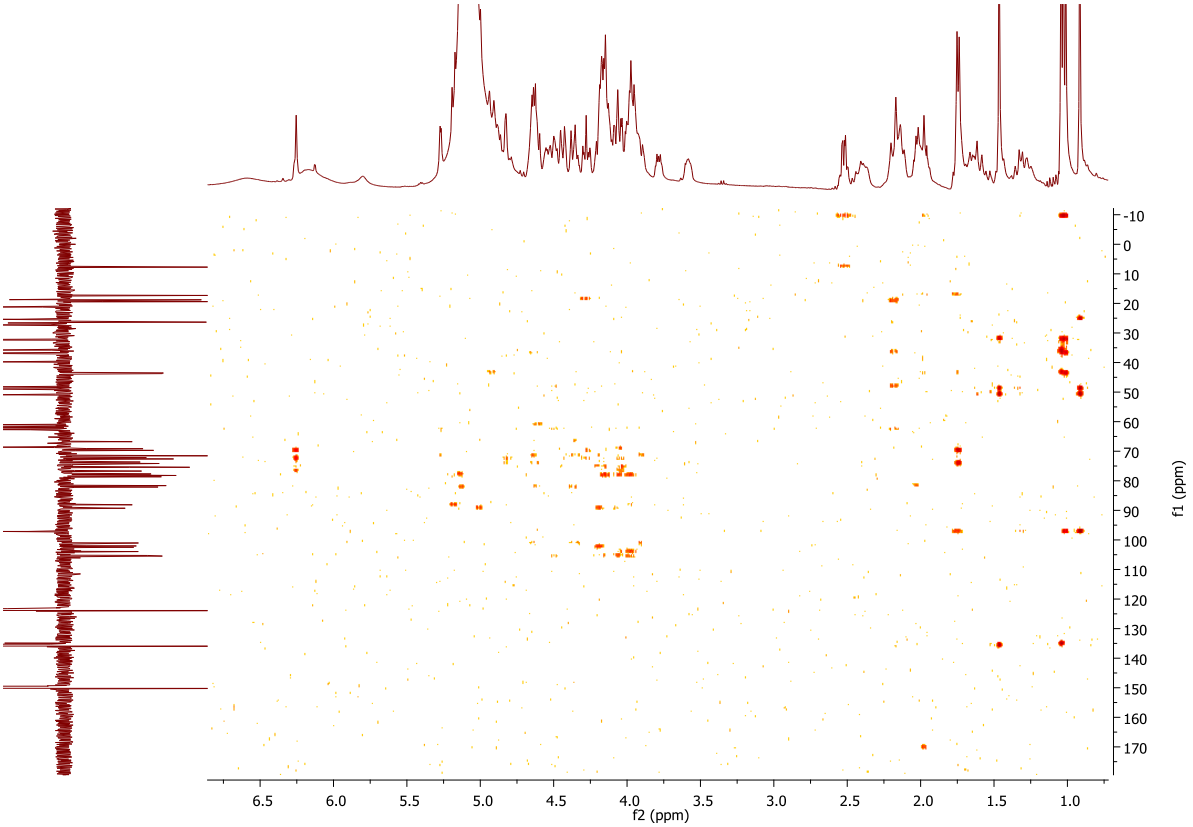

Figure 102 ^{1}H-^{13}C HMBC of DR5 in pyridine-D_5.

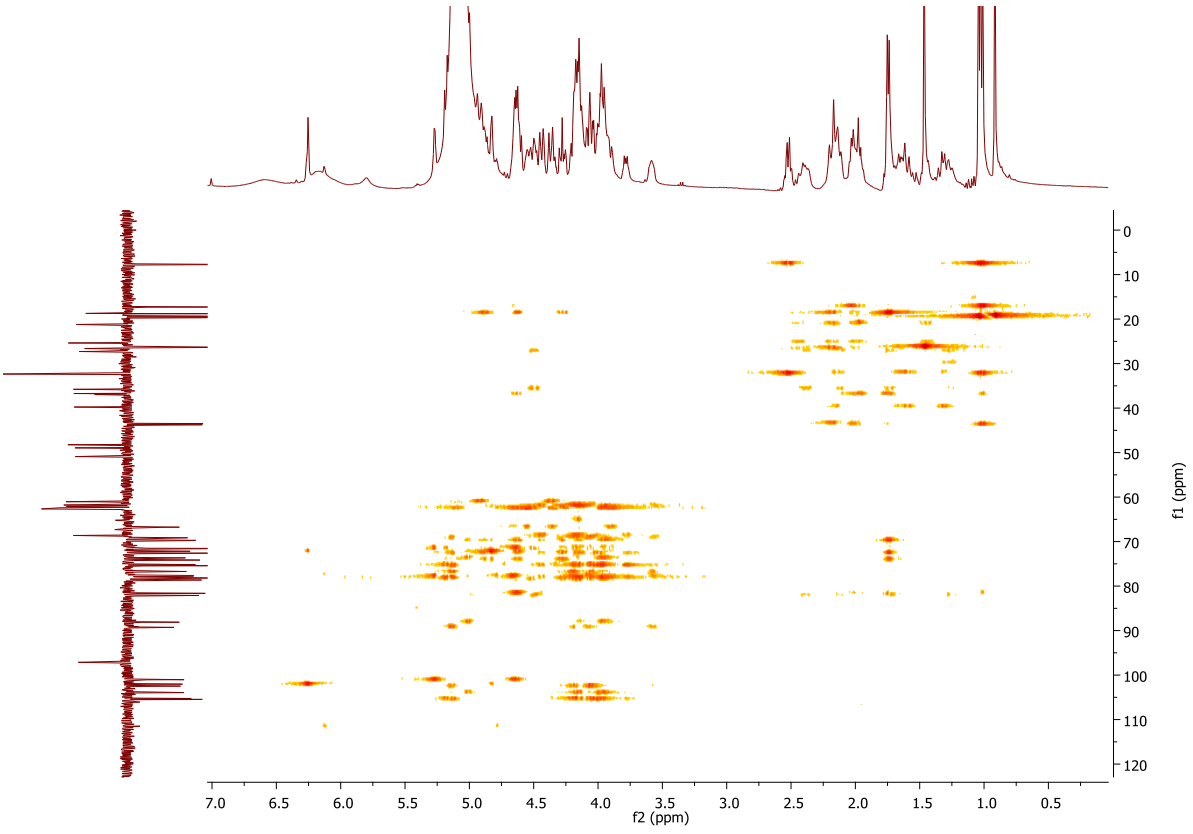

Figure 103 HSQC-TOCSY of DR5 in pyridine-D_5

4.3.3.2. LC-ESI-MS

The molecular formula $C_{64}H_{103}O_{34}$ established from NMR was confirmed with HR-ESI-MS. The negative mode ionisation (Figure 105) showed a formate adduct of the molecular mass 1445.64 and a low intensity peak of $[M-H]^-$ at m/z 1399. MS/MS analysis in this mode confirmed the mass of the oligosaccharide part which by deduction from the molecular ion gave the mass of the aglycone. On the other hand, the positive-mode ionisation (Figure 106) gave valuable information about the number, sequence and types of the sugars present in the oligomeric chain. Figure 104 shows the main mass spectral fragments of DR5 in this mode. Fragments were found at m/z 447 and 418 corresponding to the loss of ethyl and propanoyl fragment from the aglycone. Table 15 summarises the mass fragments obtained in both modes.

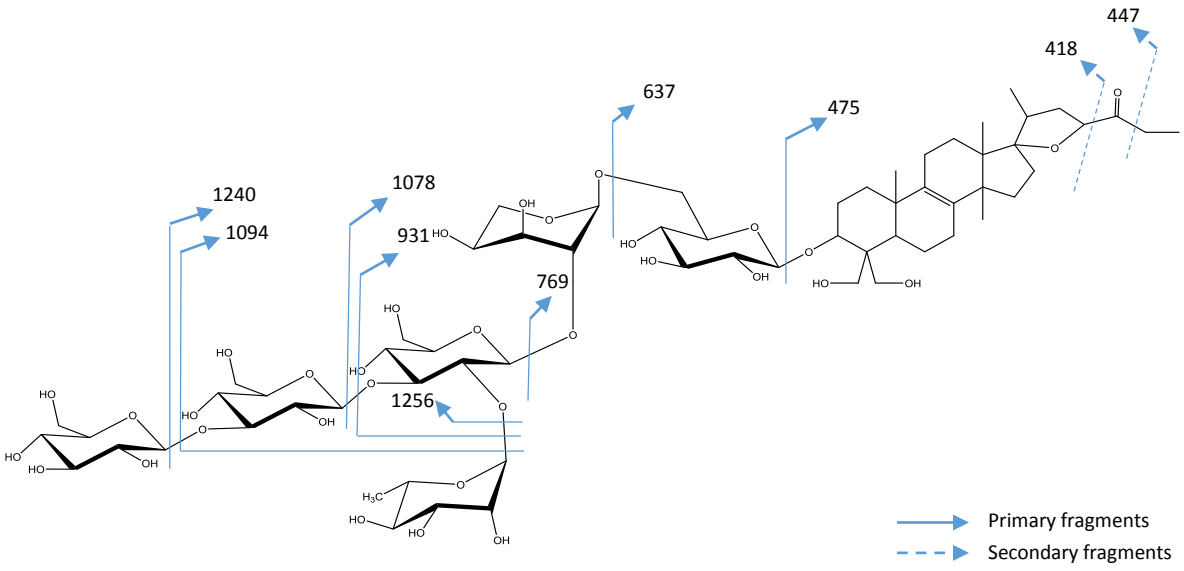

Figure 104 ESI-MS positive mode spectral fragments of DR5

Table 15 ESI-MS/MS fragments for compound DR5 in negative and positive fragmentation mode.

	m/z
Negative mode fragments	
Molecular ion $[M - H]^-$	1400
Molecular ion + formate	1446
The glycan part + formate	974
Positive mode fragments	
Molecular ion $[M+H]^+$	1402
$[M - glucose + H]^+$	1240
$[M - rhamnose + H]^+$	1256

[M – glucose - rhamnose + H]$^+$	1094
[M – (2 x glucose) + H]$^+$	1078
[M – (2 x glucose) - rhamnose + H]$^+$	931
[M – (3 x glucose) - rhamnose + H]$^+$	769
[M – (3 x glucose) - rhamnose - arabinose + H]$^+$	637
The aglycone	475
The aglycone - CH_2CH_3	447
The aglycone - $C(O)CH_2CH_3$	418

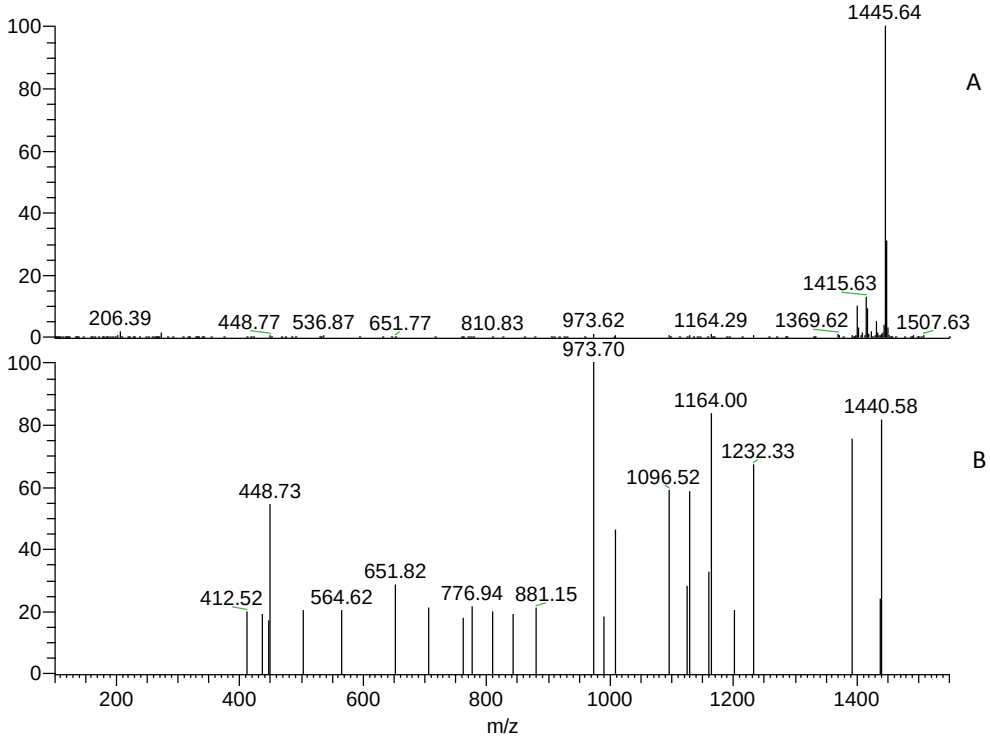

Figure 105 HR-ESI-MS (A) and MS/MS (B) OF DR5 in negative mode

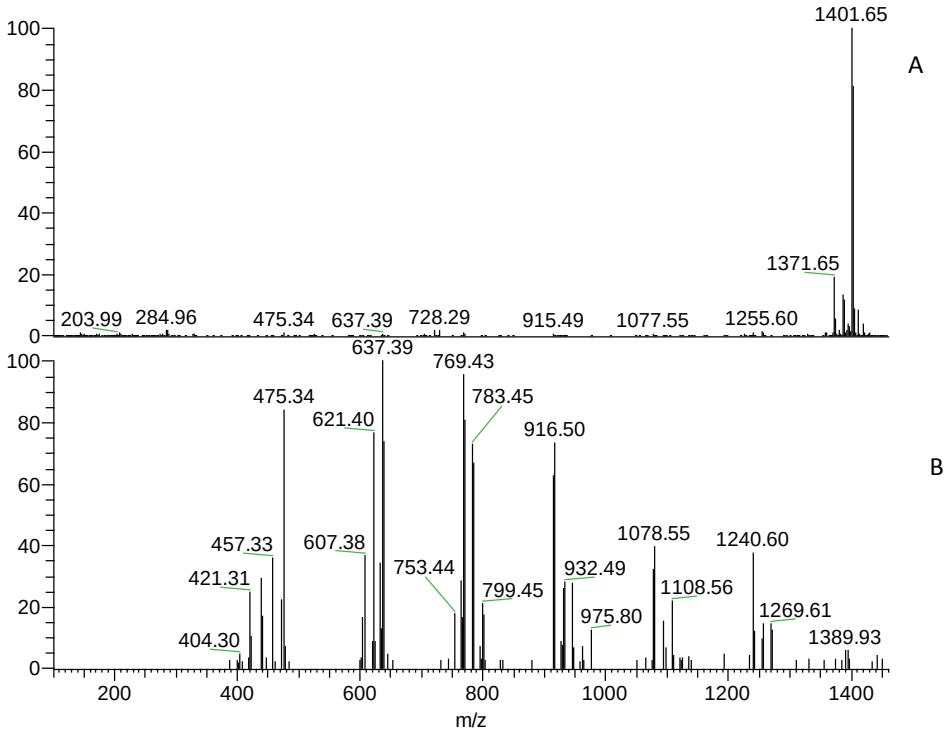

Figure 106 HR-ESI-MS (A) and MS/MS (B) OF DR5 in positive mode

4.3.3.3. GC-MS analysis

Acid hydrolysis was performed in both aqueous and methanolic HCl and the released sugars were converted into their oxime-trimethylsily derivatives for GC-MS analysis. The chromatograms obtained showed three types of sugars with their peaks matching those of glucose, rhamnose and arabinose standards. Hydrolysis in both aqueous and methanolic HCl gave matching results. However, hydrolysis in the presence of methanol resulted in the methylation of a proportion of the sugars which appeared as two extra peaks around 4.5 and 4.6 min compared to hydrolysis in water (Figure 107).

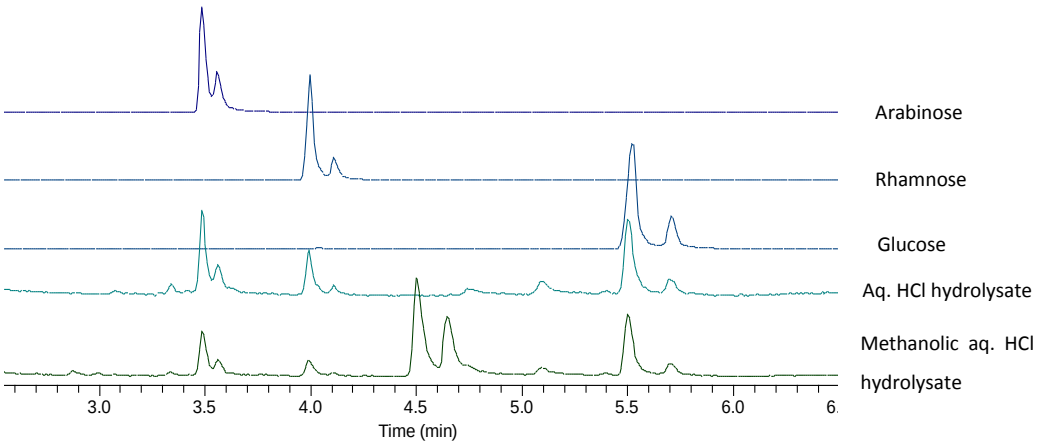

Figure 107 GC-MS chromatograms of DR5 hydrolysis products in aqueous HCl and methanolic aqueous HCl. Sugar peak identities were confirmed as arabinose, rhamnose and glucose by comparing their t_R and MS spectra with reference compounds.

4.3.4. Biological activity of bluebell saponins

DR5 showed remarkably high activity when tested against blood stream *Trypanosoma brucei* at a rate of 20 μM resulting in 98.9% inhibition. This agrees with previous literature reports of anti-trypanosomal activities of saponins (Hoet et al. 2007; Hostettmann and Marston 2005a). While studying the anti-trypanosomal activity of saponins isolated from the leaves of *Strychnos spinose* both in vitro and on mammalian cells, (Hoet et al. 2007) found that the saponins were about 4 - 7 time more toxic towards the parasite T. brucei than to the mammalian cells. They also investigated the relation of saponin structure to its activity and found that the presence of special structural features in the saponin results in higher activity. Such features included the presence of oxygenated functional group on C-17 or oxygenation of C-28.

Anti-bacterial tests showed no inhibition against *M. marinum* (an indicator species for activity against tuberculosis) and low inhibition against *K. pneumonia* and MRSA strains. DR5 didn't show anti-fungal activity when tested on 5 strains of the yeast species *C. albicans*. Additionally, compound DR5 was investigated for potential activity as pesticide which included anti-fungal activity both in artificial media and in leaf-based assays, herbicide assay and insecticide activity against aphid species. No activity was recorded in any of the tests except for a low inhibition against *Uromyces viciae-fabae* at 100 ppm. Table 16 lists a summary of the biological assays tested on DR5.

Table 16 Summary of biological assay results for the compound DR5.

Species tested	Rate	Results (as % inhibition)
Anti-trypanosoma activity		
Blood stream *Trypanosoma brucei* (S427)	20 µM	98.9
Anti-bacterial activity		
Mycobacterium marinum ATCC.BAA535	100 µM	-
Klebsiella pneumonia ATCC 13883		38.1
Klebsiella pneumonia BAA 2146		27.3
MRSA 16		9.3
MRSA 106		7.4
Anti-fungal activity		
Candida albicans SC514	20 mg/mL and 40 mg/mL	-
Candida albicans CA12		-
Candida albicans CA488		-
Candida albicans CA490		-
Candida albicans CA1008		-
Pesticidal activity		
a. Fungicidal activity		
Pythium dissimile	20 ppm	-
Alternaria solani		-
Botryotinia fuckeliana (Botrytis cinerea)		-
Gibberella zeae (Fuscarium graminearum)		-
Zymoseptoria tritici	100 ppm	-
Phytophthora infestans	200 ppm	-
Uromyces viciae-fabae	100 ppm	27
b. Herbicidal activity		
Arabidopsis thaliana	10 ppm	-
Poa annua		-
c. Insecticidal activity		
Aphid species	1000 ppm	-
Plutella xylostella	500 ppm	-
Diabrotica balteata		-

The purified bluebell saponin DR5 and crude 1-BuOH and aqueous extracts of the seeds were tested for schistosomicidal activity against *Schistosoma mansoni* at the *schistosomula* stage of its life cycle at which the parasite enters the blood vessels of the human host. The test results (Figure 108) showed activities for DR5, DR6 and DR7 higher than that of praziquantel (the current anti-schistosomal drug). This was indicated from their higher negative scores on both

the phenotype and motility axes. Although still of high activity, DR6 which is the 1-BuOH seed extract from 2013 showed lower scores than that of DR7 which could be attributed to longer storage periods of the extract. Saponins have been involved in anti-schistosomal treatments indirectly through their molluscicidal effects in controlling snails that serve as temporary host for the parasite (Goll et al. 1983; Rug and Ruppel 2000). The adjuvant effect of saponins resulting in immunisation against schistosomes has also received attention in the literature (Maghrabya et al. 2010; Smithers et al. 1989). Additionally, saponins were found to be active against the adult worm's stage of the life cycle both in vitro and in vitro (Jisaka et al. 1992; Melek et al. 2012).

Compound ID	Phenotype score	Motility score
DR5	-0.66351	-0.95038
DR6	-0.63939	-0.83815
DR7	-0.75547	-0.93826
DR8	-0.32355	-0.96731
DMSO	-0.0615	-0.05165
AUR	-0.7478	-0.9242
PZQ	-0.5788	-0.7976

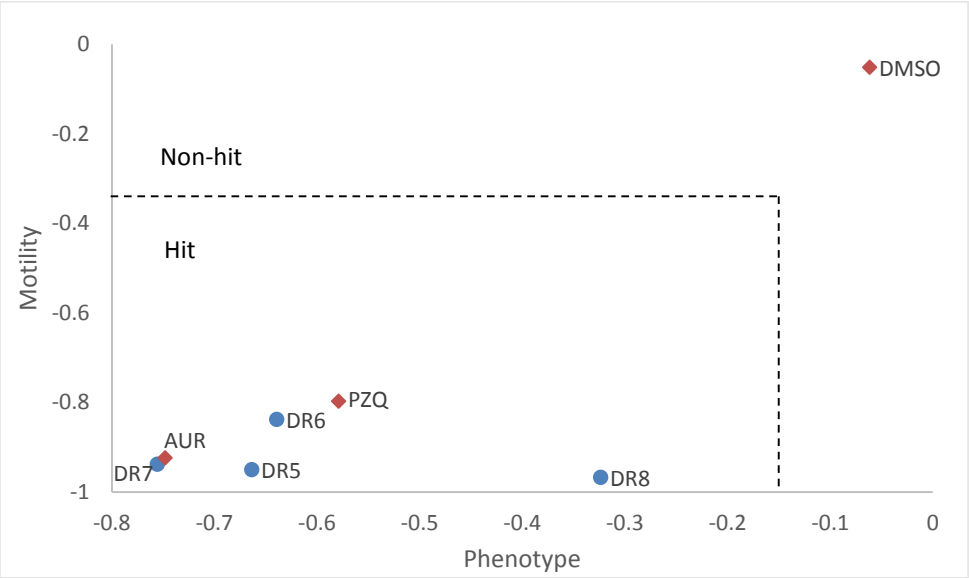

Figure 108 Tabular and graphical representation of the anti-schistosomal activity score of bluebell flower saponin and crude saponin-rich extracts from the seeds in comparison to the current anti-schistosomal drug and controls.

Chapter 5: Conclusion

5.1. Bluebell carbohydrates

Growth is limited to periods of availability of sunlight and resources prior to the growth of most other species and bracken canopy. The following undesirable seasons are avoided by the death of the above-ground organs and limiting the plant's availability to bulbs and slow underground growth phase. The bulbs comprise a large proportion of the plant's biomass and total non-structural carbohydrates. Additionally, the plant allocates a substantial amount of its photosynthate for maintaining and refilling this part to support plant's needs in the subterranean phase and early growth in the following season. Shifting from starch to fructans as the main reserve polysaccharide in bluebells is another factor to the success of the plant. Fructans have ecological significance in that their biosynthesis is of lower energy demand and continues at lower temperatures compared to starch. They accumulate to high concentrations and don't undergo severe depletion as with starch. The plant benefits from its reserve fructans for early growth by degrading the polymeric molecules and mobilising the product in the form of sucrose the growing shoots. The fructan pool was found to contain mostly short-chain fructooligosaccharides (DP3-DP9) with DP3 and DP4 oligomers being the most abundant molecules and 1-kestose the main trisaccharide. The presence of high concentrations of small molecular weight fructans can helps controlling osmotic pressure and water absorption at important for tissue expansion at early shoot growth, flowering and fruiting. Such molecules have also an advantage of protecting the plant from injury due to cold stress by stabilising cell membranes. A factor that provides a survival benefit for the plant during early growth in the cold season.

5.2. Bluebell phenolics

LC-MS investigation of bluebell phenolics revealed that the plant contains apigenin as the main flavone aglycone in addition to only minor amounts of luteolin and naringenin as *O*-glycosides and eriocictyol as *C*-glycosides. Phenolic acids such as *p*-coumaric, ferulic, sinapic and ceffeic acids were also detected as conjugates of flavonoid glycosides, sugars and organic acids. Apigenin was found to be glycosylated with hexoses, pentoses, deoxyhexoses (rhamnose) and sugar acids. The isolation of two apigenin glycosides from the flowers 7-[*O*-*β*-D-glucopuranosyl-(1→3)-*O*-*β*-D-xylopyranosyl-(1→6)-*O*-*β*-D-glucopyranosyl-(1→2)-*O*-*β*-D-glucopyranosideuronic acid-(1→)]-apigenin (DR3) and 7-[*O*-*β*-D-xylopyranosyl-(1→6)-*O*-*β*-

D-glucopyranosyl-(1→2)-*O*-*β*-D-glucopyranosideuronic acid-(1→)]-apigenin (DR4) helped identify the sugars in a glycosidic chain linked to the apigenin moiety via the C7-OH position. Investigation of the flower methanolic extract also helped identify two new metabolites (benzyl-O-β-D-glucopyranosyluronic acid-(1→2)-glucopyranoside DR1 and 2-phenylethyl-O-β-D-glucopyranosyluronic acid-(1→2)-glucopyranoside DR2). Isolation of flower metabolites was done utilising column, flash and thin layer chromatography. Structural elucidation of the compounds was based on NMR and LC-MS analysis. Apigenin and *p*-coumaric acid were quantified after simplifying the extracts using acid hydrolysis on the different plant parts. The results showed that allocation of the two compounds was mostly to the above-ground parts suggesting their contribution to plant protection from predators and oxidation damage. Anthesis is characterised with high values of phenolics in flowers and scapes. This indicates the large amount of resource the plant allocate to this stage due to its importance in reproduction, survival and continuation of the species. The results also showed that the leaves and scapes contained considerable amounts of apigenin at the end of their lives which could subsequently be transferred into the soil and contribute to nutrient cycling and symbiotic relationships.

5.3. Saponins

Metabolomics and multivariate analysis (MVA) was used to investigate the general metabolite profile in the plant at various time point of their growth cycle. The analysis was undertaken utilising high resolution mass spectrometry and data analysis software. Heatmap of the metabolites showed that the bulbs were rather different from the above-ground parts and they contained higher number of later eluting/ less polar compounds in comparison. PCA and OPLSDA score plots showed separate clustering of bulb metabolites away from the above-ground organs with bulb samples from the start of growth (March-May) and senescence and leaf death in June and July showing the greatest variability. Loading plots showed that a number of small molecular weight metabolites (200-600 Da) were responsible for the greatest variation of the bulbs. Two bulb metabolites were identified based on their MS3 data as steroidal aglycones. Previous knowledge of bluebell saponins elution behaviour and the results from dereplication analysis and comparison of bluebell metabolites with DNP database showed that compounds identified by as saponins were of MWt 1000 – 1500 Da and t_R 10 – 18 min. Thus metabolite peaks falling within this criteria were used in following the seasonal change in saponins for different parts. Saponins were found to exist in higher quantities in above ground parts compared to the bulbs. Highest contents in the bulbs were during the early growth

in March and April. The above-ground parts also showed high values for the same period. The flowers showed the highest content of saponins which decreased gradually until it reached a minimum at seed formation. The high concentrations of saponins in the start of the growth can be of survival benefits to the plant. It can help in bluebell root's colonisation with arbuscular mycorrhizal fungi necessary for phosphorous and nutrient uptake by the plant. It can also provide the young growing shoots with a defence means necessary to protect the tissues at this stage. Data dereplication helped in the tentative identification of 7 saponins of which one being the main saponin in the flowers was isolated, its structure elucidated based on NMR, GC-MS and LC-MS/MS analysis and identified as 3*β*-[(*O*-*β*-D-glucopyranosyl-(1→3)-*O*- *β*-D-glucopyranosyl-(1→3)-[*α*-L-rhamnopyranosyl-(1→2)]-*O*-*β*-D-glucopyranosyl-(1→2)-*O*-*α*-L-arabinopyranosyl-(1→6)-*O*-*β*-D-glucopyranosyl)oxy]-17,23-epoxy-28,29-dihydroxy-27-norlanost-8-en-24-one. The isolated saponin was found to be of high activity against *T. brucei* (blood stream) causing 98.9% inhibition at 20 μM, but inactive as antifungal against *C. albican*. Also no activity was noticed when the compound was tested as pesticide. The isolated saponin was further tested along with crude aqueous and 1-BuOH extracts from bluebell seeds (collected in 2013 and 2014) against *S. mansoni* at the schistosomula stage. The results showed that all the compounds were of high inhibition against the parasite.

Bibliography

Abdelmohsen, UR, Cheng, C, Viegelmann, C, Zhang, T, Grkovic, T, Ahmed, S, Quinn, RJ, Hentschel, U, Edrada-Ebel, R (2014) Dereplication strategies for targeted isolation of new antitrypanosomal actinosporins A and B from a marine sponge associated-actinokineospora sp. EG49. Marine Drugs 12:1220-1244.

Adinolfi, M, Barone, G, Lanzetta, R, Laonigro, G, Mangoni, L, Parrilli, M (1984) Glycosides from muscari comosum. 5. structure of muscaroside B. Canadian Journal of Chemistry 62:1223-1226.

Adinolfi, M, Barone, G, Corsaro, MM, Lanzetta, R, Mangoni, L, Parrilli, M (1987) Glycosides from muscari comosum. 7. structure of three novel muscarosides. Canadian Journal of Chemistry 65:2317-2326.

Agati, G, Azzarello, E, Pollastri, S, Tattini, M (2012) Flavonoids as antioxidants in plants: Location and functional significance. Plant Science 196:67-76.

Agrell, J, Oleszek, W, Stochmal, A, Olsen, M, Anderson, P (2003) Herbivore-induced responses in alfalfa (medicago sativa). J. Chem. Ecol. 29:303-320.

Appel, HM (1993) Phenolics in ecological interactions: The importance of oxidation. J. Chem. Ecol. 19:1521-1552.

Augustin, JM, Kuzina, V, Andersen, SB, Bak, S (2011) Molecular activities, biosynthesis and evolution of triterpenoid saponins. Phytochemistry 72:435-457.

Bacic, A, Harris, PJ, Stone, BA (1988) Structure and function of plant cell walls. In: Stumpf, PK, Conn, EE (eds) The Biochemistry of Plants: A Comprehensive Treatise, Volume 14, Carbohydrates. Academic Press, Inc., , pp. 297.

Baldwin, IT, Halitschke, R, Kessler, A, Schittko, U (2001) Merging molecular and ecological approaches in plant–insect interactions. Curr. Opin. Plant Biol. 4:351-358.

Bancal, P, Carpita, N, Gaudillere, J (1992) Differences in fructan accumulated in induced and field-grown wheat plants: An elongation-trimming pathway for their synthesis. New Phytol. 120:313-321.

Barz, W, Köster, J (1981) Turnover and degradation of secondary (natural) products. In: Conn, EE (ed) The Biochemistry of Plants: A Comprehensive Treatise. Volume 7, Secondary Plant Products. Academic Press: New York, , pp. 35.

Barz, W, Hoesel, W (1979) Metabolism and degradation of phenolic compounds in plants. In: Swain, T, Harborne, J. B.: Van Sumere, C. F. (eds) Biochemistry of plant phenolics. Springer, , pp. 339.

Bazzaz, F (1997) Allocation of resources in plants: State of the science and critical question. In: Bazzaz, F, Grace, J (eds) Plant resource allocation, pp. 1.

Beck, E, Ziegler, P (1989) Biosynthesis and degradation of starch in higher plants. Annual Review of Plant Physiology and Plant Molecular Biology (USA) .

Beckman, CH (2000) Phenolic-storing cells: Keys to programmed cell death and periderm formation in wilt disease resistance and in general defence responses in plants? Physiol. Mol. Plant Pathol. 57:101-110.

Bennett, RN, Wallsgrove, RM (1994) Tansley review no. 72. secondary metabolites in plant defence mechanisms. New Phytol. 617-633.

Bhat, S, Nagasampagi, B, Sivakumar, M (2005) Chemistry of natural products.

Blackman, GE, Rutter, AJ (1950) Physiological and ecological studies in the analysis of plant environment: V. an assessment of the factors controlling the distribution of the bluebell (scilla non-scripta) in different communities. Annals of Botany 14:487-520. doi: http://0-aob.oxfordjournals.org.unicat.bangor.ac.uk/content/14/4/487.short.

Blackman, GE, Rutter, AJ (1949) Physiological and ecological studies in the analysis of plant environment IV. the interaction between light intensity and mineral nutrient supply on the uptake of nutrients by the bluebell (scilla non-scripta). Annals of Botany 13:453-488.

Blackman, GE, Rutter, AJ (1948) Physiological and ecological studies in the analysis of plant environment: III. the interaction between light intensity and mineral nutrient supply in leaf development and in the net assimilation rate of the bluebell (scilla non-scripta) Annals of Botany 12:1-26.

Blackman, GE, Rutter, AJ (1947) Physiological and ecological studies in the analysis of plant environment: II. the interaction between light intensity and mineral nutrient supply in the growth and development of the bluebell (scilla non-scripta). Annals of Botany 11:125-158.

Blackman, GE, Rutter, AJ (1946) Physiological and ecological studies in the analysis of plant environment: 1. the light factor and the distribution of the bluebell (scilla non-scripta) in woodland communities. Annals of Botany 10:361-390.

Blackman, G, Rutter, A (1954) Endymion nonscriptus (L.) garcke. The Journal of Ecology 629-638.

Bonnett, G, Sims, I, Simpson, R, Cairns, A (1997) Structural diversity of fructan in relation to the taxonomy of the poaceae. New Phytol. 136:11-17.

Bornman, JF, Reuber, S, Cen, YP, Weissenböck, G (1997) Ultraviolet radiation as a stress factor and the role of rrotective pigments. In: Lumsden, P (ed) Plants and UV-B: Responses to Environmental Change. Cambridge University Press, , pp. 157.

Brocklebank, KJ, Hendry, GAF (1989) Characteristics of plant species which store different types of reserve carbohydrates. New Phytol. 112:255-260. doi: 10.1111/j.1469-8137.1989.tb02381.x.

Brouillard, R (1988) Flavonoids and flower colour. In: Harborne, JB (ed) The flavonoids. Springer, , pp. 525.

Calub, TM, Waterhouse, AL, Chatterton, NJ (1990) Proton and carbon chemical-shift assignments for 1-kestose, from two-dimensional nmr-spectral measurements. Carbohydr. Res. 199:11-17.

Cesco, S, Mimmo, T, Tonon, G, Tomasi, N, Pinton, R, Terzano, R, Neumann, G, Weisskopf, L, Renella, G, Landi, L (2012) Plant-borne flavonoids released into the rhizosphere: Impact on soil bio-activities related to plant nutrition. A review. Biol. Fertility Soils 48:123-149.

Chaieb, I (2010) Saponins as insecticides: A review. Tunisian Journal of Plant Protection 5:39-50.

Chalker-Scott, L (1999) Environmental significance of anthocyanins in plant stress responses. Photochem. Photobiol. 70:1-9.

Chapin, FS, Schulze, E, Mooney, HA (1990) The ecology and economics of storage in plants. Annu. Rev. Ecol. Syst. 423-447.

Cheok, CY, Salman, HAK, Sulaiman, R (2014) Extraction and quantification of saponins: A review. Food Res. Int. 59:16-40.

Coleman, JJ, Okoli, I, Tegos, GP, Holson, EB, Wagner, FF, Hamblin, MR, Mylonakis, E (2010) Characterization of plant-derived saponin natural products against candida albicans. ACS Chemical Biology 5:321-332.

Commenges, D, Scotet, V, Renaud, S, Jacqmin-Gadda, H, Barberger-Gateau, P, Dartigues, J (2000) Intake of flavonoids and risk of dementia. Eur. J. Epidemiol. 16:357-363.

Compain, P, Martin, OR (2007) Iminosugars: From synthesis to therapeutic applications. Wiley, .

Cuyckens, F, Claeys, M (2004) Mass spectrometry in the structural analysis of flavonoids. Journal of Mass Spectrometry 39:1-15.

Dai, J, Mumper, RJ (2010) Plant phenolics: Extraction, analysis and their antioxidant and anticancer properties. Molecules 15:7313-7352.

Darbyshire, B, Henry, R (1978) The distribution of fructans in onions. New Phytol. 29-34.

De Bruyn, A, Van Loo, J (1991) The identification by 1 H-and 13 cn. mr spectroscopy of sucrose, 1-kestose, and neokestose in mixtures present in plant extracts. Carbohydr. Res. 211:131-136.

De Geyter, E, Lambert, E, Geelen, D, Smagghe, G (2007) Novel advances with plant saponins as natural insecticides to control pest insects. Pest Technol 1:96-105.

de Rijke, E, Out, P, Niessen, WM, Ariese, F, Gooijer, C, Udo, AT (2006) Analytical separation and detection methods for flavonoids. Journal of Chromatography A 1112:31-63.

Denness, L, McKenna, JF, Segonzac, C, Wormit, A, Madhou, P, Bennett, M, Mansfield, J, Zipfel, C, Hamann, T (2011) Cell wall damage-induced lignin biosynthesis is regulated by a reactive oxygen species- and jasmonic acid-dependent process in arabidopsis. Plant Physiol. 156:1364-1374. doi: 10.1104/pp.111.175737 [doi].

Dettmer, K, Aronov, PA, Hammock, BD (2007) Mass spectrometry-based metabolomics. Mass Spectrom. Rev. 26:51-78.

Domon, B, Costello, CE (1988) A systematic nomenclature for carbohydrate fragmentations in FAB-MS/MS spectra of glycoconjugates. Glycoconj. J. 5:397-409.

Domon, B, Hostettmann, K (1984) New saponins from phytolacca dodecandra l'herit. Helv. Chim. Acta 67:1310-1315.

Edelman, J, Jefford, T (1968) The mechanisim of fructosan metabolism in higher plants as exemplified in helianthus tuberosus. New Phytol. 517-531.

Egan, MJ, Porter, EA, Kite, GC, Simmonds, MSJ, Barker, J, Howells, S (1999) High performance liquid chromatography quadrupole ion trap and gas chromatography/mass spectrometry studies of polyhydroxyalkaloids in bluebells. Rapid Communications in Mass Spectrometry 13:195-200. doi: 10.1002/(SICI)1097-0231(19990228)13:4<195::AID-RCM433>3.0.CO;2-D.

Ellis, B (1983) Production of hydroxyphenylethanol glycosides in suspension cultures of syringa vulgaris. Phytochemistry 22:1941-1943.

Ernst, M, CHATTERTON, J, Harrison, PA (1996) Purification and characterization of a new fructan series from species of asteraceae. New Phytol. 132:63-66.

Fitzgerald, MC, Parr, GR, Smith, LM (1993) Basic matrixes for the matrix-assisted laser desorption/ionization mass spectrometry of proteins and oligonucleotides. Anal. Chem. 65:3204-3211.

Forsythe, KL, Feather, MS (1989) The detection of isokestose and neokestose in plant extracts by 13 cn. mr spectroscopy. Carbohydr. Res. 185:315-319.

Fossen, T, Andersen, ØM (2006) Spectroscopic techniques applied to flavonoids. In: Andersen, ØM, Markham, KR (eds) Flavonoids: Chemistry, Biochemistry and Applications. CRC Press LLC, , pp. 37.

Francis, G, Kerem, Z, Makkar, HP, Becker, K (2002) The biological action of saponins in animal systems: A review. Br. J. Nutr. 88:587-605.

Franzen, CA, Amargo, E, Todorovic, V, Desai, BV, Huda, S, Mirzoeva, S, Chiu, K, Grzybowski, BA, Chew, TL, Green, KJ, Pelling, JC (2009) The chemopreventive bioflavonoid apigenin inhibits prostate cancer cell motility through the focal adhesion kinase/Src signaling mechanism. Cancer. Prev. Res. (Phila) 2:830-841. doi: 10.1158/1940-6207.CAPR-09-0066 [doi].

Fujishima, M, Sakai, H, Ueno, K, Takahashi, N, Onodera, S, Benkeblia, N, Shiomi, N (2005) Purification and characterization of a fructosyltransferase from onion bulbs and its key role in the synthesis of fructo-oligosaccharides in vivo. New Phytol. 165:513-524.

Gianinazzi-Pearson, V (1996) Plant cell responses to arbuscular mycorrhizal fungi: Getting to the roots of the symbiosis. Plant Cell 8:1871-1883. doi: 10.1105/tpc.8.10.1871 [doi].

Giusti, MM, Wrolstad, RE (2001) Characterization and measurement of anthocyanins by UV-visible spectroscopy. Current Protocols in Food Analytical Chemistry .

GIUSTI, MM, WROLSTAD, RE (1996) Characterization of red radish anthocyanins. J. Food Sci. 61:322-326.

Goławska, S, Łukasik, I, Leszczyński, B (2008) Effect of alfalfa saponins and flavonoids on pea aphid. Entomol. Exp. Appl. 128:147-153.

Goll, PH, Lemma, A, Duncan, J, Mazengia, B (1983) Control of schistosomiasis in adwa, ethiopia, using the plant molluscicide endod (phytolacca dodecandra). Tropenmed. Parasitol. 34:177-183.

Gómez-Caravaca, AM, Iafelice, G, Lavini, A, Pulvento, C, Caboni, MF, Marconi, E (2012) Phenolic compounds and saponins in quinoa samples (chenopodium quinoa willd.) grown under different saline and nonsaline irrigation regimens. J. Agric. Food Chem. 60:4620-4627.

Goto, T, Kondo, T, Tamura, H, Takase, S (1983) Structure of malonylawobanin, the real anthocyanin present in blue-colored flower petals of commelina communis. Tetrahedron Lett. 24:4863-4866. doi: 10.1016/S0040-4039(00)94027-9.

Gould, KS, Lister, C (2006) Flavonoid functions in plants. In: Andersen, ØM, Markham, KR (eds) Flavonoids: Chemistry, Biochemistry and Applications. CRC Press LLC, , pp. 397.

Grabham, PW, Packham, JR (1983) A comparative study of the bluebell hyacinthoides non-scripta (L.) chouard in two different woodland situations in the west midlands, england. Biol. Conserv. 26:105-126. doi: 10.1016/0006-3207(83)90061-7.

Grayer, RJ, Kite, GC, Abou-Zaid, M, Archer, LJ (2000) The application of atmospheric pressure chemical ionisation liquid chromatography–mass spectrometry in the chemotaxonomic study of flavonoids: Characterisation of flavonoids from ocimum gratissimum var. gratissimum. Phytochem. Anal. 11:257-267.

Hagerman, AE, Robbins, CT (1993) Specificity of tannin-binding salivary proteins relative to diet selection by mammals. Can. J. Zool. 71:628-633.

Hanuš, LO, Řezanka, T, Dembitsky, VM (2003) A trinorsesterterpene glycoside from the north american fern woodwardia virginica (L.) smith. Phytochemistry 63:869-875.

Haralampidis, K, Trojanowska, M, Osbourn, AE (2002) Biosynthesis of triterpenoid saponins in plants. In: Anonymous History and Trends in Bioprocessing and Biotransformation. Springer, , pp. 31.

Harborne, J (1989) General procedures and measurement of total phenolics. In: Dey, PM, Harborne, JB (eds) Methods in Plant Biochemistry, Volume 1, Plant Phenolics, pp. 1.

Harborne, J (1965) Plant polyphenols—XIV.: Characterization of flavonoid glycosides by acidic and enzymic hydrolyses. Phytochemistry 4:107-120.

Harborne, JB (1993) Biochemistry of plant pollination. In: Anonymous Introduction to Ecological Biochemistry. Academic Press, .

Harborne, JB (1988) The flavonoids: Advances in research since 1980. Springer, .

Harborne, JB (1979) Variation in and functional significance of phenolic conjugation in plants. In: Swain, T, Harborne, JB, Sumere, C (eds) Biochemistry of plant phenolics. Springer Science & Business Media, , pp. 457.

Harborne, JB, Williams, CA (1988) Flavone and flavonol glycosides. In: Harborne, JB (ed) The flavonoids. Springer, , pp. 303.

Harborne, JB, Nash, RJ (1984) Flavonoid pigments responsible for ultraviolet patterning in petals of the genus potentilla. Biochem. Syst. Ecol. 12:315-318.

Harris, P, Hartley, R (1976) Detection of bound ferulic acid in cell walls of the gramineae by ultraviolet fluorescence microscopy.

Harvey, DJ (2015) Analysis of carbohydrates and glycoconjugates by matrix-assisted laser desorption/ionization mass spectrometry: An update for 2009–2010. Mass Spectrom. Rev. 34:268-422.

Harvey, DJ (2003) Matrix-assisted laser desorption/ionization mass spectrometry of carbohydrates and glycoconjugates. International Journal of Mass Spectrometry 226:1-35.

Harvey, D (1993) Quantitative aspects of the matrix-assisted laser desorption mass spectrometry of complex oligosaccharides. Rapid Communications in Mass Spectrometry 7:614-619.

He, Z, Qiao, C, Han, Q, Wang, Y, Ye, W, Xu, H (2005) New triterpenoid saponins from the roots of platycodon grandiflorum. Tetrahedron 61:2211-2215.

Heller, W, Forkmann, G (1988) Biosynthesis. In: Harborne, JB (ed) The Flavonoids. Springer, , pp. 399.

Hendry, GA, Wallace, RK (1993a) The origin, distribution and evolutionary significance of fructans. In: Michio Suzuki and N. Jerry Chatterton (ed) Science and Technology of Fructans. CRC Press, , pp. 119.

Hendry, GA, Wallace, RK (1993b) The origin, distribution, and evolutionary significance of fructans. Science and Technology of Fructans 119-139.

Hendry, G (1987) The ecological significance of fructan in a contemporary flora. New Phytol. 106:201-216.

Hertog, MG, Feskens, EJ, Kromhout, D, Hollman, P, Katan, M (1993) Dietary antioxidant flavonoids and risk of coronary heart disease: The zutphen elderly study. The Lancet 342:1007-1011.

Hertog, MG, Hollman, PC, Katan, MB (1992) Content of potentially anticarcinogenic flavonoids of 28 vegetables and 9 fruits commonly consumed in the netherlands. J. Agric. Food Chem. 40:2379-2383.

Hillenkamp, F, Karas, M, Beavis, RC, Chait, BT (1991) Matrix-assisted laser desorption/ionization mass spectrometry of biopolymers. Anal. Chem. 63:1193A-1203A.

Hincha, DK, Hellwege, EM, Heyer, AG, Crowe, JH (2000) Plant fructans stabilize phosphatidylcholine liposomes during freeze-drying. European Journal of Biochemistry 267:535-540.

Hoet, S, Pieters, L, Muccioli, GG, Habib-Jiwan, J, Opperdoes, FR, Quetin-Leclercq, J (2007) Antitrypanosomal activity of triterpenoids and sterols from the leaves of strychnos spinosa and related compounds. J. Nat. Prod. 70:1360-1363.

Horne, G, Wilson, FX, Tinsley, J, Williams, DH, Storer, R (2011) Iminosugars past, present and future: Medicines for tomorrow. Drug Discov. Today 16:107-118. doi: 10.1016/j.drudis.2010.08.017.

Horvath, DP, Anderson, JV, Chao, WS, Foley, ME (2003) Knowing when to grow: Signals regulating bud dormancy. Trends Plant Sci. 8:534-540.

Hostettmann, K, Marston, A (2005a) Saponins. Cambridge University Press, .

Hostettmann, K, Marston, A (2005b) Saponins. Cambridge University Press, .

Housley, TL, Daughtry, CS (1987) Fructan content and fructosyltransferase activity during wheat seed growth. Plant Physiol. 83:4-7.

Hu, XW, Meng, D, Fang, J (2008) Apigenin inhibited migration and invasion of human ovarian cancer A2780 cells through focal adhesion kinase. Carcinogenesis 29:2369-2376. doi: 10.1093/carcin/bgn244 [doi].

Hutzler, P, Fischbach, R, Heller, W, Jungblut, TP, Reuber, S, Schmitz, R, Veit, M, Weissenböck, G, Schnitzler, J (1998) Tissue localization of phenolic compounds in plants by confocal laser scanning microscopy. J. Exp. Bot. 49:953-965.

Inderjit (1996) Plant phenolics in allelopathy. The Botanical Review 186-202.

Ishii, H, Kitagawa, I, Matsushita, K, Shirakawa, K, Tori, K, Tozyo, T, Yoshikawa, M, Yoshimura, Y (1981) The configuration and conformation of the arabinose moiety in platycodins, saponins isolated from platycodongrandiflorum, and mi-saponins from madhucalongifolia based on carbon-13 and hydrogen-1 nmr spectroscopic evidence: The total structures of the saponins. Tetrahedron Lett. 22:1529-1532.

Iwashina, T (2000) The structure and distribution of the flavonoids in plants. J. Plant Res. 113:287-299.

Iwashina, T, Matsumoto, S, Nishida, M, Nakaike, T (1995) New and rare flavonol glycosides from asplenium trichomanes-ramosum as stable chemotaxonomic markers. Biochem. Syst. Ecol. 23:283-290.

Jia, J, Zhang, F, Li, Z, Qin, X, Zhang, L (2015) Comparison of fruits of forsythia suspensa at two different maturation stages by NMR-based metabolomics. Molecules 20:10065-10081.

Jiménez, C, Riguera, R (1994) Phenylethanoid glycosides in plants: Structure and biological activity. Nat. Prod. Rep. 11:591-606.

Jisaka, M, Kawanaka, M, Sugiyama, H, Takegawa, K, Huffman, MA, Ohigashi, H, Koshimizu, K (1992) Antischistosomal activities of sesquiterpene lactones and steroid glucosides from vernonia amygdalina, possibly used by wild chimpanzees against parasite-related diseases. Biosci. Biotechnol. Biochem. 56:845-846.

Kamenetsky, R, Shafir, IL, Zemah, H, Barzilay, A, Rabinowitch, H (2004) Environmental control of garlic growth and florogenesis. J. Am. Soc. Hort. Sci. 129:144-151.

Kamenetsky, R, Zaccai, M, Flaishman, MA (2012) Florogenesis. In: Kamenetsky, R, Okubo, H (eds) . CRC Press, , pp. 197.

Kato, A, Adachi, I, Miyauchi, M, Ikeda, K, Komae, T, Kizu, H, Kameda, Y, Watson, AA, Nash, RJ, Wormald, MR, Fleet, GWJ, Asano, N (1999) Polyhydroxylated pyrrolidine and pyrrolizidine alkaloids from hyacinthoides non-scripta and scilla campanulata. Carbohydr. Res. 316:95-103. doi: 10.1016/S0008-6215(99)00043-9.

Kerem, Z, German-Shashoua, H, Yarden, O (2005) Microwave-assisted extraction of bioactive saponins from chickpea (cicer arietinum L). J. Sci. Food Agric. 85:406-412.

Kesselmeier, J, Urban, B (1983) Subcellular localization of saponins in green and etiolated leaves and green protoplasts of oat (avena sativa L.). Protoplasma 114:133-140.

Kettaneh, N, Berglund, A, Wold, S (2005) PCA and PLS with very large data sets. Comput. Stat. Data Anal. 48:69-85.

Khoddami, A, Wilkes, MA, Roberts, TH (2013) Techniques for analysis of plant phenolic compounds. Molecules 18:2328-2375.

Knight, GH (1964) Some factors affecting the distribution of endymion nonscriptus (L.) garcke in warwickshire woods. J. Ecol. 52:405-421.

Kondo, T, Yoshida, K, Nakagawa, A, Kawai, T, Tamura, H, Goto, T (1992) Structural basis of blue-colour development in flower petals from commelina communis.

Koops, AJ, Jonker, HH (1996) Purification and characterization of the enzymes of fructan biosynthesis in tubers of helianthus tuberosus colombia (II. purification of sucrose:Sucrose 1-fructosyltransferase and reconstitution of fructan synthesis in vitro with purified sucrose:Sucrose 1-fructosyltransferase and fructan:Fructan 1-fructosyltransferase). Plant Physiol. 110:1167-1175. doi: 110/4/1167 [pii].

Krygier, K, Sosulski, F, Hogge, L (1982) Free, esterified, and insoluble-bound phenolic acids. 1. extraction and purification procedure. J. Agric. Food Chem. 30:330-334.

Kuroda, M, Mimaki, Y, Ori, K, Sakagami, H, Sashida, Y (2004) 27-norlanostane glycosides from the bulbs of muscari p aradoxum. J. Nat. Prod. 67:2099-2103.

Kuwatsuka, S, Shindo, H (1973) Behavior of phenolic substances in the decaying process of plants: I. identification and quantitative determination of phenolic acids in rice straw and its decayed product by gas chromatography. Soil Sci. Plant Nutr. 19:219-227.

Lacaille-Dubois, M, Wagner, H (1996) A review of the biological and pharmacological activities of saponins. Phytomedicine 2:363-386.

Lapointe, L (2001) How phenology influences physiology in deciduous forest spring ephemerals. Physiol. Plantarum 113:151-157.

Larsson, S, Wirén, A, Lundgren, L, Ericsson, T (1986) Effects of light and nutrient stress on leaf phenolic chemistry in salix dasyclados and susceptibility to galerucella lineola (coleoptera). Oikos 205-210.

Le Roy, K, Vergauwen, R, Cammaer, V, Yoshida, M, Kawakami, A, Van Laere, A, Van den Ende, W (2007) Fructan 1-exohydrolase is associated with flower opening in campanula rapunculoides. Functional Plant Biology 34:972-983.

Lee, HS, ROUSEFF, RL, NAGY, S (1986) HPLC determination of furfural and 5-Hydroxymethylfurfural in citrus juices. J. Food Sci. 51:1075-1076.

Lee, S, Chun, H, Lee, C, Min, B, Lee, E, Kho, Y (2002) Eucosterol oligoglycosides isolated from scilla scilloides and their anti-tumor activity. Chemical and Pharmaceutical Bulletin 50:1245-1249.

Li, H, Wong, C, Cheng, K, Chen, F (2008) Antioxidant properties in vitro and total phenolic contents in methanol extracts from medicinal plants. LWT-Food Science and Technology 41:385-390.

Li, Q, Van den Heuvel, H, Dillen, L, Claeys, M (1992) Differentiation of 6-C-and 8-C-glycosidic flavonoids by positive ion fast atom bombardment and tandem mass spectrometry. Biol. Mass Spectrom. 21:213-221.

Li, Z, Wang, Q, Ruan, X, Pan, C, Jiang, D (2010) Phenolics and plant allelopathy. Molecules 15:8933-8952.

Lin, S, Mullin, CA (1999) Lipid, polyamide, and flavonol phagostimulants for adult western corn rootworm from sunflower (helianthus annuus L.) pollen. J. Agric. Food Chem. 47:1223-1229.

Liu, J, Waterhouse, AL, Chatterton, NJ (1991) Proton and carbon chemical-shift assignments for 6-kestose and neokestose from two-dimensional nmr measurements. Carbohydr. Res. 217:43-49.

Livingston III, DP, Hincha, DK, Heyer, AG (2009) Fructan and its relationship to abiotic stress tolerance in plants. Cellular and Molecular Life Sciences 66:2007-2023.

Livingston, DP, Chatterton, NJ, Harrison, PA (1993) Structure and quantity of fructan oligomers in oat (avena spp.). New Phytol. 123:725-734.

Livingston, DP, Henson, CA (1998) Apoplastic sugars, fructans, fructan exohydrolase, and invertase in winter oat: Responses to second-phase cold hardening. Plant Physiol. 116:403-408.

Ma, Y, Li, Q, Van den Heuvel, H, Claeys, M (1997) Characterization of flavone and flavonol aglycones by collision-induced dissociation tandem mass spectrometry. Rapid Communications in Mass Spectrometry 11:1357-1364.

Mackie, A, Singh, H, Owen, J (1977) Studies on the distribution, biosynthesis and function of steroidal saponins in echinoderms. Comparative Biochemistry and Physiology Part B: Comparative Biochemistry 56:9-14.

Maghrabya, AS, Hamed, MAA, Alyb, HF, Alib, SA (2010) The antischistosomal activity of fasciola gigantica and schistosoma mansoni eggs is influenced by saponin extracted from atriplex nummularia. Journal of American Science 6:.

Mahato, S, Ganguly, A, Sahu, N (1982) Steroid saponins. Phytochemistry 21:959-978.

Mahmood, A (2013) Minor componenets in vegetable oils. Master dissertation. School of Chemistry, Bangor University.

Man, S, Gao, W, Zhang, Y, Huang, L, Liu, C (2010) Chemical study and medical application of saponins as anti-cancer agents. Fitoterapia 81:703-714.

Mandal, SM, Chakraborty, D, Dey, S (2010) Phenolic acids act as signaling molecules in plant-microbe symbioses. Plant Signaling & Behavior 5:359-368.

March, RE, Lewars, EG, Stadey, CJ, Miao, X, Zhao, X, Metcalfe, CD (2006) A comparison of flavonoid glycosides by electrospray tandem mass spectrometry. International Journal of Mass Spectrometry 248:61-85.

Markham, KR (1989) Flavones, flavonols and their glycosides. In: Dey, PM, Harborne, JB (eds) Methods in Plant Biochemistry, Volume 1, Plant Phenolics, pp. 197.

Markham, KR, Ryan, KG, Bloor, SJ, Mitchell, KA (1998) An increase in the luteolin: Apigenin ratio in marchantia polymorpha on UV-B enhancement. Phytochemistry 48:791-794.

Marston, A, Hostettmann, K (2006) Separation and quantification of flavonoids. In: Andersen, Ø, Markham, K (eds) Flavonoids: Chemistry, Biochemistry and Applications. CRC Press LLC, , pp. 1.

Marx, SP, JOSEF, N, Frehner, M (1997a) Hydrolysis of fructan in grasses: A β-(2-6)-linkage specific fructan-β-fructosidase from stubble of lolium perenne. New Phytol. 135:279-290.

Marx, SP, NÖSBERGER, J, Frehner, M (1997b) Seasonal variation of fructan-β-fructosidase (FEH) activity and characterization of a β-(2-1)-linkage specific FEH from tubers of jerusalem artichoke (helianthus tuberosus). New Phytol. 135:267-277.

Massiot, G, Lavaud, C (1995) Structural elucidation of saponins. In: Atta-ur-Rahman (ed) Studies in Natural Product Chemistry, Volume 15, Structure and Chemistry (Part C). Elsevier Science, The Netherlands, pp. 187.

Matern, U, Reichenbach, C, Heller, W (1986) Efficient uptake of flavonoids into parsley (petroselinum hortense) vacuoles requires acylated glycosides. Planta 167:183-189.

McClure, JW (1979) The physiology of phenolic compounds in plants. In: Swain, T, Harborne, JB, Van Sumere, C (eds) Biochemistry of plant phenolics. Springer, , pp. 525.

Meier, H, Reid, J (1982) Reserve polysaccharides other than starch in higher plants. In: Anonymous Plant Carbohydrates I. Springer, , pp. 418.

Melek, FR, Tadros, MM, Yousif, F, Selim, M, Hassan, MH (2012) Screening of marine extracts for schistosomicidal activity in vitro. isolation of the triterpene glycosides echinosides A and B with potential activity from the sea cucumbers actinopyga echinites and holothuria polii. Pharm. Biol. 50:490-496.

Merryweather, J, Fitter, A (1995a) Arbuscular mycorrhiza and phosphorus as controlling factors in the life history of hyacinthoides non-scripta (L.) chouard ex rothm. New Phytol. 129:629-636.

Merryweather, J, Fitter, A (1995b) Phosphorus and carbon budgets: Mycorrhizal contribution in hyacinthoides non-scripta (L.) chouard ex rothm. under natural conditions. New Phytol. 619-627.

Meyer, VR (2013) Practical high-performance liquid chromatography. John Wiley & Sons, .

Milgate, J, Roberts, D (1995) The nutritional & biological significance of saponins. Nutr. Res. 15:1223-1249.

Miller, R, Owens, SJ, Rørslett, B (2011) Plants and colour: Flowers and pollination. Optics & Laser Technology 43:282-294.

MOJŠIŁOVÊ, G, Kuchta, M (2001) Dietary flavonoids and risk of coronary heart disease. Physiol. Res. 50:529-535.

Molnár-Perl, I (2000) Role of chromatography in the analysis of sugars, carboxylic acids and amino acids in food. Journal of Chromatography A 891:1-32. doi: 10.1016/S0021-9673(00)00598-7.

Mulholland, DA, Schwikkard, SL, Crouch, NR (2013) The chemistry and biological activity of the hyacinthaceae. Nat. Prod. Rep. 30:1165-1210.

Müller, V, Albert, A, Winkler, JB, Lankes, C, Noga, G, Hunsche, M (2013) Ecologically relevant UV-B dose combined with high PAR intensity distinctly affect plant growth and accumulation of secondary metabolites in leaves of centella asiatica L. urban. Journal of Photochemistry and Photobiology B: Biology 127:161-169.

Narwal, SS, Sampietro, DA (2009) Allelopathy and allelochemicals. In: Sampietro, DA, Catalan, CA, Vittuone, MA (eds) Isolation, Identification and Characterization of Allelochemicals/Natural Products. Science Publishers, USA, pp. 1.

Nash, RJ, Kato, A, Yu, C, Fleet, GW (2011) Iminosugars as therapeutic agents: Recent advances and promising trends. Future Medicinal Chemistry 3:1513-1521.

Ndakidemi, PA, Dakora, FD (2003) Legume seed flavonoids and nitrogenous metabolites as signals and protectants in early seedling development. Functional Plant Biology 30:729-745.

Neuwinger, HD (2004) Plants used for poison fishing in tropical africa. Toxicon 44:417-430.

Nuutila, A, Kammiovirta, K, Oksman-Caldentey, K (2002) Comparison of methods for the hydrolysis of flavonoids and phenolic acids from onion and spinach for HPLC analysis. Food Chem. 76:519-525.

Ohyama, T, Ikarashi, T, Baba, A (1985) Determination of the structure of oligofructan in the tulip bulb. Soil Sci. Plant Nutr. 31:293-298.

Okubo, H (2012) Dormancy. In: Kamenetsky, R, Okubo, H (eds) . CRC Press, , pp. 233.

Oleszek, W, Bialy, Z (2006) Chromatographic determination of plant saponins—an update (2002–2005). Journal of Chromatography A 1112:78-91.

Oleszek, W (2002) Chromatographic determination of plant saponins. Journal of Chromatography A 967:147-162.

Oleszek, W, Hoagland, R, Zablotowicz, R (1999) Ecological significance of plant saponins. In: Dakshini, K, Foy, C (eds) Principles and practices in plant ecology: allelochemical interactions. CRC press, , pp. 451.

Oleszek, W (1993) Allelopathic potentials of alfalfa (medicago sativa) saponins: Their relation to antifungal and hemolytic activities. J. Chem. Ecol. 19:1063-1074.

Oliveira, I, Sousa, A, Ferreira, IC, Bento, A, Estevinho, L, Pereira, JA (2008) Total phenols, antioxidant potential and antimicrobial activity of walnut (juglans regia L.) green husks. Food and Chemical Toxicology 46:2326-2331.

Oren-Shamir, M, Shaked-Sachray, L, Nissim-Levi, A, Ecker, R (1999) Anthocyanin pigmentation of lisianthus flower petals. Plant Science 140:81-86. doi: 10.1016/S0168-9452(98)00198-8.

Ori, K, Koroda, M, Mimaki, Y, Sakagami, H, Sashida, Y (2003) Lanosterol and tetranorlanosterol glycosides from the bulbs of muscari paradoxum. Phytochemistry 64:1351-1359.

Orthen, B (2001) Sprouting of the fructan-and starch-storing geophyte lachenalia minima: Effects on carbohydrate and water content within the bulbs. Physiol. Plantarum 113:308-314.

Orthen, B, Wehrmeyer, A (2004) Seasonal dynamics of non-structural carbohydrates in bulbs and shoots of the geophyte galanthus nivalis. Physiol. Plantarum 120:529-536.

Osbourn, A (1996) Saponins and plant defence—a soap story. Trends Plant Sci. 1:4-9.

Pan, M, Lai, C, Ho, C (2010) Anti-inflammatory activity of natural dietary flavonoids. Food & Function 1:15-31.

Parrilli, M, Lanzetta, R, Adinolfi, M, Mangoni, L (1980) Glycosides from m uscari comosum—III: The structure of further authentic aglycones. Tetrahedron 36:3591-3596.

Pelzer, LE, Guardia, T, Juarez, AO, Guerreiro, E (1998) Acute and chronic antiinflammatory effects of plant flavonoids. Il Farmaco 53:421-424.

Phillips, D, Tsai, S (1992) Flavonoids as plant signals to rhizosphere microbes. Mycorrhiza 1:55-58.

Pieles, U, Zurcher, W, Schar, M, Moser, HE (1993) Matrix-assisted laser desorption ionization time-of-flight mass spectrometry: A powerful tool for the mass and sequence analysis of natural and modified oligonucleotides. Nucleic Acids Res. 21:3191-3196.

Pollock, C (1986) Tansley review no. 5. fructans and the metabolism of sucrose in vascular plants. New Phytol. 1-24.

Pollock, C (1984) Sucrose accumulation and the initiation of fructan biosynthesis in lolium temulentum L. New Phytol. 96:527-534.

Pollock, C (1982) Patterns of turnover of fructans in leaves of dactylis glomerata L. New Phytol. 645-650.

Pollock, C, Chatterton, N (1988) Fructans. In: Preiss, J (ed) The Biochemistry of Plants, A Comprehensive Treatise. Academic Press, Inc.(London) Ltd., , pp. 109.

Pollock, C, Lloyd, E (1994) The metabolism of fructans during seed development and germination in onion (allium cepa L.). New Phytol. 128:601-605.

Porretta, S, Sandei, L (1991) Determination of 5-(hydroxymethyl)-2-furfural (HMF) in tomato products: Proposal of a rapid HPLC method and its comparison with the colorimetric method. Food Chem. 39:51-57.

Poulton, JE (1981) Transmethylation and demethylation reactions in the metabolism of secondary plant products. In: Conn, EE (ed) The Biochemistry of Plants: A Comprehensive Treatise, Volume 7, Secondary Plant Products. Academic Press New York, , pp. 667.

Radine, C (2015) Chemical composition of unexplored plant seed oils. Master dissertation. Rheinische Friedrich-Wilhelms-Universitat Bonn.

Rao, JR, Cooper, JE (1994) Rhizobia catabolize nod gene-inducing flavonoids via C-ring fission mechanisms. J. Bacteriol. 176:5409-5413.

Raskin, I (1992) Role of salicylic acid in plants. Annual Review of Plant Biology 43:439-463.

Rehwald, A, Meier, B, Sticher, O (1994) Qualitative and quantitative reversed-phase high-performance liquid chromatography of flavonoids in crataegus leaves and flowers. Journal of Chromatography A 677:25-33.

Rix, M (2004) PLATE 481. HYACINTHOIDES NON-SCRIPTA HYACINTHACEAE. Curtis's Botanical Magazine 21:20-25.

Robards, K (2003) Strategies for the determination of bioactive phenols in plants, fruit and vegetables. Journal of Chromatography A 1000:657-691.

Rocher, Y (1969) Method of Extracting Saponins .

Roessner, U, Beckles, DM (2009) Metabolite measurements. In: Schwender, J (ed) Plant metabolic networks. Springer, , pp. 39.

Roessner, U, Bowne, J (2009) What is metabolomics all about? BioTechniques 46:363.

Rosnitschek-Schimmel, I (1983) Biomass and nitrogen partitioning in a perennial and an annual nitrophilic species of urtica. Zeitschrift Für Pflanzenphysiologie 109:215-225.

Rug, M, Ruppel, A (2000) Toxic activities of the plant jatropha curcas against intermediate snail hosts and larvae of schistosomes. Tropical Medicine & International Health 5:423-430.

Ruiz-Matute, AI, Hernández-Hernández, O, Rodríguez-Sánchez, S, Sanz, ML, Martínez-Castro, I (2011) Derivatization of carbohydrates for GC and GC–MS analyses. Journal of Chromatography B 879:1226-1240. doi: http://0-dx.doi.org.unicat.bangor.ac.uk/10.1016/j.jchromb.2010.11.013.

Saimaru, H, Orihara, Y (2010) Biosynthesis of acteoside in cultured cells of olea europaea. Journal of Natural Medicines 64:139-145.

Sakai, A, Larcher, W (1987) Frost survival of plants. responses and adaptation to freezing stress. Springer-Verlag, .

Sakushima, A, Nishibe, S, Takeda, T, Ogihara, Y (1988) Positive and negative ion mass spectra of flavonoid glycosides by fast atom bombardment. Journal of the Mass Spectrometry Society of Japan 36:71-80.

Saleem, M, Nazir, M, Ali, MS, Hussain, H, Lee, YS, Riaz, N, Jabbar, A (2010) Antimicrobial natural products: An update on future antibiotic drug candidates. Nat. Prod. Rep. 27:238-254.

Sardans, J, Penuelas, J, Rivas-Ubach, A (2011) Ecological metabolomics: Overview of current developments and future challenges. Chemoecology 21:191-225.

Schmitz-Hoerner, R, Weissenböck, G (2003) Contribution of phenolic compounds to the UV-B screening capacity of developing barley primary leaves in relation to DNA damage and repair under elevated UV-B levels. Phytochemistry 64:243-255.

Schulze, E (1982) Plant life forms and their carbon, water and nutrient relations. In: Anonymous Physiological plant ecology II. Springer, , pp. 615.

Sherwin, HW, Farrant, JM (1998) Protection mechanisms against excess light in the resurrection plants craterostigma wilmsii and xerophyta viscosa. Plant Growth Regulation 24:203-210.

Shiomi, N (1978) Isolation and identification of 1-kestose and neokestose from onion bulbs. Journal of the Faculty of Agriculture, Hokkaido University = 北海道大學農學部紀 58:548-556.

Shiomi, N (1989) Properties of fructosyltransferases involved in the synthesis of fructan in liliaceous plants. J. Plant Physiol. 134:151-155.

Shiomi, N (1981) Two novel hexasaccharides from the roots of asparagus officinalis. Phytochemistry 20:2581-2583.

Shirley, BW (1996) Flavonoid biosynthesis:'new'functions for an 'old'pathway. Trends Plant Sci. 1:377-382.

Shirley, BW (1998) Flavonoids in seeds and grains: Physiological function, agronomic importance and the genetics of biosynthesis. Seed Science Research 8:415-422.

Shukla, S, Gupta, S (2010) Apigenin: A promising molecule for cancer prevention. Pharm. Res. 27:962-978.

Simões, C, Amoros, M, Girre, L (1999) Mechanism of antiviral activity of triterpenoid saponins. Phytotherapy Research 13:323-328.

Smith, D, Paulsen, GM, Raguse, CA (1964) Extraction of total available carbohydrates from grass and legume tissue. Plant Physiol. 39:960-962.

Smithers, S, HACKETT, F, ALI, PO, Simpson, A (1989) Protective immunization of mice against schistosoma mansoni with purified adult worm surface membranes. Parasite Immunol. 11:301-318.

Solovchenko, A (2010) Photoprotection in plants: Optical screening-based mechanisms. Springer Science & Business Media, .

Sparg, S, Light, M, Van Staden, J (2004) Biological activities and distribution of plant saponins. J. Ethnopharmacol. 94:219-243.

Stafford, HA (1990a) Genral aspects of chemistry and metabolism of flavonoids. In: Anonymous Flavonoid metabolism. CRC press, , pp. 1.

Stafford, HA (1990b) Secondary changes: Recycling and degradation of flavonoids. In: Anonymous Flavonoid Metabolism. CRC press, , pp. 171.

Stahl, B, Linos, A, Karas, M, Hillenkamp, F, Steup, M (1997) Analysis of fructans from higher plants by matrix-assisted laser desorption/ionization mass spectrometry. Anal. Biochem. 246:195-204.

Stalikas, CD (2007) Extraction, separation, and detection methods for phenolic acids and flavonoids. Journal of Separation Science 30:3268-3295.

Steele, JM, Ratliff, RD, Ritenour, GL (1984) Seasonal variation in total nonstructural carbohydrate levels in nebraska sedge. J. Range Manage. 465-467.

Švehlíková, V, Bennett, RN, Mellon, FA, Needs, PW, Piacente, S, Kroon, PA, Bao, Y (2004) Isolation, identification and stability of acylated derivatives of apigenin 7-O-glucoside from chamomile (chamomilla recutita [L.] rauschert). Phytochemistry 65:2323-2332.

Sweeley, CC, Bentley, R, Makita, M, Wells, W (1963) Gas-liquid chromatography of trimethylsilyl derivatives of sugars and related substances. J. Am. Chem. Soc. 85:2497-2507.

Swislocka, R, Kowczyk-Sadowy, M, Kalinowska, M, Lewandowski, W (2012) Spectroscopic (FT-IR, FT-raman, 1 H and 13 C NMR) and theoretical studies of p-coumaric acid and alkali metal p-coumarates. Journal of Spectroscopy 27:35-48.

Szakiel, A, Pączkowski, C, Henry, M (2011a) Influence of environmental abiotic factors on the content of saponins in plants. Phytochemistry Reviews 10:471-491.

Szakiel, A, Pączkowski, C, Henry, M (2011b) Influence of environmental biotic factors on the content of saponins in plants. Phytochemistry Reviews 10:493-502.

Tahvanainen, J, Julkunen-Tiitto, R, Kettunen, J (1985) Phenolic glycosides govern the food selection pattern of willow feeding leaf beetles. Oecologia 67:52-56.

Takeda, K, Harborne, JB, Self, R (1986) Identification of malonated anthocyanins in the liliaceae and labiatae. Phytochemistry 25:2191-2192. doi: 10.1016/0031-9422(86)80089-9.

Tapondjou, LA, Ponou, KB, Teponno, RB, Mbiantcha, M, Djoukeng, JD, Nguelefack, TB, Watcho, P, Cadenas, AG, Park, H (2008) In vivo anti-inflammatory effect of a new steroidal saponin, mannioside A, and its derivatives isolated from dracaena mannii. Arch. Pharm. Res. 31:653-658.

Tarkowski, ŁP, Van den Ende, W (2015) Cold tolerance triggered by soluble sugars: A multifaceted countermeasure. Frontiers in Plant Science 6:.

Tawaha, K, Alali, FQ, Gharaibeh, M, Mohammad, M, El-Elimat, T (2007) Antioxidant activity and total phenolic content of selected jordanian plant species. Food Chem. 104:1372-1378.

Tawfike, AF, Viegelmann, C, Edrada-Ebel, R (2013) Metabolomics and dereplication strategies in natural products. In: Anonymous Metabolomics Tools for Natural Product Discovery. Springer, , pp. 227.

Teklemariam, T, Blake, TJ (2003) Effects of UVB preconditioning on heat tolerance of cucumber (cucumis sativus L.). Environ. Exp. Bot. 50:169-182.

Thompson, J, Jones, J (1964) The glucomannan of bluebell seed (scylla nonscripta L.). Canadian Journal of Chemistry 42:1088-1091.

THOMPSON, PA, COX, SA (1978) Germination of the bluebell (hyacinthoides non-scripta (L.) chouard) in relation to its distribution and habitat. Annals of Botany 42:51-62.

Thompson, WR, Meinwald, J, Aneshansley, D, Eisner, T (1972) Flavonols: Pigments responsible for ultraviolet absorption in nectar guide of flower. Science 177:528-530.

Thoss, V, Murphy, PJ, Marriott, R, Wilson, T (2012) Triacylglycerol composition of british bluebell (hyacinthoides non-scripta) seed oil. Rsc Advances 2:5314-5322. doi: 10.1039/c2ra20090b.

Treutter, D (2006) Significance of flavonoids in plant resistance: A review. Environmental Chemistry Letters 4:147-157.

Valluru, R, Lammens, W, Claupein, W, Van den Ende, W (2008) Freezing tolerance by vesicle-mediated fructan transport. Trends Plant Sci. 13:409-414.

Valluru, R, Van den Ende, W (2008) Plant fructans in stress environments: Emerging concepts and future prospects. Journal of Experimental Botany 59:2905-2916. doi: 10.1093/jxb/ern164.

Vereyken, IJ, Chupin, V, Demel, RA, Smeekens, SC, De Kruijff, B (2001) Fructans insert between the headgroups of phospholipids. Biochimica Et Biophysica Acta (BBA)-Biomembranes 1510:307-320.

Vergauwen, R, Van den Ende, W, Van Laere, A (2000) The role of fructan in flowering of campanula rapunculoides. J. Exp. Bot. 51:1261-1266.

Vermerris, W, Nicholson, R (2007) Phenolic compound biochemistry. Springer Science & Business Media, .

Vierheilig, H, Bago, B, Albrecht, C, Poulin, M, Piché, Y (1998) Flavonoids and arbuscular-mycorrhizal fungi. In: Anonymous Flavonoids in the living system. Springer, , pp. 9.

Vijn, I, Van Dijken, A, Sprenger, N, Van Dun, K, Weisbeek, P, Wiemken, A, Smeekens, S (1997) Fructan of the inulin neoseries is synthesized in transgenic chicory plants (cichorium intybus L.) harbouring onion (allium cepa L.) fructan: Fructan 6G-fructosyltransferase. The Plant Journal 11:387-398.

Vijn, I, Smeekens, S (1999) Fructan: More than a reserve carbohydrate? Plant Physiol. 120:351-360.

Villas-Boas, SG, Nielsen, J, Smedsgaard, J, Hansen, MA, Roessner-Tunali, U (2007) Metabolome analysis: An introduction. John Wiley & Sons, .

Vincken, J, Heng, L, de Groot, A, Gruppen, H (2007) Saponins, classification and occurrence in the plant kingdom. Phytochemistry 68:275-297.

Vukics, V, Guttman, A (2010) Structural characterization of flavonoid glycosides by multi-stage mass spectrometry. Mass Spectrom. Rev. 29:1-16.

Vukics, V, Ringer, T, Kery, A, Bonn, GK, Guttman, A (2008) Analysis of heartsease (viola tricolor L.) flavonoid glycosides by micro-liquid chromatography coupled to multistage mass spectrometry. Journal of Chromatography A 1206:11-20.

Wagner, W, Wiemken, A, Matile, P (1986) Regulation of fructan metabolism in leaves of barley (hordeum vulgare L. cv gerbel). Plant Physiol. 81:444-447.

Wang, S, Ridsdill-Smith, T, Ghisalberti, E (1998) Role of isoflavonoids in resistance of subterranean clover trifoliates to the redlegged earth mite halotydeus destructor. J. Chem. Ecol. 24:2089-2100.

Watson, A, Nash, R, Wormald, M, Harvey, D, Dealler, S, Lees, E, Asano, N, Kizu, H, Kato, A, Griffiths, R, Cairns, A, Fleet, G (1997) Glycosidase-inhibiting pyrrolidine alkaloids from hyacinthoides non-scripta. Phytochemistry 46:255-259. doi: 10.1016/S0031-9422(97)00282-3.

Watson, AA, Fleet, GWJ, Asano, N, Molyneux, RJ, Nash, RJ (2001) Polyhydroxylated alkaloids — natural occurrence and therapeutic applications. Phytochemistry 56:265-295. doi: 10.1016/S0031-9422(00)00451-9.

Weinmann, H (1947) Determination of total available carbohydrates in plants. Plant Physiol. 22:279-290.

WILSON, JY (1959) Verification of the breeding system in the bluebell endymion nonscriptus (L.) garcke Annals of Botany 23:201-203.

Wishart, DS, Knox, C, Guo, AC, Eisner, R, Young, N, Gautam, B, Hau, DD, Psychogios, N, Dong, E, Bouatra, S, Mandal, R, Sinelnikov, I, Xia, J, Jia, L, Cruz, JA, Lim, E, Sobsey, CA, Shrivastava, S, Huang, P, Liu, P, Fang, L, Peng, J, Fradette, R, Cheng, D, Tzur, D, Clements, M, Lewis, A, De Souza, A, Zuniga, A, Dawe, M, Xiong, Y, Clive, D, Greiner, R, Nazyrova, A, Shaykhutdinov, R, Li, L, Vogel, HJ, Forsythe, I (2009) HMDB: A knowledgebase for the human metabolome. Nucleic Acids Res. 37:D603-10. doi: 10.1093/nar/gkn810 [doi].

Wold, S, Sjöström, M, Eriksson, L (2001) PLS-regression: A basic tool of chemometrics. Chemometrics Intellig. Lab. Syst. 58:109-130.

Wollenweber, E, Harborne, J, Mabry, T (1982) The flavonoids: Advances in research. By Harbone JB, Mabry TJ, Chapman & Hall, London 240.

Worley, B, Powers, R (2013) Multivariate analysis in metabolomics. Current Metabolomics 1:92-107.

Xie, ZP, Staehelin, C, Vierheilig, H, Wiemken, A, Jabbouri, S, Broughton, WJ, Vogeli-Lange, R, Boller, T (1995) Rhizobial nodulation factors stimulate mycorrhizal colonization of nodulating and nonnodulating soybeans. Plant Physiol. 108:1519-1525. doi: 108/4/1519 [pii].

Yoshida, K, Mori, M, Kondo, T (2009) Blue flower color development by anthocyanins: From chemical structure to cell physiology. Nat. Prod. Rep. 26:884-915.

Yuliana, ND, Khatib, A, Choi, YH, Verpoorte, R (2011) Metabolomics for bioactivity assessment of natural products. Phytotherapy Research 25:157-169.

Zappala, M, Fallico, B, Arena, E, Verzera, A (2005) Methods for the determination of HMF in honey: A comparison. Food Control 16:273-277.

Zenobi, R, Knochenmuss, R (1998) Ion formation in MALDI mass spectrometry. Mass Spectrom. Rev. 17:337-366.

Zhang, J, Cao, Y, Xu, Z, Sun, H, An, M, Yan, L, Chen, H, Gao, P, Wang, Y, Jia, X (2005) In vitro and in vivo antifungal activities of the eight steroid saponins from tribulus terrestris L. with potent activity against fluconazole-resistant fungal. Biological and Pharmaceutical Bulletin 28:2211-2215.

Zucker, WV (1982) How aphids choose leaves: The roles of phenolics in host selection by a galling aphid. Ecology 972-981.

Appendices

1. NMR spectra of 1-kestose

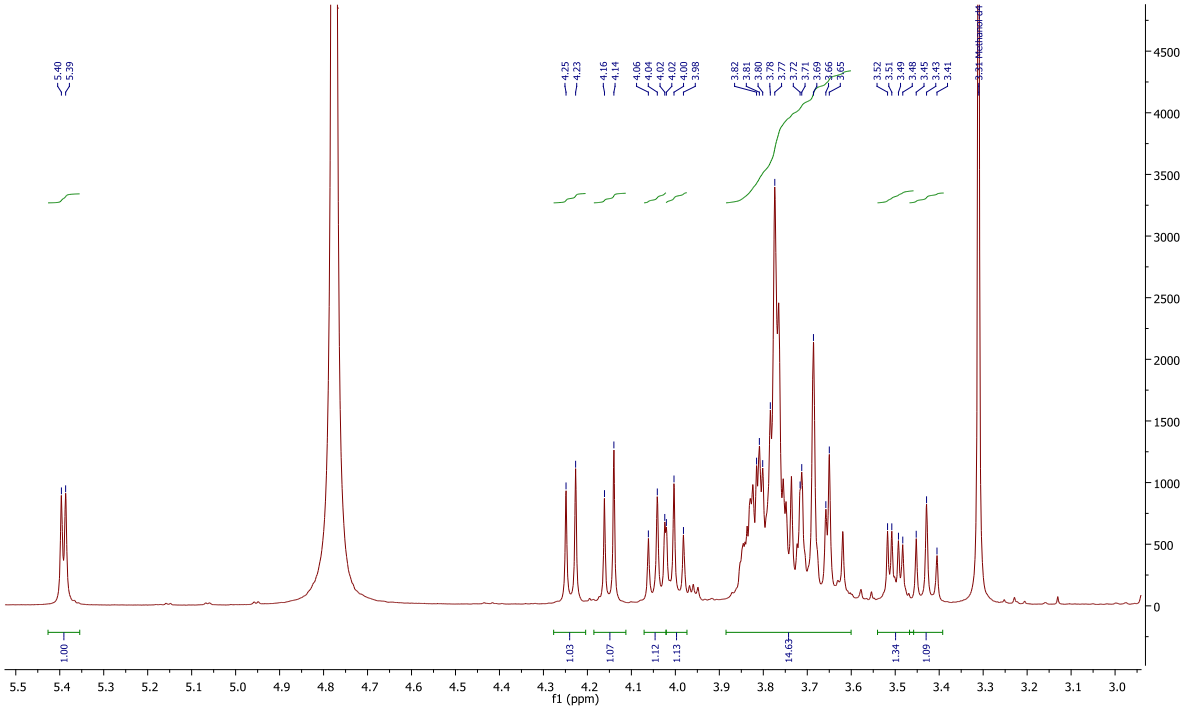

Figure 109 ^{1}H NMR of 1-kestose isolated from bluebell bulbs in D_2O.

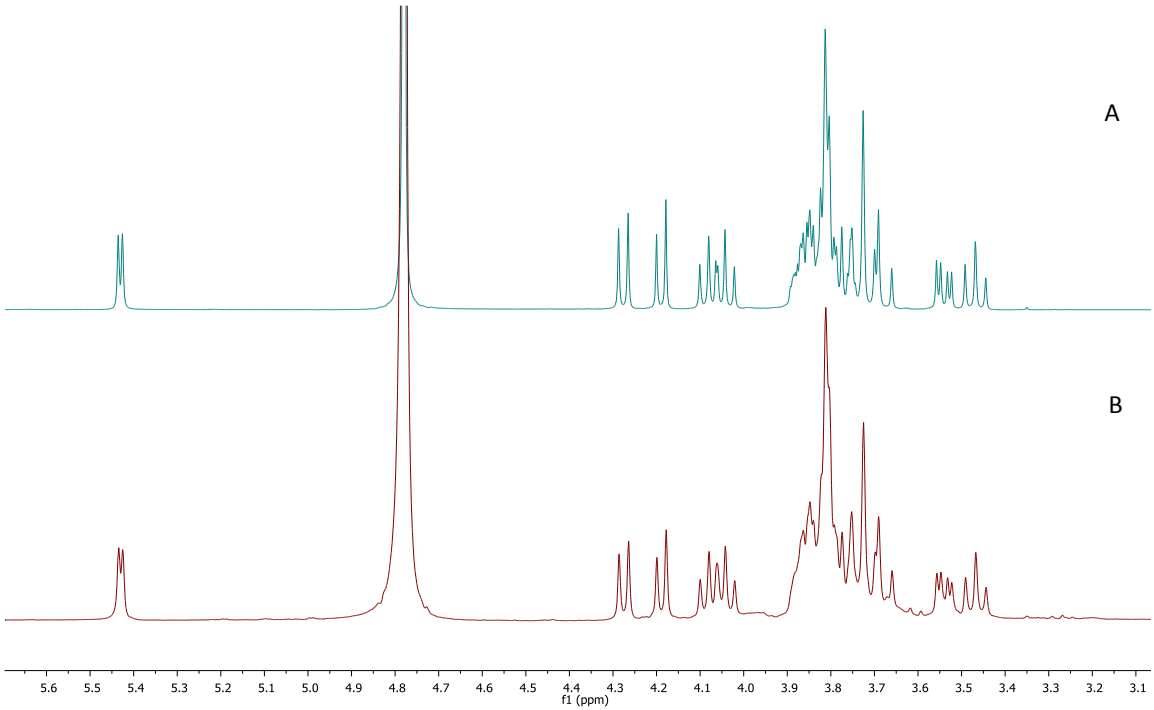

Figure 110 Comparison between ^{1}H NMR spectra of A, standard 1-kestose and B, 1-kestose isolated from bluebell bulbs in D_2O.

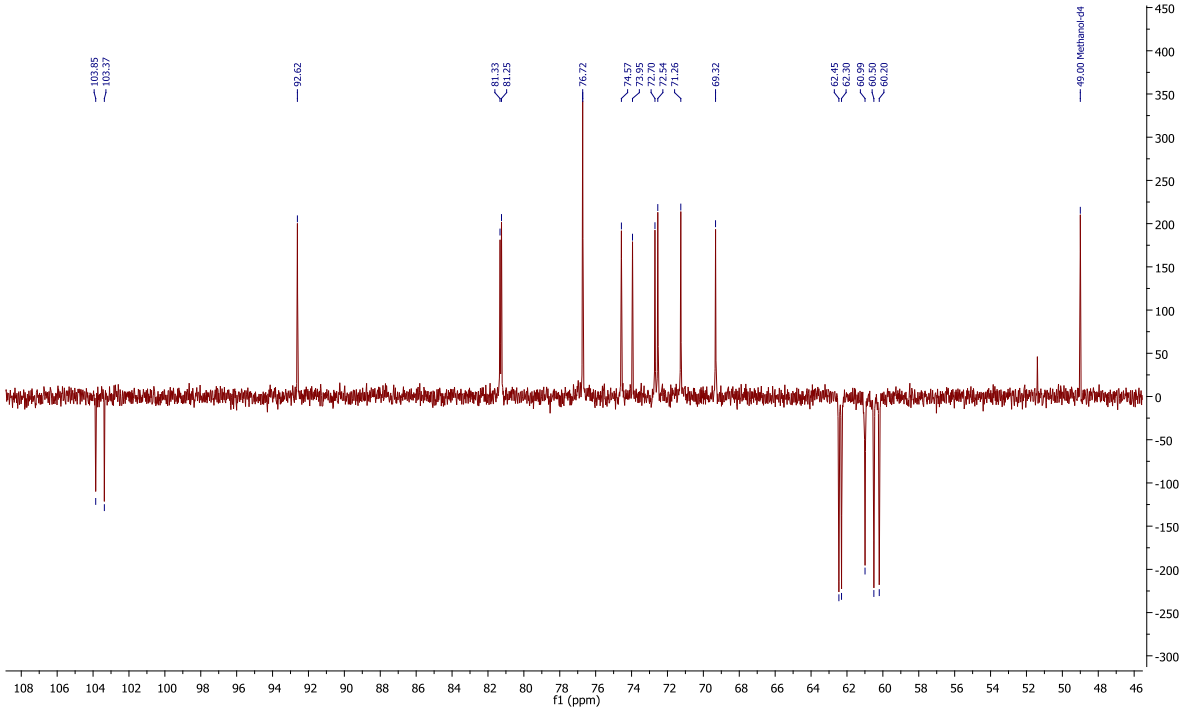

Figure 111 DEPTQ of 1-kestose isolated from bluebell bulbs in D_2O.

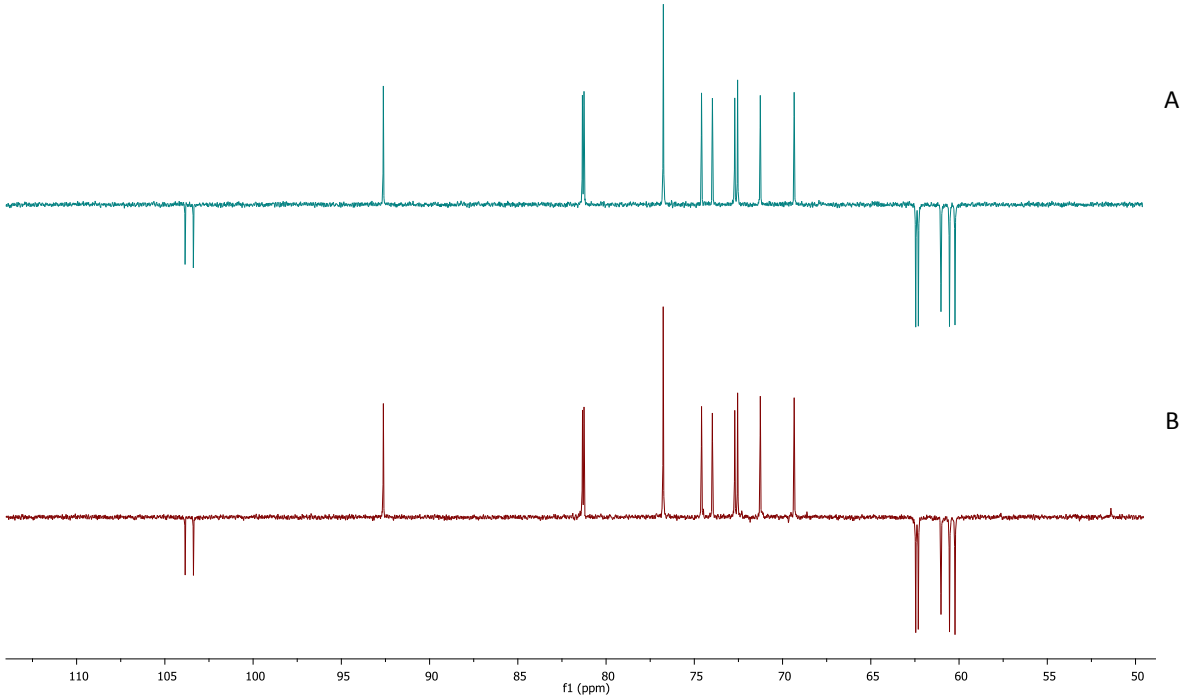

Figure 112 Comparison between DEPTQ spectra of A, standard 1-kestose and B, 1-kestose isolated from bluebell bulbs in D_2O.

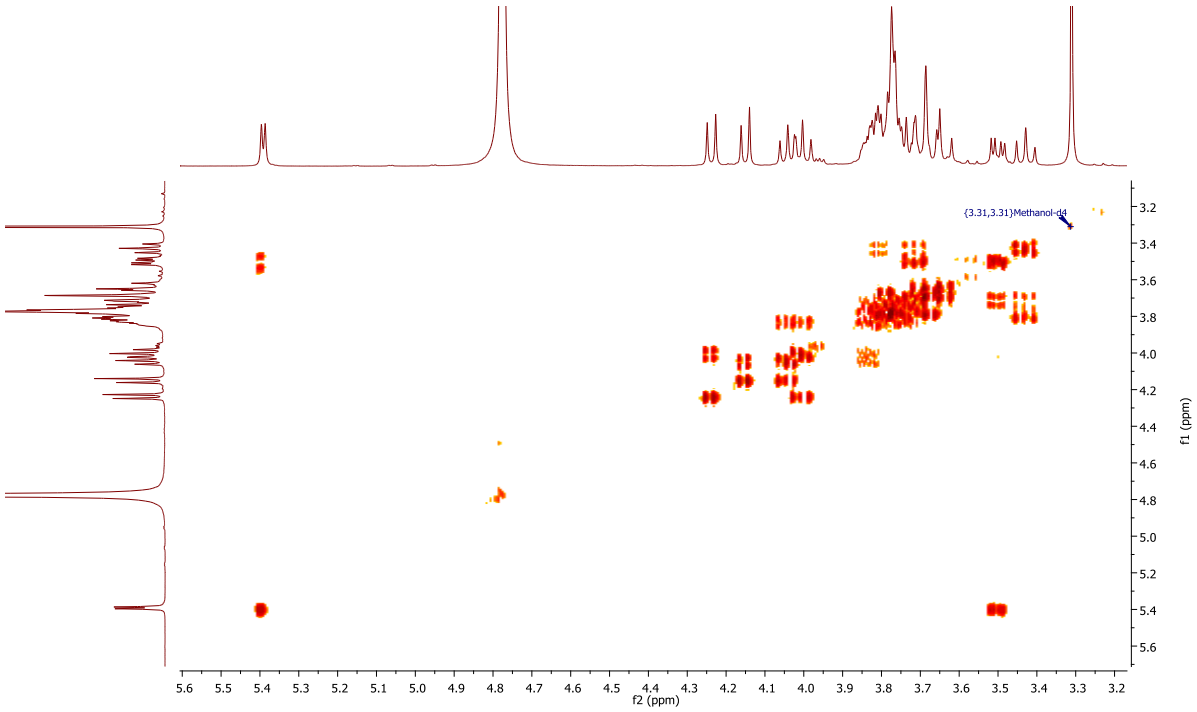

Figure 113 COSY of 1-kestose isolated from bluebell bulbs in D_2O.

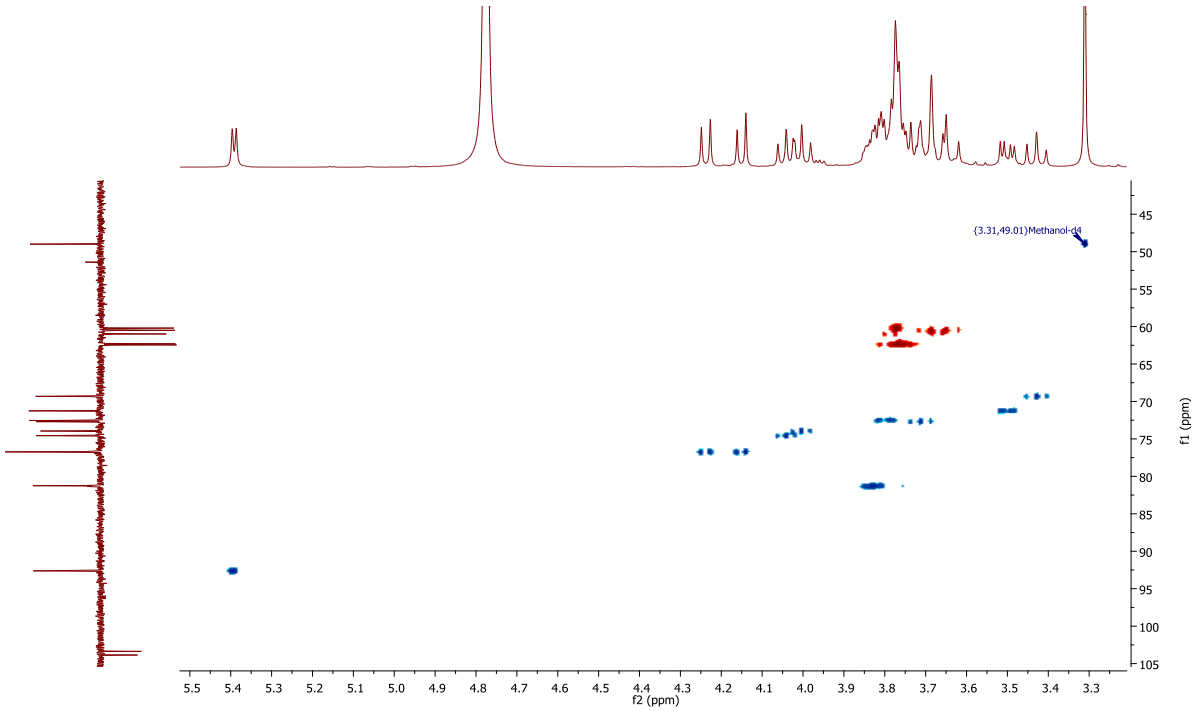

Figure 114 HSQC of 1-kestose isolated from bluebell bulbs in D_2O.

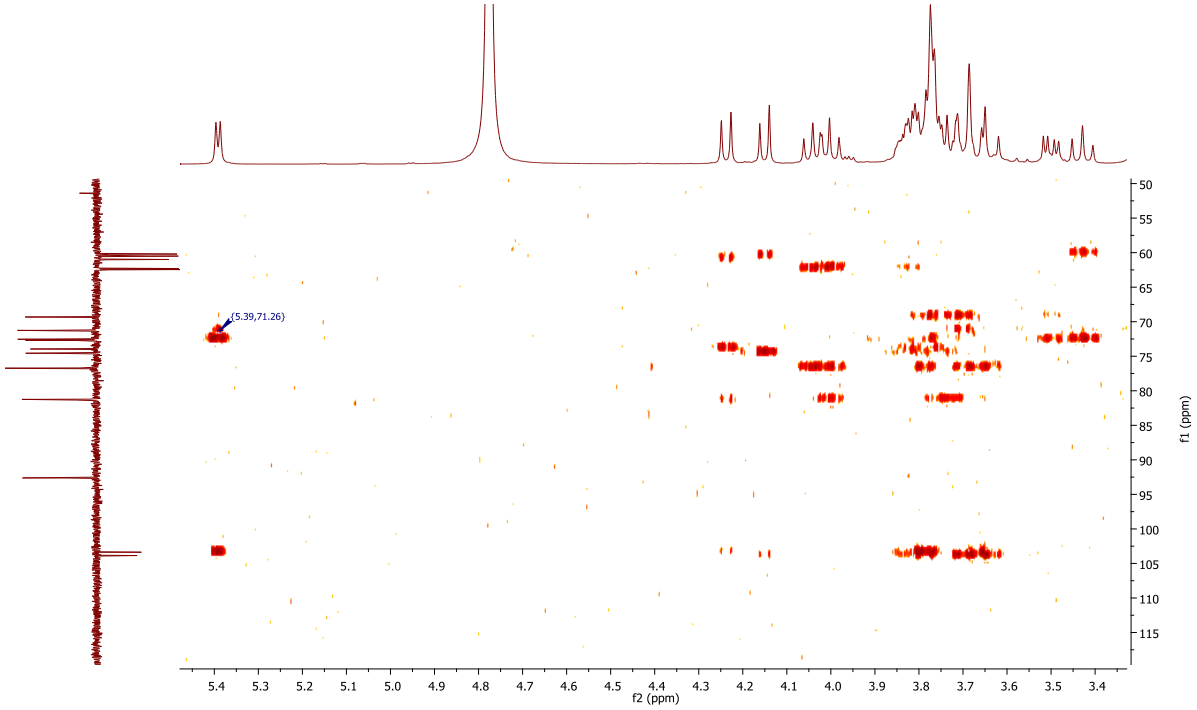

Figure 115 HMBC of 1-kestose isolated from bluebell bulbs in D_2O.

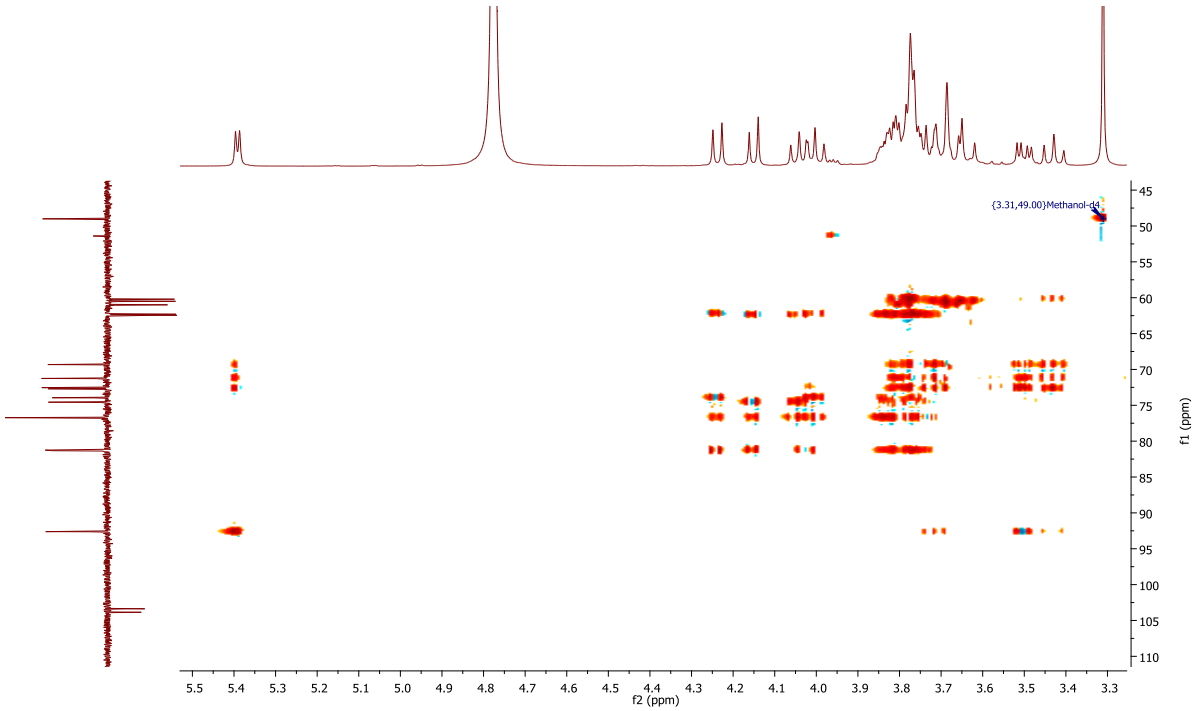

Figure 116 HSQC-TOCSY of 1-kestose isolated from bluebell bulbs in D_2O.

2. NMR spectra of peracetylated 1-kestose

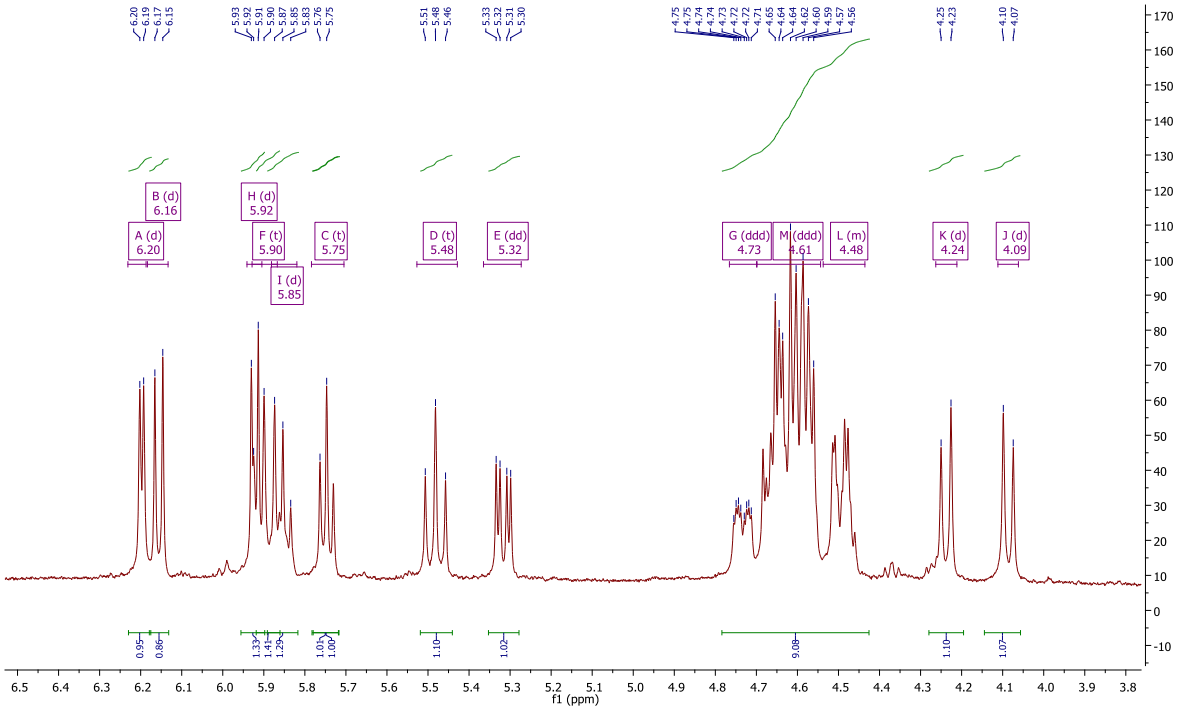

Figure 117 ^{1}H NMR of the peracetylated derivative of 1-kestose isolated from bluebell bulbs in pyridine-D_5.

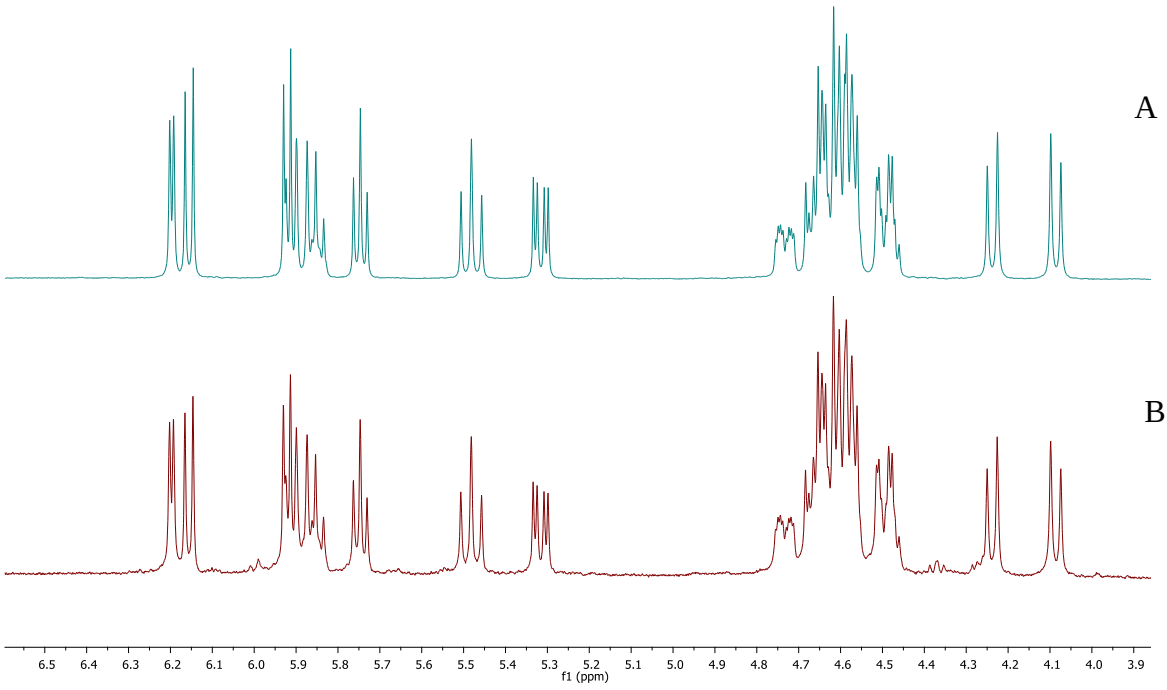

Figure 118 Comparison of ^{1}H NMR spectra of the peracetylated derivatives of A, standard 1-kestose and B, 1-kestose isolated from bluebell bulbs in pyridine -D_5.

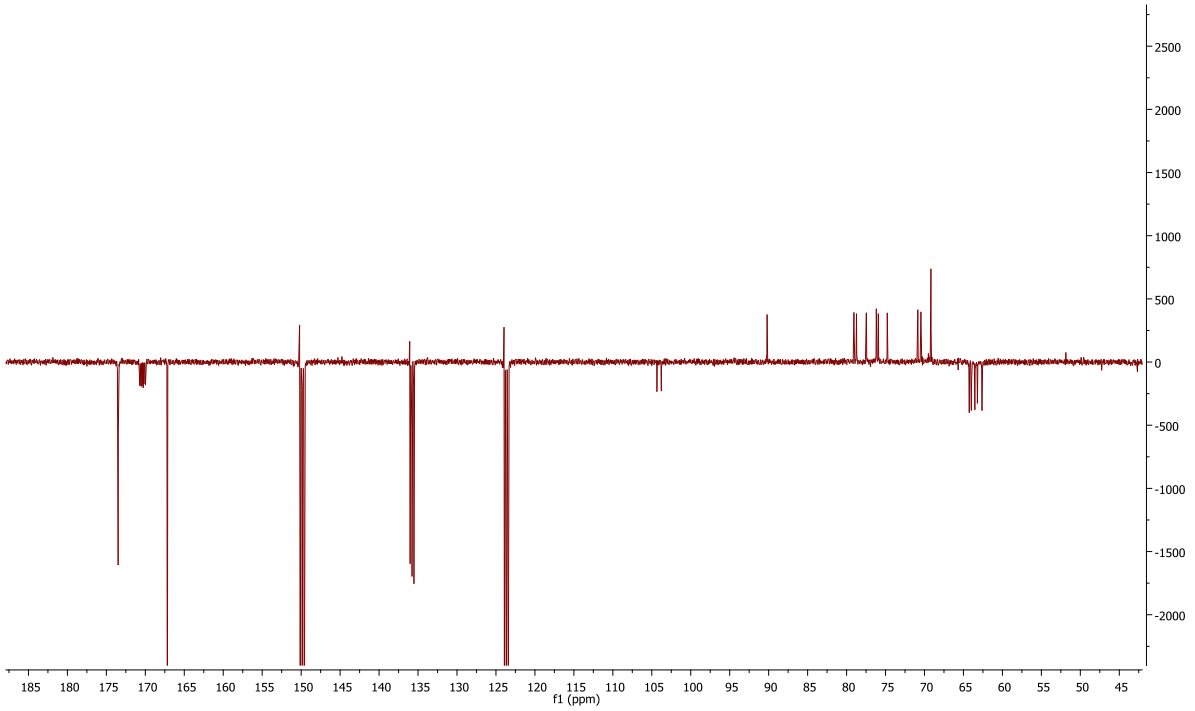

Figure 119 DEPTQ spectrum of the peracetylated derivative of 1-kestose isolated from bluebell bulbs in pyridine-D_5.

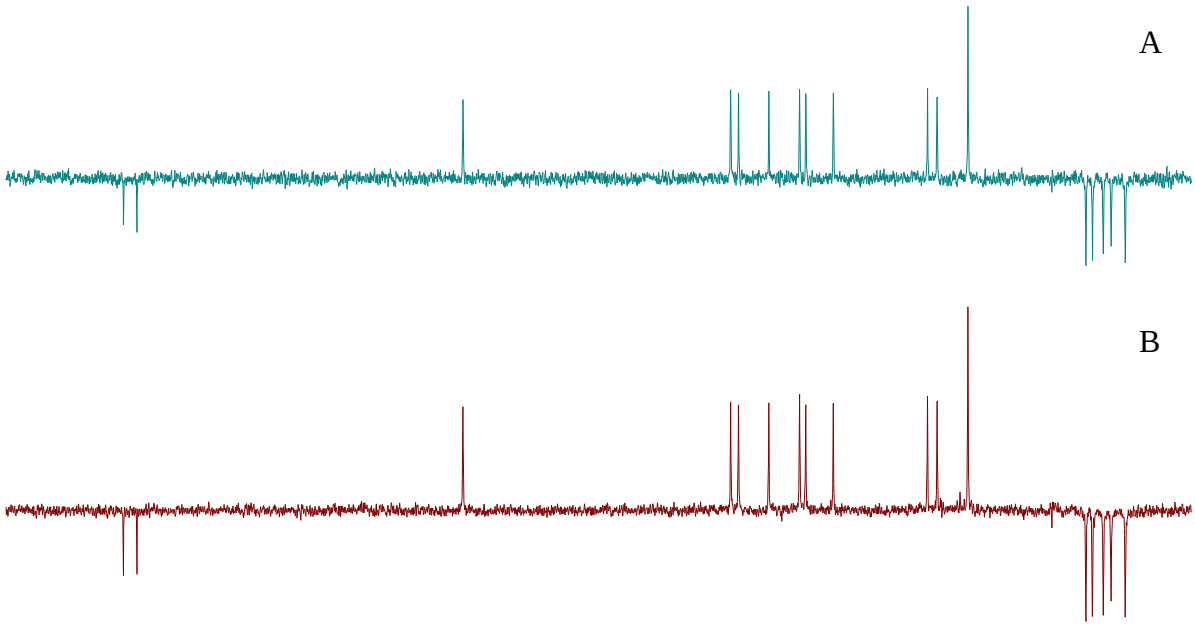

Figure 120 Comparison of DEPTQ spectra of the peracetylated derivatives of A, standard 1-kestose and B, 1-kestose isolated from bluebell bulbs in pyridine -D_5.

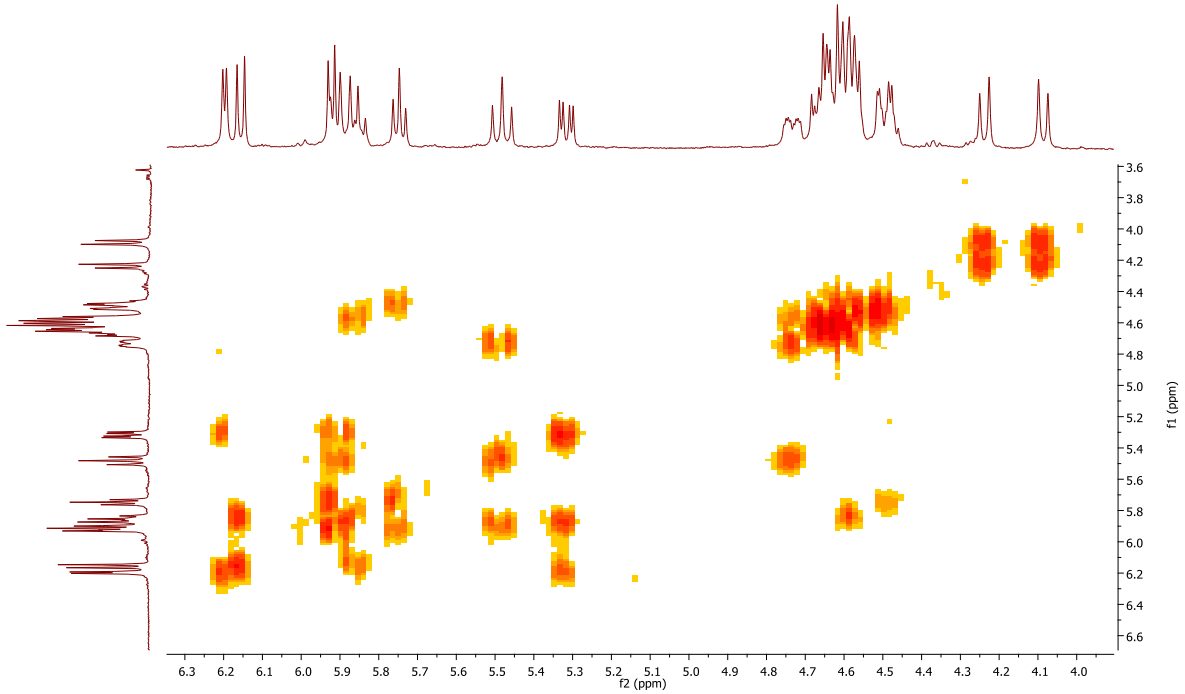

Figure 121 COSY spectrum of the peracetylated derivative of 1-kestose isolated from bluebell bulbs in pyridine-D_5.

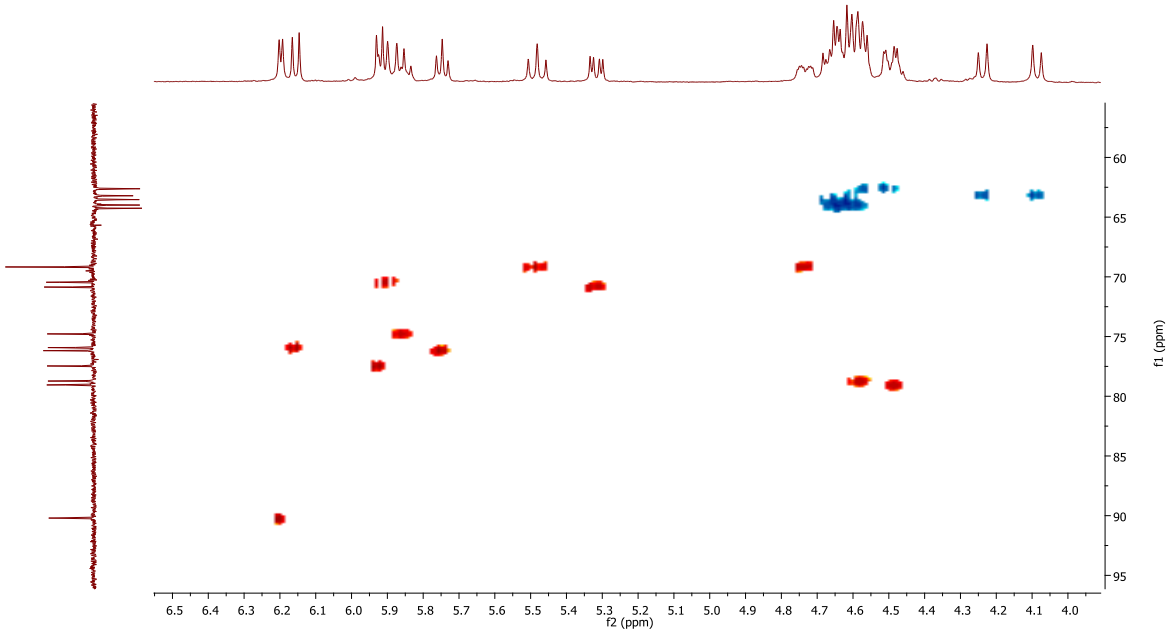

Figure 122 HSQC spectrum of the peracetylated derivative of 1-kestose isolated from bluebell bulbs in pyridine-D_5.

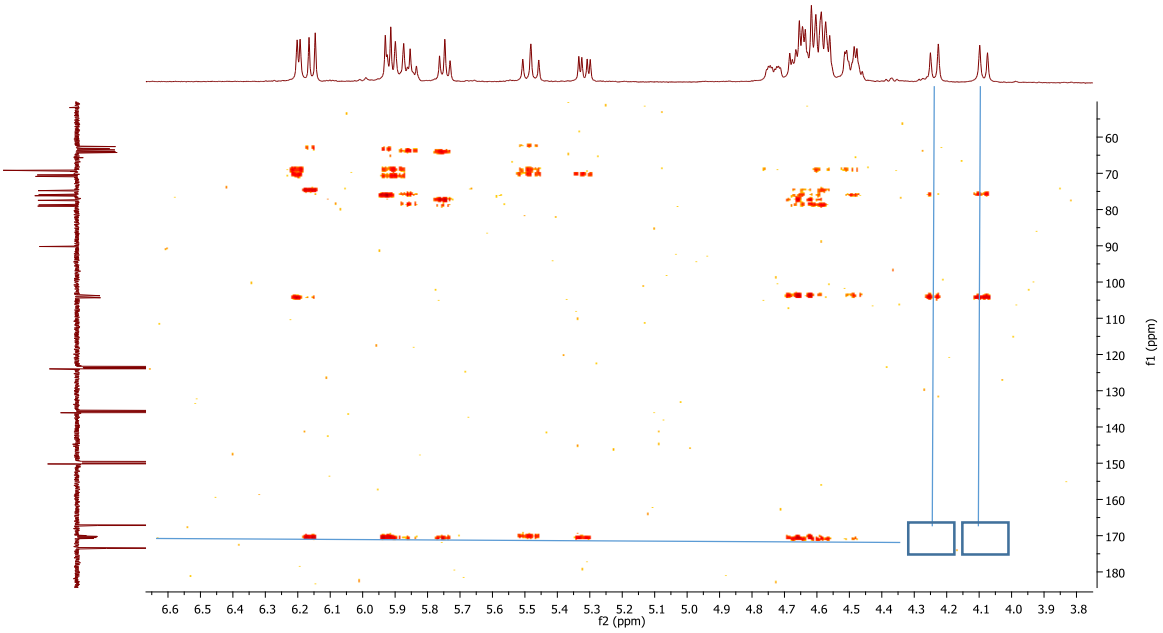

Figure 123 HMBC spectrum of the peracetylated derivative of 1-kestose isolated from bluebell bulbs in pyridine-D_5. The two rectangles show where cross peaks would have appeared had the hydroxyl group on C1-f1 been free.

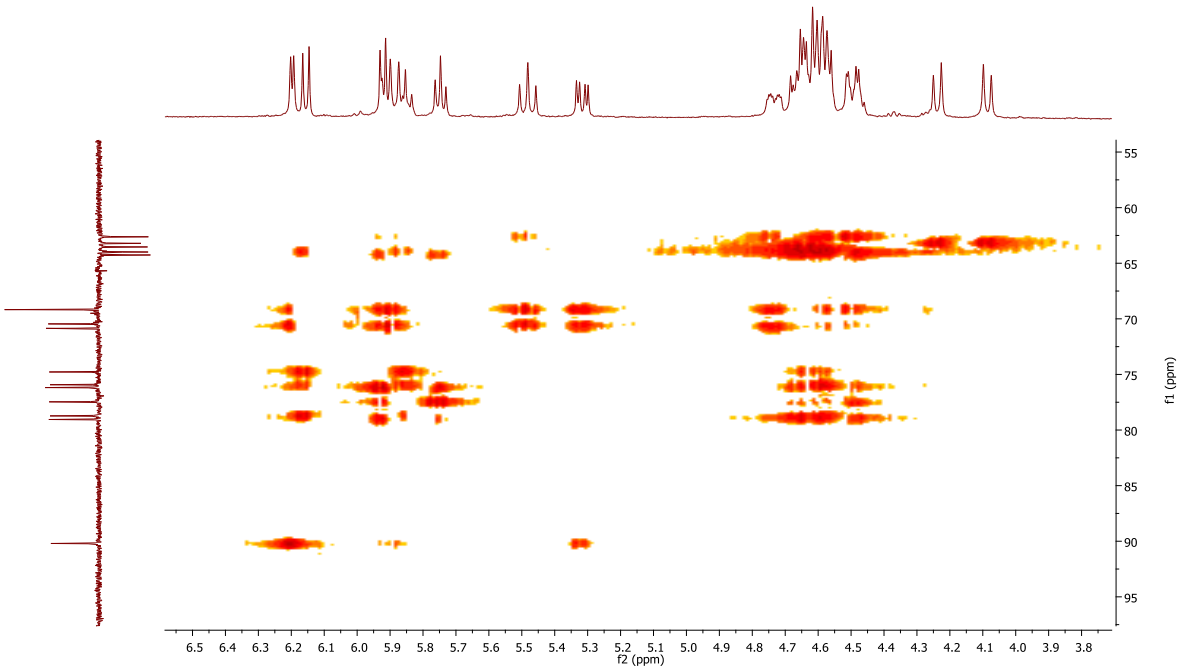

Figure 124 HSQC-TOCSY spectrum of the peracetylated derivative of 1-kestose isolated from bluebell bulbs in pyridine-D_5.

3. Mass spectra of bluebell flower metabolites DR1 – DR4

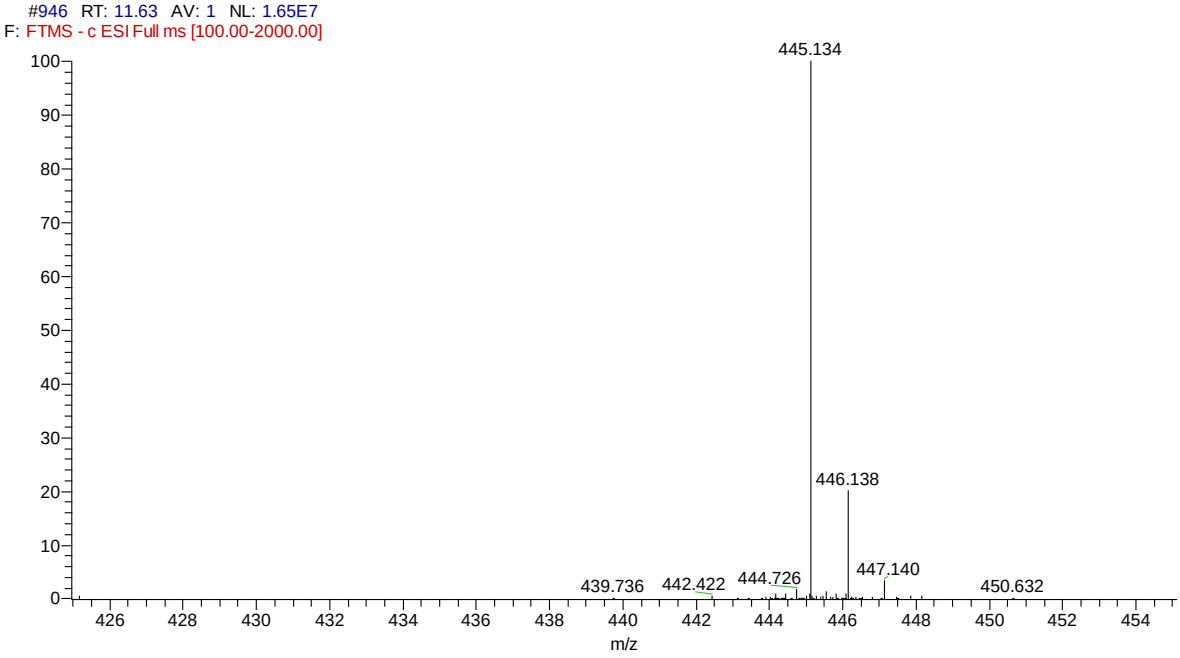

Figure 125 Negative mode HR-ESI-MS of DR1.

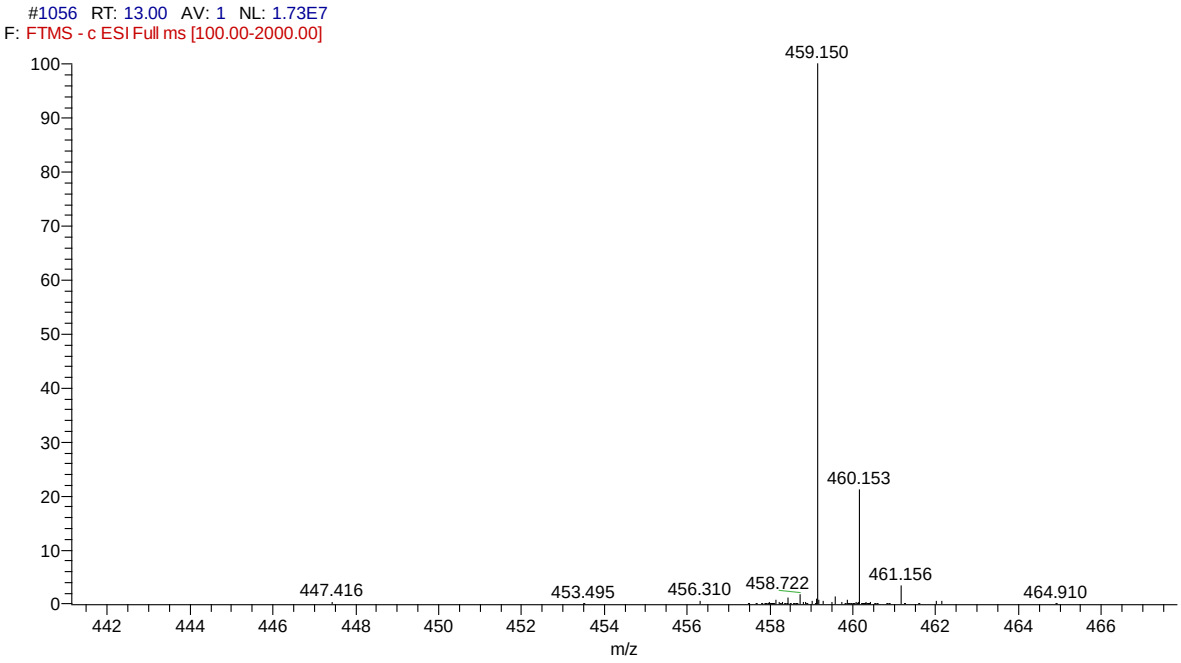

Figure 126 Negative mode HR-ESI-MS of DR2.

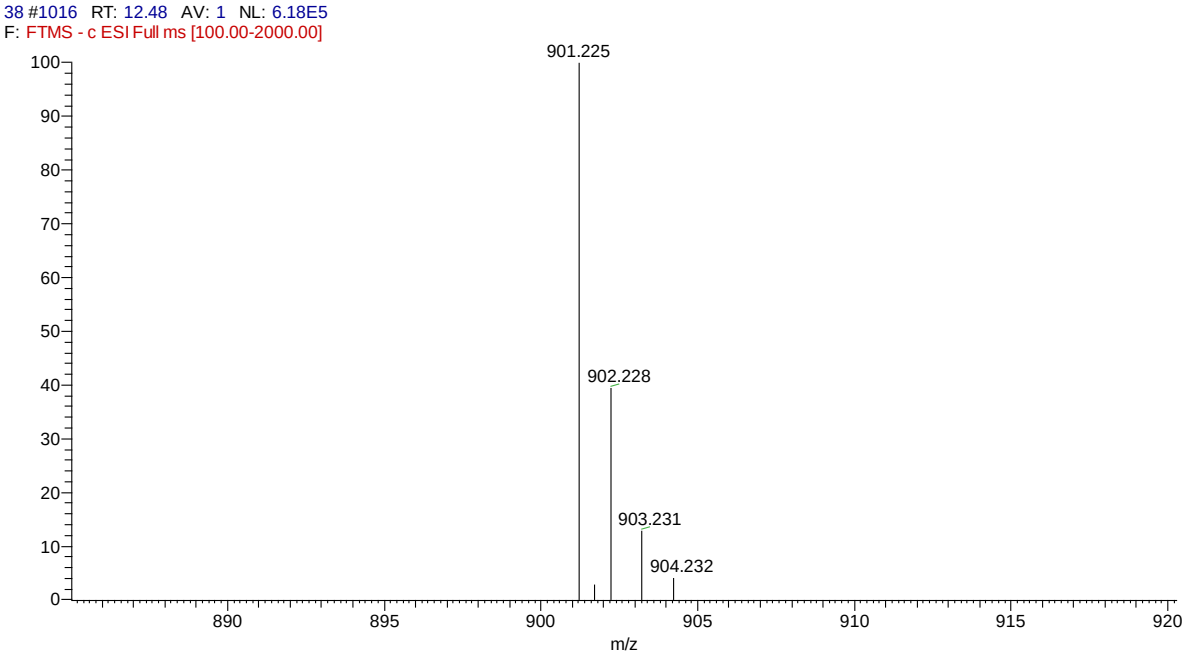

Figure 127 Negative mode HR-ESI-MS of DR3.

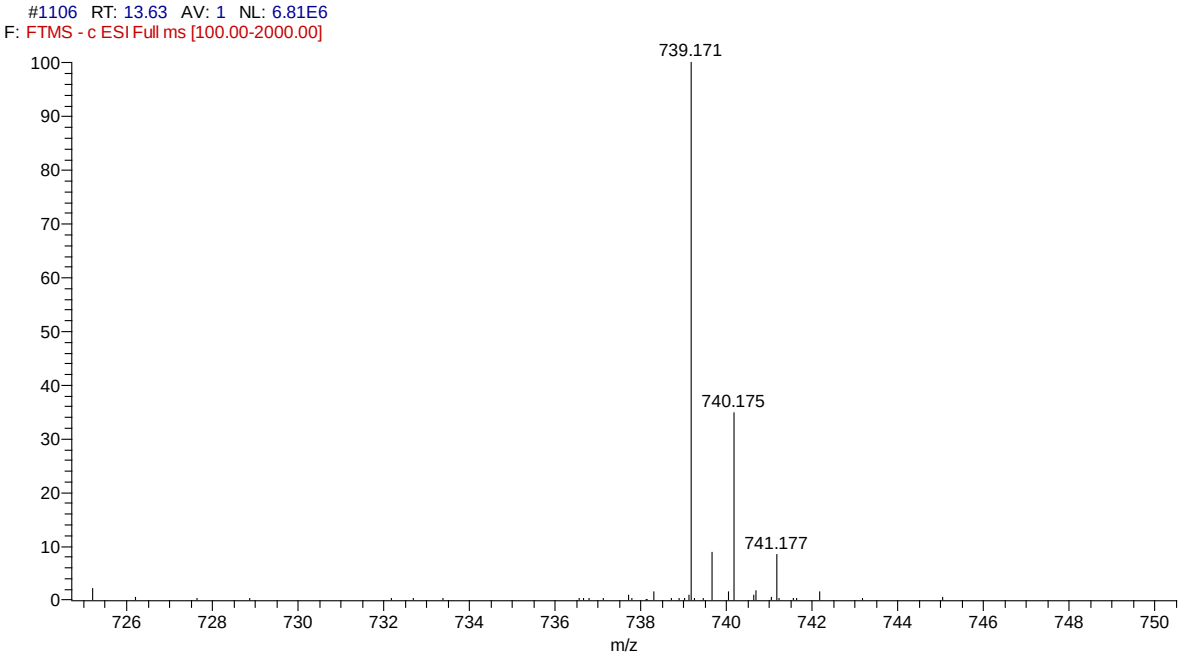

Figure 128 Negative mode HR-ESI-MS of DR4.

4. NMR spectra of *p*-coumaric acid (1)

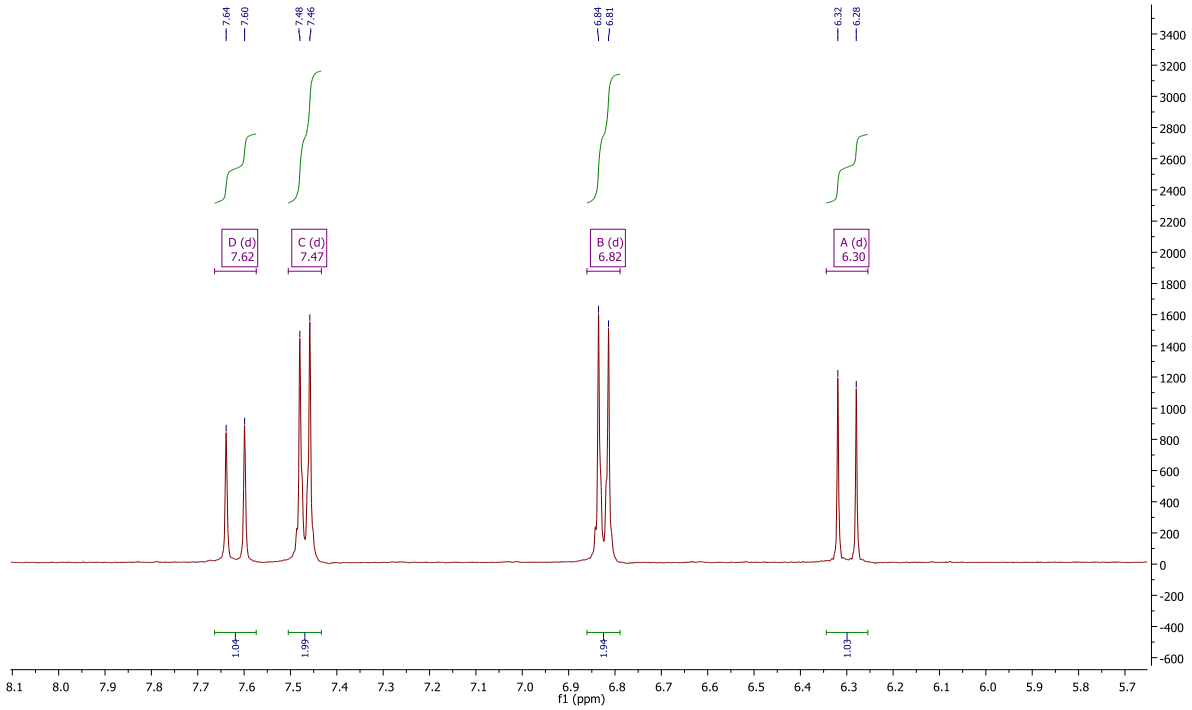

Figure 129 ^{1}H NMR of *p*-coumaric acid in MeOD.

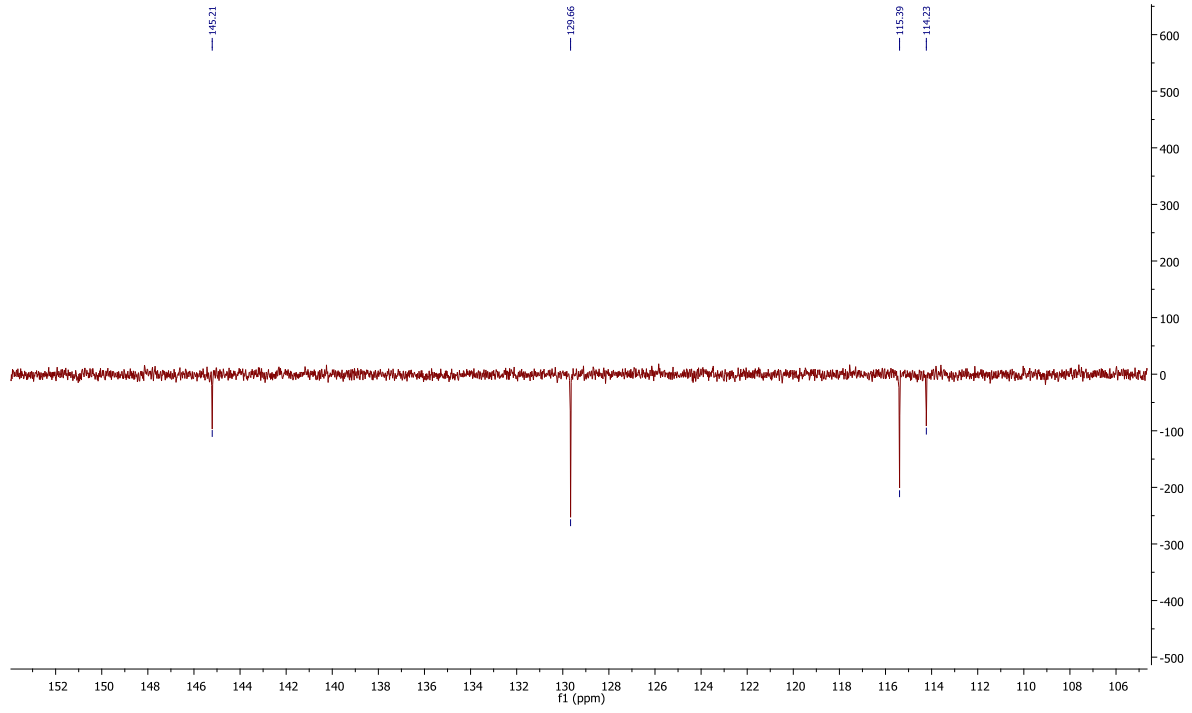

Figure 130 DEPTQ of *p*-coumaric acid in MeOD.

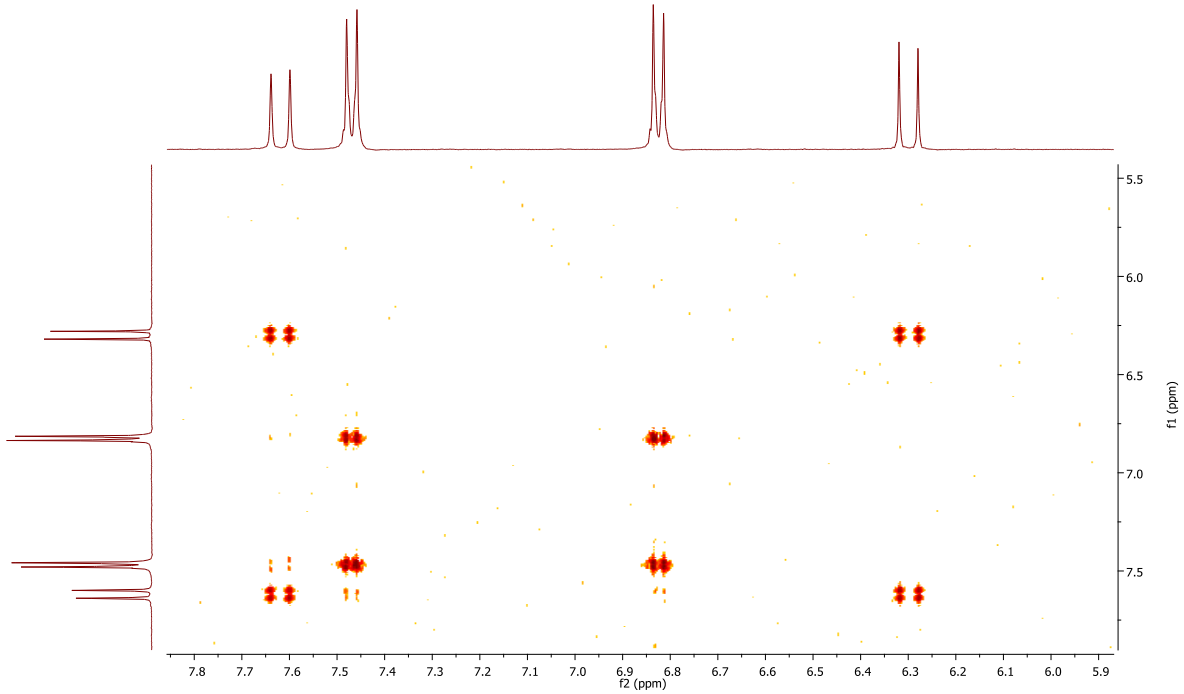

Figure 131 COSY NMR of *p*-coumaric acid in MeOD.

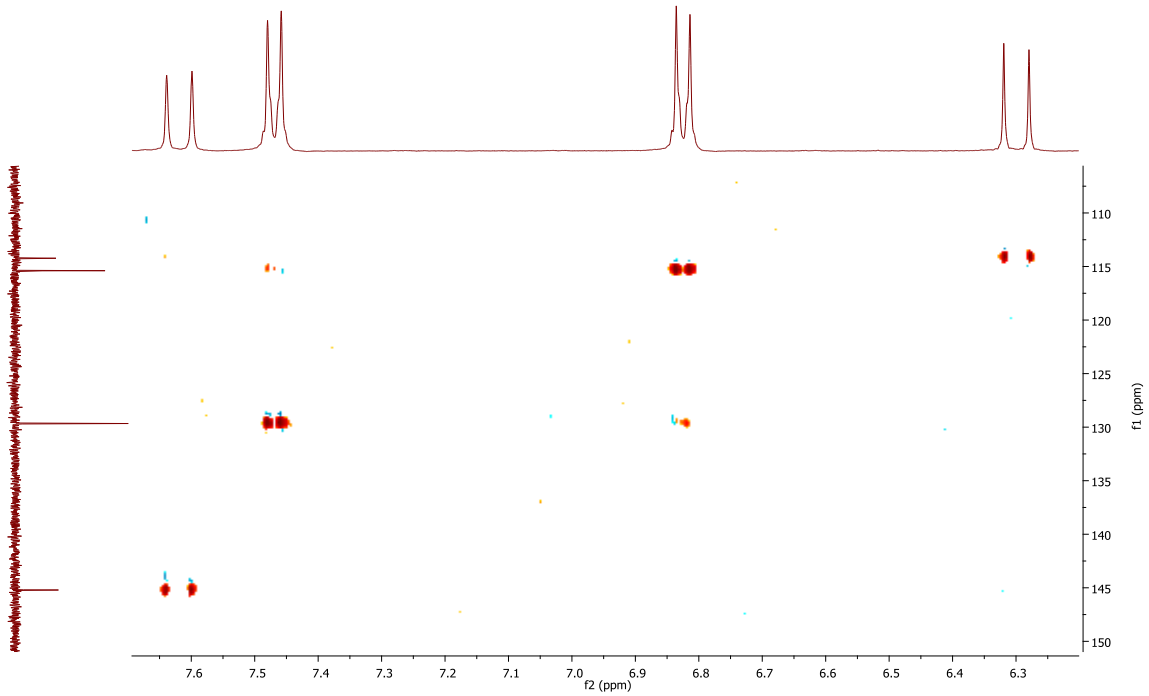

Figure 132 HSQC of *p*-coumaric acid in MeOD.

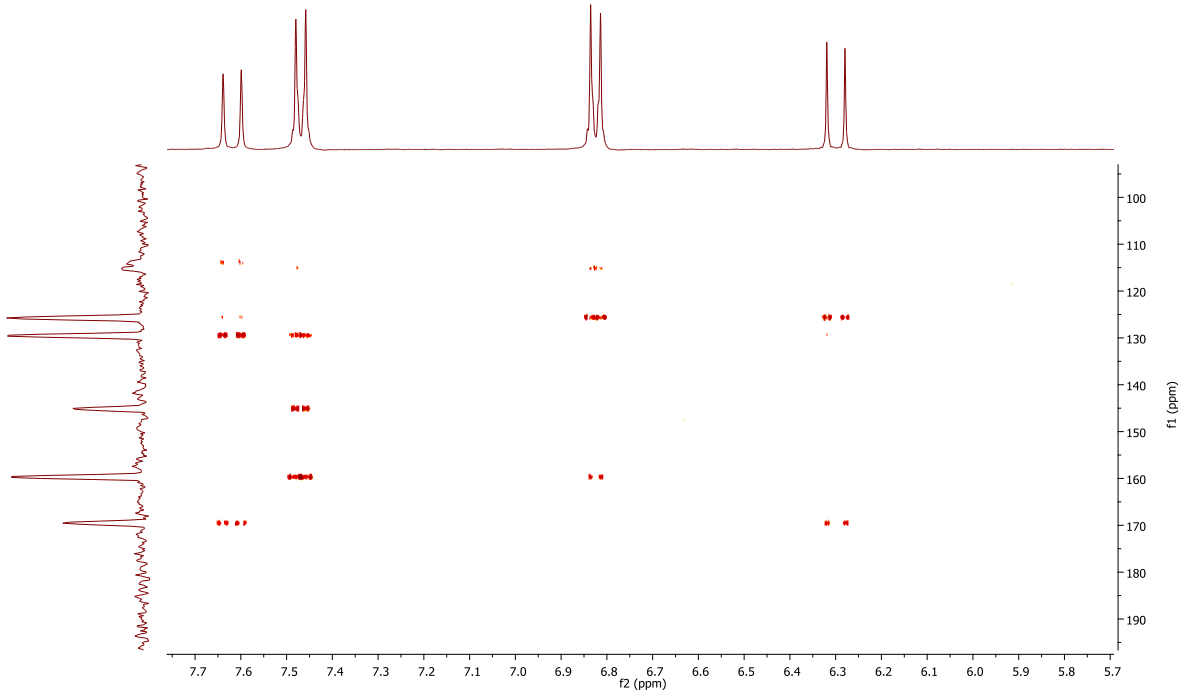

Figure 133 HMBC of *p*-coumaric acid in MeOD.

5. NMR spectra of apigenin (2)

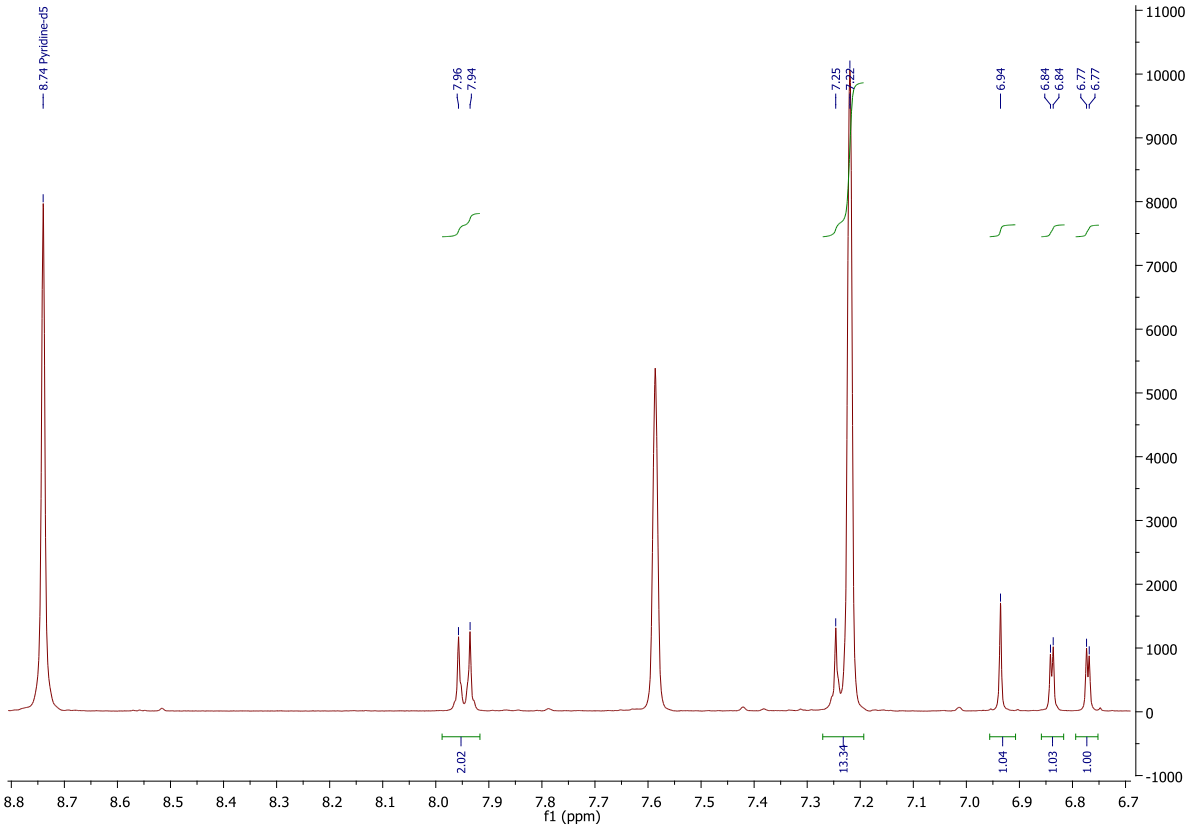

Figure 134 ^{1}H NMR of apigenin in 500 µL pyridine-D5 + 100 µL MeOD.

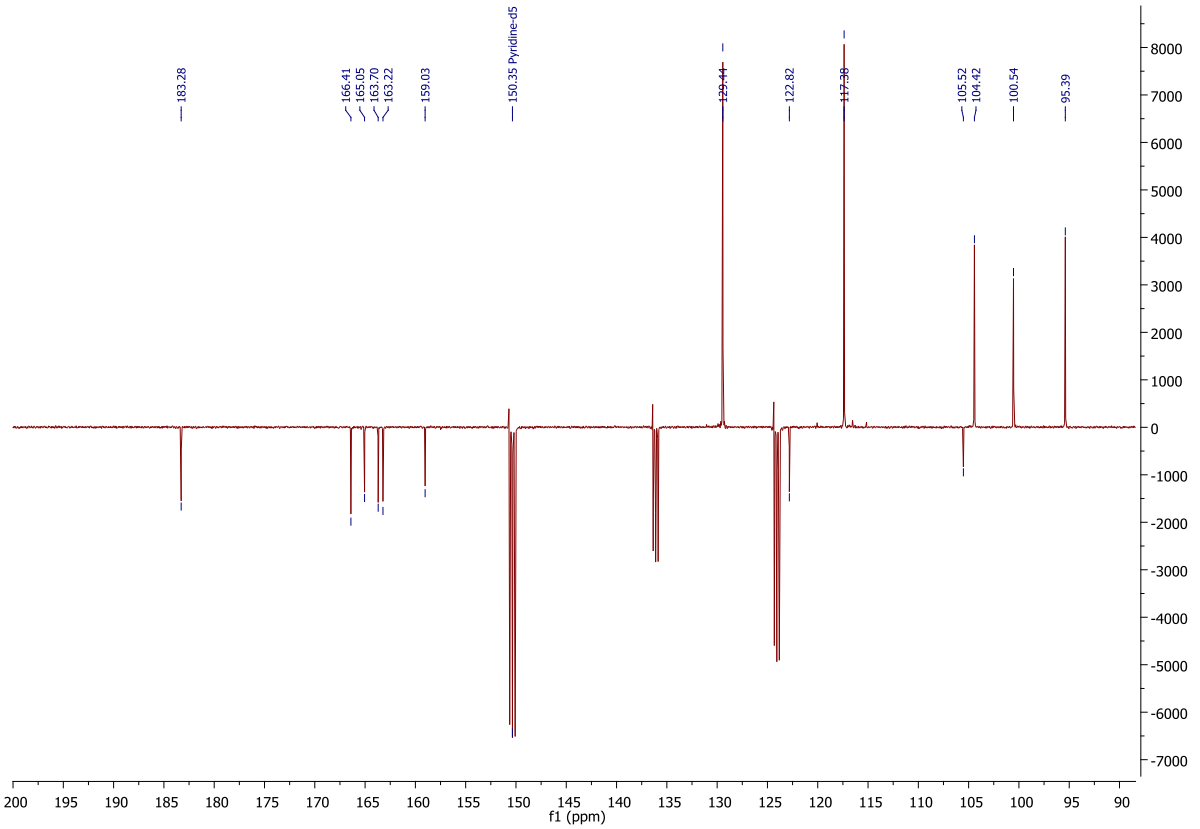

Figure 135 DEPTQ of apigenin in 500 µL pyridine-D5 + 100 µL MeOD.

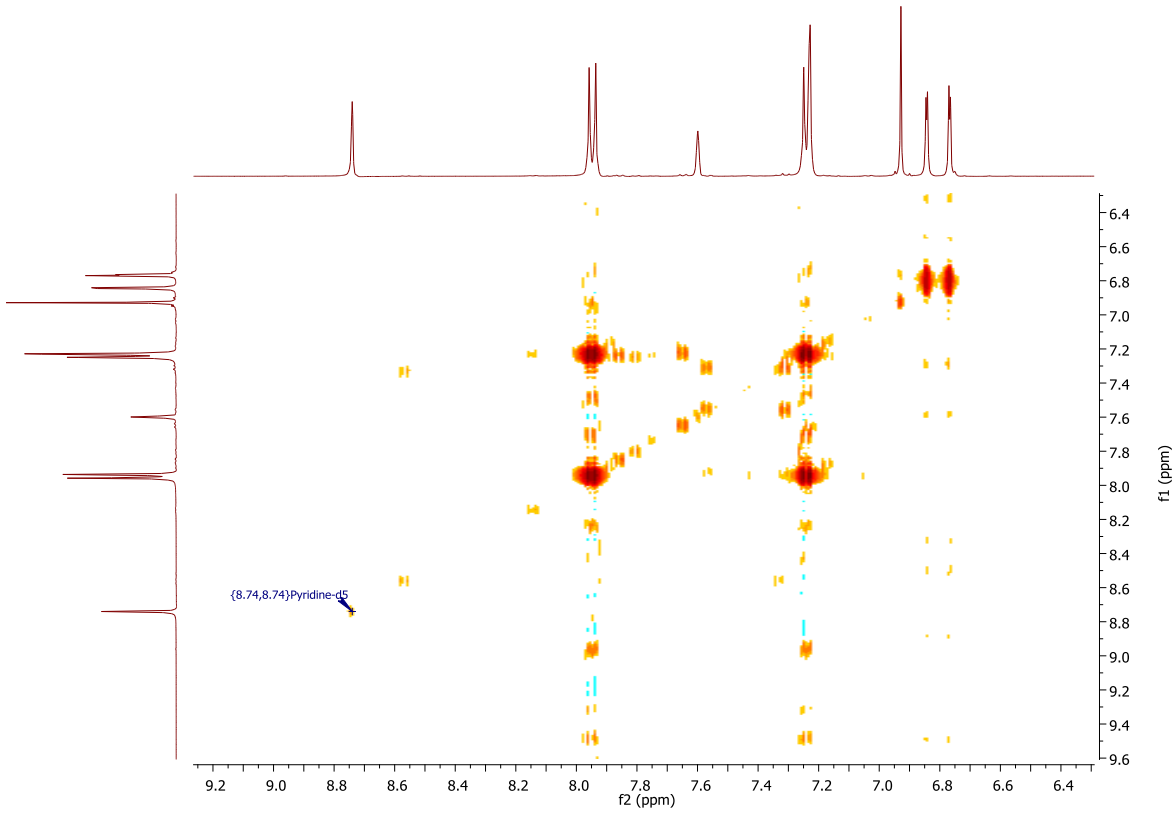

Figure 136 COSY of apigenin in 500 µL pyridine-D5 + 100 µL MeOD.

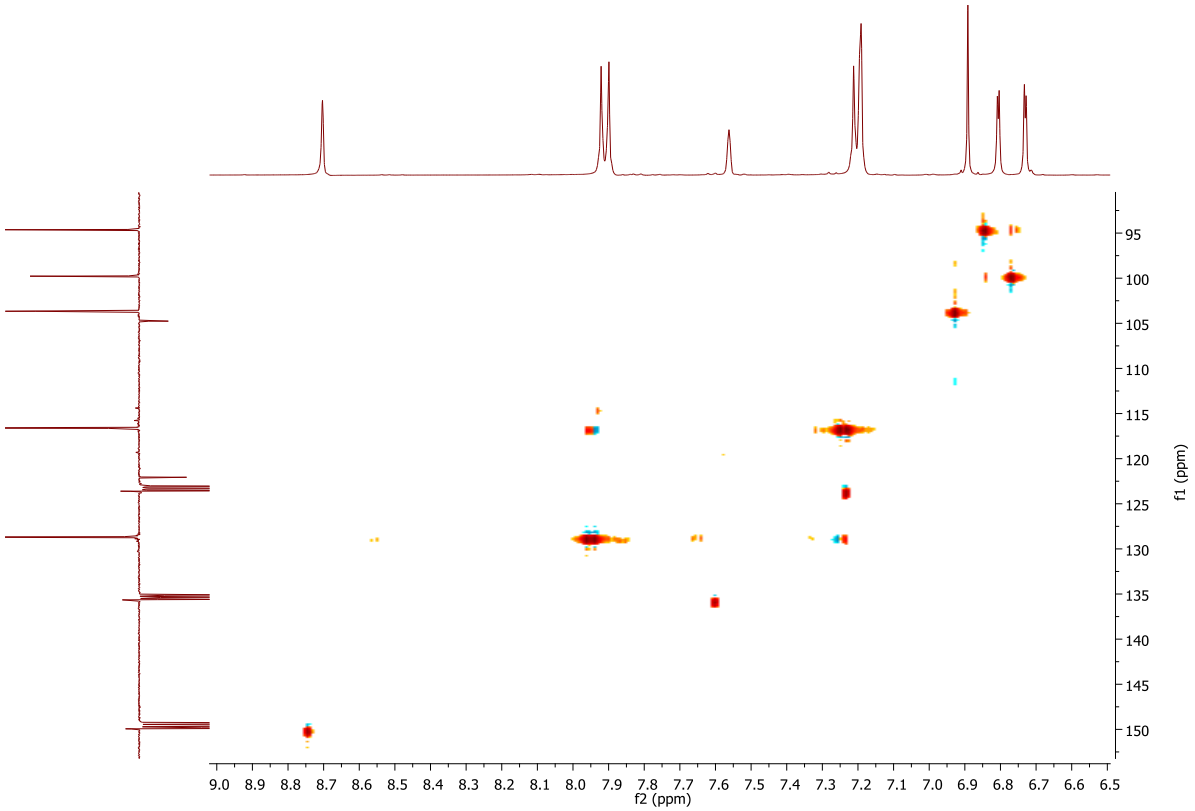

Figure 137 HSQC of apigenin in 500 µL pyridine-D5 + 100 µL MeOD.

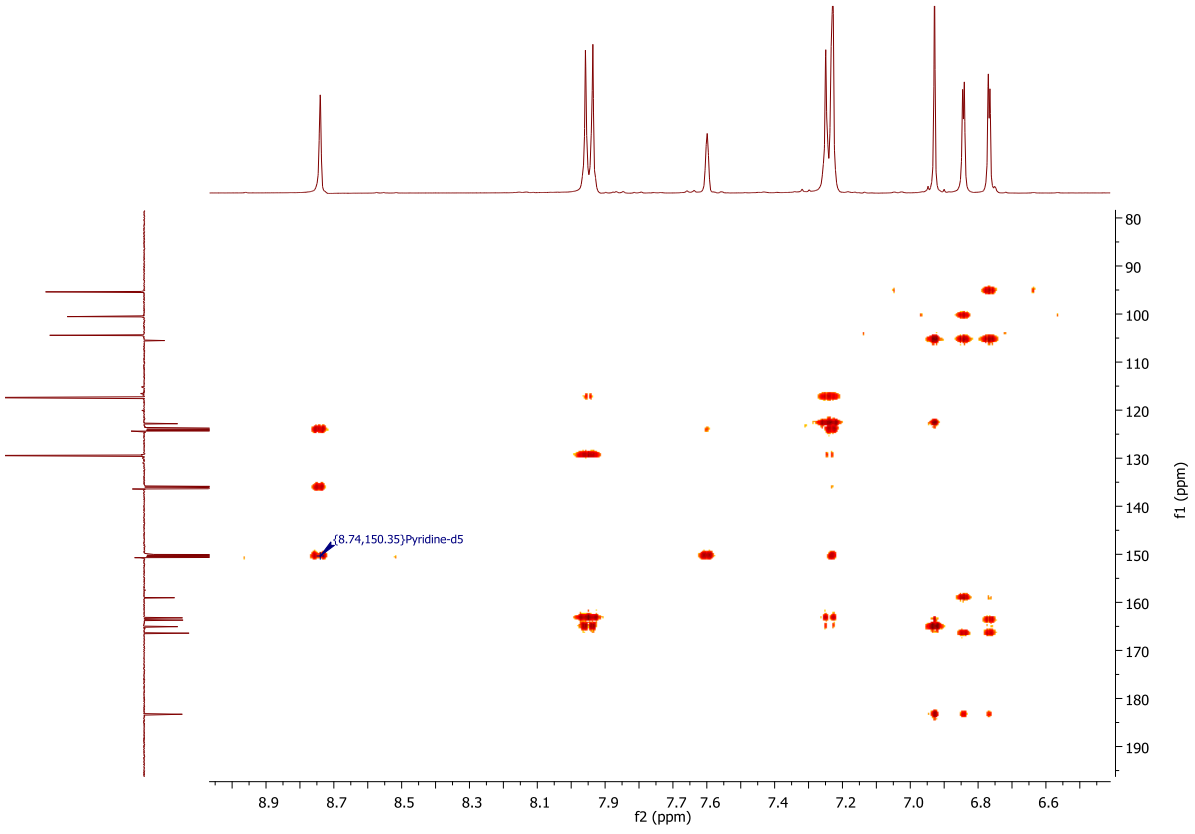

Figure 138 HMBC of apigenin in 500 µL pyridine-D5 + 100 µL MeOD.

6. NMR spectra of 7-*O*-(*β*-D-glucopyranoside methyl uronate) apigenin (3)

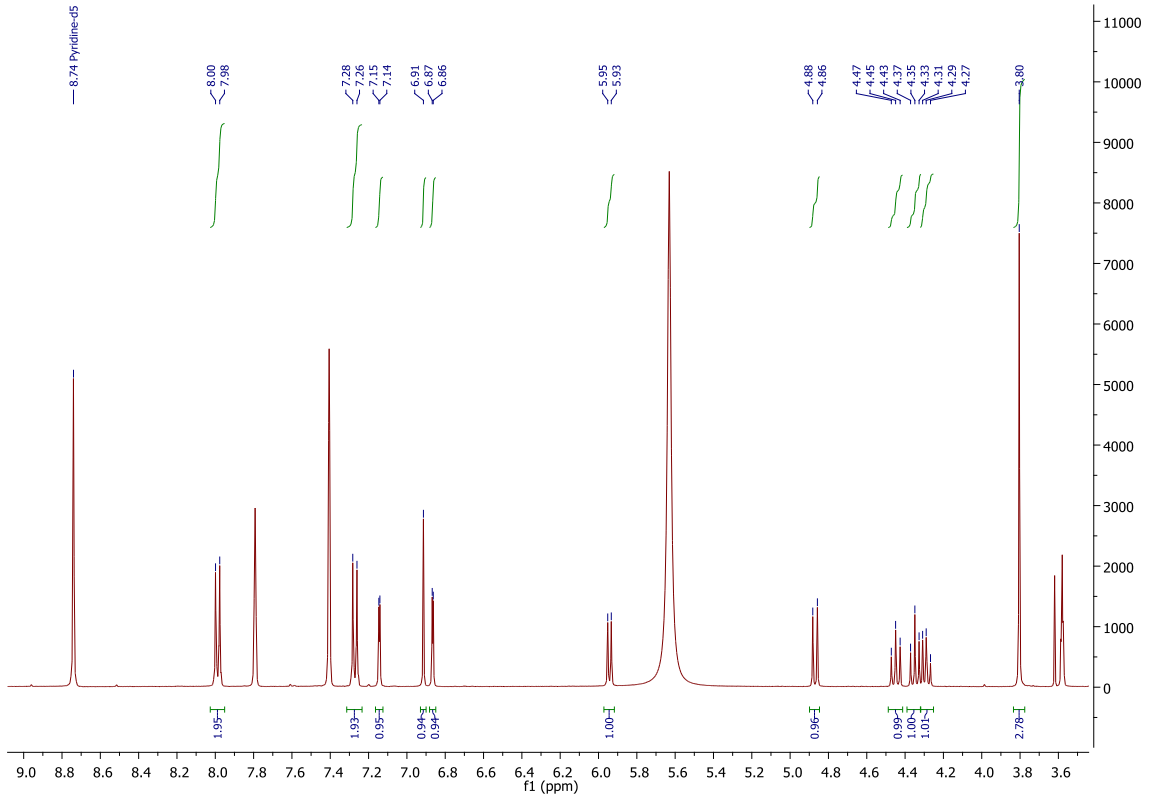

Figure 139 H NMR of methyl apigenin -7-*O*-*β*-D-glucuronate

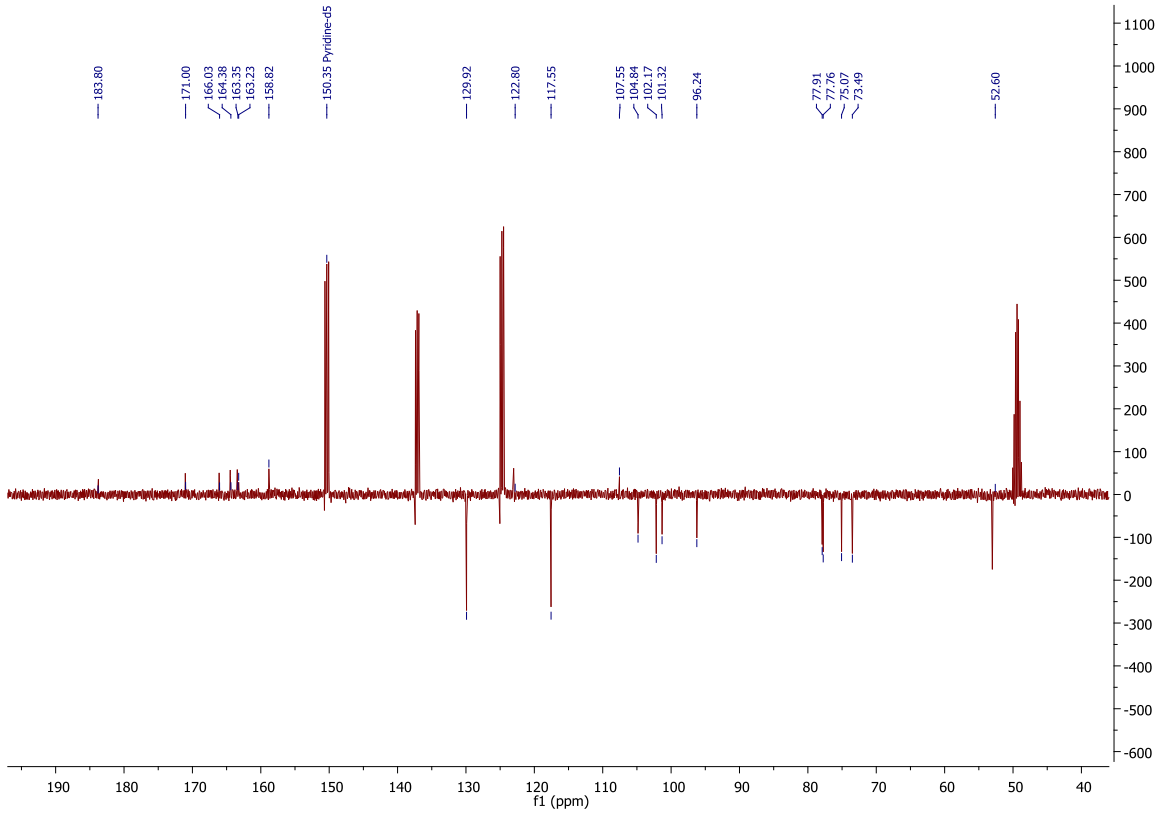

Figure 140 DEPTQ of methyl apigenin -7-*O*-*β*-D-glucuronate

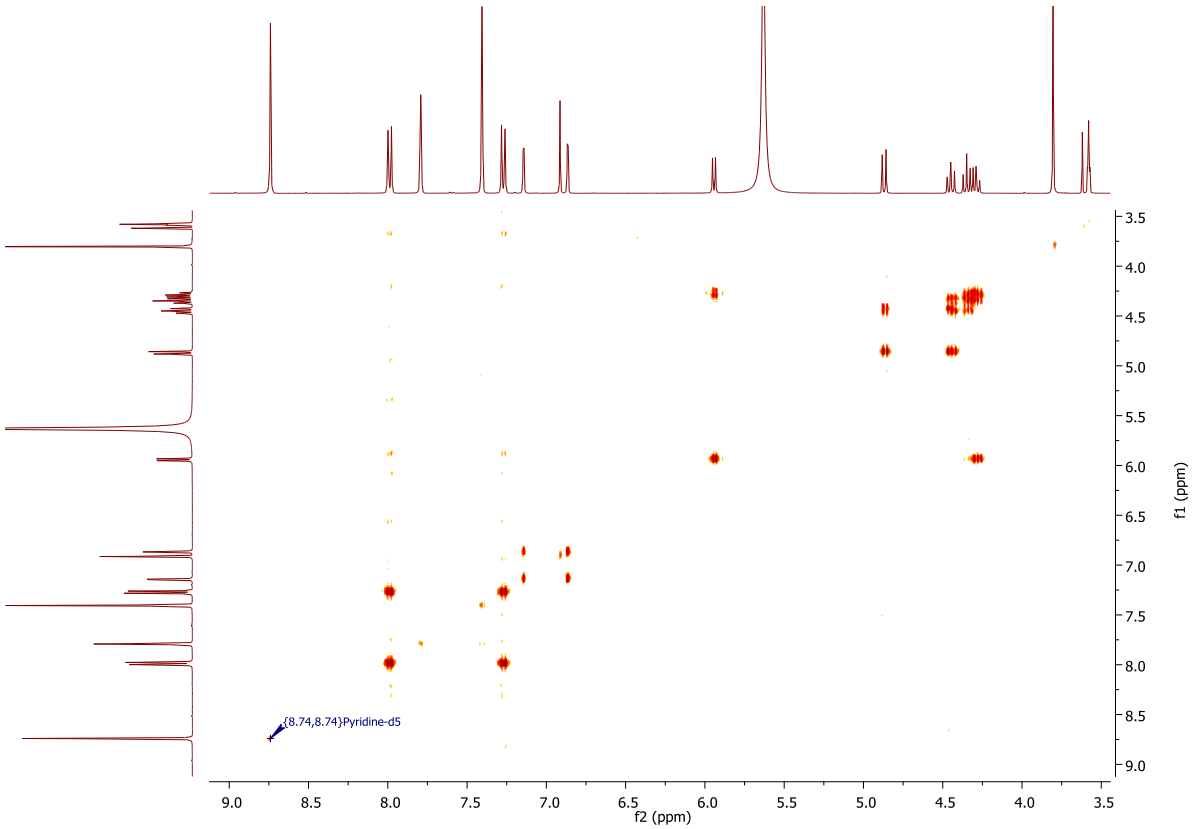

Figure 141 COSY of methyl apigenin -7-*O*-*β*-D-glucuronate

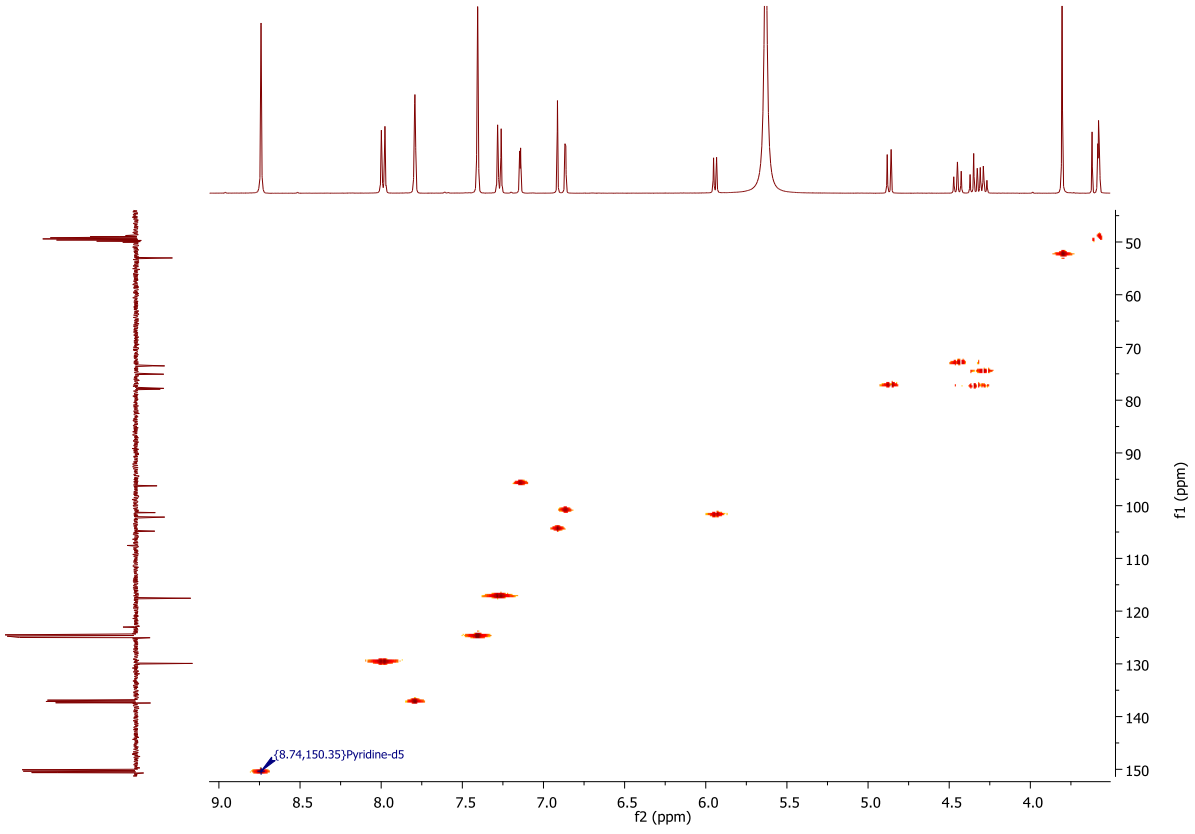

Figure 142 HSQC of methyl apigenin -7-*O*-*β*-D-glucuronate

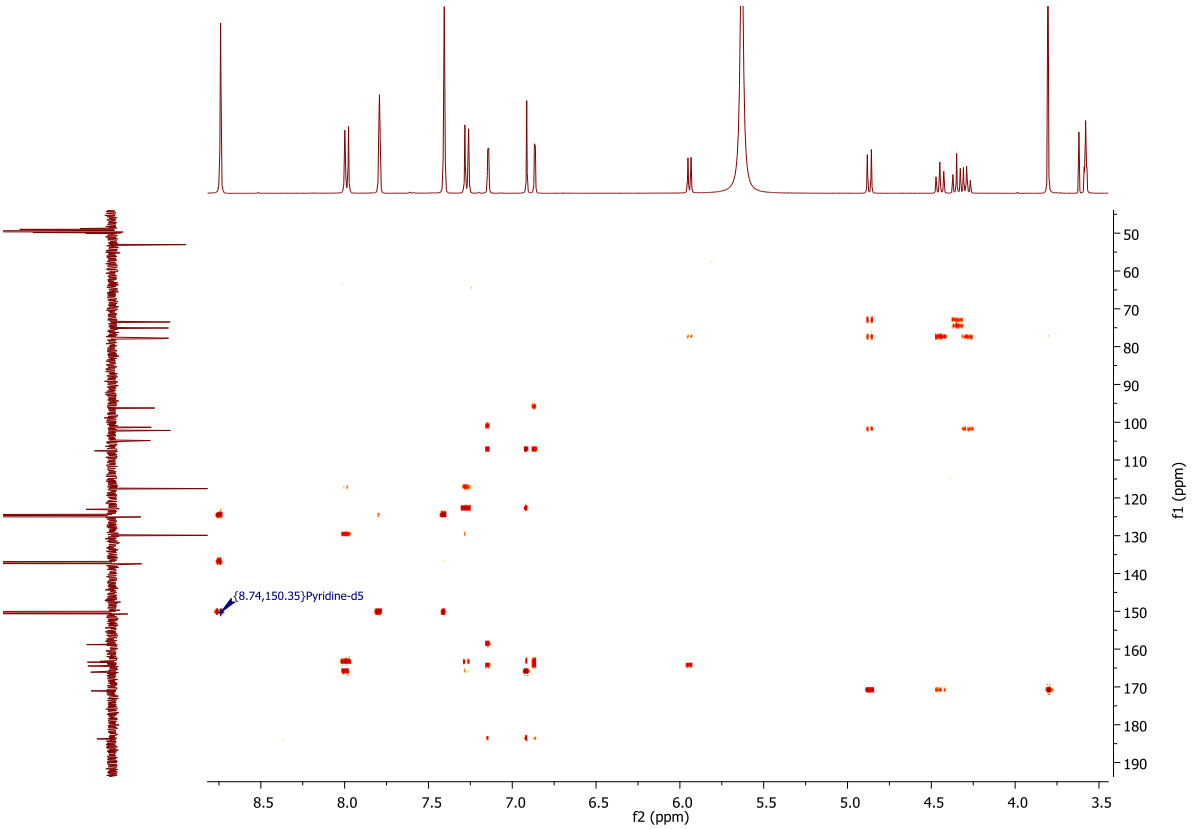

Figure 143 HMBC of methyl apigenin -7-*O*-*β*-D-glucuronate

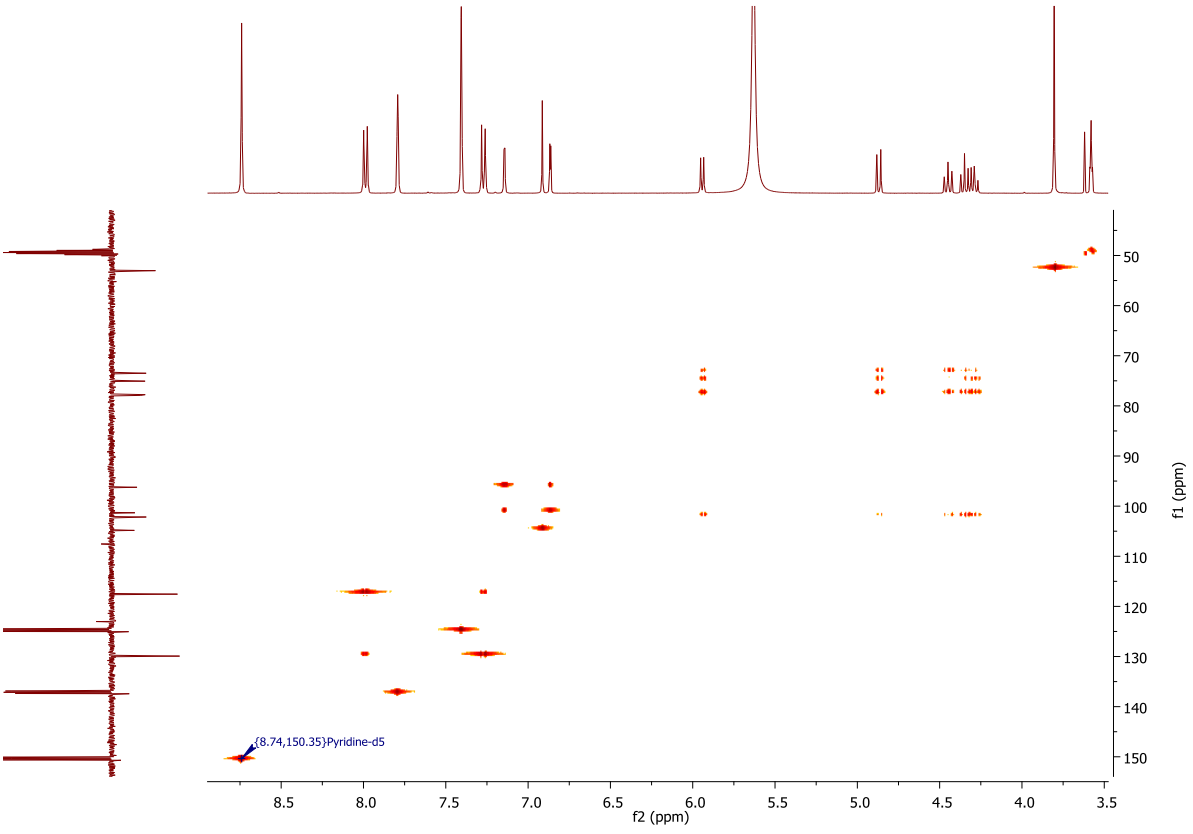

Figure 144 HSQC-TOCSY of methyl apigenin -7-*O*-*β*-D-glucuronate

7. NMR spectra of 7-*O*-(*β*-D-glucopyranosideuronic acid) apigenin (4).

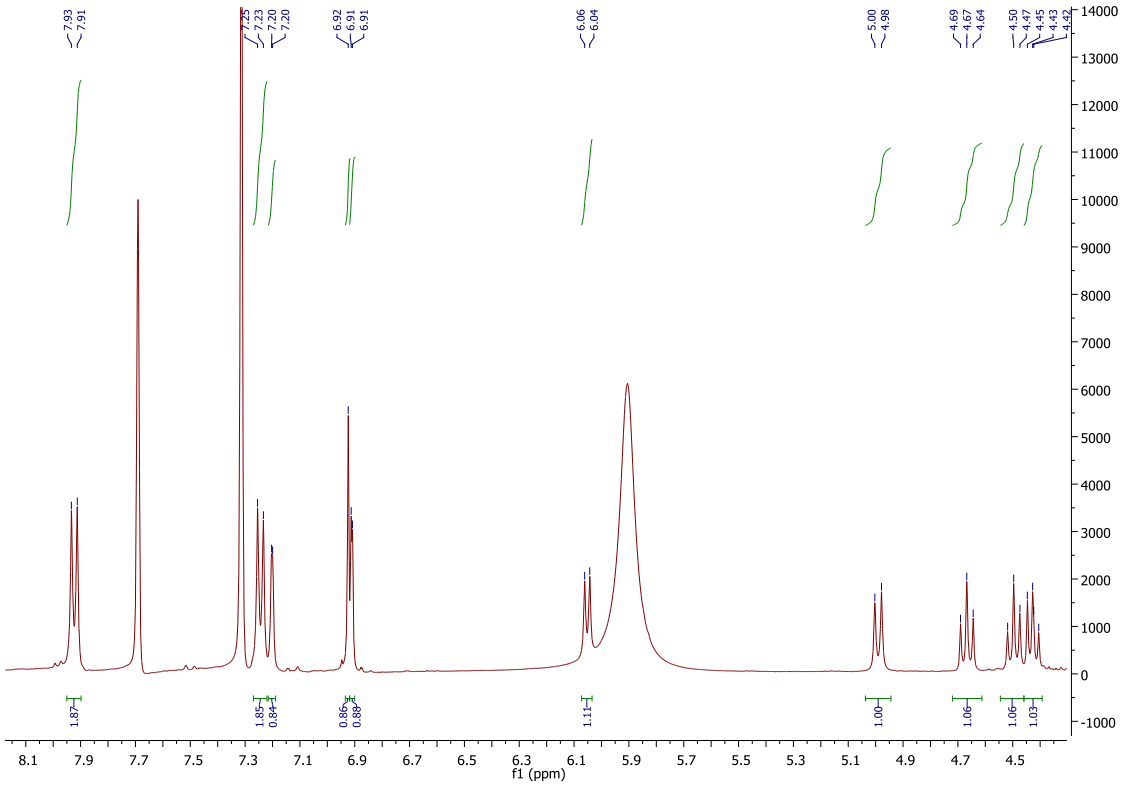

Figure 145 ^{1}H NMR of 7-*O*-(*β*-D-glucopyranosideuronic acid) apigenin

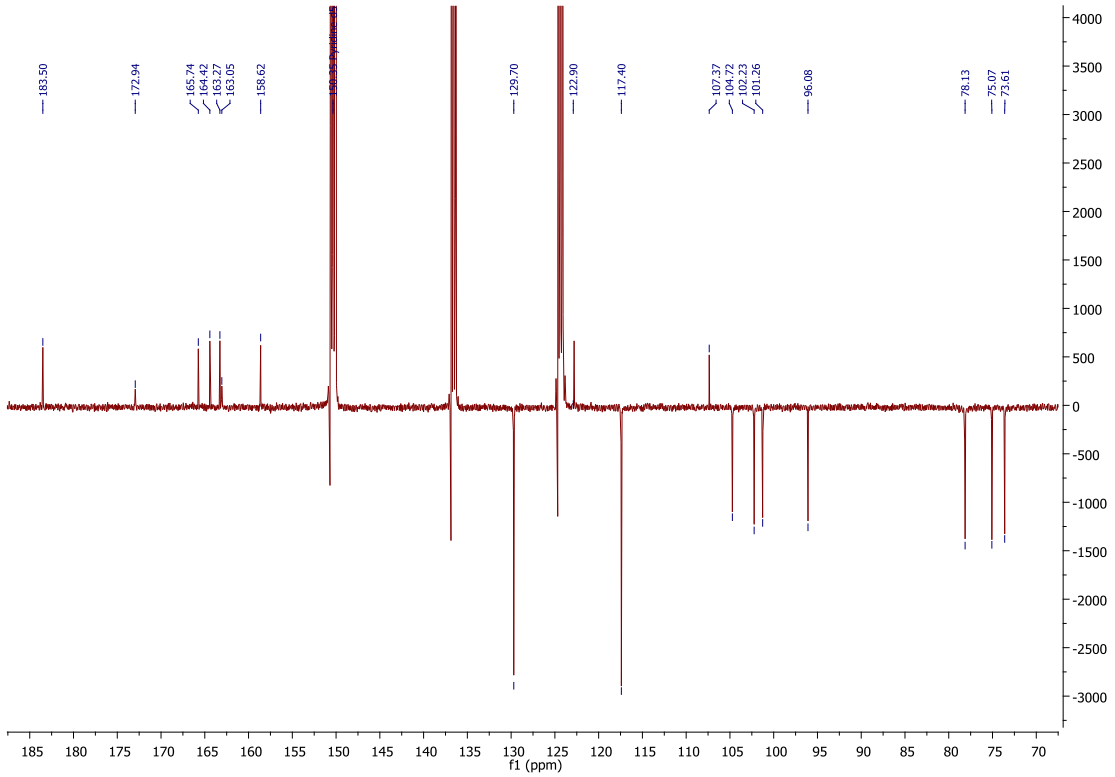

Figure 146 DEPTQ of 7-*O*-(*β*-D-glucopyranosideuronic acid) apigenin

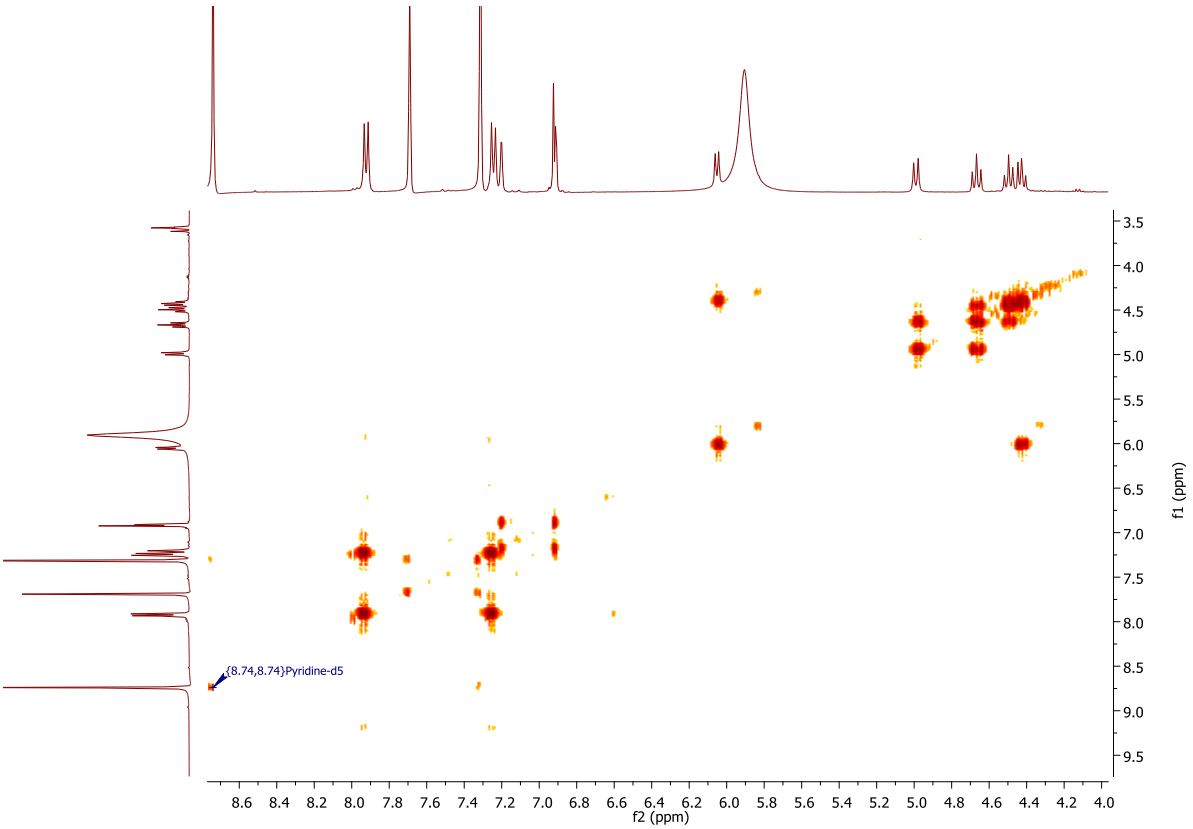

Figure 147 COSY of 7-*O*-(*β*-D-glucopyranosideuronic acid) apigenin

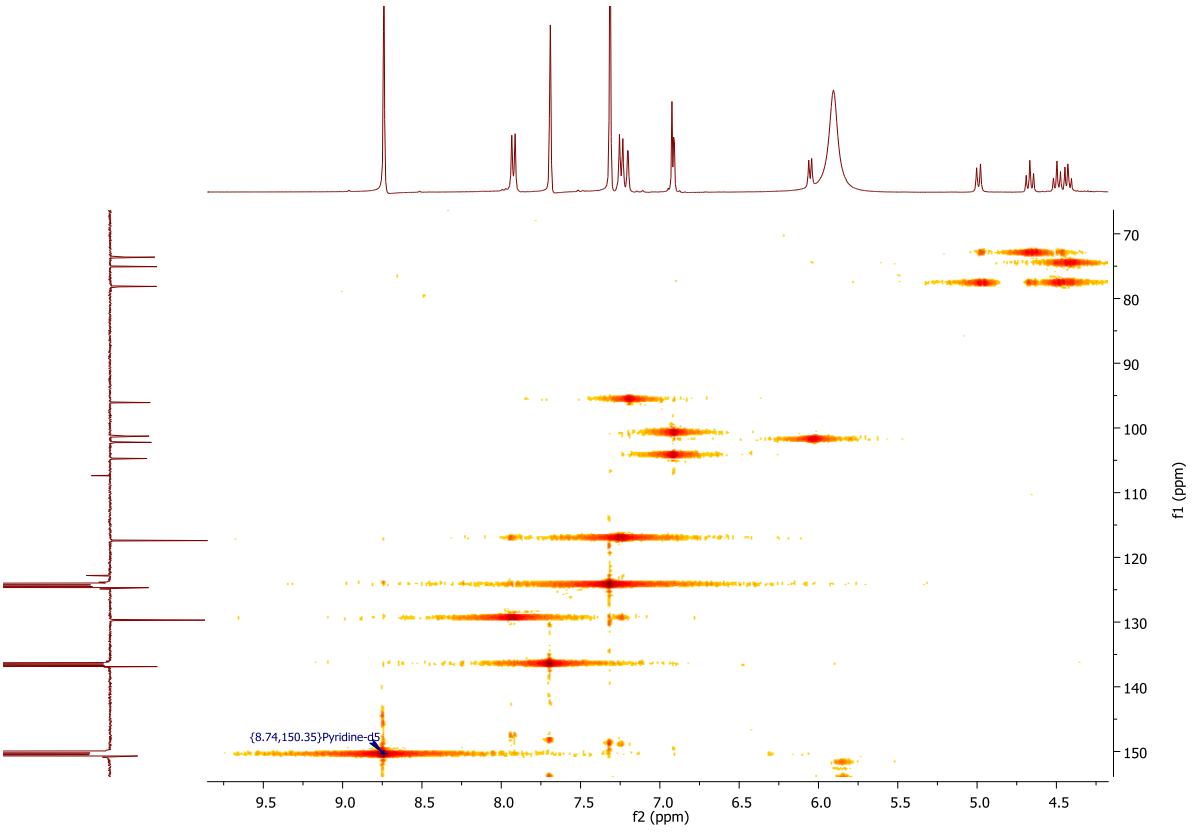

Figure 148 HSQC of 7-*O*-(*β*-D-glucopyranosideuronic acid) apigenin

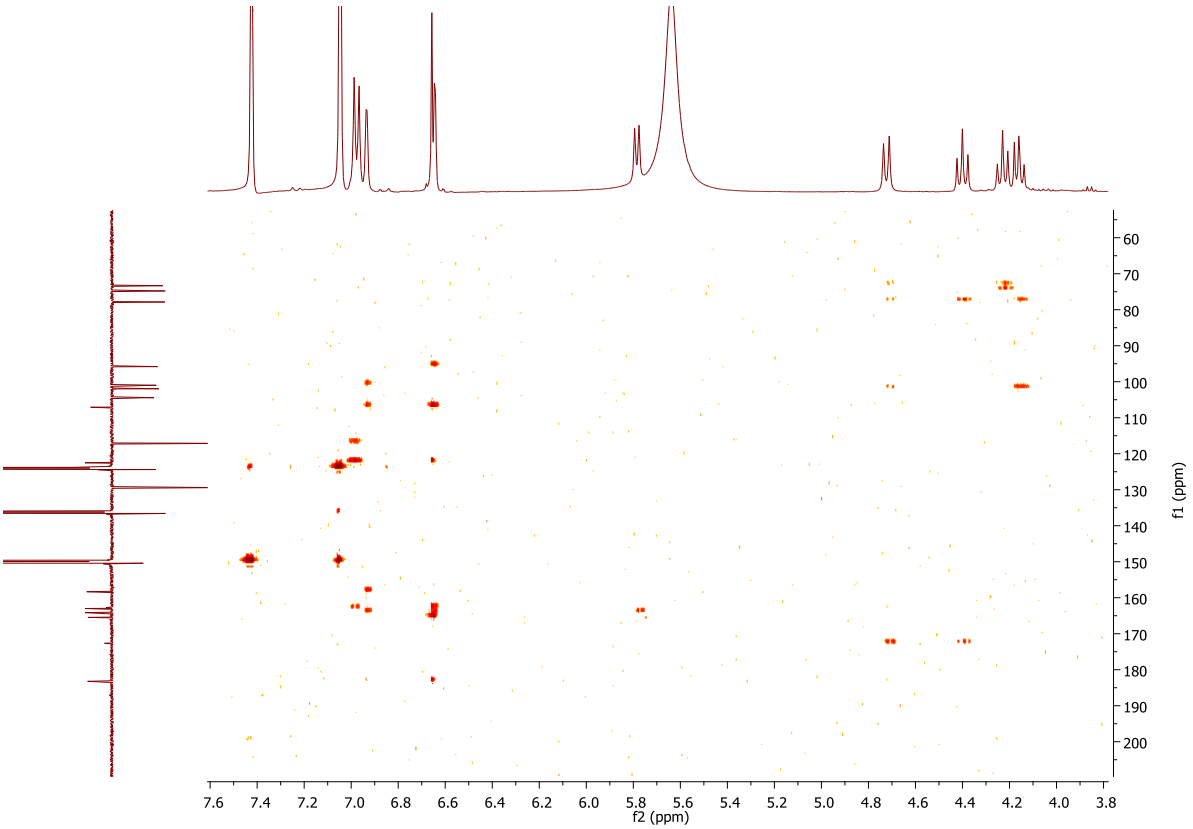

Figure 149 HMBC of 7-*O*-(*β*-D-glucopyranosideuronic acid) apigenin

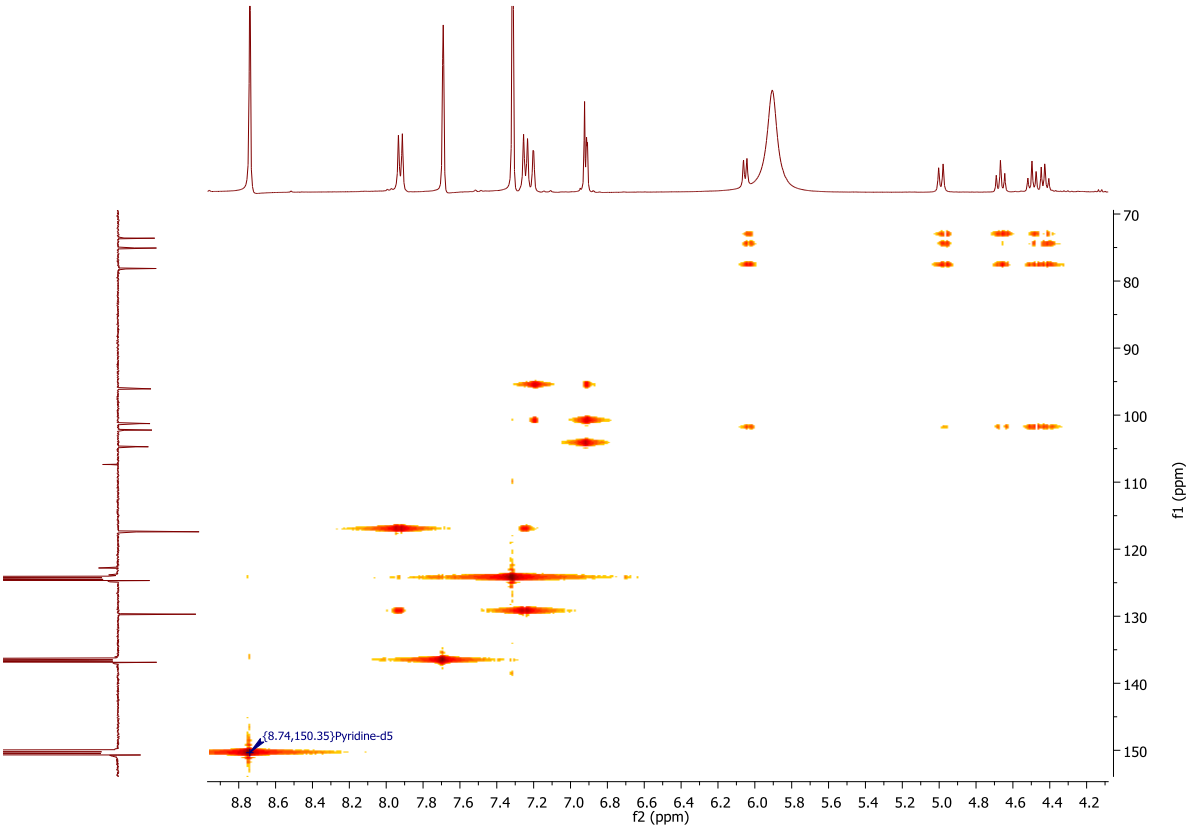

Figure 150 HSQC-TOCSY of 7-*O*-(*β*-D-glucopyranosideuronic acid) apigenin